논문개요집

ISSN 2233-9485(Print)
ISSN 2233-9574(Online)

2021년 한국자기학회 동계학술대회

2021 KMS Winter Conference

논문개요집

일시 2021. 11. 24(수) ~ 26(금)

장소 강릉 세인트존스호텔

주최 한국자기학회

후원 GWTO 강원도관광재단 Gangwon Tourism Organization · 강릉시 · 강릉관광개발공사 Gangneung Tourism Development Corporation · KIMS 한국재료연구원

Digests of the 2021 KMS Winter Conference

The Korean Magnetics Society

사단법인 한국자기학회

2021년 한국자기학회 동계학술대회

2021 KMS Winter Conference

논문개요집

일시 2021. 11. 24(수) ~ 26(금)

장소 강릉 세인트존스호텔

주최 한국자기학회

후원 GWTO 강원도관광재단 Gangwon Tourism Organization · 강릉시 · 강릉관광개발공사 Gangneung Tourism Development Corporation · KIMS 한국재료연구원

공지사항

1. 포스터 발표를 하시는 회원은 아래의 사항을 지켜주시기 바랍니다.

1) 포스터보드 크기는 한 명당 가로 100cm X 세로 200cm 사용할 수 있습니다.

2) 포스터 발표자료는 아래 해당 시간까지 행사장 로비에 설치된 판넬에 부착해 주시면 됩니다.
[포스터 발표 1] 11월 24일(수) 14:00 까지 / [포스터 발표 2] 11월 25일(목) 09:00 까지

3) 포스터 발표 질의응답(Q&A)은 코로나19 확산 방지를 위해 11월 24일(수) 17:00~17:30, 11월 25일(목) 17:00~17:30 사이에 비대면으로 온라인 홈페이지를 통해 댓글 형태로 진행됩니다.

2. 일정

11월 24일(수)	14:00~	참가자 등록			
	14:00~18:00	포스터발표1 (로비)			
	14:00~16:50	강습회 (Antigua1)			
	17:00~17:30	포스터발표1 Discussion (온라인Q&A)			
11월 25일(목)	08:30~	참가자 등록			
	09:00~18:00	포스터발표2 (로비)			
	09:00~12:30	Oral Session 1 (Antigua1)	Symposium 1 (Antigua2)	Symposium 2 (Barbuda1)	Symposium 3 (Barbuda2)
	12:30~13:30	점심식사			
	13:30~17:00	Symposium 4 (Antigua1)	Oral Session 2 (Antigua2)	Symposium 5 (Barbuda1)	Symposium 3 (Barbuda2)
	17:00~17:30	포스터발표2 Discussion (온라인 Q&A)			
	17:30~17:50	총회초청강연 (Antigua1)			
	18:00~19:00	한국자기학회 정기총회 및 시상식 (Antigua1)			
	19:00~	만찬취소			
11월 26일(금)	08:30~	참가자 등록			
	09:00~12:45	Symposium 6 (Antigua1)		Oral Session 3 (Antigua2)	
	13:00~	포스터 시상식 및 폐회(Antigua1)			

3. 11월 25일(목) 저녁 만찬은 코로나19 확산에 따른 영향으로 부득이하게 취소되었습니다.

11월 24일[수]

시간	프로그램
14:00 ~	참가자 등록
14:00 ~ 18:00	포스터발표 1 [SS] Spintronics [MD] Magnetization Dynamics [QM] Quantum Magnetism (Oxide Magnetics) [SD] Magnetic Sensors and Magnetic Micro-Devices [LM] Low Dimensional Magnetics [OS] Others (로비)
	강습회 - Ferromagnetic Resonance(FMR) - (Antigua1) 좌장 : 조영훈(KBSI)
14:00 ~ 14:50	T-1. Analysis of Magnetic Properties using FMR Signals 김동영(안동대)
14:50 ~ 15:00	Coffee Break
15:00 ~ 15:50	T-2. 극저온용 강자성 공명 측정 시스템 개발 박정민(KBSI)
15:50 ~ 16:00	Coffee Break
16:00 ~ 16:50	T-3. Introduction of Brillouin Light Scattering for Spintronics Research 유천열(DGIST)
17:00 ~ 17:30	포스터발표 1 Discussion (온라인 Q&A) 좌장 : 박지훈(KIMS)

11월 25일[목]

시간	프로그램							
08:30 ~	참가자 등록							
09:00 ~ 18:00	포스터발표 2 [MS] Magnetics in Medical Science [PM] Permanent Magnetics [SM] Soft Magnetics [TC] Theory and Computational Magnetics (로비)							
	Oral Session 1 'Spintronics / Magnetization Dynamics' (Antigua1) 좌장 : 고경춘(KAIST)		Symposium 1 'Permanent Magnetics' & 'Electro-Magnetic Energy Conversion' 공동세션 (Antigua2)		Symposium 2 'Theory and Computational Magnetics' (Barbuda1) 좌장 : 박노정(UNIST)		Symposium 3 'Quantum Magnetism' (Barbuda2) 좌장 : 한명준(KAIST)	
09:00 ~ 09:20	초O-1-1. Stabilization and dynamical switching of skyrmions and skyrmioniums in magnetic hemispherical shells 김상국(서울대)	09:00 ~ 09:05	개회사 이우영(연세대) 좌장 : 이정구(KIMS)	09:00 ~ 09:25	초S-2-1. Field-induced Bose-Einstein condensation and supersolid in the two-dimensional Kondo necklace 이현용(고려대)	09:00 ~ 10:00	초S-3-1. Machine Learning Quantum Data Eun-ah Kim(Cornell University)	
09:20 ~ 09:40	초O-1-2. Spin accumulation and spin-orbit torque driven by Rashba-Edelstein effect in an InAs quantum well layer 최경민(성균관대)	09:05 ~ 09:25	초S-1-1. 로봇용 서보모터 개발 및 고특성 분말 Soft Magnet Composite (SMC) 소재 개발에 관한 연구 양상선(KIMS)	09:25 ~ 09:50	초S-2-2. Design of MgAl2O4 Spinel-Oxide-Based Tunnel Barriers for Advanced Spintronics Devices Kenji Nawa(미에대학)			
09:40 ~ 10:00	초O-1-3. Coupling of Distant Magnets via Standing Acoustic Waves 안경모(KRISS)	09:25 ~ 09:45	초S-1-2. 순철 SMCs(Soft Magnetic Composites)의 절연막 내열성 향상 연구 변지영(KIST)	09:50 ~ 10:15	초S-2-3. Magnetics in the two-dimensional layered materials Wei Ren(Shanghi University)	10:00 ~ 10:45	초S-3-2. Artificial Neural Networks for Analyzing Quantum Many-Body Problems Y. Nomura(RIKEN)	
10:00 ~ 10:20	초O-1-4. Coexistence of coupling-induced transparency and absorption in photon-magnon coupling 비스와낫보이(서울대)	09:45 ~ 10:05	초S-1-3. 열간변형 공정을 이용한 고특성 희토자석 제조기술 차희령(KIMS)					
		10:05 ~ 10:25	초S-1-4. 영구자석 설계의 중요 파라미터, 인공지능에 물어보다 박현규(서울대)	10:15 ~ 10:25	Coffee Break			
10:20 ~ 10:30	Coffee Break	10:25 ~ 10:35	Coffee Break 좌장 : 임명섭(한양대)	10:25 ~ 10:50	초S-2-4. Manipulating emergent properties of Hund metal: SrRuO3-SrTiO3 heterostructure 김민재(KIAS)	10:45 ~ 11:30	초S-3-3. Ground-state Properties via Machine Learning Quantum Constraints Y. Zhang(Peking University)	
10:30 ~ 10:50	O-1-5. Highly efficient heat-dissipation power driven by ferromagnetic resonance in ferrite nanoparticles for hyperthermia application 김용섭(서울대)	10:35 ~ 10:55	초S-1-5. 신소재 적용 200W급 서보모터 및 1kW급 제너레이터 개발 전연도(한국전기연구원)	10:50 ~ 11:15	초S-2-5. 2-Dimensional van der Waals Antiferromagnets Studies with Optical Spectroscopy 정현식(서강대)			
10:50 ~ 11:10	O-1-6. Thickness-dependent spin-orbit torques in normal metal/Nb/ ferromagnet tri-layers 이민혁(고려대)	10:55 ~ 11:15	초S-1-6. 신소재 적용 200W급 서보모터 출력 특성 개선 설계 박예지(한양대)					

11월 25일[목]

시간	프로그램				
11:10 ~ 11:30	O-1-7. Prediction of large anomalous Hall conductivity in a compensated ferrimagnet quaternary Heusler compound TiZrMnAl 호앙투투이(울산대)	11:15 ~ 11:35	초S-1-7. 신소재 적용 1 kW 급 제너레이터 출력 특성 개선 설계 김정원(한양대)		
11:30 ~ 11:50	O-1-8. 자구벽 운동 임계전류의 보편성 이해 장준영(서울대)	11:35 ~ 11:55	초S-1-8. 회전 전기 기기의 기계적 성능 검증 프로세스 개발 장민준(부산대)		
		11:55 ~ 12:35	사업단 진도점검 회의 (비공개세션)		
12:30 ~ 13:30	점심식사				

11월 25일[목]

시간	프로그램							
	Symposium 4 '미래소재디스커버리 사업' (Antigua1)		Oral Session 2 'Permanent Magnetics' & 'Electro-Magnetic Energy Conversion' 구두발표 (Antigua2)		Symposium 5 'Soft Magnetics' (Barbuda1)		Symposium 3 'Quantum Magnetism' (Barbuda2)	
	좌장 : 최석봉(서울대)		좌장 : 김태훈(KIMS)		좌장 : 임혜인(숙명여대)		좌장 : 김재욱(KAERI)	
13:30 ~ 13:50	초S-4-1. 스핀궤도소재연구단의 연구 현황과 성과	김영근(고려대)	13:35 ~ 13:50	O-2-1. High-performance Ce-substituted Nd-Fe-B hot-deformed magnets produced by dual alloy method	김가영(KIMS)	13:30 ~ 13:50	초S-5-1. Fabrication of high-Ms amorphous /nanocrystalline soft magnetic materials for high-frequency and high-efficiency electromagnetic applications	정재원(KIMS)
13:50 ~ 14:10	초S-4-2. New spin hall system for high spin efficiency materials	임상호(고려대)	13:50 ~ 14:05	O-2-2. Synthesis and Characterization of SmFe12-based compounds prepared by reaction-diffusion reaction	이강혁(서울대)	13:50 ~ 14:10	초S-5-2. Changes in magnetic properties and microstructure according to composition and annealing conditions of Fe-based nanocrystalline alloys	이귀영(한양대)
14:10 ~ 14:30	초S-4-3. Pd/Co/Pd 구조에서 강자성층 두께에 따른 전자기적 특성 변화	홍종일(연세대)	14:05 ~ 14:20	O-2-3. Magnetic performance of hybrid Nd-Fe-B /Ce-Fe-Bhot-deformed magnets	장예령(연세대)	14:10 ~ 14:30	초S-5-3. Soft magnetic properties and nanocrystallization behavior of cast-iron based bulk amorphous alloy	정효연(한국생산기술연구원)
14:30 ~ 14:50	초S-4-4. Field-free spin-orbit torque switching of perpendicular magnetization	박병국(KAIST)	14:20 ~ 14:35	O-2-4. Fabrication and magnetic properties of Iron-rich intermetallic compounds with ThMn12 structure	천휘동(KIMS)	14:30 ~ 14:40	Coffee Break	
							좌장 : 정재원(KIMS)	
						14:40 ~ 15:00	초S-5-4. Development of hexaferrite-based electromagnetic wave absorbers	강영민(한국교통대)
14:50 ~ 15:10	초S-4-5. Various approaches for the more effective spin-orbit torque switching	유천열(DGIST)	14:35 ~ 14:45	Coffee Break		15:00 ~ 15:20	초S-5-5. Machine Learning Directed Prediction of Saturation Magnetization	남충희(한남대)
15:10 ~ 15:20	Coffee Break		좌장 : 박지훈(KIMS)			15:20 ~ 15:40	초S-5-6. Current Status and Research Trend of Soft Magnetic Core	김진배(LG Electronics)
			14:45 ~ 15:00	O-2-5. Microstructure and Magnetic Properties of Sn added MnBi Bulk Magnets	양양(KIMS)			
	좌장 : 이경진(KAIST)		15:00 ~ 15:15	O-2-6. Giant Magnetic Anisotropy in Metastable FePt Alloy	어취르(인천대)	좌장 : 정재원(KIMS)		
15:20 ~ 15:40	초S-4-6. Interfacial Dzyaloshinskii-Moriya Interaction in Ferromagnetic Thin Films	최석봉(서울대)	15:15 ~ 15:30	O-2-7. Effect of Cu addition on the magnetic and microstructural properties of multi-main phase Nd-Ce-Fe-B sintered magnet	배경훈(KIMS)	15:40 ~ 16:00	초S-5-7. Manufacturing strategy for a powder-based Fe-6.5%Si steel with high density	권기혁(RIST)
13:30 ~ 14:30							초S-3-4. Thermal transport and thermodynamic properties of Kitaev quantum spin liquid candidate material α-RuCl	Y. Matsuda(Kyoto University)
14:30 ~ 15:15							초S-3-5. Terahertz spectroscopy of antiferromagnetic resonances in $YFe_{1-x}Mn_xO_3$ ($0 \le x \le 0.4$) across a spin reorientation transition	김재훈(연세대)
15:15 ~ 16:00							초S-3-6. Oxide Heterostructures for Quantum Magnetism	손창희(UNIST)
16:00 ~ 16:45							초S-3-7. Finite-Temperature Spin Dynamics and Transport Phenomena in Kitaev Quantum Spin Liquids	J. Nasu(Tohoky University)
16:45 ~ 17:30							초S-3-8. Assessments of Kitaev physics in 3d transition metal magnets via first-principles calculations	김흥식(강원대)

11월 25일[목]

시간	프로그램					
15:40 ~ 16:00	초S-4-7. SRAM 기반 cache memory 대체를 위한 SOT-MRAM의 설계 사양 검증 박종선(고려대)	15:30 ~ 15:45	O-2-8. Fabrication of fine-grained Nd-Fe-B hot-pressed magnet using anisotropic HDDR powders aligned by a pulsed magnetic field 유재경(KIMS)	16:00 ~ 16:20	초S-5-8. Strategies for improved properties of soft magnetic composites: heat-resistant insulation and powder engineering 장민선(KIMS)	
16:00 ~ 16:20	초S-4-8. Spin Hall conductivity of Tungsten alloys 임성현(울산대)	15:45 ~ 15:55	Coffee Break	16:20 ~ 16:40	초S-5-9. A Study on the Magnetic Properties of Soft Magnetic Powder using Water Atomized Iron Powder for Eco-Friendly Automotive Application 윤준철(현대제철)	
		좌장 : 이정종(KETI)				
		15:55 ~ 16:10	O-2-9. 화학공정용 마그네틱 드라이브 펌프에 적용되는 영구자석에 대한 연구 윤명환(KETI)			
16:20 ~ 16:40	초S-4-9. Ferromagnet-induced spin-orbit torques 이경진(KAIST)	16:10 ~ 16:25	O-2-10. 할박 배열 영구자석을 갖는 비접촉 동력 장치의 구조에 따른 특성 해석 및 검증 우종현(충남대)	16:40 ~ 17:00	초S-5-10. Additive manufacturing of soft magnetic Fe-Si alloys: a new strategy for 3D components of novel high-performance motors 구본욱(KIMS)	
		16:25 ~ 16:40	O-2-11. 방향성 전기 강판을 적용한 고고도 장기체공 무인항공기용 외전형 방식 표면 부착형 영구자석 동기전동기의 성능 분석 안종민(울산대)			
		16:40 ~ 16:55	O-2-12. 고정투자율법을 이용한 고조파 전류 입력 철손 해석 방법 유준열(한양대)			
17:00 ~ 17:30	**포스터발표2 Discussion (온라인 Q&A)** 좌장 : 김상훈(울산대)					
(Antigua1)	**총회초청강연** 좌장 : 이기석(UNIST)					
17:30 ~ 17:50	초P-1-1. 총회초청강연 오환원 대표(㈜우원테크놀로지)					
17:50 ~ 18:00	Coffee Break					
18:00 ~ 19:00	(Antigua1) **한국자기학회 정기총회 및 시상식**					
19:00 ~	**만찬취소**					

11월 26일[금]

시간	프로그램		
08:30 ~	참가자 등록		
	Symposium 6 'Magnetics in Medical Science' (Antigua1)		Oral Session 3 'Theory and Computational Magnetics' / 'Others' (Antigua2)
	좌장 : 백철하(강원대)		좌장 : 이기석(UNIST)
09:00 ~ 09:20	초S-6-1. Effects of Neuromuscular Electrical Stimulation Applied After 1 Hz Low Frequency Repetitive Transcranial Magnetic Stimulation on Upper Limb Motor Function and Electroencephalography in Chronic Stroke Patients 정중우(보바스기념병원)	09:00 ~ 09:20	O-3-1. Semimetallic Nature of and Magnetic Polarons in EuB6 Studied by using Angle-Resolved Photoemission Spectroscopy 김형도(포항가속기연구소)
09:20 ~ 09:40	초S-6-2. A Computational Algorithm to Classify Active and Resting Motion during Finger Tapping Task for evaluation of Rehabilitation Therapy 서나연(전남대)		
09:40 ~ 10:00	초S-6-3. Effect of Gradient physical linearity and Static Magnetic Field homogeneity on diffusion weighted image : A phantom study 이호범(서울아산병원)	09:20 ~ 09:40	O-3-2. 자동차 럼버서포트용 모터의 토크향상을 위한 전자기해석 이만기(한국로봇융합연구원)
10:00 ~ 10:20	초S-6-4. Conjugation element analysis and Brownian motion observation of magnetic nanoparticle structure conjugated with Corona-19 immune antibody 이상석(상지대)		
10:20 ~ 10:50	초S-6-5. New CT Scanner with Photon-Counting Detector 이창래(삼성전자)		
10:50 ~ 11:00	Coffee Break	09:40 ~ 10:00	O-3-3. Weyl points in magnetic metals 박민규(울산대)
	좌장 : 안소현(연세대)		
11:00 ~ 11:20	초S-6-6. 몬테카를로 시뮬레이션을 이용한 친환경 의료용 차폐 시트개발 권다은(강원대)		
11:20 ~ 11:50	초S-6-7. A review of AAPM Task Group 241: A medical physicist's guide to MRI-guided focused ultrasound body systems 박소현(제주대)		
11:50 ~ 12:15	초S-6-8. Implementation and Clinical Considerations of Elekta MR-linac 추광현(일렉타 코리아)		
12:15 ~ 12:45	초S-6-9. Experience with 1.5T MR-Linac system: a medical physicist's point of view 이호(연세대)		
13:00 ~	포스터 시상식 및 폐회 (Antigua1)		

CONTENTS

○ Session MD [Magnetization Dynamics]

11월 25일(목) 09:00~18:00
Session : 포스터발표 2

로비

비대면 진행

○ Session MS [Magnetics in Medical Science]

○ Session PM [Permanent Magnetics]

○ Session SM [Soft Magnetics]

○ Session TC [Theory and Computational Magnetics]

11월 25일(목) 09:00~11:50
Oral Session 1 'Spintronics' / 'Magnetization Dynamics'

Antigua1

좌 장 : 고경춘(KAIST)

11월 25일(목) 09:00~12:35
Symposium 1 'Permanent Magnetics' & 'Electro-Magnetic Energy Conversion' 공동세션

Antigua2

❀ 좌 장 : 이정구(KIMS) / 임명섭(한양대)

11월 25일(목) 09:00~11:15
Symposium 2 'Theory and Computational Magnetics'

Barbuda1

좌 장 : 박노정(UNIST)

11월 25일(목) 09:00~17:30
Symposium 3 'Quantum Magnetism'

Barbuda2

좌 장 : 한명준(KAIST) / 김재욱(KAERI)

11월 25일(목) 13:30~16:40
Symposium 4 '미래소재디스커버리 사업'

Antigua1

❀ 좌 장 : 최석봉(서울대) / 이경진(KAIST)

11월 25일(목) 13:30~16:55

Oral Session 2 'Permanent Magnetics' & 'Electro-Magnetic Energy Conversion'

Antigua2

❀ 좌 장 : 김태훈(KIMS) / 박지훈(KIMS) / 이정종(KETI)

11월 25일(목) 13:30~17:00
Symposium 5 'Soft Magnetics'

Barbuda1

좌 장 : 임혜인(숙명여대) / 정재원(KIMS)

11월 25일(목) 17:30~17:50
총회초청강연

Antigua1

좌 장 : 이기석(UNIST)

11월 26일(금) 09:00~12:45
Symposium 6 'Magnetics in Medical Science'

Antigua1

좌 장 : 백철하(강원대) / 안소현(연세대)

11월 26일(금) 09:00~10:00
Oral Session 3 'Theory and Computational Magnetics' / 'Others'

Antigua2

좌 장 : 이기석(UNIST)

2021 KMS Winter Conference

강습회

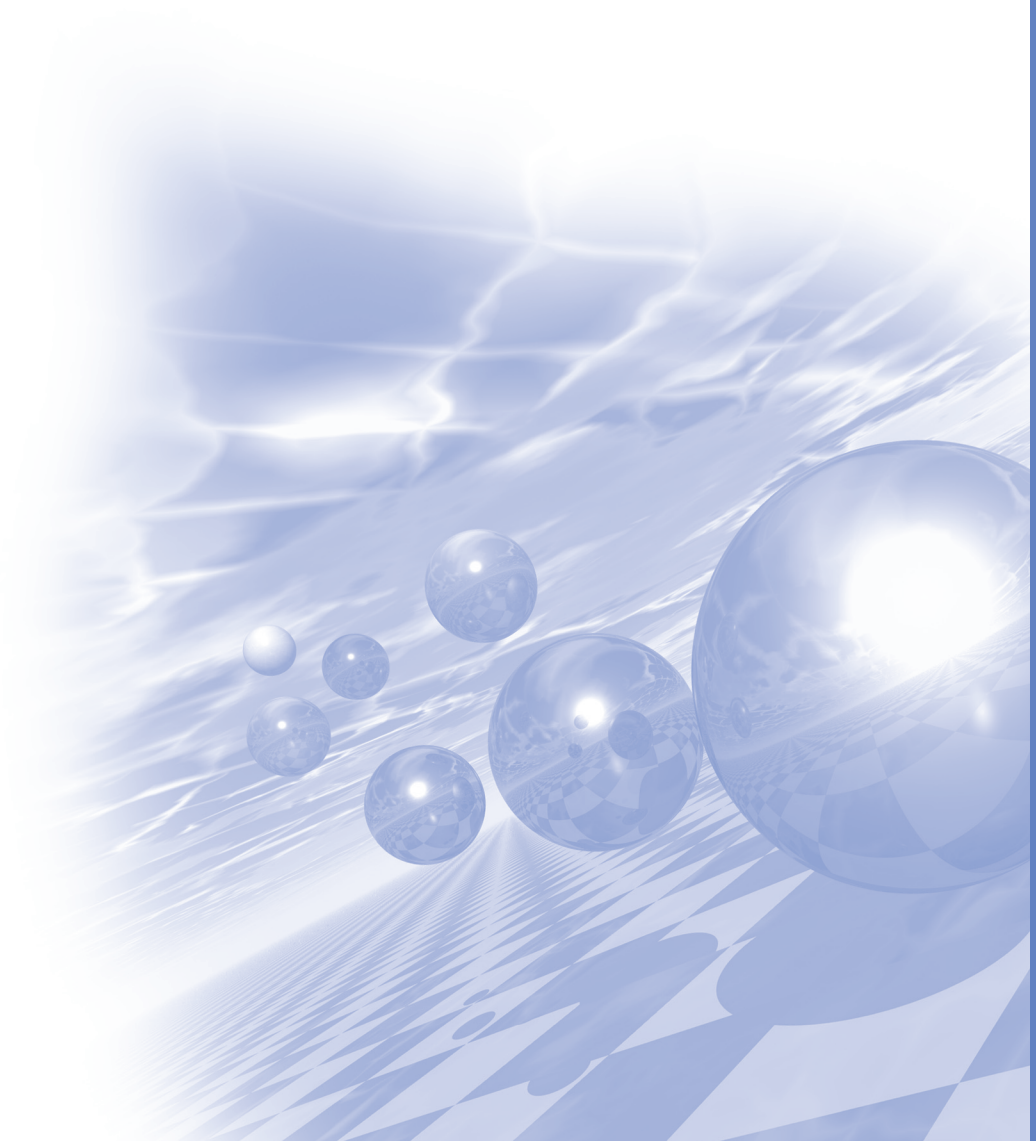

Analysis of Magnetic Properties using FMR Signals

Dong Young Kim*
Department of Physics, Andong National University, Andong, Korea

이번 강습회에서는 강자성 공명(Ferromagnetic resonance, FMR) 신호를 측정하는 장치의 하나인 Cavity-FMR 장치의 소개 및 강자성 재료에서 측정한 공명 신호의 현상학적 분석 방법을 소개하고자 한다. 강자성 박막, 나노 튜브, 나노 입자 등에서 측정한 강자성 공명 신호를 분석하여 자성 재료의 유효 자화량, g-factor, 이방성 자기장, Gilbert 감쇄 상수 등 자성 재료의 물성을 구하는 방법과 재료의 비균질성을 평가하는 방법을 소개하고자 한다.

T-2

극저온용 강자성 공명 측정 시스템 개발

박정민[1*], 이아연[2], 조영훈[1]
[1]한국 기초 과학 지원연구원, 연구장비 개발부, 대전 유성구 과학로 169-148 (34133)
[2]한국 기초 과학 지원연구원, 연구장비 운영부, 대전 유성구 과학로 169-148 (34133)

강자성 공명 현상은 강자성체 자구(magnetic domain)의 자기 모멘트가 외부 자기장에 의해 세차운동을 하고 이때 발생하는 주파수(Larmor frequency)와 외부에서 인가한 전자기파의 주파수가 일치할 때 공명이 일어나고 인가한 주파수의 에너지를 흡수한다. 강자성 공명은 강자성체의 감쇠상수(damping constant), 유효 자화(effective magnetization), 자기 회전비(gyromagnetic ratio), 자기 이방성, 미세 자기 구조, 다층 박막의 계면 효과 등 자성 특성을 분석하는 데 이용하고 있다. 여기에 더해 공명이 일어날 때 발생하는 스핀 펌핑은 일반금속, 2차원 물질 및 위상학적 절연체의 역 스핀 홀 효과(Inverse spin Hall effect, ISHE), 스핀-전하 변환 효율 등을 분석할 수 있다.

이번 강습회에서는 FMR(ferromagnetic resonance) 및 스핀 펌핑의 원리와 현재 대부분 외산 장비에 의존해서 사용하고 있는 극저온용 ISHE-FMR 측정 장비의 국산화를 위한 장비 개발 과정을 간략하게 소개한다. 강자성 공명 장비는 PPMS (physical property measurement system) 장비에 사용할 수 있게 개발되었으며 ISHE-FMR을 동시에 측정이 가능 하다. 측정 가능한 온도 범위는 PPMS 사용 온도와 유사한 4~350K에서 사용할 수 있다. 개발된 장비로 상전이 온도가 220K인 분자기반 강자성 절연체 Cr-PBA와 Co (10nm) 박막의 FMR 신호 및 ISHE 전압을 측정하고 각 시료의 감쇠상수를 얻어 그 값을 참고 문헌의 결과와 비교한다.

Introduction of Brillouin Light Scattering for Spintronics Research

Jaehun Cho[1], June-Seol Kim[1] and Chun-Yeol You[2*]
[1]Division of Nanotechnology, Institute of Convergence, DGIST, Daegu 42988, Korea
[2]Department of Emerging Materials Science, DGIST, Daegu 42988, Korea

We will explain about Brillouin Light Scattering (BLS), which is an in-elastic light scattering with magnon of the magnetic samples [1]. Magnon excitation frequency (or spin-wave (SW) resonance frequency) is determined by the dispersion relations of SW as a function of the basic magnetic properties of the samples, sample's geometrical structure, SW wavevector, and external magnetic field. In BLS measurement, we varied the external magnetic field and obtained the basic magnetic properties of the sample by non-linear regression process, so that we can determine the saturation magnetization, anisotropy energy, exchange stiffness. In addition, we can also determine the interfacial Dzyaloshinskii-Moriya Interaction (iDMI) energy density by using non-reciprocal nature of the SW with non-zero iDMI. Since BLS is based on optical measurement, BLS has a lateral resolution of the laser beam spot size (~50 um), and BLS can measure the magnetic properties of the sub-nm ferromagnetic films. In this lecture, we will discuss about basic principles of BLS measurement and application of BLS for spintronics devices researches.

Reference

[1] J. Cho, J.-S. Kim, and C.-Y. You, J. of Mag. **31**, 69 (2021).

2021 KMS Winter Conference

포스터발표

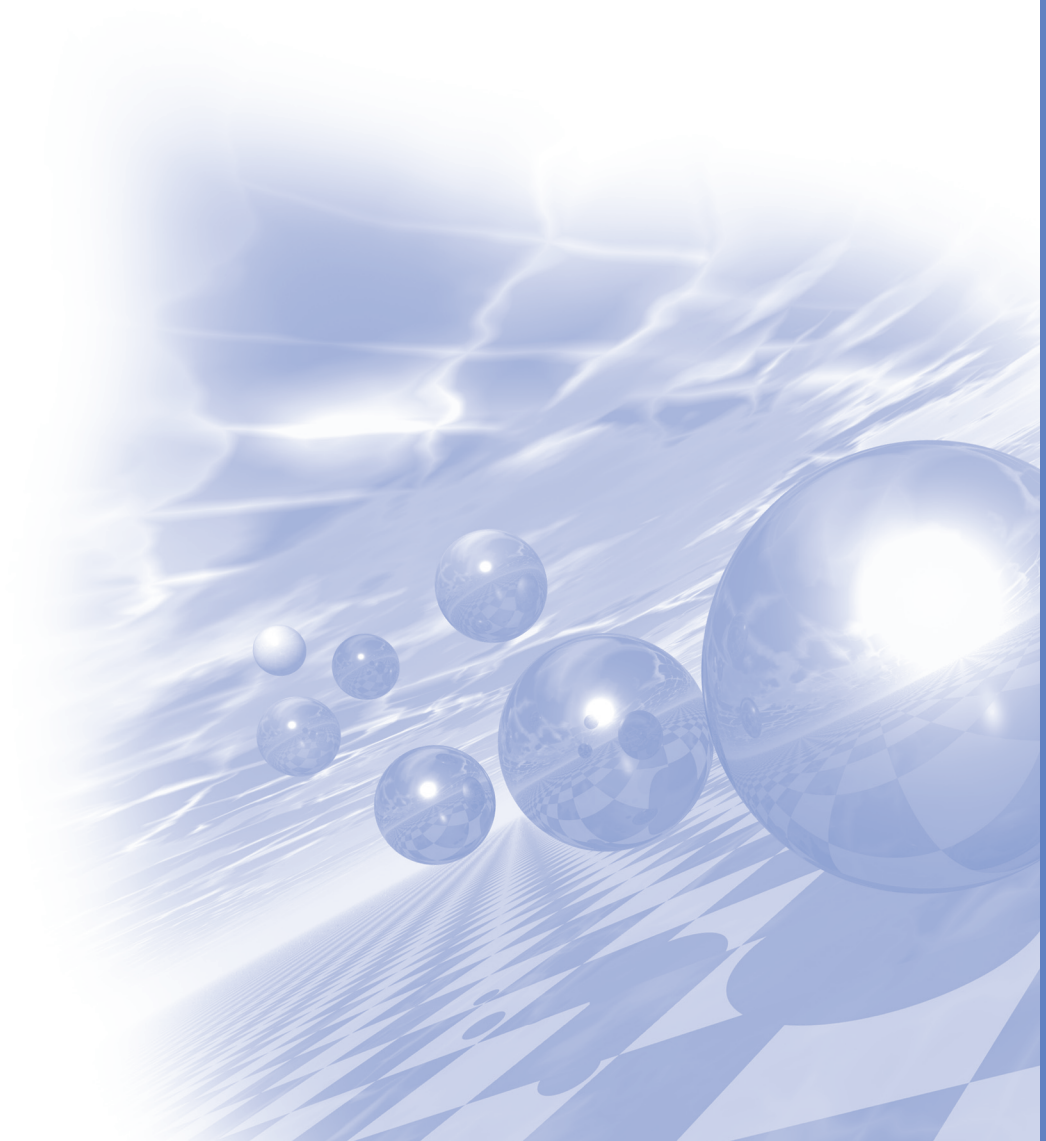

Skewed In-plane Uniaxial Magnetic Anisotropy in Pt/Co/MgO by Using Miscut Sapphire Substrate

Jin-A Kim*, Suhyeok An and Chun-Yeol You†
Department of Emerging Materials Science, DGIST, Daegu, 42988, Korea
*Correspond to cyyou@dgist.ac.kr

Recently, the magnetic memory devices using spin-orbit torque(SOT) have been investigated actively. The writing process in SOT magnetic memory devices takes advantage of simple heavy metal(HM)/ferromagnet(FM) bilayer without extra ferromagnetic layer, which is required in spin transfer torque memory devices. Strong spin-orbit coupling in HM layer generates SOT in FM layer so that the direction of magnetization of FM layer changed by the torque. Efficient SOT based magnetic memory devices usually adopt perpendicular magnetic anisotropy(PMA) system. Generally, SOT makes the magnetization direction to in-plane, additional external in-plane magnetic field is required to achieve deterministic switching. In order to realize field-free SOT switching, in-plane symmetry breaking in PMA system is needed. According to recent researches, breaking in-plane symmetry has been achieved by means of using exchange bias[1], Rashba interface modulation[2], or crystal structural symmetry breaking[3].

In this study, we tried to find lateral symmetry breaking of Pt/Co/MgO heterostructure which is a typical layer structure in SOT based memory devices. We used 3°miscut Al_2O_3 as substrate to get imperfect symmetry through the in-plane direction while deposited heterostructure still shows PMA through the out of plane direction. In-plane magnetic anisotropy is measured by anomalous Hall effect with external field in Hall bar and calculated by using Generalized Sucksmith-Thompson(GST) method[4,5]. The notable finding is the difference between the samples deposited on miscut substrate and the flat Al_2O_3 substrate. The former presents slanted uniaxial anisotropy [6] whereas the latter doesn't as shown in Fig.1(b).

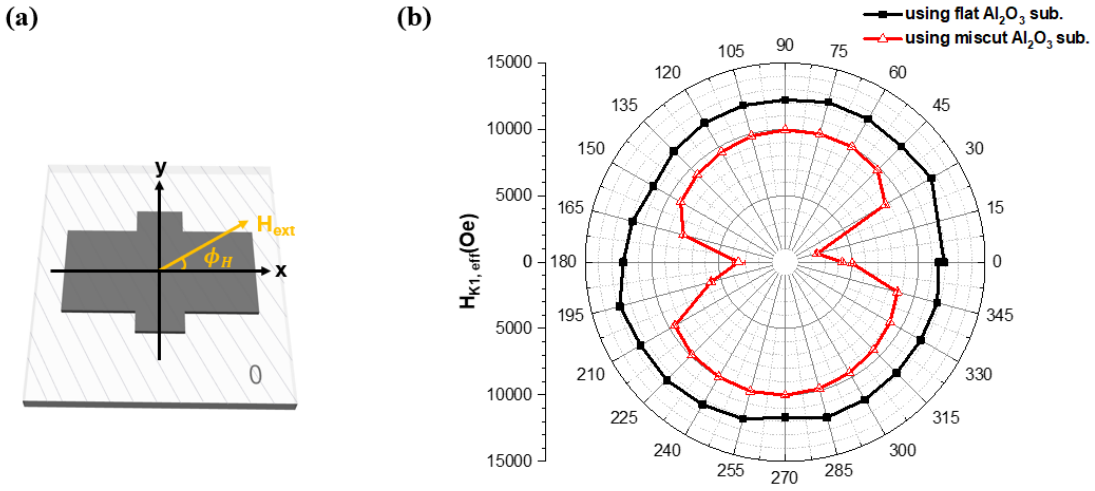

Figure 1. (a) Simple schematic of sample deposited on miscut sapphire substrate and applied in-plane field with the azimuthal angle ϕ_H. (Gray solid lines represent step and terrace structures.), (b) Effective anisotropy field calculated by GST method as a function of angle ϕ_H.

We successfully introduce additional in-plane symmetry breaking with miscut Al_2O_3 substrate, and this result is important because of the proven association between lateral symmetry breaking and field-free SOT based switching.

References

[1] van den Brink, A. *et al*. Field-free magnetization reversal by spin-Hall effect and exchange bias. *Nat Commun* 7 (2016).

[2] Cui, B. S. *et al*. Field-Free Spin-Orbit Torque Switching of Perpendicular Magnetization by the Rashba Interface. *Acs Appl Mater Inter* 11, 39369-39375 (2019).

[3] Liu, L. *et al*. Symmetry-dependent field-free switching of perpendicular magnetization. Nat Nanotechnol 16, 277-+ (2021).

[4] Okamoto, S. *et al*. Chemical-order-dependent magnetic anisotropy and exchange stiffness constant of FePt (001) epitaxial films. *Phys Rev B* 66 (2002).

[5] Okamoto, S., Nishiyama, K., Kitakami, O. & Shimada, Y. Enhancement of magnetic surface anisotropy of Pd/Co/Pd trilayers by the addition of Sm. *J Appl Phys* 90, 4085-4088 (2001).

[6] You, C.-Y., *et al*. Slant-perpendicular magnetic anisotropy axis induced by steps in 4°-miscut Si(111)/ Cu/Au/Co/Au system. *Physical Review B* 69(13), 134402 (2014).

Simulation of Multiple Walker Breakdowns

Jaesung Yoon[1*], Joon Moon[1], Kitae Kim[1], Seong-Hyub Lee[1], Dae-Yun Kim[2], Sug-Bong Choe[1†]
[1]Department of Physics and Astronomy, Seoul National University, Seoul, 08826, Republic of Korea
[2]Department of Electrical and Computer Engineering, National University of Singapore, Singapore,117582, Singapore

Recently, magnetic thin films have drawn great technological attention due to their prospects for use in next-generation memory and logic devices. Particular focuses are given on their domain wall dynamics, which means how to move them effectively. The domain wall dynamics and its characteristics are usually determined by magnetic properties, such as perpendicular magnetic anisotropy (PMA), Dzyaloshinskii-Moriya interaction (DMI), and the spin-orbit coupling effect (SOC), etc. As these properties mostly depend on the interfaces adjacent to the magnetic layers, the magnetic multilayered structures which have multiple interfaces are highlighted.

For this study, we did micromagnetic simulation using so-called OOMMF. For the case of in-plane field – domain wall velocity plot, in contrast to the magnetic single layer which shows single minimum conventionally, double minima are observed in magnetic double layers. The results reveal that each magnetic layer has different internal dipolar magnetic field and thus, the domain wall in each magnetic layer feels different magnetic field. Consequently, each layer has different Walker breakdown field for each domain wall, the domain wall can go through multiple Walker breakdowns assisted by the in-plane field.

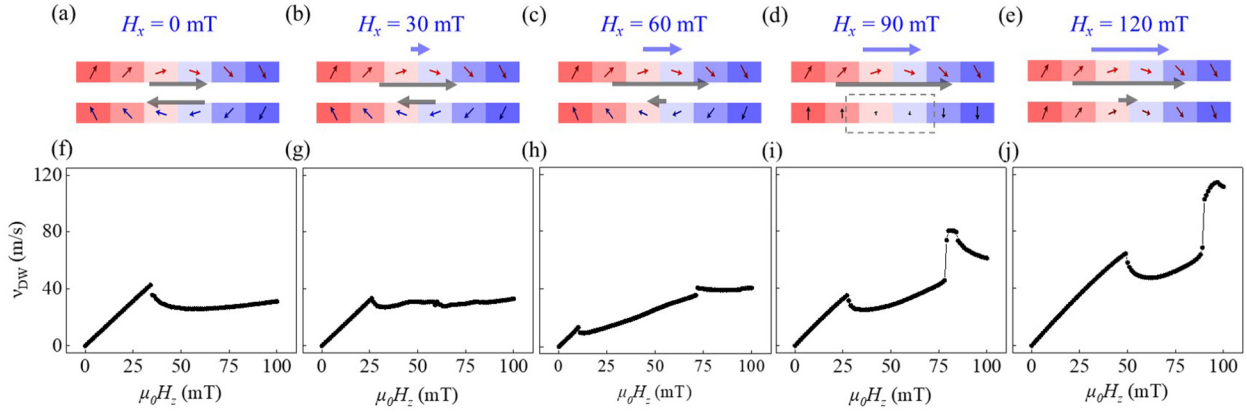

Fig. 1. DW configurations under various H_x values of (a) 0 mT, (b) 30 mT, (c) 60 mT, (d) 90 mT, and (e) 120 mT. The arrow inside each mesh shows the direction of the magnetization. The colors of arrows and meshes correspond to the x and z components of the magnetization, respectively. The gray arrows show H_{tot} at the upper and lower magnetic layer. The blue arrow shows the strength of H_x. (f)-(j) Plots of v_{DW} with respect to H_z for different H_x values.

Electrical detection of magnetic domain wall in Hall bar structure

Seong-Hyub Lee*, Myeonghoe Kim, Yune-Seok Nam and Sug-Bong Choe†
Physics and Astronomy, Seoul National University, Seoul 151-742, Republic of Korea

Here we report electrical detection of magnetic domain wall in Hall bar structure in various wire dimensions within perpendicular magnetic anisotropy system. To examine as many as possible device structures in one coupon sample, wire width and Hall bar width combination was arranged as 8 by 5 matrix. Using Dc magnetron sputtering, our conventional perpendicular magnetic anisotrpy thin film Ta [5 nm] / Pt [2.5 nm] / Co [0.3 nm] / Pt [1.5 nm] trilayer structure was deposited on the commercial Si [525μm] / SiO_2 [100 nm] diced to 12 mm by 12 mm wafer substrate. Then Hall bar pattern was transferred to this film by using photolithograpy and ion milling process. And finally electrode pattern was also tranferred followed by Ta [5 nm] / Au [80 nm] electrode deposition and lift off process. Now in this microstructure, magnetic domain wall position was optically detected by laser p-MOKE with anomalous Hall signal simultaneously. Wire width dimension (W_M) is assigned as [40, 30, 25, 20, 15, 10, 5, 2 μm] and Hall bar width (W_H) is assigned as [10, 8, 6, 4, 2 μm]. Hall signal of magnetic domain wall was fitted as $a*\tanh\{b(x-c)\}$ and if the value of a reach 90 % of total anomalous Hall signal, detection range of magnetic domain (R) is defined as $\frac{[2\tanh^{-1}(0.9)]}{b}$. Fig. 1 is our example data of Hall signal versus position of magnetic domain wall (DW). Interestingly, maximum value of ratio between detection range and Hall bar width was 23.4 which is very seneitive to the position of magnetic domain wall. In conclusion by measuring the detection range of magnetic domain wall via anomalous Hall signal in diverse wire dimensions, we investigate the sensitivity of anomalous Hall signal to magnetic domain wall position.

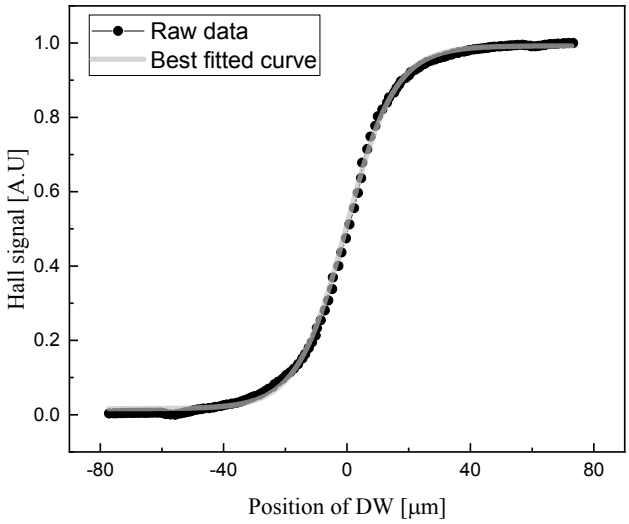

Fig. 1 Hall signal versus position of domain wall in wire width 40 μm and Hall bar width 10 μm device.

Asymmetry of Spin-Orbit Torque induced Magnetization Switching by Local Helium Ion Irradiation

Suhyeok An*, Jin-A Kim, Hyeong Joo Seo, Chun-Yeol You†
Department of Emerging Materials Science, DGIST, Daegu, Korea
Correspondent to cyyou@dgist.ac.kr

The spin-orbit torque (SOT) induced magnetization switching based memory devices with perpendicular magnetic anisotropy (PMA) [1,2] has a perspective as replacement of spin transfer torque (STT). However, magnetization switching using SOT, unlike STT, requires in-plane magnetization symmetry breaking, thus the applying an in-plane external magnetic field is essential. Therefore, several methods have been proposed to break the in-plane magnetization symmetry without the application of an external magnetic field. Among them, there is a few reports that magnetization switching caused by in-plane non-uniformity of PMA creates deterministic SOT-based magnetic field-free switching [3,4], but the discussion on how the magnetization reversal starts is still insufficient. In this report, we prepared the sample having in-plane non-uniformity of PMA by locally irradiated He^+ ion in Pt(5)/Co(0.8)/MgO(2) structure. And the asymmetry of SOT induced magnetization switching current is observed according to magnetization initial status (+z or -z direction). By local irradiation of He^+ ion, the sample is divided two (irradiated and non-irradiated) regions. The PMA energies of two regions are districted and its differences between them increase gradually with higher dose irradiation. The results show different critical switching current according to initial direction of magnetization and this asymmetry reaches ~ 12.3% at dose amount of 45 ions/nm^2. The domain patterns measured by magneto-optical Kerr microscopy display lower switching current when the domain starts to nucleation at PMA boundary, and it implies that SOT switching can be assisted by internally-formed effective field caused by PMA energy gradient.

References

[1] Miron, I. M. *et al*. *Nature* **476**, 189–193 (2011)
[2] Liu, L. *et al. Phys. Rev. Lett.* **109**, 096602 (2012)
[3] Yu, G. *et al. Nat. Nanotechnol.* **9**, 548-554 (2014)
[4] Wu, H. *et al. Nano Letter* **21**, 515-521 (2020)

Exploring the role of magnetic clusters in Ce and Cr-substituted $La_{1.2}Ce_{0.2}Ca_{1.6}Mn_{1.9}Cr_{0.1}O_7$ Ruddlesden-Popper compound

Akshay Kumar[1*], Kavita Kumari[2], Minji Shin[1], Seok Hwan Huh[1] and Bon Heun Koo[1,2†]

[1]School of Materials Science and Engineering, Changwon National University, Changwon, Gyeongnam, 51140, Republic of Korea

[2]School of Materials Science and Engineering, Changwon National University, Changwon, Gyeongnam, 51140, Republic of Korea

In this work, the Simultaneous doping on A and B sites were performed in $La_{1.2}Ce_{0.2}Ca_{1.6}Mn_{1.9}Cr_{0.1}O_7$ (LCCMCO) compound to analyze the influence of Cerium (Ce) and Chromium (Cr) on the structural, magnetic and magnetocaloric properties. The bulk ceramics were prepared through solid-state sintering method by sequentially monitoring the heating episodes. The samples crystallized in tetragonal symmetry of double layer Ruddlesden-Popper phase. Parent compound ($La_{1.4}Ca_{1.6}Mn_2O_7$) acquired pure phase while the co-doped sample has a mixed cubic perovskite phase. The samples possess well-connected microstructure with clearly defined grain boundaries. secondary oxide phases appeared at the surface of LCCMCO. The temperature dependent magnetization revealed ferromagnetic state of the compounds, meanwhile multiple magnetic transitions were observed in LCCMCO, which were ascribed to the magnetic clusters and/or due to the involvement of secondary phase. The ferromagnetic-paramagnetic transition temperature (T_C) was reduced from a value of 275 K for the parent compound to 235 K for LCCMCO. In general, Arrott plots disclosed second order phase transition for both samples, while the spin-clusters clearly revealed for LCMCO sample throughout the transition. The maximum magnetic entropy change (ΔS_M) at 2.5 T was 3.02 J/kgK for LCMO and 2.48 for LCCMCO sample. The relative cooling power (RCP) enhanced from 98 J/kg to 109 J/kg at an applied field of 2.5 T respectively for parent and LCCMCO compound.

Keywords: Ruddlesden-Popper phase; magnetocaloric; ferromagnetic state; magnetic entropy change; relative cooling power.

Spin-orbit torque properties of W-V alloy based magnetic heterostructures

Jeong Kyu Lee[1*], Gyu Won Kim[1], Taehyun Kim[1], Min Hyeok Lee[1],
In Ho Cha[1], Jiung Cho[2], Young Keun Kim[1]

[1]Department of Materials Science and Engineering, Korea University, Seoul 02481, Republic of Korea
[2]Western Seoul Center, Korea Basic Science Institute, Seoul 03759, Republic of Korea

β-W is considered the most promising transition metal due to its outstanding charge-to-spin conversion efficiency. Despite this exceptional property, alloys based on β-W as a spin current generating layer have been rarely studied due to their lack of phase stability [1]. This study examines various properties of W-V alloy layers in $W_{100-x}V_x$ (5)/CoFeB (2.5)/MgO (1)/Ta (2) magnetic heterostructures with different W-V compositions.

Samples were sputtered onto thermally oxidized Si wafers under a base pressure below 5×10^{-9} Torr. Diverse $W_{100-x}V_x$ compositions were fabricated by changing sputtering power densities of W and V targets during co-deposition. X-ray diffraction verified the existence of β-W up to a V content of 20 at%. It also confirmed that Co-V alloys are formed when V content exceeded 60 at%. Spin-orbit torque properties were analyzed by harmonics Hall measurement [2]. Out of all the samples measured, the sample with W content of 80 at% and V of 20 at% showed the maximum damping-like torque efficiency of -0.45 ± 0.04. ξ_{DL} decreased drastically when V content exceeded 20 at% because phase transition from β-W to α-W occurred [3]. We also fabricated heterostructures of W (5)/CoFeB (0.9)/MgO (1)/Ta (2) and $W_{80}V_{20}$ (5)/CoFeB (0.9)/MgO (1)/Ta (2) to obtain perpendicular magnetic anisotropy. These samples were used to acquire optical microscope images and determine switching current densities. We utilized Magneto-Optic Kerr Effect microscope to observe and obtain current-induced spin-orbit torque switching images for the $W_{80}V_{20}$ alloy-based sample. The change in the contrast of the images successfully depicted the magnetization switching of the ferromagnetic CoFeB layers. The switching current (current density) was 11 mA (2.2×10^7 A cm^{-2}) and 6 mA (1.2×10^7 A cm^{-2}) for β-W and $W_{80}V_{20}$, respectively. The switching current is clearly reduced when $W_{80}V_{20}$ is used instead of pristine W. We hope that this work will play as a key role in the field of spintronics in the future.

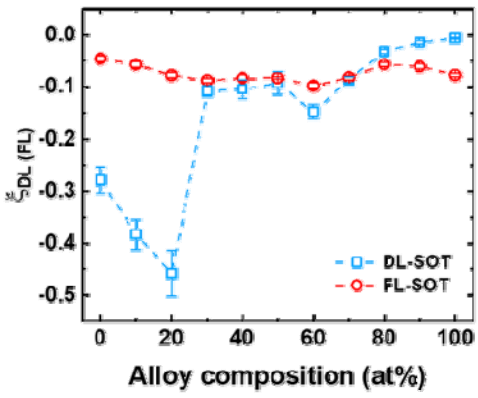

Fig. 1. Damping-like and field-like spin-orbit torque efficiencies of $W_{100-x}V_x$/CoFeB/MgO/Ta structures

References

[1] K.U. Demasius *et al*., Nat. Commun. 7, 10644 (2016)

[2] C. O. Avci *et al*., Phys. Rev. B 90, 224427 (2014)

[3] C.F. Pai *et al*., Appl. Phys. Lett. 101, 122404 (2012)

Investigation of Magnetic Anisotropy in Ultra-thin Co Films Grown on 2-D Materials

Pham Trang Huyen Cao[2*], Nguyen Dan Chi[1,2], Thi-Nga Do[1,2], Soo Min Kim[3], Chanyong Hwang[4], Tae Hee Kim[1,2]

[1]Center for Quantum Nanoscience, Ewha Womans University, Seoul, 03760, Korea
[2]Department of Physics, Ewha Womans University, Seoul, 03760, Korea
[3]Institute of Functional Composite Materials, Korea Institute of Science and Technology, Jeonbuk, 55324, Korea
[4]Korea Research Institute of Standards and Science, Daejeon, 34113, Korea

2D materials have unique physical and chemical properties which can be used for spintronic device applications, such as the long spin relaxation time of graphene. Additionally, the related heterostructures provide the unprecedented probability of combining the different characteristics via the proximity effect.[1]

In this work, ultra-thin Co films were grown on CVD-grown Gr and h-BN layers using the UHV-MBE system. In order to characterize unconventional magnetic properties of 6 ~ 8 nm thick Co films, anisotropy of magnetic tunnel junctions (MTJs) was investigated. The MTJs of x-nm Co (x = 6 and 8)\1.6-nm MgO\12-nm Co were prepared using UHV-MBE system on CVD-grown Gr and h-BN. Perpendicular magnetic anisotropy (PMA) was clearly shown at room temperature (RT) in all the Co bottom electrodes prepared on both graphene and h-BN. Interestingly, for the MTJs grown on h-BN, a very large MR value of more than 700%, was observed with the large PMA, while a few tenth percent of MR values were measured for the Co films grown on Gr layers. Considering theoretical report of an active role of the Co/graphene interface in the magnetism of Co [2], which allows us to sustain PMA, analysis of interface properties between Co and 2-D materials layers is a prerequisite for understanding their magnetic properties. The development of high-quality ferromagnetic thin films in contact with 2D materials is a state-of-the-art growth technique, whereas only thick polycrystalline or three-dimensional morphologies have been demonstrated so far. We report on the growth of flat, epitaxial ultrathin Co films on h-BN and graphene using UHV-MBE deposition technique.

References

[1] Igor Zutic et al., Materials Today, 22, 85-107 (2018).

[2] Chi Vo-Van et al., Materials Science, arXiv:1004.1463 (2010).

온도에 따른 FePt-X(X=C, TiO_2, Ta_2O_5) 입상 박막의 결정 및 자기특성 연구

임은지*, 이동현, 이년종, 박정민, 김상훈
울산대학교 물리학과, 한국

자성 입상 박막(magnetic granular film)은 작은 자기 결정(grain)이 절연체 혹은 비자성 금속에 박혀 있는 형태의 박막이다. 이 박막들의 자기적 전기적 특성들은 결정의 크기, 결정 간의 거리 등에 의존한다. 이러한 입상 자성 박막은 작은 결정의 크기와 높은 자기 이방성 때문에 자성 센서와 하드 디스크 드라이브(Hard Disk Drive, HDD)에 활용되고 있다. FePt-X(X=C, TiO_2, Ta_2O_5)는 대표적인 입상 박막이며, 열 보조 자기기록(Heat-Assisted Magnetic Recording, HAMR) 기술에 활용하고 있다. 여기서 FePt-X(X=C, TiO_2, Ta_2O_5)의 결정 크기 및 밀집도는 소자 응용면에서 중요한 요소가 된다.

이번 연구에서는 높은 자기 이방성을 가지는 FePt-X(X=C, TiO_2, Ta_2O_5) 박막을 온도 별 (300 ^oC ~ 700 ^oC)로 성장시켜 결정 크기의 변화와 표면의 거칠기에 대해 분석한다. FePt-X(X=C, TiO_2, Ta_2O_5) 박막은 여러 물질들을 동시에 증착 할 수 있는 Co-sputter 방법으로 증착 되었다. 각 열처리 온도에 따른 결정성과 자기적 특성을 비교하기 위해 투과 전자 현미경(Transmission Electron Microscope, TEM)으로 결정의 두께를 관측하여 비교하였으며, X 선 회절 분석 (X-ray Diffraction, XRD)으로 결정성(Crystal structure)을 확인하였다. 또한 입상 박막의 표면은 원자간력 현미경 (Atomic Force Microscope, AFM)으로 표면 거칠기를 분석하고 최종, 비정상 홀 효과 (Anomalous Hall Effect, AHE)를 측정하여 입상 박막소자의 자기 이방성 및 전기적 특성을 평가하였다. 끝으로 온도에 따른 입상 박막의 결정 크기 및 자기 특성을 비교 분석한다.

p-MTJ 구조에서 RKKY 상호작용의 Joule heating 효과

임수빈[1*], 정세엽[1], 이택현[2], 박정민[2], 김갑진[2], 김상훈[1]
[1]울산대학교 물리학과
[2]한국과학기술원 물리학과

자기 다층 및 초격자 구조에서 나타나는 Rudeman-Kittel-Kasuya-Yoshida (RKKY) 상호작용은 주로 비자성층에 인접한 두 자성 층 사이의 층간 교환 결합에 기인한다. RKKY 상호작용은 자기 터널 접합의 열적 안정성을 높이기 위해 자기 터널 접합 구조에 활용될 수 있다. 특히 최근에는 열적 안정성이 높은 수직 자기 터널 접합 구조(Perpendicular-Magnetic tunnel junction, p-MTJ)에 활용하기 위해 수직 자기 이방성을 갖는 박막의 RKKY 상호작용에 관한 연구가 발표되고 있다 [1]. 한편, 스핀 토크를 활용하여 p-MTJ의 자화 컨트롤을 하는 경우, Joule heating이 일어나는데, 이때 소자의 자성 특성이 영향을 받게 된다. 수직 자기 이방성 뿐만 아니라, 교환 결합 바이어스 (exchange bias), RKKY 상호작용 등의 물성도 발열에 의해 변화할 것으로 예상되기 때문에, 해당 물리 변수들의 온도 의존성을 이해하는 것이 중요하다. RKKY 상호작용은 디바이스에서 Joule heating이 증가함에 따라 감소한다고 알려져 있는 반면 [1], p-MTJ 구조에서의 RKKY에 온도에 대한 연구는 활발히 진행되지 않고 있다.

이번 발표에서, 우리는 Si/SiO2 기판 위에 수직 자기 이방성을 갖는 Ta/Pt/Co/[Ni/Co]/Ta/CoFeB/MgO/Ta 구조를 magnetron sputtering 시스템을 이용하여 제작했으며 Synthetic Ferrimagnet이 갖는 RKKY 상호작용의 온도 의존성 관측 결과를 다룬다. 극저온 측정 시스템 (Cryogenic Free Measurement System)을 이용하여 비정상적인 홀 효과 (anomalous Hall effect)를 5 K에서 300 K까지 측정했으며 보자력, 스핀 오빗 토크 스위칭 특성 등 다른 물리 변수들의 온도에 따른 경향성과 비교하고, 그 미시적인 원인에 대해서 논의하고자 한다.

References

[1] Jyotirmoy Chatterjee, *et al.*, Scientific Reports **8,** 11724 (2018)
[2] A. Chavent, *et al.*, PHYS.REV.APPLIED **6**, 034003 (2016)

Field free switching of ferrimagnetic GdCo with artificially broken symmetry

Jisu Kim[1*], Seyeop Jeong[1], Taekhyeon Lee[2], Suhyeok An[3], Kab-Jin Kim[2], Ki-Seung Lee[3], Chun-Yeol You[3], Soogil Lee[4], Byong-Guk Park[4], Sanghoon Kim[1†]

[1]Department of Physics, University of Ulsan, Korea

[2]Department of Physics, Korea Advanced Institute of Science and Technology, Korea

[3]Department of Emerging Materials Science, Daegu Gyeongbuk Institute of Science & Technology

[4]Department of Materials Science and Engineering, Korea Advanced Institute of Science and Technology, Korea

[*]Corresponding author: sanghoon.kim@ulsan.ac.kr

During the last decade, current-induced magnetization switching by spin-orbit torque (SOT) is of great importance to nanoelectronics due to energy-efficient control of spintronic memory and logic devices [1,2]. However, it has a problem that an external magnetic field is required to switch magnetization of a device when magnetic layers are perpendicularly magnetized [2]. This implies that there should be limitation of scalability and low energy efficiency because of necessity to use the external magnetic field. Therefore, field-free switching of a magnetization should be achieved for realization of the energy efficient and ultra-fast SOT-driven devices.

Here, we report field-free SOT switching of ferrimagnetic GdCo thin films with a He ion microscope (HIM) technique [3]. The Pt(5)/$Gd_{36}Co_{64}$(5)/Ta(3) structure is irradiated by He ions with the dose range from 5 to 50 ions/nm^2. We find that magnetic properties of the GdCo layer such as coercivity (H_C) and magnetization compensation temperature (T_M) strongly depend on ion dose of a He irradiation. Based on the idea that ferrimagnetic properties can be controlled using He ion irradiation method, we introduced a lateral gradient of magnetization by the HIM to form a broken mirror symmetry in the device [4]. The mirror symmetry breaking was observed after the local modulation; T_M and perpendicular magnetic anisotropy (PMA) properties were locally modulated by He ion irradiation. As the magnetic mirror symmetry is broken, we observed the field-free SOT switching behavior. The S_z component of the spin current generated by the broken mirror symmetry was also observed. We will discuss details about structural change in the ferrimagnetic GdCo by the He ion irradiation.

References

[1] Liu, L. Q. et al., *Science* **336**, 555-558, (2012)

[2] Miron, I. M. et al., *Nature* **476**, 189-193 (2011)

[3] John Notte et al., *Microscopy Today* **14**, Issue 4, 24-31 (2006)

[4] Guoqiang Yu et al., *Nature Nanotechnology* **9**, 548-554 (2014)

Hopping Nature of Magnetic Skyrmion Motion

Mujin You[1*], Moojune Song[1], Seungmo Yang[2], Tae-Seong Ju[2], Min Gyu Albert Park[1], Kyoung-Whan Kim[3] and Kab-Jin Kim[1†]

[1]Department of Physics, KAIST, Daejeon 34141, Korea

[2]Spin Convergence Research Team, Korea Research Institute of Standards and Science, Daejeon 34113, Republic of Korea

[3]Center for Spintronics, Korea Institute of Science and Technology, Seoul 02792, Republic of Korea

It is essential to study the dynamics of magnetic solitons such as domain walls (DWs), vertical Bloch lines (VBLs), and vortices for understanding physical features of emergent excitation. Skyrmion, a topologically protected magnetic soliton, drew a lot of attention because of its nanoscale size, low current controllability, and topological stability, which makes it an attractive candidate for technological applications, such as magnetic memory and logic devices [1, 2]. However, due to the complicated energy landscape and stochastic thermal motion, analyzing the current-induced dynamics of a skyrmion in the actual world is difficult, necessitating statistical treatment. Using magneto-optical Kerr effect (MOKE) microscopy and a blob-tracking method, we discover the current-induced hopping motion of skyrmions in the W/CoFeB/Ta/MgO ferromagnetic thin film. Skyrmions follow a different scaling behavior compared with magnetic DWs, which follow the conventional creep scaling law in the 2D regime [3]. We show that skyrmions display a stochastic particle-like hopping motion, as evidenced by the stop-start characteristics of skyrmion motion at low current density ($7.0 \times 10^7 \sim 1.6 \times 10^9$ A/m^2), thermal diffusion, and forward-and-backward movement. Collective segment theory [4] with the bottleneck process shows that skyrmions exhibit hopping-like scaling behavior because of geometric constraints coming from the closed boundaries. Our study on the rigid-particle model further verifies the hopping nature of skyrmions. Our findings provide fundamental and physical insights into the stochastic motion of particles in the weakly-driven regime, which will be useful to many pioneers in the field.

References

[1] A. Fert et al., Nat. Nanotechnol. 8, 152 (2013)

[2] M. Song et al., IEEE Trans. Electron. Dev. 68, 1939 (2021)

[3] K. -J. Kim et al., Nature 458, 740 (2009)

[4] J. Ryu et al., Phys. Rev. B 84, 075469 (2011)

Antiferromagnetic interfaces in $CoFe_2O_4/Fe_3O_4$ superlattices

Van Quang Nguyen[1,2*], June Hyuk Lee[2], and Sunglae Cho[1*]
[1]Department of Physics and Energy Harvest Storage Research Center,
University of Ulsan, Ulsan 44610, Republic of Korea
[2]Neutron Science Division, Korea Atomic Energy Research Institute, Daejeon, 34057, Republic of Korea

$CoFe_2O_4$ and Fe_3O_4 have been focused in bi-layer system due to their potential used as the magnetic tunnel barrier and electrode in spin dependent tunneling devices and due to their small lattice mismatch. A strong antiferromagnetic coupling at their interface has been reported due to the exchange coupling between two oxides. Here, we provide a first study on the transport and magnetic properties of $[CoFe_2O_4(d)/Fe_3O_4(d)]_n$ superlattices (d = 25 Å, n = 40 and d = 100 Å, n = 10), epitaxially grown on MgO (100) substrate using molecular beam epitaxy. Different from bi-layer system, magnetization curves were centered not only at zero but also at high fields, assigned to a combination of magnetizations of antiferromagnetic interfaces and ferrimagnetic layers. As expected, this behavior becomes more obvious, when the superlattice's wave length decreases due to the dominance of interfaces. Anomalous anisotropic magneto-resistance was also observed due to the presence of these interfaces.

Manipulation of Magnetic Topological Structures Using Localized Magnetic Field

Sooseok Lee[1*], Hee-Sung Han[1,2], Dae-Han Jung[1], Myeonghwan Kang[1], Hye-Jin Ok[1], Namkyu Kim[1], and Ki-Suk Lee[1†]

[1]Department of Materials Science and Engineering, Ulsan National Institute of Science and Technology, Ulsan 44919, Republic of Korea

[2]Center for X-ray Optics, Lawrence Berkeley National Laboratory, Berkeley, CA94720, USA.

Magnetic skyrmions are topologically stable swirling spin configuration and they hold promise as information carriers in future spintronic devices due to their impressive stability. [1-5] For magnetic skyrmions to be practical, establishing controlling method in a selected area of the magnetic thin film is an essential prerequisite. In this presentation, we show experimental demonstration of skyrmion creation and annihilation in a Pt/Co/Ta multi-layered film with perpendicular magnetic anisotropy (PMA) by using highly localized magnetic field. To apply the local magnetic field, we utilized magnetized tip of the magnetic force microscopy (MFM) which generates highly localized stray field (H_{tip}). [6]. As the tip-sample distance decreases, H_{tip} becomes stronger and it reaches to the switching field of the PMA film, and the local magnetization direction of the films can be switched, and it induces creation of magnetic topological structures such as the magnetic skyrmions. Moreover, we demonstrate that the skyrmion polarization can be selectively reversed by changing the tip magnetization as well as they can remain stably without an external magnetic field [7]. Our findings can provide a useful manipulation method for skyrmion based spintronic devices.

References

[1] W. Kang *et al.*, *IEEE Electron Device Lett.*, **37**, 924–927 (2016)

[2] G. Yu *et al.*, *Nano Lett.*, **17**, 261–268 (2017)

[3] A. Fert, V. Cros, and J. Sampaio, **8**, 152–156 (2013)

[4] R. Tomasello *et al.*, *Sci. Rep.*, **4**, 1–7 (2014)

[5] S. L. Zhang *et al.*, *Nat. Commun.*, **9**, 2115 (2018)

[6] A. Casiraghi *et al.*, *Commun. Phys.*, **2**, 1–9 (2019)

[7] S. Lee *et al*., *J. Magn.*, **25**, 458–462 (2020)

Exploring Spin orbit torque efficiency of A15 phase W_3Ta heavy metal

Jeongwoo Seo[1*], Jeonghun Shin[2], Jungyup Yang[3], Jinpyo Hong[1,2]

[1]Department of Physics, Hanyang University, Seoul 133-791, South Korea

[2]Division of Nanoscale Semiconductor Engineering, Hanyang University, , Seoul 133-791, South Korea

[3]Department of physics, Kunsan national University, South Korea 54150

Magnetization manipulation by a Spin Orbit Torque (SOT) phenomena using novel heavy materials has intense focus on the efficient operation of spintronic devices at lower powers. The previously published theoretical work suggested that a W_3Ta layer might have a large spin hall angle, compared with those of the well-known Heavy Metals such as W, Ta. Here, we address the SOT Efficiency of W_3Ta material in a W_3Ta/ CoFeB/MgO hetero-frame. Our in-plane DC analyses confirmed the SOT efficiency of W_3Ta by means of spin orbit torque-driven effective fields and spin hall angle, where the W_3Ta layer were systematically prepared by adjusting different parameters, such as working pressure and annealing temperature. Experimental observation indicate that the enhanced SOT efficiency strongly depends on the crystal structure of particular A15 phase(β-phase) existing in an extremely narrow growth ranges, as seen in fig 1.

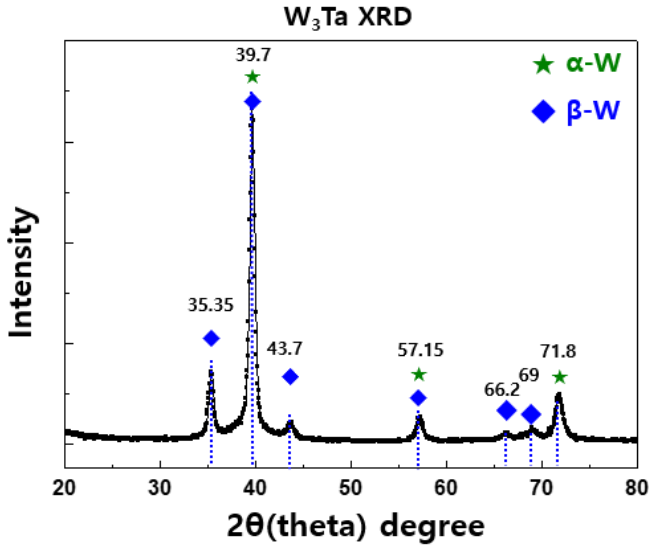

Fig. 1. W_3Ta XRD data with α-phase and β-phase(A15 phase) tungsten

Temperature and bias dependent magnetoresistance in a vertical spin valve CoFe/TiO_2/CoFe based structure

Ehsan Elahi[1*], Ghulam Dastgeer[1], Pradeep Raj Sharma[1],
Abdul Subhan Siddiqui[2], Hwayong Noh[1†]

[1]Department of Physics and Astronomy, Sejong University, Seoul, Korea
[2]Department of Physics, University of Sialkot, Punjab, Pakistan
[†]Corresponding author e-mail: hnoh@sejong.ac.kr

The metal-oxides spin valve junctions are the building blocks for spintronic devices and to utilize for miniaturized magnetic sensors. Here, we describe the fabrication and characterization of vertical spin valve based on CoFe/TiO_2/CoFe structure. CoFe was deposited on Si/SiO_2 substrate and TiO_2(1 nm) deposited on CoFe directly by an e-beam evaporator, in a high vacuum. A reasonable positive magnetoresistance (MR) is obtained via this vertical spin valve at low temperatures. We have observed a maximum value of MR about 0.33% at 28K and 0.20% at 300K. At various current bias, a significant variation in MR is observed. The value of MR was high at lower current (15 μA) and then decreased for the higher bias current which saturates at 40 μA. The decrement in MR at higher bias current can be accredited to the excitation of magnons, to band bending, and probably to the contribution of interface states at higher currents. This trend was also observed in other previous reports. The linear I-V curve demonstrates the ohmic trend of the TiO_2 and FM contacts. The demonstrated device identifies TiO_2 as favorable spacer material in spin valve and opens the way to integrate high-performance memory storage devices.

Development of a new spin hole layer using AlN

Jae Ho Jeong*, Sang Ho Lim
Department of Material Science and Engineering, Korea University, Seoul 02841, Korea)

본 연구에서는 SOT 장치를 위한 새로운 시스템을 개발하기 위해 다양한 실험을 수행하였다. SOT 연구에 자주 활용되고 있는 Pt/Co/MgO 구조에 Pt 층 사이에 AlN 층을 얇게 쌓았다. VSM를 통해 PMA의 변화를 측정하고 홀 측정을 통해 DLT efficiency를 계산해 본 결과 AlN 층을 Pt 가운데 삽입하였을 때 두 데이터에서 모두 큰 향상을 관찰할 수 있었다.

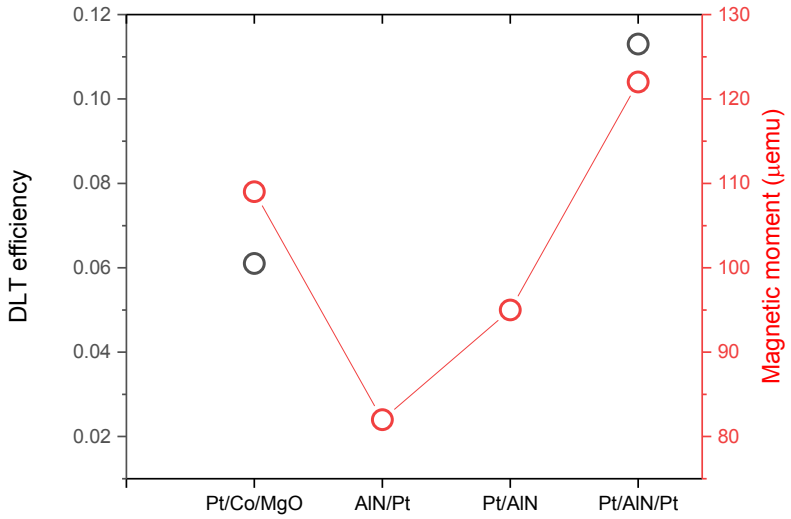

Fig. 1. Results of magnetic moment and damping like torques efficiency values

Effect on perpendicular magnetic anisotropy and spin-orbit torque efficiency with insertion of the W-Ge layer in Pt/Co/W structure

Jun Yeong Heo*, Sang Ho Lim†
Department of Materials Science and Engineering, Korea University, Seoul 136-713, Korea

Pt\Co\W multilayers are evaluated as a novel material composition for the use in perpendicular nanomagneticlogic (pNML) applications. For practical applications of SOT devices, write efficiency parameters such as SOT efficiency (or effective spin hall angle), switching current and write latency need to be improved. SOT efficiency can be improved by reducing anisotropy energy density (K_{eff}). In this study, we compare and analyze SOT efficiency in Pt/Co/W structures with insertion of the W-Ge layer between Co and W layers.

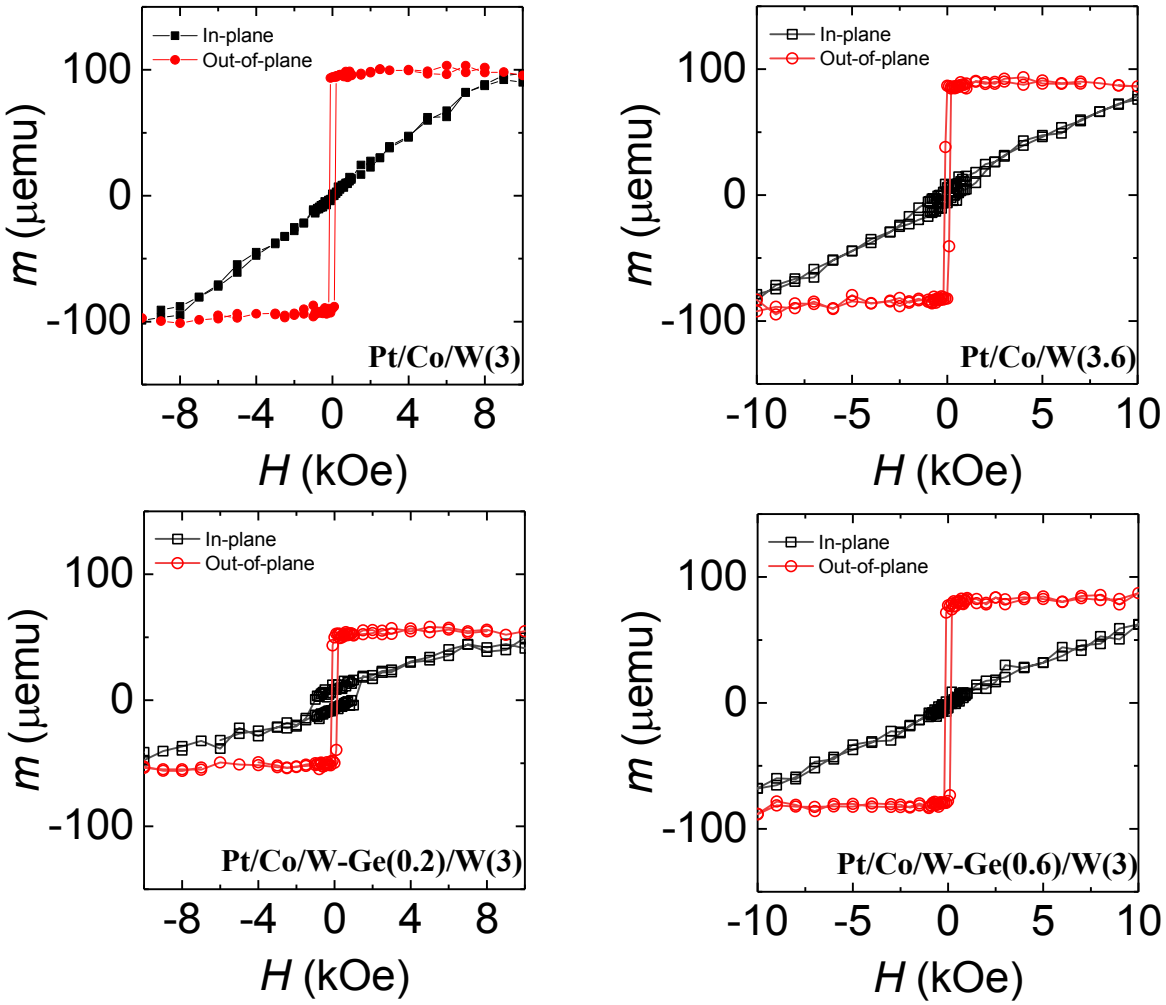

Fig. 1. Hysteresis loops of Pt/Co/W and Pt/Co/W-Ge/W structures.

Magnetic sensor core thin film properties

Hyun Woo Jung*, Sang Ho Lim
Department of Materials Science and Engineering, Korea University, Seoul 136-713, Republic of Korea

Magnetic head core material are required to have higher saturation magnetization (4πMs) and low coecivity. Co-based amorphous films and Ni-Fe (permalloy) alloy films have low coecivity and high saturation magnetization values. So we prepared a Co-based thin films. The thin film was made of Co, Nb, Zr. The cobalt (Co) has good properties suitable for magnetic sensor films. However, cobalt has hcp structure crystalline, which is not good for magnetic sensor core. Than zirconium (Zr) helps to amorphize the crystallinity of cobalt. But, zirconium has negative magnetostrction value. If the magnetostrction value becomes negative, thin film structure become unstale due to stress. Niobium has positive magnetostrction value and help high thermal stability.

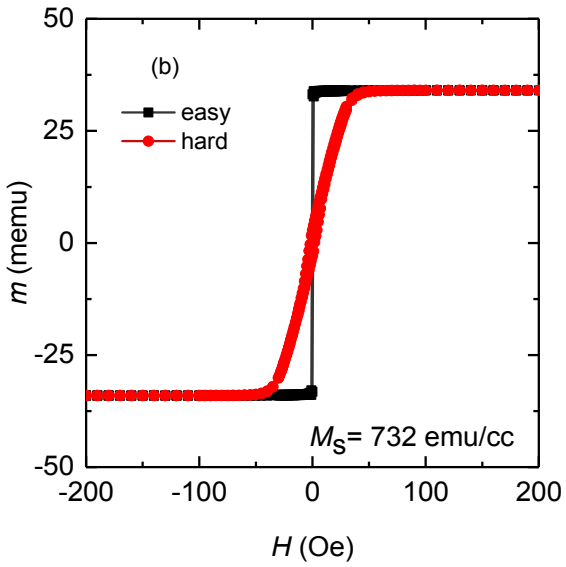

Magnetic Domain-wall Tilting Mechanism during the Transition of Domain-wall Chiralilty

Jung-Hyun Park[1*], Dae-Yun Kim[2], Yune-Seok Nam[1], Hyun-Seok Whang[1], and Sug-Bong Choe[1]

[1]Department of Physics, Seoul National University, Seoul, 08826, Republic of Korea

[2]Department of Electrical and Computer Engineering, National University of Singapore, 117576 Singapore

Spin structure inside domain wall (DW) has attracted great attention due to its potential application on data storage or logic memory. Among terms affecting chirality of DW, Dzyaloshinskii-Moriya interaction (DMI) has been investigated in magnetic thin layer with perpendicular magnetization anisotropy. Based on such platform, most of experimental schemes have measured the chirality change under application of external in-plane field. By changing in-plane field, the direction of magnetization inside DW is changed, resulting in modification of chirality, DW energy, DW dynamics, etc. But those schemes have an assumption that DW is straightly placed across wire and only one variable, direction of the magnetization inside DW, is changed. Here, we propose generalized equation of equilibrium chirality with not only the degree of freedom of DW chirality (Ψ), but also the DW tilting angle (θ). With coordinate system in fig. 1, we numerically calculated equilibrium angle of Ψ and θ, giving a result of DW tilting in the transition regime of DW chirality (fig. 2). This result is counterintuitive in a sense that DW would not be tilted in transition regime as its energy is maximum at Ψ=0. Tilting angle of DW is maximum when in-plane field is applied as much as effective DMI field. Interestingly, the transition regime is widened as both Ψ and θ contribute to reduction of DW energy when in-plane field is changed. Additionally, we analytically calculated the critical field at which the DW starts and ends tilting. This study provides more realistic understanding of chirality and tilting mechanism by considering both contribution to DW energy.

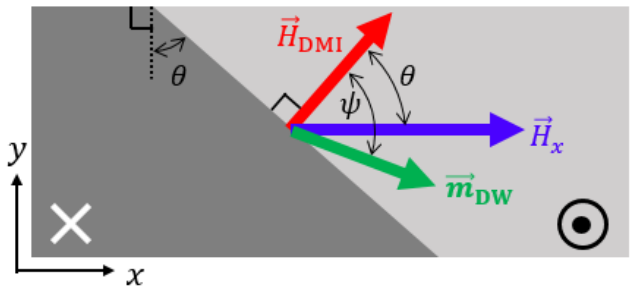

Fig. 1. A schematic coordinate system.

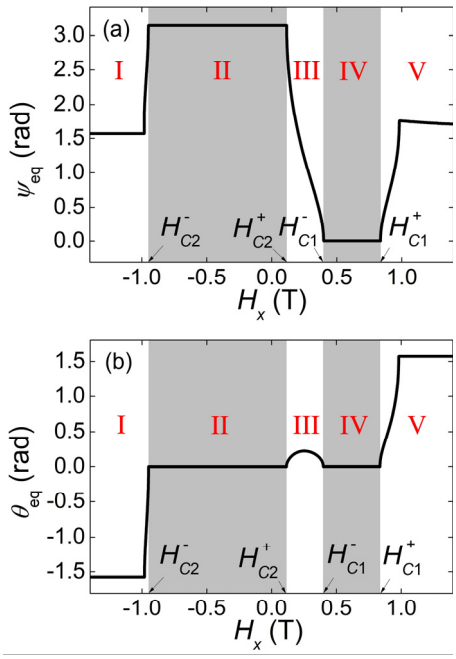

Fig. 2. Equilibrium angle of (a) Ψ and (b) Θ.

In-Situ Measurement of Single Interface Dzyaloshinskii-Moriya Interaction

Ji-Sung Yu[1*], Seong-Hyub Lee[1], Min-Hwan Kim[1], Joon Moon[1],
Dae-Yun Kim[2], and Sug-Bong Choe[1†]

[1]Department of Physics & Astronomy, Seoul National University, Seoul 151-742, Republic of Korea
[2]Spin and Energy Laboratory, Dept. of Electrical & Computer Engineering, National University of Singapore

There have been numerous efforts devoted to quantifying the DMI both theoretically and experimentally, because Dzyaloshinskii-Moriya interaction (DMI) that occurs in structural inversion asymmetric systems stabilizes chiral domain-walls (DWs) which is a key issue to achieve high performance spintronic applications such as memory and data storage devices with high speed and high durability [1-4]. Unfortunately, the inconsistency between theory and experiment inevitably occurs because the theory predicts the strength of DMI based on single interface, however, the experiments must be implemented based on at least, double interface because of Ex-Situ nature [2-6]. Here, we first, measure the strength of DMI in Pt/Co single interface in In-Situ nature. To measure the strength of DMI in single interface, we set up In-Situ magneto-optical-Kerr-effect (MOKE) microscopy with UHV magnetron sputtering chamber. Figure 1 clearly shows the plot of v_{DW} with respect to H_x to quantify the strength of DMI based on Je's method [5].

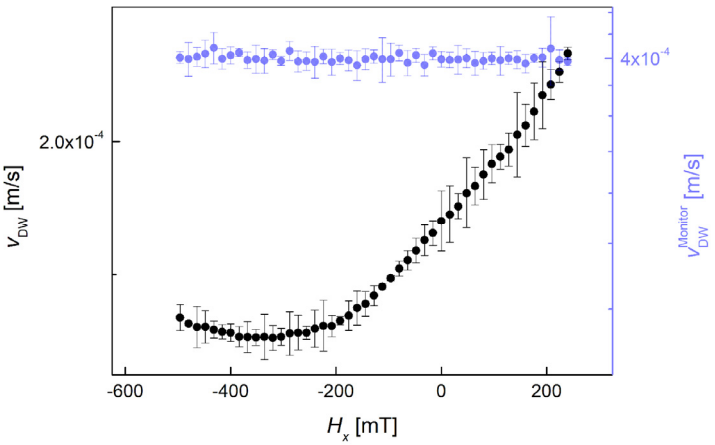

Figure 1. The Plot of the plot of v_{DW} with respect to H_x

References

[1] Stuart S. P. Parkin,* Masamitsu Hayashi and Luc Thomas, Science 320 (5873), 190-194. (2008).
[2] I. E. Dzialoshinskii, Sov. Phys. JETP 5, 1259 (1957).
[3] T. Moriya, Phys. Rev. 120, 91 (1960).
[4] Albert Fert, Vincent Cros and João Sampaio, Nat. Nanotechnol. 8, 152 (2013).
[5] S.-G. Je, K.-J. Lee, and S.-B. Choe, Phys. Rev. B 88, 214401 (2013).
[6] J. Cho, B. Koopmans, and C.-Y. You, Nat. Commun. 6, 7635 (2015).

Experiment Verification of Thiele Equation of Skyrmion Hall Effect

Kitae Kim*, Seong-Hyub Lee, Sug-Bong Choe†
Department of Physics and Astronomy, Seoul National University, Seoul, 08826, Republic of Korea

Magnetic skyrmion is topologically stable spin configuration, which is extensively studied nowadays as promising information carrier in future. Such skyrmion is composed of the Néel-type domain wall with energy stabilization by the Dzyaloshinskii-Moriya interaction. When electric current flows through the skyrmion, the effect based on the Berry phase makes skyrmion deflected from the direction of the current. This effect is called skyrmion Hall effect, which consequently causes information loss by inducing skyrmion annihilation near boundary of device. Therefore, the skyrmion Hall effect attracts great attention with caution in development of skymions to memory device.

In this study, we made series of samples, Ta (5) / Pt (2.5) / Co (X) / W (3) / Ta (2 nm), with varying the magnetic layer thickness X = 0.9, 1.0, 1.1, 1.2, 1.6, 1.7, and 1.9 nm using DC magnetron sputtering. We measure then the skyrmion Hall angle by means of a magneto-optical Kerr effect (MOKE) microscope. In Thiele equation, the skyrmion Hall angle is predicted in terms of Gilbert damping α and anisotropy field H_k. The results are shown in Fig. 1. Although Ideal skyrmion moves remaining circular, in case of half-skyrmion observed in our samples, one half part is extended inclined to the current direction while the other half is pinned. Topological structure is same between skyrmion and half skyrmion so that our result shows verification of Thiele equation experimentally.

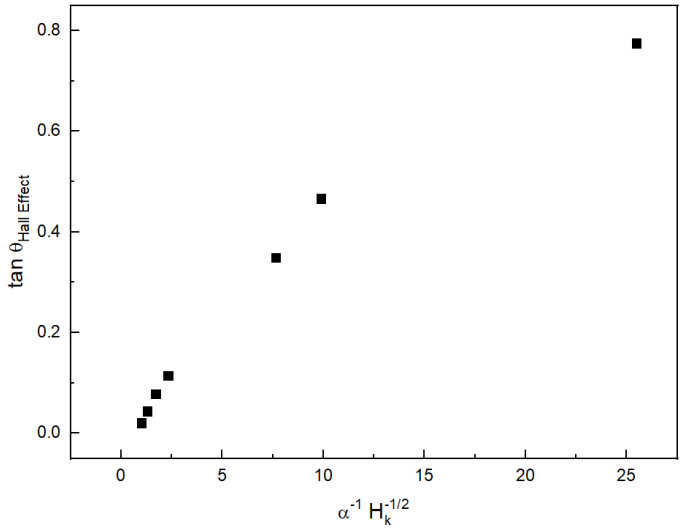

Fig. 1. Skyrmion hall angle with respect to α^{-1} $H_k^{-1/2}$

Statistical properties of telegraph noise generated by magnetic domain wall

Seyyoung Jeon*, Seong-Hyub Lee, Jiho Shin, Sug-Bong Choe
Department of Physics and Institute of Applied Physics, Seoul National University, Seoul, Korea

Telegraph noise, the certain type of signals which consists of sudden jumps between two or more levels, can be observed in several systems for example CMOS, memristor, and magnetic domain wall. The behavior of telegraph noise looks so random that there have been several approaches to utilize this noise to generate random numbers. In this study, as the foundation work for random number generator, some statistical properties are extracted from the telegraph noise generated by domain wall between two metastable states. Telegraph noise is measured by magneto-optic Kerr effect (MOKE) signal from the domain wall of the perpendicularly magnetized Pt/Co/W thin film. Applying field in the direction which makes domain wall escape from the pinning site results in telegraph noise of MOKE signal. As shown in figure 1, signal jumps up when the domain wall is depinned. By fitting cumulative probability function depending on depinning time, the energy barrier of domain wall depinning is also estimated.

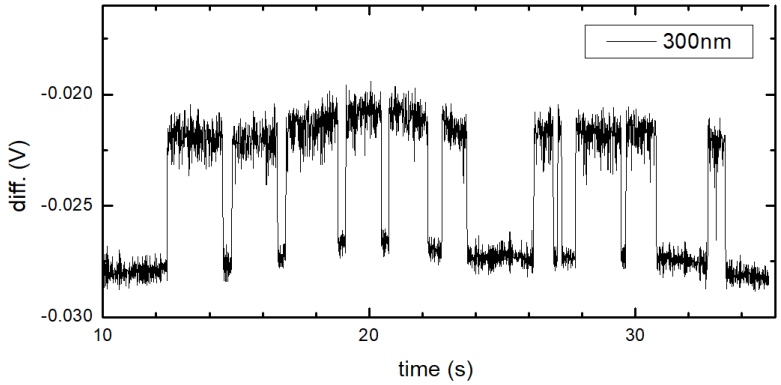

Fig. 1. Telegraph noise measured from notch of the 300nm nanowire by applying field

Frequency response of anomalous Nernst effect with sinusoidal laser pulses

Nayeon Kim, Sung Hwang, Seungha Yoon*
Green energy and nano technology R&D group, Korea Institute of Industrial Technology, Gwangju, South Korea

Because the anomalous Nernst effect (ANE) involves the effective electric field generated by the combination between the thermal gradient and the magnetization direction, it has been well applied to not only the measurement of the static magnetization but also the experiments for low frequency magnetization dynamics. In this work, the frequency response of the ANE was examined to provide two implications: First, as a method to separate Nernst effects from other signals in the homo or heterodyne method, and second, as a timing reference of the phase-sensitive measurement for the magnetization dynamics. The 1550 nm laser power was modulated up to 2.4 GHz and successfully produced the equivalent speed of the ANE signals on the 10 nm permalloy block on the sapphire substrate. The two implications could be sufficiently supported, when the system consists of well-designed radio frequency components and the better heat sink substrate for the fast thermal gradient on the magnets.

Spin-torque ferrimagnetic resonance near angular momentum compensation

Seok-Jong Kim[1,2*], Dong-Kyu Lee[3], Se-Hyeok Oh[4], Hyun Cheol Koo[1,5*], and Kyung-Jin Lee[2†]

[1]KU-KIST Graduate School of Converging Science and Technology, Korea University, Seoul 02841, Korea

[2]Department of Physics, Korea Advanced Institute of Science and Technology, Daejeon 34141, Korea

[3]Department of Materials Science and Engineering, Korea University, Seoul 02841, Korea

[4]Department of Nano-Semiconductor and Engineering, Korea University, Seoul 02841, Korea

[5]Center for Spintronics, Korea Institute of Science and Technology, Seoul 02792, Korea

Compensated ferrimagnets show both ferromagnetic and antiferromagnetic dynamics, i.e., fast magnetization dynamics [1-5] and vanishing Skyrmion Hall effect [6] with finite magnetization. As the dynamics of ferrimagnets can be driven with current-induced spin torques [7, 8], it is important to find a way of quantifying spin torques in ferrimagnetic materials. One of the main methods to quantify the spin torque in ferromagnets is the spin torque ferromagnetic resonance (ST-FMR) technique [9, 10]. For ferromagnets, the damping-like (DL) and field-like (FL) torque components are separately determined through ST-FMR line-shape analysis. However, it is unclear if this line-shape analysis is valid even for ferrimagnets. In this work, we report a theory of spin torque ferrimagnetic resonance (ST-FiMR) in ferrimagnet/heavy metal bilayer structures. The mixing voltage originating from the DL torque is linearly proportional to the effective net spin density of the system, resulting in sign reversal at the angular momentum compensation condition. Our result suggests that the line-shape analysis established for ferromagnets is invalid for ferrimagnets especially near the compensation condition so that the proposed theory must be implemented to analyze the spin torque ferrimagnetic resonance.

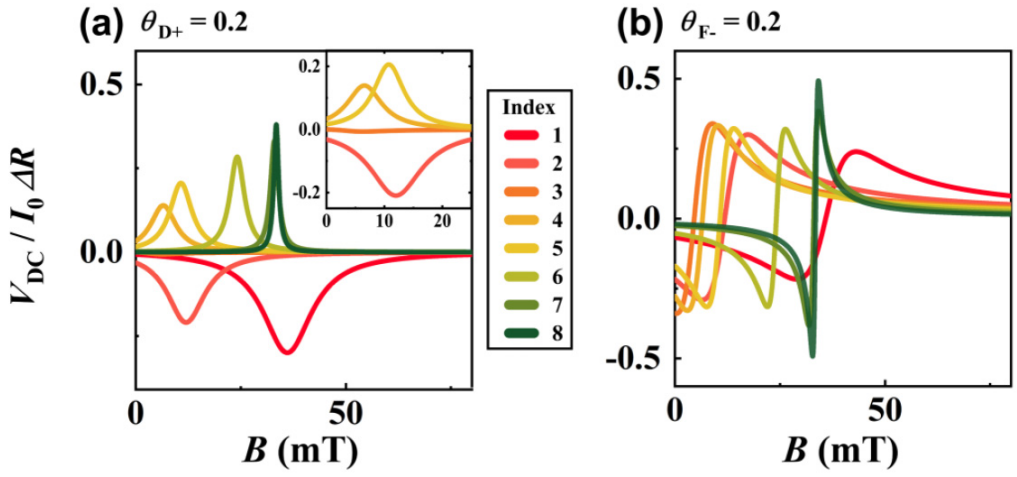

Fig. 1. ST-FiMR signals for various values of net spin density as a function of external field B.

References

[1] K.-J. Kim et al., Nat. Mater. 16, 1187 (2017).

[2] S.-H. Oh et al., Phys. Rev. B 96, 100407(R) (2017).

[3] L. Caretta et al., Nat. Nanotechnol. 13, 1154 (2018).
[4] S. A. Siddiqui et al., Phys. Rev. Lett. 121, 057701 (2018).
[5] S.-H. Oh and K.-J. Lee, J. Magn. 23, 196 (2018).
[6] Y. Hirata et al., Nat. Nanotechnol. 14, 232 (2019).
[7] J. Yu et al., Nat. Mater. 18, 29 (2019).
[8] T. Okuno et al., Nat. Electron. 2, 389 (2019).
[9] A. A. Tulapurkar et al., Nature 438, 339 (2005).
[10] J. C. Sankey et al., Phys. Rev. Lett. 96, 227601 (2006).

MD07

HM/TmIG 이중층 구조에서 SOT 스위칭의 온도의존성 연구

이동현[1*], 조하은[1], 장희찬[3], Ikebuchi Tetsuya[3], Funada Shinsaku[3], Yoichi Shiota[3], Yoshinori Kotani[4], 이년종[1], 이수길[5], Teruo Ono[3], 정종률[2], 김상훈[1†]

[1]울산대학교 물리학과
[2]충남대학교 신소재공학과
[3]교토대학교 화학연구소
[4]일본 가속기 연구소 (SPring-8)
[5]한국과학기술원 신소재공학과

중금속(heavy metal, HM)/강자성체 이중층 구조에서 중금속과 같이 스핀-궤도 결합 (spin-orbit coupling)이 매우 큰 물질에서 전류가 흐르면 스핀 홀 효과 (spin Hall effect, SHE)에 의해전자의 스핀 방향에 따라 경로가 나뉘게 된다. 이 스핀 편극된 전자가 강자성체로 주입하여스핀-궤도 돌림힘(spin-orbit torque, SOT)이 발생되고, 이를 이용하여 강자성 층의 자화를 제어할 수 있다. 나노 기술의 발전에 따라 스핀트로닉스에 주요한 자성 물질이 함께 연구가 되기 시작하였다. 자성물질은 초격자 물질, 다층 구조 물질, 수직 자화 이방성 물질 등 여러 가능성으로 연구와 특성에 대한 조사가 진행되고 있다.

최근 스핀트로닉스 분야에서 강자성 절연체(FMI)에 대한 연구가 활발히 이루어지고 있다. 강자성체/중금속 혹은 강자성체/위상절연체 이종구조에서 강자성 금속과 달리 FMI층으로의 전류흐름이 없다. 이로 인해 스핀 펌핑, 스핀 제벡 및 근접 효과 및 스핀-궤도 돌림힘 (spin-orbit torque, SOT)에 의한 다양한 현상 연구에서 스핀 전달 토크의 영향 등을 배제할 수 있다. 특히 수직자기이방성(perepndicular magnetic anisotropy, PMA)를 갖는 경우, 스핀 전류 및 비정상 홀 효과 등을 이용한 racetrack 메모리나 논리 장치의 응용성이 있다. 본 연구에서는 PMA를 갖는 FMI인 TmIG를 이용하여 HM/TmIG구조에서 SOT 스위칭 현상의 온도의존성에 대해 살펴보았다. 선행연구에서 우리는 다양한 온도에서의 X선 자기원형이색성(X-ray magnetic circular dichroism, XMCD)측정함으로써 저온에서 자화보상점(magnetic compensation point)을 갖는 TmIG의 페리자성 특성을 관측한 바 있다. 스핀 홀 각도의 부호가 다른 Pt와 W을 이용한 10 nm의 TmIG 두께를 가진 (Pt/W)/TmIG 이중층 구조에서 온도에 따른 SOT 스위칭을 특성을 관측함으로써 자화보상점 전후의 특이점 등에 대해 논하고자 한다.

Enhanced Superconductivity of Sr_2RuO_4 and $La_{2-x}Sr_xCuO_4$ Thin Films by Atomic-Scale Interface Engineering

Jinkwon Kim[1,2*], Junsik Mun[3], Youngdo Kim[1,2], Bongju Kim[1,2], Jeong Rae Kim[1,2], Lingfei Wang[1,2], Miyoung Kim[3], Changyoung Kim[1,2], Jason W. A. Robinson[4], Yoshiteru Maeno[5], Tae Won Noh[1,2]

[1]Center for Correlated Electron Systems, Institute for Basic Science (IBS), Seoul 08826, Korea

[2]Department of Physics and Astronomy, Seoul National University, Seoul 08826, Korea

[3]Department of Materials Science and Engineering and Research Institute of Advanced Materials, Seoul National University, Seoul 08826, Korea

[4]Department of Materials Science & Metallurgy, University of Cambridge, Cambridge CB3 0FS, United Kingdom

[5]Department of Physics, Kyoto University, Kyoto 606-8502, Japan

Ruddlesden-Popper (RP) phase oxides ($A_{n+1}B_nO_{3n+1}$, n = 1, 2, ...) have been spotlighted with versatile physical properties such as high-temperature superconductivity, colossal magnetoresistance. [1-2] These emergent phenomena provide a platform for novel oxide-based electronic devices including spintronics application. However, high-quality RP-phase thin film growth has been disturbed by extended structural defects, such as out-of-phase boundaries (OPBs).[3] OPB is a translational boundary between neighboring unit cells, shifted in a specific crystallographic direction. For instance, if RP-phase thin films grown on ABO_3 perovskite substrates, the structural mismatch between film and substrates induces a crystallographic shift in the *c*-axis direction, thus OPBs form at the film-substrate interface. Since OPB formation hampers the physical properties of RP-phase thin films, the suppression of the structural defects is highly required to carry out the high-performance RP-phase based functional devices.[4-5]

In this study, we suppressed OPB suppression in RP-phase oxide thin films by atomic-scale interface engineering. As model systems, the unconventional superconductor Sr_2RuO_4 (bulk T_c ~ 1.5 K) and $La_{2-x}Sr_xCuO_4$ (bulk T_c ~ 39 K) thin films were employed. Despite the structural similarities between films and substrates, Sr2RuO4 and $La_{2-x}Sr_xCuO_4$ films exhibited huge OPB formations. By controlling the atomic-scale interface engineering, the OPBs were significantly suppressed in the film structure. Notably, these OPB-free Sr_2RuO_4 and $La_{2-x}Sr_xCuO_4$ thin films exhibited highly enhanced superconductivity than the film with huge OPB formation. Our study suggests a comprehensive method to suppress OPB formation in RP thin films, enabling superconducting spintronics devices based on the unconventional superconductivity.[5-6]

References

[1] J. G. Bednorz *et al.*, *Science* **236**, 73 (1987).

[2] Y. Moritomo *et al.*, *Nature* **380**, 141 (1996).

[3] M. A. Zurbuchen *et al.*, *J. Mater. Res.,* **22**, 1439 (2007).

[4] A. Tsurumaki-Fukuchi *et al.*, *ACS Appl. Mater. Interfaces* **12**, 28368 (2020).

[5] J. Kim *et al.*, *Nano Lett.* **21**, 4185 (2021).

[6] S. B. Chung *et al.*, *Phys. Rev. Lett.* **121**, 167001 (2018).

$La_{1-x}Sr_xMnO_3/NdNiO_3$ 계면에서 $NdNiO_3$층의 두께에 따라 발현되는 전자기적 상전이 현상에 대한 연구

조하은[1*], 이종민[2], 이년종[1], 양미현[3], 이상훈[3], 심은지[4], 이상한[2†], 임규욱[3†], 김상훈[1†]
[1]울산대학교 물리학과
[2]광주과학기술원 신소재공학부
[3]포항가속기연구소 나노계면연구팀
[4]성균관대학교 지능형 팹테크 융합전공

최근 강자성/$RNiO_3$ 이종구조에서 관측된 특이현상에 대하여 산화물 계면에서의 전하 이동(charge transfer)과 오비탈의 재구성(orbital reconstruction) 관점에서 활발한 연구가 진행되고 있다. 희토류 금속과 니켈산염(nickelate)으로 구성된 $RNiO_3$는 전자 사이의 강한 결합 및 상호작용으로 인해 다양한 물리적 상전이가 발현된다. 본 연구에서는 $La_{1-x}Sr_xMnO_3$(LSMO)/$NdNiO_3$(NNO) 이중층으로 강상관계 전자 시스템을 구성하여 NNO 두께에 따른 전자기적 상전이 특성[1]에 대해 살펴보고자 한다. NNO는 $RNiO_3$ 물질 중, 상자성 (paramagnetism)에서 반강자성(antiferromagnetism)으로 전환되는 자기 상전이(magnetic phase transition)와 금속-절연체 전이(MIT, metal-insulator transition)를 함께 가지는 대표적인 물질이며, LSMO는 반금속(half metallic) 성질[2]을 가진 강자성 산화물이다.

시스템의 온도에 따른 전기적 자기적 특성을 측정한 결과 전자기적 상전이의 NNO두께 의존성이 뚜렷하게 관측되었다. 상전이 온도는 각각 자화율의 온도 의존성 곡선(*M-T* curve)에서의 Néel 온도 (T_N)와 저항의 온도 의존성 곡선 (*R-T* curve)에서의 전이 온도 (T_t) 값을 기준으로 하였다. 더하여 연 X선 흡수 분광법(XAS, X-ray absorption spectroscopy)을 이용하여 계면에서의 전하 이동 상태 변화를 직접 관측하였다. 상전이 특성의 NNO층 의존성은 NNO층 두께가 8 u.c.보다 얇아질 때 차원효과(dimensionality effect)가 나타나고, 20 u.c.보다 두꺼워지면 인장 또는 압축에 의한 변형작용이 더 지배적으로 작용한 것으로 이해할 수 있다.

References

[1] María Luisa Medarde, J. Phys.: Condens. Matter 9 1679 (1997)
[2] B Nadgorny, J. Phys.: Condens. Matter 19 315209 (2007)
[3] Torrance, J. B. et al., Phys. Rev. B 45 8210 (1992)
[4] Jian Liu et al., Nature Comm. 4 2714 (2013).
[5] Natalia Palina et al., Nanoscale 9 6094 (2017)

AI를 이용한 PEC 측정 데이터 내의 결함 검출

박덕근[1,2*], 김재민[1,5], 손대락[3], 유권상[4], 서호건[1], 김경모[1]
[1]한국원자력연구원, 덕진동 유성 34057, 대전
[2]주식회사 AIPIT , 덕진동 유성 34057, 대전
[3]주식회사 Sensorpia, 전민동 유성 34054, 대전
[4]한국표준과학연구원 , 도룡동 유성 34113, 대전
[5]신형원자력시스템공학과, 과학기술연합대학원대학교, 도룡동 유성 34113, 대전

1. PEC(Pulse eddy current) 기법은 단열재하부식(CUI) 검출에 광범위하게 적용되는 전자기 비파괴 진단법이며, 여타 전자기 비파괴 측정 방식들보다 높은 투과성을 이용해 심도깊은 비접촉식 진단이 가능하나 전통적인 측정 방법보다 분석이 어려워 더욱 신뢰성 있는 측정을 위해 더욱 많은 연구가 필요하다. PEC 측정 데이터 분석의 난해함은 검사 시간 및 비용 증가의 원인이 되며, 검사자의 경험과 직관에 대한 의존성이 커 오류 발생 가능성을 높인다. 이 문제를 해결하기 위해서는 방대한 양의 데이터를 정량적으로 분석할 수 있는 인공지능 알고리즘의 도입이 필요하며, 인공지능 도입 가능성과 방안에 대한 연구가 필수적이다. 이 연구에서는 주식회사 AIPIT사가 개발한 PEC 측정 장비를 이용해 배관을 모사한 시편 검사 데이터 취득후 AI 알고리즘을 통해 분석하였다. 시료의 두께가 얇아질수록 일반적인 방법으로는 단차간의 구분이 어려웠으며, 이를 해결하기 위해 SVM과 CNN을 도입하였다.

2. AIPIT 사가 제작한 PEC 측정 장비를 이용하여 시계열의 펄스 와전류 신호를 취득하였으며, 취득한 신호 중 실제 데이터 분석에 이용한 부분은 진폭의 변화량, 최대진폭 및 최대진폭 도달 후 진폭이 펄스 와전류 인가 전 시간으로 돌아오는데 걸린 시간이다. 시편에 PEC를 인가 후 장비의 수신 코일에는 먼저 도체 표면에서 유도된 전류가 수신되며, 그 다음 도체내 전도로 유도된 전류가 그 다음으로 감지되며, 이후로는 인가 지점에서 먼 곳에서 유도된 전류가 수신된다. 그러므로 수신된 시계열 전류 신호의 데이터의 중후반부에 도체내 발생한 결함, 도체의 두께에 정보가 있어 이를 분석해 결함 및 두께 정보를 추정할 수 있다. 보온재에 둘러싸인 배관의 내부 두께 측정이 가능한 것인지 확인해 보기 위해 다섯 개의 단차를 가진 탄소강 배관을 준비하였다. 0.5 mm 두께의 스테인레스 크래딩 안에 50 mm 두께의 플라스틱 보온재가 ASTM A106 Grade B 소재의 배관을 둘러싸고 있다. 배관의 총 길이는 1500 mm이며, 300 mm의 동일간격으로 두께가 단계적으로 일정하게 줄어들도록 제작하였다. 배관 표면부를 동경 방향 매 45도마다 분할해 8 지점 및 길이 방향으로 5개의 계단 부 및 4개의 변곡 지점 총합 9 지점을 측정 지점으로 선정하였다. 총 측정지점은 72곳이며, 각 지점에서 10회씩 총 720개의 펄스 와전류 측정을 수행하였다. 데이터의 정규화 수행을 통해 측정간에 발생한 오차 및 노이즈의 영향을 완화하였다. 잘 알려진 CNN 처리 모델 중 VGG19 및 Inception을 이용하였으며, 모델 내 Convolution 부분은 실험 데이터에 맞게 1차원으로 수정되었다. 도입한 모델 중 높은 성능을 가진 모델 및 Sampling Length를 구별하기 위한 성능 지표로 Mean Absolute Error를 기존으로 삼아 측정을 수행하였다.

3. 펄스 와전류 측정을 통해 취득한 실험 데이터의 AI를 이용한 분석을 수행해 기존 방식의 숙련자의 경험에 의존하지 않으며 인간적 오류의 영향 여지가 적은 정량적 분석을 해내는 딥러닝 모델 개발의 가능성 및 한계를 확인하였으며, 이 모델의 배관 단차 추정 성능이 통계적 방법으로 분석이 어려운 구간에서도 두께를 추정할 수 있음을 확인하였다. 또한 각 모델의 성능 특성 및 최적 작동 환경을 분석을 통해 적합한 알고리즘과 작동 환경 및 이들의 경향성을 확인하였다. Sampling Length가 길어질수록 MAE는 낮아지는 경향을 보였고, 이는 펄스 와전류 진폭이 줄어드는 양상을 충분히 반영할 수 있는 길이의 데이터를 투입하여 성능을 더욱 높일 수 있음을 의미한다.

근지구 우주환경 관측위성 탑재체용 3-축 플럭스게이트 자기센서의 개발 및 제작

김은애[2*], 홍기민[2], 손대락[1]
[1]㈜센서피아
[2]충남대학교, 물리학과

본 연구에서는 한국천문연구원에서 '근지구 우주환경 관측위성 탑재체 개발 연구' 사업의 일환으로 진행되고 있는 근지구 우주환경 탑재체 개발 미션 (SNIPE)의 탑재체의 FM 용 3-axis Flux-gate를 개발 및 제작하였다. SNIPE 위성은 4대가 편대로 비행을 하며, 자기장의 경우 근지구 우주환경의 자기장 분포와 시간에 따른 자기장 변화를 관측한다. 탑재되는 자력계의 경우 요구조건이 입력전압 +5 V, 소비전력 2 W 미만, 측정범위가 ±60,000 nT, 자기잡음이 1 Hz bandwidth에서 1 nTrms 이하를 요구하고 있다.

자력계의 구조는 아날로그부 전자회로보드 1장과 디지털부 전자회로보드 1장, 3-축의 flux-gate sensor 2개로, 동시에 2개의 MAG가 구동되도록 설계하였다. 2개의 MAG가 동시에 구동되도록 설계한 이유는 내부에서 발생되는 주변환경자기장을 보상하고, 1개의 MAG에 이상이 생겼을 시를 대비하기 위함이다.

Fig. 1-(a)는 SNIPE 위성의 3차원 조감도이다. Fig. 1-(b)는 본 연구에서 개발 및 제작한 자력계의 구조도로 대각선 위치에 3-축 센서가 각각 1개씩 배치되어 있다. Fig. 1-(c)는 제작된 자력계의 선형도를 비자성실험실에서 3-축 Helmholtz coil 장치로 측정한 결과로 선형도가 0.05% 이상이었다. Fig. 1-(d)는 자기잡음 특성으로 자력계를 차폐율이 80dB 이상인 자기차폐장치에 넣어서 측정한 결과이다. 자기잡음의 크기는 1 Hz bandwidth에서 rms 값이 0.5 nT 이하로 측정되었다.

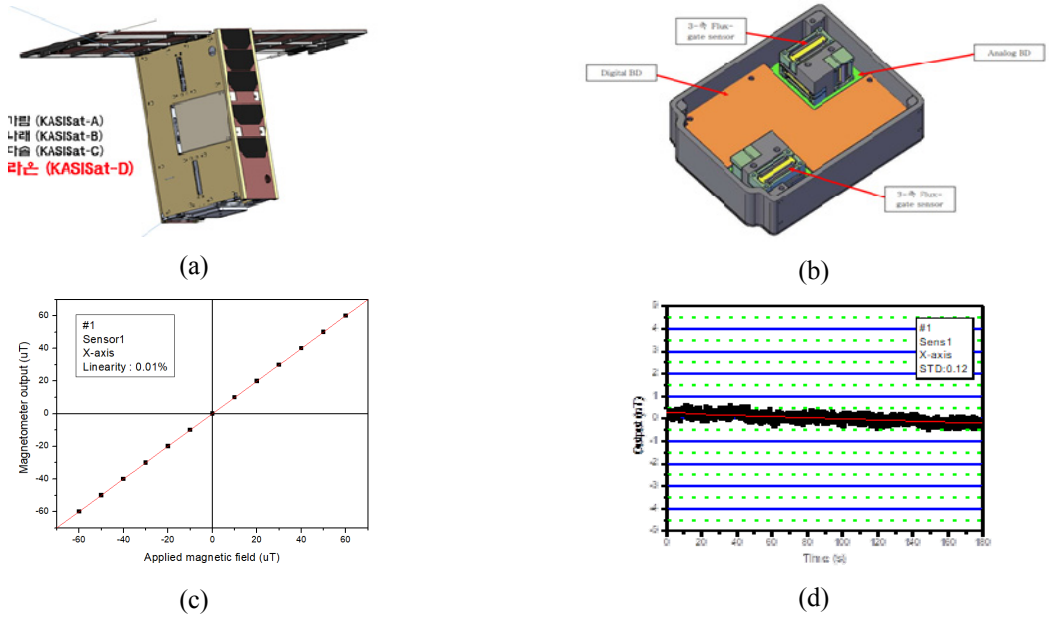

(a) (b)

(c) (d)

Fig. 1. (a)위성전체구조, (b)자력계의 내부구조, (c)자기센서 선형도 (d)자기센서 noise level.

Reference

[1] 손대락, "NEXTSat-1용 TAM 제작에 관한 연구", 한국자기학회지, pp.106-107 (2014)

Electrical and magnetic properties of in-plane graphene/graphene oxide junction devices

Eun Hee Kee[1*], DaYea Oh[1], Minjeong Shin[1], Woohyeon Ryu[1], Duc Minh Tran[1], Mohd Musaib Haidari[1], Ji Hye Lee[2,3], Jin Sik Choi[1], and Bae Ho Park[1†]

[1]Division of Quantum Phases & Devices, Department of Physics, Konkuk University, Seoul 143-701, Korea

[2]Department of Physics, Seoul National University, Seoul 08826, Korea

[3]Center for Correlated Electron Systems (CCES),Institute of Basic Science (IBS), Seoul 08826, Korea

E-mail address: *baehpark@konkuk.ac.kr

In the past decade, the study of graphene has been tremendously exploited due to its phenomenal physical and electromagnetic properties such as high flexibility, high thermal conductivity, high electron mobility and long spin diffusion length. Especially, research using long spin life-time and spin diffusion length of graphene have been extensively investigated for the application to spintronics. However, low spin-injection efficiency (~1%) of graphene is an obstacle to realize for spintronic devices. Recently, there have been reports to overcome this problem by using insulating oxide films or a material which has a similar hexagonal lattice constant of graphene such as Ni (111) between the ferromagnetic electrode and graphene. Also, it has been known that a magnetic exchange field (MEF) induced by a magnetic insulator adjacent to graphene can effectively control local spin generation and spin modulation in a 2D device without modulating the structural properties of the material.

In this study, we fabricated graphene (G) / graphene oxide (GO) junction devices in which GO was formed by oxidation technique by applying ultraviolet(UV) light, directly. One of the shortcut to fabricate large area GO, which can make the process of fabrication device easy, minimizing contamination on graphene surface is using ozone induced by UV light. We examined the proximity effect of GO adjacent graphene in the transport of this G/GO heterostructure device with external magnetic field. We showed that week localization and Shubinikov-de Haas oscillations were larger than that of pristine graphene. And we measured magnetoresistance(MR) that revealed negative MR at low temperature in this G/GO heterostructure device. We expect the ferromagnetic properties of GO improve the spin-orbit coupling of the graphene.

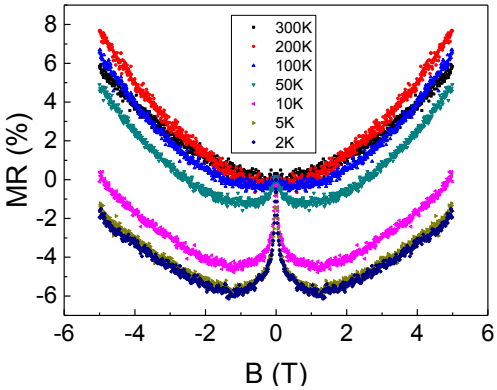

Fig. 1. Magnetoresistance (MR) VS Magnetic field
MR (%) = {Rxx(B)-Rxx(B=0)/Rxx(B=0)}*100,
graph shows enhanced weak localization effect at low temperature.

LM02

Neutron scattering for large-area 2D magnetic materials

June Hyuk Lee*
Korea Atomic Energy Research Institute, Daejeon, Korea

2D magnetic materials have attracted attention as a material for next-generation spintronic and magneto-optical devices. These technological applications require the large-area synthesis and characterization of high crystalline ultrathin films. Recently the family of Fe-based 2D magnetic materials has been fabricated in wafer-scale by molecular beam epitaxy. These 2D materials exhibit Curie temperatures at or above room temperature along with various magnetic effects. To analyze the magnetic structure of large-area ultrathin samples, neutron scattering, especially reflectivity can be useful because of its large beam size and magnetic sensitivity. This can be achieved by transferring 2D van der Waals materials on top of substrate with additional layers, which amplify the reflectivity from ultrathin film. In this presentation, molecular beam epitaxy for large-area 2D magnetic materials and neutron reflectivity analysis will be discussed.

Anomalous Hall and Nernst effect in a few to bulk layer 2D van der Waals ferromagnetic material Fe_3GeTe_2

Pradeep Raj Sharma[1*], Tae Wan Kim[2,3], Hwayong Noh[1†]

[1]Department of Physics and Astronomy, Sejong University, Seoul, Korea

[2]Department of Nano and Advanced Materials Engineering, Sejong University, Seoul, Korea

[3]Nanogate, Cheorwon, Gangwon-do, Korea

[†]Corresponding author e-mail: hnoh@sejong.ac.kr

Two-dimensional (2D) van der Waals (vdW) ferromagnetic materials have emerged as promising candidates and are recently providing a huge platform for the study of spin-related phenomena and their potential applications. Here we report the thickness and temperature-dependent anomalous Hall and anomalous Nernst effect in h-BN/FGT/SiO_2 van der Waals heterostructures. Interestingly, we have observed the polarity reversal of AHE in a thin flakes of FGT ~15 nm. The anomalous Hall and Nernst effects in a few-layer FGT flake show single domain magnetic structure with nearly square-shaped hall signals and large coercivity, indicating strong perpendicular magnetic anisotropy (PMA). On the other hand, thick (bulk) FGT shows gradual switching with the magnetic field evolution, indicating the presence of multi-domain structures and demonstrate weak PMA. The variation of Curie temperature (T_C) and H_C with a flake thickness are also presented.

A Study on Increasing the Useful Field of View by Minimizing the Edge Effect of Gamma Camera

Hyeon Jeong Yang[1], Ji Eun Jeong[1], Hye Ri Shin[1], Su Rim Lee[1], Seung-Jae Lee[1,2*]
[1]Department of Radiological Science, Dongseo University, Korea
[2]Center for Radiological Environment & Health Science, Dongseo University, Korea

It is intended to increase the detection area by minimizing the phenomenon that the uniformity is lowered at the edge of the scintillator of the gamma camera. The light generated by the interaction between the scintillator and gamma rays is reflected or blocked from the side of the scintillator, resulting in a phenomenon in which the uniformity of the edge portion is deteriorated. To minize this, a gamma camera was designed by placing the optical sensor on the side of the scintillator. A gamma camera was designed using the DETECT2000 simulation tool capable of simulating the movement of light, and a flood image was acquired by generating a gamma ray event at the edge and the entire detection area. The acquired flood image was compared and analyzed with the flood image acquired by a general gamma camera. In general, in a gamma camera with an optical sensor on the bottom, a phenomenon in which the position of a gamma ray event generated at the edge cannot be distinguished occurs, resulting in a decrease in the detection area and a decrease in uniformity. On the other hand, the gamma camera designed by adding an optical sensor to the side of the scintillator showed an increase in the detection area by distinguishing gamma ray events at the edge. A gamma camera was designed that improved the detection area by adding an optical sensor to the side of the scintillator. As a result, the uniformity was improved and the detection area was increases compared to the general gamma camera. When this gamma camera is used for clinical application, it is considered that the imaging area will be expanded without deterioration of uniformity.

Acknowledgments: This work was supported by the Korea Foundation for the Advancement of Science & Creativity (KOFAC), and funded by the Korean Government(MOE).

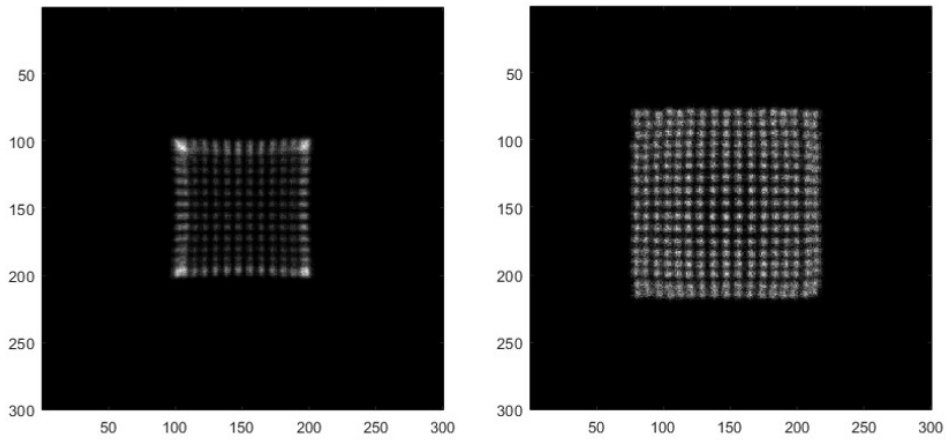

Bottom sensors　　Bottom + Side sensors

Fig. 1. Flood image acquired when a gamma ray event is generated at 3 mm intervals. Left: gamma camera with bottom sensors, Right: gamma camera with bottom and side sensros.

A Study on the magnetic field of eddy current caused by the rolling of the Ship

Sang Hyeon Im*
Dong Eui University, Korea

In warships made of ferromagnetic materials, permanent magnetic fields generated during the manufacturing process, induced magnetic fields due to changes in the Earth's magnetic field, and eddy current magnetic fields due to fluctuations of underwater bodies are generated. The above magnetic fields cause damage by magnetically sensitive mines using high-sensitivity magnetic field sensors equivalent to thousands to tens of thousands of the earth's magnetic field.[1] In order to remove the permanent and induced magnetic fields that account for the majority of the above magnetic fields, research on demagnetization and devices to reduce the permanent and induced magnetic fields of ships is being actively conducted, and damage caused by mines is effectively reduced by reducing the magnetic field of underwater vehicles. [1][2][3]

However, the relative weight of the eddy current magnetic field is increasing as the permanent and induced magnetic fields are reduced through demagnetization and demagnetization processes. Therefore, in order to prevent damage to the ship by mines, it is necessary to predict the eddy current magnetic field generated by the fluctuation of the ship and generate a magnetic field to offset it. However, if the correct offset current is not passed, the magnetic field measured from the outside becomes larger, which may increase the possibility of damage. In order to prevent such a situation, it should be possible to accurately measure the eddy current when the ship fluctuates. Therefore, it is necessary to quickly and accurately respond to the generated eddy current magnetic field, so immediate calculation by formulas rather than FEM simulation analysis is required.

In this paper, the formula for calculating the eddy current in the equivalent model of the ship is summarized. In addition, the eddy current calculation method was verified by simulating the ship's fluctuations through the 2D FEM program, analyzing the eddy currents generated accordingly, and comparing the analyzed results with the calculated results.

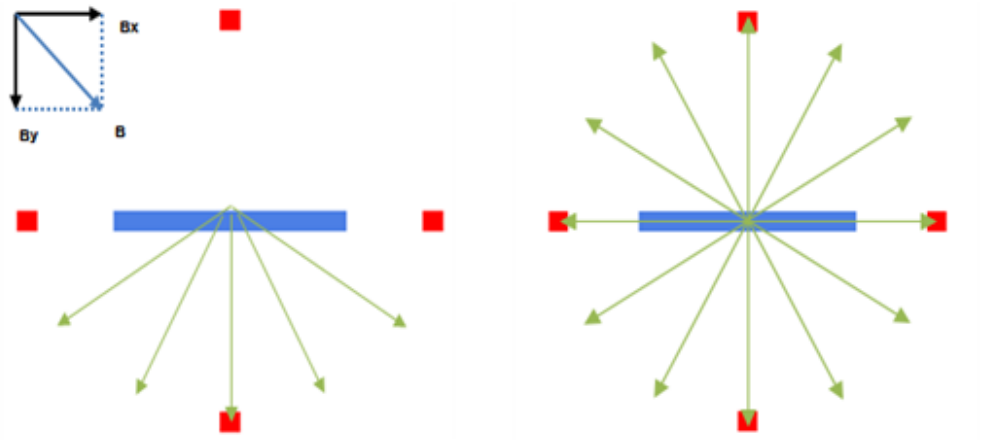

(a) Rolling simulation modeling (b) Revised modeling

Fig. 1. Rolling simulation modeling in warships

Lunar Magnetic field investigations of Korea Pathfinder Lunar Orbiter

Ho Jin[1*], Khan-Hyuk Kim[1], Derac Son[2], Hyojeong Lee[3], Jehyuk Shin[1], Eunae Kim[2]
[1]School of Space Research, Kyung Hee University, Korea
[2]Sensorpia Inc, Korea
[3]NARA Space Technology, Korea

Korea Pathfinder Lunar Orbiter (KPLO) is the first Korean Lunar exploration mission. Kplo-MAGnetometer (KMAG) is one of the scientific instruments of KPLO set to be launched in 2022. Its scientific objectives are the investigations of the lithospheric magnetism of the Moon and measure the electromagnetic wave properties near Moon's orbit space.

KMAG consists of three fluxgate magnetometers on a 1.2 m long boom. The three magnetometers are used for scientific measurements, redundancy checks, and multi-sensor technical investigation. The magnetometers and an inner Anisotropic Magneto-Resistive sensor perform simultaneous sampling to correct for the magnetic field interference caused by the spacecraft. The fully integrated flight model assembly showed that the magnetometer noise level was less than 30 pT Hz−1/2 at 1 Hz and stability was within ±0.2 nT at the 10 Hz sampling rate. This paper describes the configuration and performance of the KMAG using the multi-sensing method. The KMAG will be able to contribute to multi-site in-situ measurements of the lunar magnetic field with others lunar mission during KPLO operation phase. We expect that the KMAG will provide an up-to-date lunar observation data set and an opportunity to perform the multi-sensor observation.

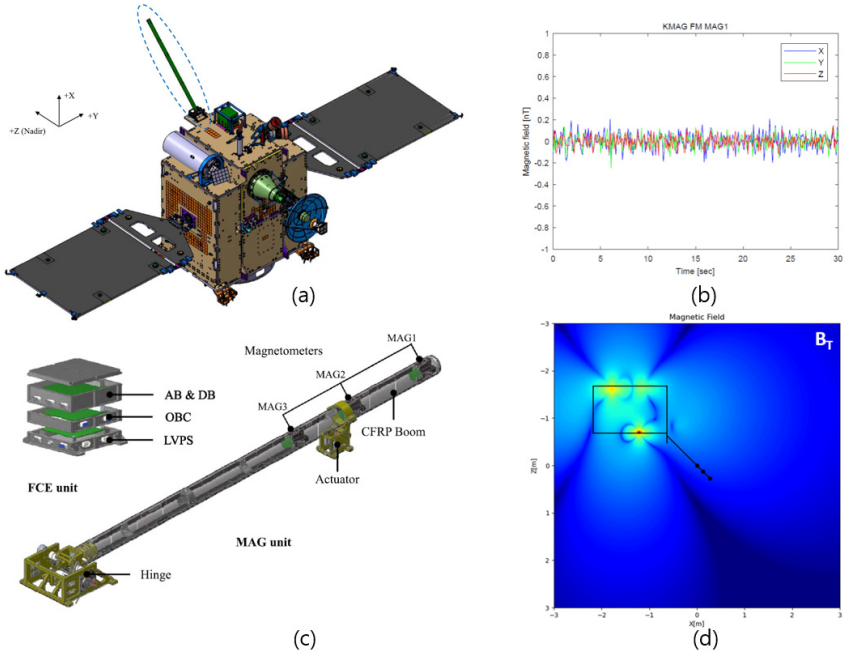

Fig. 1. KMAG instrument of KPLO. (a)KPLO, (b) Magnetometer stabilities, (c) KMAG configuration, (d) simulation of spacecraft interference.

Quantitative iDPC-STEM observations of oxygen octahedral connectivity control at perovskite oxide interfaces via epitaxial strain engineering

Junsik Mun[1,2†], Eun Kyo Ko[1,3†], Tae Won Noh[1,3*], and Miyoung Kim[1,2*]

[1]Center for Correlated Electron Systems, Institute for Basic Science (IBS), Seoul 08826, Republic of Korea

[2]Department of Materials Science and Engineering and Research Institute of Advanced Materials, Seoul National University, Seoul 08826, Republic of Korea

[3]Department of Physics and Astronomy, Seoul National University, Seoul 08826, Republic of Korea

[†]These authors contributed equally.

[*]twnoh@snu.ac.kr, and mkim@snu.ac.kr

Since the oxygen octahedral rotation (OOR) of ABO_3 perovskite oxide provides various functionalities, controlling the OOR plays an important role in device applications development and fundamental physics exploration. One of the most efficient ways to control the OOR is using the oxygen octahedral coupling at heterointerfaces which have two different structural symmetries. [1] Thanks to the interfacial coupling, structures that cannot be accessed in bulk can be realized in thin films. [2-4] For exploring further functionalities, investigating and engineering the length-scale of the interfacial coupling is an important issue. However, precise length-scale and control method of the oxygen octahedral coupling remain open questions.

Here, we made $SrRuO_3/SrTiO_3$ (SRO/STO) heterostructure on various substrates by pulsed laser deposition and succeeded controlling the length-scale of the oxygen octahedral coupling via epitaxial strain. Since SRO has $a^-b^+c^-$ (in pseudo-cubic notation) and STO has $a^0a^0c^0$ rotating pattern, we could observe how the $a^0a^0c^0$ symmetry of STO penetrates into SRO. The precise OOR angle depending on the each atomic layer was investigated using integrated differential phase contrast-scanning transmission electron microscopy (iDPC-STEM) technique. We found that the critical thickness for saturated OOR angle is engineered via epitaxial strain from 3 unit cells to 13 unit cells of SRO. This study provides an effective method to control the oxygen octahedral interfacial coupling, and suggests a potential model system for investigating how the interfacial coupling occurs between the two different symmetries.

References

[1] J. M. Rondinelli et al., MRS Bulletin 37, 262 (2012)

[2] T. H. Kim et al., Nature 553, 68 (2016)

[3] J. R. Kim et al., Nature Communications 11, 4944 (2020)

[4] S. G. Jeong et al., Advanced Science 7, 2001643 (2020)

신호 비율을 통한 디지털 위치 및 깊이 정보 측정 양전자방출단층촬영기기 검출기 개발

이승재[1,2], 백철하[3*]
[1]동서대학교 방사선학과
[2]동서대학교 방사선보건환경연구센터
[3]강원대학교 방사선학과

Positron emission tomography (PET)의 공간분해능 향상과 검출기의 섬광 픽셀의 디지털 좌표 획득을 위한 새로운 검출기를 설계하였다. Field of view (FOV) 외곽에서 발생하는 parallax error로 인한 공간분해능 저하현상을 해결하기 위해 반응 깊이를 측정하는 방법을 개발하였으며, 이는 디지털 좌표 획득과 함께 이루어졌다. 섬광 픽셀의 디지털 좌표 획득과 두 층의 반응 깊이를 측정하기 위해 4 × 4 × 2의 GAGG 섬광체를 사용한 검출기를 DETECT2000 시뮬레이션 툴을 통해 설계하였다. 모든 섬광 픽셀에서 감마선 반응을 일으켜 4 × 4 배열의 SiPM 픽셀에서 신호를 획득하였다. 16채널의 광센서 신호는 4개 채널의 신호로 감소시켰으며, 이를 각 신호의 비율로 계산하였다. 모든 섬광 픽셀에서의 신호의 비율을 획득하였으며, 이를 통해 새로운 위치에서 발생된 감마선 반응에 의한 신호의 비율과 비교하여 위치를 디지털 좌표로 획득하였다. 섬광체와 감마선이 반응한 층과 섬광 픽셀의 디지털 좌표의 획득 정확도를 평가하기 위해, 각 섬광 픽셀의 전체 길이에 대한 감마선 반응을 발생시켜 신호를 획득하였다. 0.1 mm ~ 19.9 mm까지 0.2 mm 간격으로 감마선 반응을 발생시켰으며, 획득한 신호를 사전에 획득한 각 섬광 픽셀의 신호와 비교하여 X, Y, Z 축에 대한 위치 측정 정확도를 평가하였다. X, Y 축에 대한 정확도는 모두 완벽한 결과를 보였으며, Z축에 대해서는 91.46%의 정확도를 보였다.

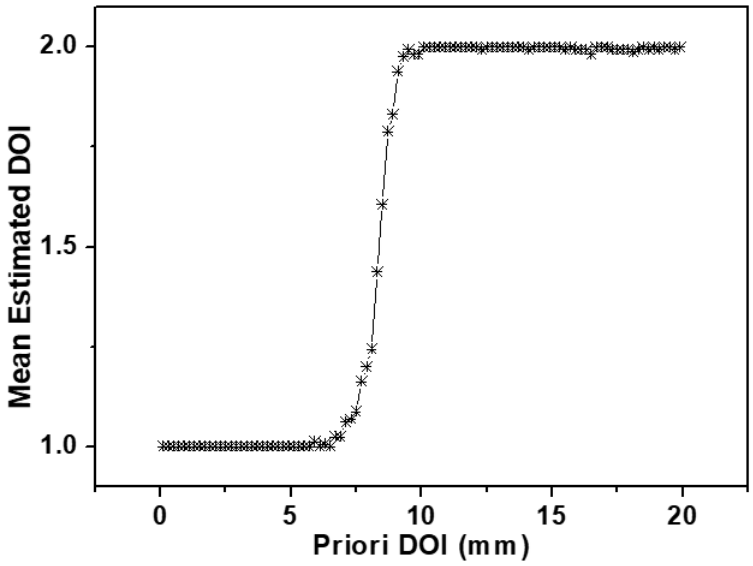

Fig. 1. DOI positioning results in each crystal layer. The horizontal axis is the true position from simulation input, and the vertical axis is the mean estimated position for different true positions.

비접촉식 3D 자기장 스캐너

김이슬, 김선규, 손무근, 박세준, 김상우, 김종민*, 양현식†, 박병열, 고재생
파인원 주식회사, R&D Center, 서울특별시, 대한민국

자속선은 자기장의 방향과 세기를 나타내는 가상의 선으로, 자속밀도(Magnetic Flux Density)는 균일하게 자화된 재료에서의 단위 면적당의 자속, 자속의 방향과 수직인 단위 면적당 자속선의 수를 의미하여 자계의 세기를 측정하는데 사용하고 있으며, 가우스 미터로 자속밀도를 측정할 수 있다.

현재, OLED 디스플레이의 화소를 생성해 주는 증착기(Evaporator)는 6.5세대 Half (1,500mm x 900mm)가 주력이며, 메탈 마스크(Metal Mask)의 처짐을 해결하기 위해 영구 자석이 일정하게 배열된 마그넷 플레이트가 사용되고 있다.

기존에는 영구 자석이 배열된 마그넷 플레이트의 자속 밀도를 측정하기 위해서 가우스 미터를 이용하여 각 포인트 마다 수작업으로 일일이 측정을 진행하였고, 그로 인해 위치 및 작업자 별 측정값의 부정확성, 많은 시간 소요, Data 의 낮은 신뢰도, 등의 다양한 문제가 발생하여, 측정값의 신뢰도가 하락하였고, 최근 8.5세대 OLED 디스플레이의 개발이 대두된 상황에서 지속적으로 마그넷 플레이트의 크기는 증가할 것으로 예상되므로, 비접촉식 3D 자기장 스캐너의 필요성이 절실해지고 있는 상황이다.

본 발표는 비접촉식 3D 자기장 스캐너의 자속밀도 측정값의 정확도를 확인하기 위해 전사모사(FEMM4.2)를 통한 영구자석 배열 시뮬레이션을 진행하였고, 시뮬레이션 결과를 토대로 Test 용 마그넷 플레이트 실물을 제작하였다. 제작된 Test 용 마그넷 플레이트는 비접촉식 3D 자기장 스캐너로 측정을 진행하여 x, y, z 축의 가우스 값을 비교하였다.

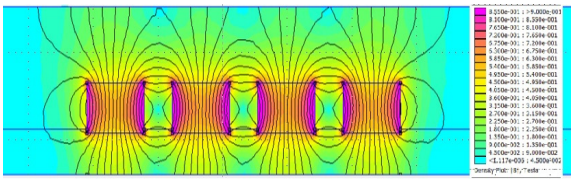

그림 1. 전산모사를 통한 영구자석 배열

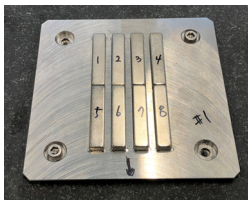

그림 2. Test용 마그넷 플레이트 실물

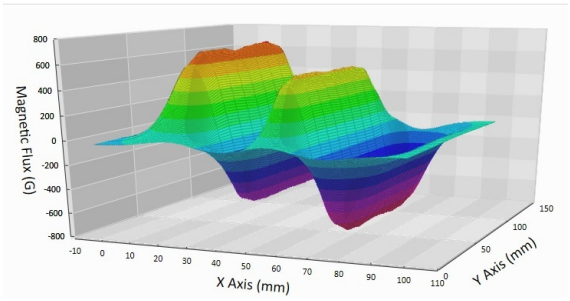

그림 3. Test용 마그넷 플레이트의
3D 자기장 측정(Z축)

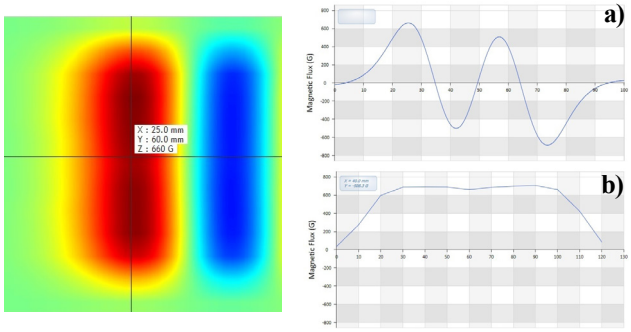

그림 4. 위치 별 자속 밀도(G) 값,
a)는 x축 b)는 y축의 가우스 값

Acknowledgement: The research was supported by a grant (S3040790) from Ministry of SMEs and Startups in 2021.

MS01

Analysis of Commercial Fluoride-containing Mouthwashes for Children Using Nuclear Magnetic Resonance Spectroscopy

Yu-Rin Kim[1], Seoul-Hee Nam[2*], and Man-Seok Han[3*]

[1]Dept. of Dental Hygiene, Silla University, Busan, Korea

[2]Dept. of Dental Hygiene, Kangwon National University, Korea

[3]Dept. of of Radiological Science, Kangwon National University, Korea

[*]These authors contributed equally to this work

Fluoride-containing mouthwash easily used at home are preferred. Children under the age of 6 have difficulty gargling, so when using fluoride-containing mouthwash, fluoride may remain in the oral cavity and may even be swallowed. Therefore, this study measured the total fluoride (TF) of mouthwash for children containing fluoride sold in Korea using Fluorine (^{19}F) Nuclear magnetic resonance (NMR) spectroscopy and confirmed the amount of fluoride remaining in the saliva of the oral cavity after using mouthwashes.

In this result, the fluoride content of 2080 Kids was 90ppm, but the detected TF was about 29% less. The fluoride content indicated in Chikachika was 226ppm, but the average TF was about 32% less. On the other hand, in the case of Garglin Kids Care marked as 226.1ppm, TF was 102% more. After 2 minutes of using mouthwash, very little fluoride was present in the oral saliva in all three types of mouthwashes.

So, there was no possibility of exposure to side effects. Therefore, fluoride-containing mouthwash is a safe method of preventing dental caries for children under six who have difficulty brushing teeth. Therefore, this study confirmed the mouthwash has no effect on the human body as toxicity even when children swallow the fluoride remained in the saliva after using fluoride-containing mouthwash for children. In conclusion, for children under the age of 6 who have difficulty brushing their teeth, mouthwash containing fluoride can prevent dental caries and contribute to oral health.

High-Energy Electromagnetic Wave Radiation Analysis Study of Laboratories Using Digital Medical Imaging Devices

Chang Gyu Kim*
Department of Radiological Science, Gimcheon University, Gyung Sang Buk - Do, South Korea

Abstracts Devices that acquire digital medical images using radiation (DR; Digital Radiography) are widely used in medical institutions to obtain information necessary for patient diagnosis. Compared to the existing film-sensitization method and computerized radiography system (CR, computed radiography system) method, digital medical imaging radiation generator has advantages such as image processing speed, diverse image parameters, image quality improvement through utilization, wide dynamic range, image post-processing method to remove noise from output instability, and artifact correction. This study was conducted to measure the 3-month cumulative dose of the radiation protection facility shielding wall of the radiation generating device that acquires digital medical images using a glass dosimeter for environmental monitoring, and to improve the diagnostic radiation safety management method by comparing it with foreign standards and to present it as basic data for education.

In this study, DK medical system Innovision (Ceiling Type - ELIN T5) was used to measure the radiation dose of the digital medical imaging radiation generator examination room protection wall [Figure 1]. Innovision device is a device that can quickly check a clear image with a low radiation dose and can be used easily and safely. This device is widely used as a device that supports conversion of standard medical images.

By selecting 3 hospitals that perform more than 50 digital X-ray medical imaging tests per day, a glass dosimeter for environmental measurement was installed outside the protection wall of the examination room, and the leakage radiation dose was measured for one month from May 16 to June 21, 2021.

The glass dosimeter was installed at 150 - 190cm from the floor considering the safety of the patient entrance and exit door, the entrance door of the digital medical image acquisition radiation generator control room, the shielding wall, and the patient viewing window based on the medical image X-ray examination room.

To measure and evaluate the shielding efficiency of the patient viewing window, multiple glass dosimeters were installed inside and outside the laboratory to measure environmental radiation dose and verify statistical significance. The dosimeter recovered after measurement was delivered by air to Chiyoda Technol, Japan, without the procedure of passing the X-ray screening station, and the results were analyzed. By multiplying the measurement result by a factor of 3, a comparative analysis was performed with the Japanese medical radiation safety management standard.

Using a glass dosimeter, the cumulative leakage dose from the shielding wall, entrance, and patient viewing window of the digital medical image acquisition radiation generator examination room was measured and analyzed for 3 months.

The 1cm dose equivalent value of the glass dosimeter accumulated for 3 months was 0.96mSv at the maximum and 0.18mSv on average at the outer side of the shielding wall at the entrance of the digital medical image acquisition radiation generator examination room. In addition, the cumulative dose equivalent of 1 cm in the glass dosimeter for 3 months outside the shielding wall on the control room showed a maximum of 3.03

mSv and an average of 0.41 mSv.

At the outside of the entrance to the patient waiting room for the digital medical image acquisition radiation generator examination room, the glass dosimeter accumulated dose equivalent of 1 cm for 3 months was maximum of 8.31 mSv and average of 2.09 mSv. Also, outside the entrance to the control room, in 3 months, the cumulative dose equivalent of 1 cm in the glass dosimeter showed a maximum of 14.04 mSv and an average of 3.84 mSv.

It is expected that these research results can be used as basic data for conducting medical radiation safety management in the future. In addition, it is expected that it will be greatly useful in setting measurement methods and regulatory standards for environmental radiation safety management of medical radiation generators [Table1].

It is proposed to continue research at the national level by expanding to all medical institutions distributed throughout the country on the shielding wall performance of diagnostic radiation shielding facilities.

Fig. 1. Digital medical image acquisition radiation generator

Table 1 Digital medical image radiation generator examination room shielding wall dose analysis result

Examination Room	Entrance Shielding Wall	Control Room Shielding Wall
1	-	-
2	-	0.24
3	0.96	-
4	0.57	-
5	-	3.03
6	-	0.33
7	-	0.30
8	-	0.18
9	0.30	-
10	-	-
Average	0.18	0.41

Effects of Pulsed Electro-Magnetic Fields on Dry Eye Syndrome

Subin Park*, Hyunseon Yu, Donghwan Ko, Sangmin Shim and Byungjo Jung
Yonsei Univ. Biomedical Engineering, Korea

Pulsed Electro-Magnetic Fields (PEMF) is known as a technology used in clinical trials for the purpose of pain control and treatment due to its non-invasive, safe, and convenient use. PEMF has been found to affect physiological processes such as increased cell activity, depolarization of cell membranes and changes in membrane potential, improvement of inflammation, and improvement of blood flow, but the specific mechanism is not clearly defined. Pulsed electromagnetic fields (PEMFs) are emerging as innovative therapies for the control of inflammation that can significantly affect tissue regeneration. [1]

Dry eye syndrome is a disorder of the tear film caused by insufficient or excessive evaporation of tears, which causes damage to the ocular surface between the eyelids and is associated with symptoms of ocular discomfort. The causes of dry eye syndrome are diverse, including aging, chronic conjunctivitis, decreased female hormones, and environmental factors. Among them, we focused on dry eye syndrome caused by chronic conjunctivitis. When cells that function as mucous glands in the conjunctiva decrease due to chronic inflammation, mucus secretion decreases. As a result, water cannot be held in the mucus layer, and the aqueous layer of the tear layer flows out through the tear duct into the nose. [2] In this study, we tried to observe the improvement effect of dry eye syndrome through stimulation of PEMF.

This study was conducted with an approval from the Institutional Review Board at the Mirae campus of the Yonsei University (Protocol 1041849-202101-BM-019-03). Experiment was conducted on 9 subjects with dry eye syndrome in their 20s. The subjects had previously been diagnosed with dry eye syndrome or had been diagnosed with conjunctivitis or the like. It was observed continuously for 5 days, and PEMF (20Hz, 7mT) equipment was worn under the eyelids for 30 minutes every day. Dry eye examination was performed at the hospital on the 1st and 5th days. There are two tests for dry eye syndrome, Break-Up Time test and Schirmer test. [3] Schirmer Test (ST) measures the amount of tears secreted in 5 minutes by hanging a piece of paper of a certain length on the lower eyelid. Break-Up Time (BUT) test measures the time it takes for the tear film to break through an ophthalmic microscope and fluorescein. Subjective evaluation of subjects through a survey was also carried out.

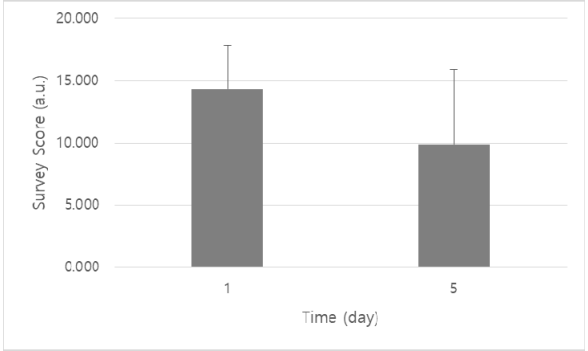

Fig. 1 Survey results according to PEMF stimulation

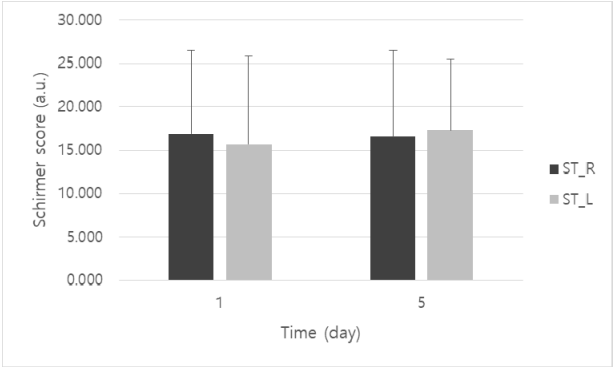

Fig. 2 Schirmer test results according to PEMF stimulation

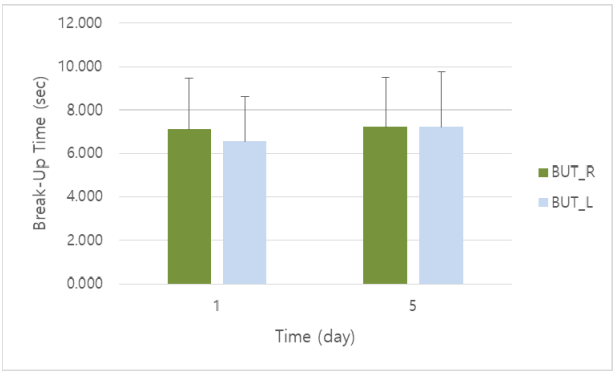

Fig. 3 Break-Up Time test results according to PEMF stimulation

In the survey, it showed a decrease of 31.008% from 14.333 points to 9.898 points on average, and 7 out of 9 people showed a subjective improvement effect. In ST, 4 out of 9 patients showed an increase in tear volume in the left and right eyes. In BUT test, 3 out of 9 subjects increased the BUT value 5 days after PEMF stimulation. It was confirmed that all three people with improved BUT showed an improvement effect in the survey and ST.

The results of this study may be of limited improvement in subjects with chronic conjunctivitis. It seems that long-term monitoring for improvement of dry eye syndrome is necessary, and additional research on this is also required.

References

[1] Christina L. Ross, Yu Zhou, Charles E. McCall, “The use of Pulsed Electromagnetic Field to Modulate Inflammation and Improve Tissue Regeneration: A Review”, Bioelectrocity, 1.4, 2019

[2] MA Lemp, GN Foulks, “The definition and classification of dry eye disease”, The Ocular Surface, 2007 tearfilm.org

[3] AJ Bron, “Diagnosis of dry eye”, Survey of ophthalmology, 2001

Evaluation of low-dose lung computed tomography (CT) using deep-learning: A phantom study

Daehong Kim[1], Kihong Son[2], Sooyeul Lee[2], Cheol-Ha Baek[3], Pil-Hyun Jeon[4*]

[1]Department of Radiological Science, Eulji University, Seongnam 13135, Republic of Korea

[2]Medical Information Research Section, Electronics and Telecommunications Research Institute, Daejeon 34129, Republic of Korea

[3]Department of Radiological Science, Kangwon National University, Samcheok 25949, Republic of Korea

[4]Department of Diagnostic Radiology, Yonsei University Wonju College of Medicine, Wonju Severance Christian Hospital, Wonju 26426, Republic of Korea

The aim of this phantom study was to evaluate the image quality of low-dose lung computed tomography (CT) achieved using a deep-learning based image reconstruction method. The chest phantom was scanned with a tube voltage of 100 kV for various CT dose index (CTDIvol) conditions: 0.4 mGy for ultra-low-dose (ULD), 0.6 mGy for low-dose (LD), 2.7 mGy for standard (SD), and 7.1 mGy for large size (LS). The signal-to-noise ratio (SNR) and noise values in reconstructions produced via filtered back projection (FBP), iterative reconstruction (IR), and deep convolutional neural network (DCNN) were computed for comparison. The quantitative results of both the SNR and noise indicate that the adoption of the DCNN makes the image reconstruction in the ULD setting more stable and robust, achieving a higher image quality when compared with the FBP algorithm in the SD condition. Compared with the conventional FBP and IR, the proposed deep learning-based image reconstruction approach can improve the ULD CT image quality while significantly reducing the patient dose.

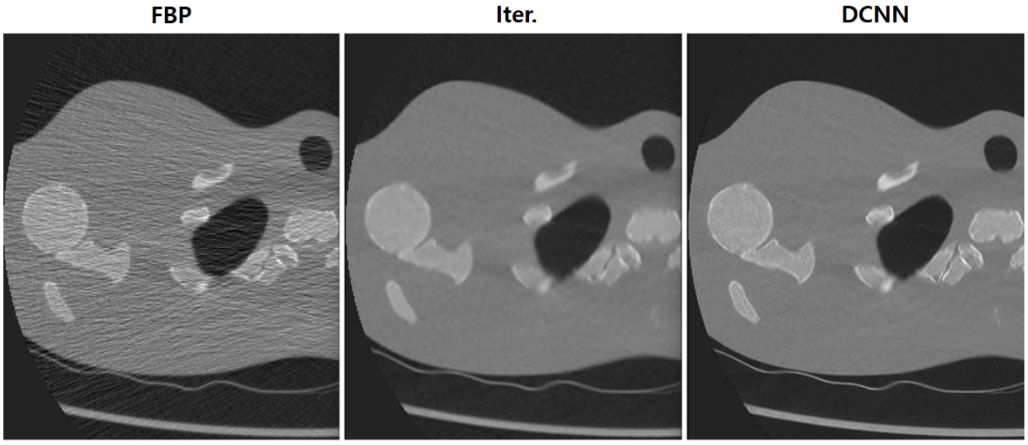

Fig. 1. Reconstructed images of the upper lung produced through filtered back projection (FBP), iterative reconstruction (IR), and deep convolutional neural network (DCNN) under a CTDIvol of 0.4 mGy for ultra-low-dose (ULD) CT

Optimization of the Design Parameters for a Thyroid Care Nuclide Monitoring Diverging Collimator using Monte Carlo Simulation

Dong-Hee Han[1,5], Seung-Jae Lee[2], Jang-Oh Kim[3], Hak-Jae Lee[4], and Cheol-Ha Baek[5,6*]

[1]Deparment of Medical Health Science, Kangwon National University, Samcheok 25949, Republic of Korea

[2]Deparment of Radiological Science, Dongseo University, Busan 47011, Republic of Korea

[3]Institute of Health Medical Education Research, Kangwon National University, Samcheok 25949, Republic of Korea

[4]ARALE Laboratory Co., Ltd., Seoul 02843, Republic of Korea

[5]Center for Radiological Science and Technology, Kangwon National University, Samcheok 25949, Republic of Korea

[6]Deparment of Radiological Science, Kangwon National University, Samcheok 25949, Republic of Korea

본 연구의 목적은 ^{131}I 동위원소에 대응하기 위한 방사선 모니터링 전용의 확산형 콜리메이터를 개발하는 것이다. 이를 위해 몬테카를로 시뮬레이션 툴 중 하나인 GATE를 이용하였으며 변수에 대한 성능을 비교하여 최적화 과정을 진행하였다. 이때 검출부는 50.0 × 50.0 × 3.5 mm^3 크기의 GAGG이며 0.7 × 0.7 mm^2 픽셀로 구성된다. 모든 변수에서 점선원 위치 판독을 위한 반치폭 하한을 약 3.0 mm로 설정하였고 결과의 정확성을 높이고자 에너지 창을 10%로 입력하였다. 실험 결과, 투과로 인해 발생되는 영상의 허상을 제거하기 위한 최소 콜리메이터 높이는 45.0 mm이고 범용의 경우, 높이 50.0 mm, 구멍 크기 1.0 mm, 격벽 두께 0.4 mm로 최적화 설계변수가 산출되었으며 이때 반치폭은 3.06 mm이다. 또한 같은 확대 인자 조건 하에 핀홀 콜리메이터와 성능을 비교하였을 때, 관심영역 내 점선원의 위치에 관계없이 일정한 성능을 보이는 것을 확인하였다.

핵심단어: ^{131}I, 방사선 모니터링, GATE, 확산형 콜리메이터

5Hz 고빈도 반복 경두개자기자극과 결합된 신경근 전기자극치료가 만성 뇌졸중 환자의 대뇌 활성도에 미치는 영향

마성룡[1*], 정중우[2], 송보경[3]
[1]조선대학교 작업치료학과
[2]보바스기념병원
[3]강원대학교 작업치료학과

본 연구는 5 Hz 고빈도 반복 경두개자기자극과 결합된 신경근 전기자극치료가 만성 뇌졸중 환자의 대뇌 활성도에 미치는 영향에 대해 알아보고자 하였다. 선정기준을 만족하는 16명의 만성 뇌졸중 환자를 대상으로 5 Hz 고빈도 반복 경두개자기자극과 결합된 신경근 전기자극집단 8명, 손의 내재근 치료와 결합된 신경근전기자극집단 8명으로 분류하여 주 4회, 3주간 연구를 실시하였다. 실험군은 5 Hz 의 고빈도 반복 경두개자기자극 15분, 신경근전기자극치료 25분으로 총 40분의 중재를 실시하였다. 대조군에서는 손 내재근 치료 15분, 신경근 전기자극치료 25분으로 총 40분 중재를 실시하였다. 본 연구는 대뇌 활성도를 확인하기 위해 뇌파 중 알파파, 감각운동리듬파를 분석하였으며, 모든 집단은 중재 전, 중재 후, 2주 후 평가를 실시하였다. 그 결과 5 Hz 고빈도 반복 경두개자기자극과 결합된 신경근 전기자극집단의 집단내 알파파의 중재 전, 후, 2주 후 평가에서 F3, P3, Cz 영역에서 유의한 차이를 보였지만($p<0.05$), 손의 내재근 치료와 결합된 신경근전기자극집단에서는 유의한 차이를 보이지 않았다($p>0.05$). 5 Hz 고빈도 반복 경두개자기자극과 결합된 신경근 전기자극집단의 집단내 감각운동리듬파에서는 중재 전, 후, 2주 후 평가에서 F3, Cz 영역에서 유의한 차이를 보였지만($p<0.05$), 손의 내재근 치료와 결합된 신경근전기자극집단에서는 유의한 차이를 보이지 않았다($p>0.05$). 두 집단간 비교에서 알파파에서는 P4영역에서 유의한 차이를 보였으며($p<0.05$), 감각운동리듬파에서는 Cz 영역에서 유의한 차이를 보였다($p<0.05$). 이러한 연구의 결과를 통해 5 Hz 고빈도 반복 경두개자기자극과 결합된 신경근 전기자극치료가 만성 뇌졸중 환자의 뇌 활성도, 근 활성도 및 근 긴장도에 긍정적인 영향을 확인 할 수 있었다.

A Comparative Analysis of Metal Shielding for Mammography Using Monte Carlo Simulation

Jang Oh Kim[1,4], Da Eun Kwon[2], Dong Hee Han[2], Kyung Hwan Jung[2],
Byung In Min[3], Cheol Ha Baek[2,4*]

[1]Health and Medical Education Research Institute, Kangwon National University,
Samcheok 25949, Republic of Korea
[2]Department of Health Medical Science, Graduate School, Kangwon National University,
Samcheok 25949, Republic of Korea
[3]Department of Nuclear Applied Engineering, Inje University, Gimhae 50834, Republic of Korea
[4]Department of Radiological Science, Kangwon National University, Samcheok 25949, Republic of Korea

인체 내 방사선 피폭의 주된 문제점 중 하나로 의료기관에서 전자기파 방사선의 빈번한 사용이 제시되고 있다. 특히 유방암 발병률이 증가함에 따라 유방엑스선검사에 따른 불필요한 피폭의 우려됨에 따라 적절한 장비가 요구되고 있다. 본 연구는 GATE code를 이용하여 관전압 30 kVp, X-선 관과 차폐체의 거리 100 cm 조건에서 실리콘(Silicon, Si), 납(Lead, Pb), 비스무트(Bismuth, Bi), 텅스텐(Tungsten, W)의 95% 차폐능을 보이는 두께와 무게를 정량적으로 평가하였다. 또한, MCNP code를 이용하여 GATE에서 도출된 최적의 결과를 기반으로 유방의 흡수선량을 도출하였다. 시뮬레이션 결과 최적의 두께는 텅스텐, 납, 비스무트, 실리콘 순 이였으며, 밀도를 고려한 총 무게는 비스무트, 납, 텅스텐, 실리콘 순으로 나타났다. 95%가 차폐될 때 물질에 따른 유방의 흡수선량은 차이가 나타나지 않았다. 따라서, 차폐체의 두께, 무게, 경제성을 고려했을 때 납이 가장 우수한 차폐체로 나타났다. 비록 유해한 성분을 가진 납이지만 최소한의 실리콘으로 감싸서 유해성분을 차단하면 두께 및 무게를 줄일 수 있는 최적의 차폐체가 될 수 있다.

핵심단어: Mammography, 몬테카를로 시뮬레이션, 차폐률, 납, 비스무스, 텅스텐

VS Line 기기를 이용한 인체의 주름 세포와 동통에 관한 양자 파동 에너지 효과

김영훈*, 김현숙[1], 이형호[2], 송승기*
*명지대학교 자연과학대학 물리학과
[1]주식회사 우리엘바이오, 동양의학표준과학원
[2]주식회사 보원

사람을 포함한 모든 생물이나 무생물체는 스스로의 존재를 유지하고자 하는 고유의 파동 에너지를 갖고 있다. 인체의 각 장기도 각각 고유한 생체에너지 파동을 가지고 있다. 인간의 육체를 이루고 있는 위, 장, 간, 심장 등의 조직을 공통적으로 연결하는 매체가 파동이다. 즉, 인체는 파동이라는 에너지로 유기적 결합을 이루고 있는 파동의 집합체이다.

우리의 인체는 미세전류가 흐름으로써 각 세포의 생리작용을 하게 되는데 우리 몸의 미세전류는 약 40~60μA로, 원활한 신체활동과 피부건강을 유지하는데 중요한 역할을 한다. 그러나 나이가 들면서 우리 몸의 미세전류는 자연스럽게 약화 또는 소멸 되는데, 이런 현상은 신체활동을 저하 시키고 피부 노화를 가속화 시킨다.

우리 몸에는 약 60조 개의 세포가 있는데 주위환경의 영향으로 인하여 많은 스트레스를 받으면 체내에 많은 수의 세포들이 정상적인 세포의 기능을 못하는 비정상 세포들이 생성된다.

이와 같은 비정상 세포들을 정상화 세포로 변화시키기 위하여 우리 몸에서 자연 발생하는 전자기 파동 에너지와 양자 파동 에너지 발생장치인 VS Line기기를 제작하여 실험을 실시하였다. VS Line기기를 통하여 우리 몸의 면역력 저하로 발생하는 항암 부작용과 동통, 그리고 피부 노후화에 따라 나타나는 세포 중에서 주름 세포 개선을 연구했다. 즉, 양자 파동에너지를 통하여 주름 세포의 개선, 항암 부작용과 동통이 정상화되는 것을 연구하였다.

VS Line기기에서 S Line을 선택하여 10~20 level을 10~40초 처리한 결과, NT 대조군을 대비해 볼 때 통계학적으로 의미 있는 세포 생존율 감소를 보이지 않았다. 이것은 VS Line기기가 피부세포인 HDF세포에 독성을 나타내지 않는다는 것을 의미한다.

HDF 세포에서 colagenase의 일종인 MMP-1 억제활성을 평가한 결과를 [그림1]에 나타냈다. HDF 세포에 S Line의 3~25 level 자극을 10초 처리한 다음, MTT법으로 세포 생존율을 측정한 결과는 [그림2]에서 볼 수 있다. 모든 처리군에서 NT 대조군에 비교한 결과, 80% 이상의 세포 생존율을 보였으며, 이것은 처리된 조건에서 VS Line기기는 피부세포인 HDF 세포에 독성을 나타내지 않는다는 것으로 보인다.

HDF 세포에 S Line의 3~24 level 자극을 60초 처리한 다음, ELISA법으로 MMP-1 억제 활성을 평가한 결과를 [그림3]에 나타냈다. S Line을 60초 처리한 결과, level 3을 제외한 6~24의 모든 level에서 NT 대조군과 비교하여 통계학적으로 의미있는 MMP-1 억제 활성을 보여주었다. 가장 우수한 활성을 보여준 level 24에서는 MMP-1 억제 활성이 60.7%로 나타났다.

양자 파동에너지 VS Line기기를 이용하여 의학 분야에 종사하는 내과 전문의를 통하여 항암 부작용 및 통증 환자 김○○ 외 10명 남녀를 선정하여 임상시험을 시행했다.

직장암 항암치료에 의해 신경 발진부위의 손상으로 통증이 발생한 곳에 양자 파동에너지를 VS Line S-2, 3 mode에서 60분간 통증 부분의 혈 자리를 접촉한 결과, 치료 후 혈액 순환이 잘되어 체온 열 색의 변화가 나타났다.

또한 환자 진술에 의하면 발진 부위의 손상으로 통증이 없어지고, 혈액 순환도 잘 이루어졌음을 확인했다.

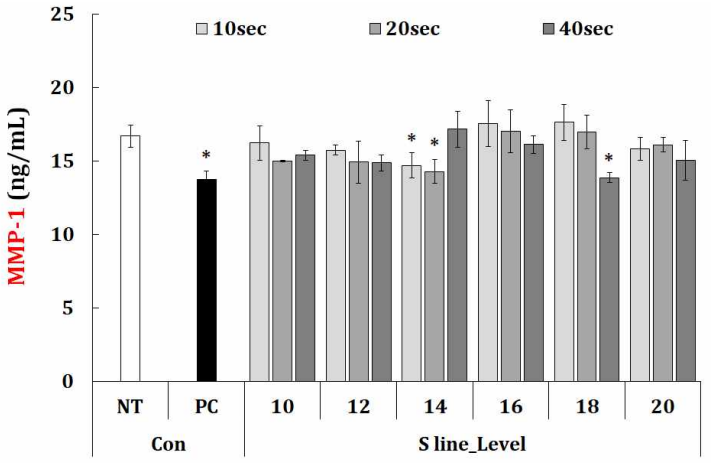

그림. 1. VS Line(10~20 level × 10~40초)이 자극된
human dermal fibroblast (HDF) 세포에서 MMP-1 억제활성 평가.

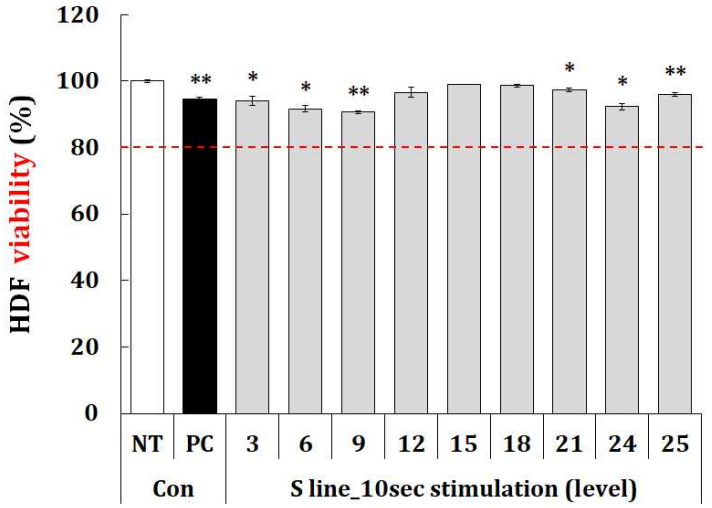

그림. 2. VS Line(3~25 level × 10초)이 자극된 human dermal fibroblast (HDF)에서 세포독성 평가.

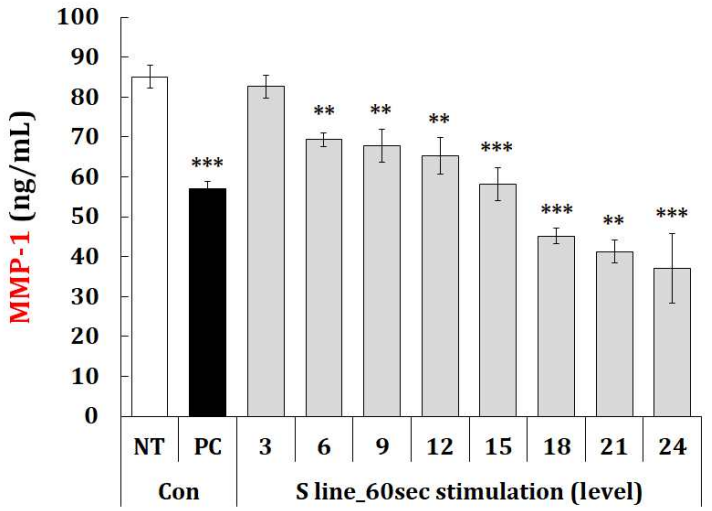

그림. 3. VS Line(3~24 level × 60초)이 자극된 human dermal fibroblast (HDF) 세포에서 MMP-1 억제활성 평가.

미세혈관순환시스템 내에서 펄스자기장이 면역세포 활성화에 미치는 영향

최유경*, 이현숙†
상지대학교 보건과학대학 한방의료공학과, 강원 원주시 상지대길 84, 26339

Ⅰ. 서론

혈액의 산-염기 불균형은 염증, 암과 같은 질병을 유발하며 대사성산증으로 인한 쇼크나 사망에 이를 수 있다. 산증이 심각한 경우에는 정맥 내에 중탄산염을 투여하는데 이는 모든 산증 치료에 적용할 수 없으며 침습적인 방법이기에 각종 부작용을 동반한다고 알려져 있다.[1] 최근 비침습적 치료방법인 자기장을 이용한 in-vitro실험에서 펄스자기장이 적혈구막 주변 이온에 영향을 주어 혈액의 pH 조절에 영향을 미친다는 연구결과가 있다.[2] 그러므로 본 연구에서는 인체의 순환시스템과 같은 in-vivo 실험을 모방한 미세순환시스템을 구축하여 순환시스템 내에서 펄스자기장이 혈액의 산-염기 균형 평가와 면역세포 배양을 통한 면역세포의 활성화에 대한 메커니즘을 연구하고자 한다.

Ⅱ. 실험 방법

실험을 위해 필요한 혈액은 IRB면제 심의 후 강원혈액원에서 공급받아 농축적혈구(RBC)와 신선동결혈장(FFP)을 인체와 동일한 적혈구용적률(HT) 45%로 맞추어 사용하였다. PDMS를 이용하여 500 μm의 크기를 갖는 인공모세혈관을 제작하였다. 내경이 0.5 mm의 크기를 가지는 micro-tube를 이용하여 인공모세혈관과 0.1~40 μl/min의 유량을 갖는 micro pump(TAKASA-GO ELECTRIC, RP-TX)를 연결하여 미세순환시스템을 구축하였다. pH meter(HORIBA, LAQUA twin)를 사용하여 펄스자기장(Pulsed Magnetic Field, PMF) 자극 전 후의 순환한 혈액의 pH를 측정하여 비교하였다.

면역세포의 활성도를 관찰하기 위하여 쥐의 대식세포인 RAW 264.7 cell을 사용하였다. DMEM, FBS 5%, penicillin-streptomycin 1%를 희석한 배양액을 사용하여 37℃, CO_2 5%, 습한 상태인 인큐베이터에 배양하였고, 염증반응 유도를 위하여 LPS(lipopolysaccharide, 1μg/ml) 처리 후 펄스자기장 자극 전 후의 세포 배양액의 pH를 측정하였다. 펄스자기장은 세기(400G, 1000G, 2700G) 별로 샘플 당 각각 3분씩 인가하였다.

Ⅲ. 결과

미세혈관순환시스템 내에서 펄스자기장 자극 전후의 혈액의 pH 변화를 관찰하였다. 자기장 자극없이 순환한 혈액과 자기장 자극을 가하며 순환한 혈액의 pH 수치는 큰 차이를 보이지 않았다. 실험 횟수가 적어 반복실험을 통해 객관적인 정량화가 필요한 것으로 보인다.

세포 배양 후 세포의 적응을 위해 24시간 지난 뒤 LPS를 유도하였으며, RAW 264.7 cell의 doubling time인 18시간 후 펄스자기장을 자극하고 다음 18시간 후 세포 배양액의 pH를 관찰하여 비교하였다. 대조군보다 LPS 처리군의 pH가 산성화되었고 LPS 유도 후 펄스자기장을 인가한 처리군은 대조군과 비슷한 정상범위로 들어오는 것을 확인하였다. 또한, 자기장 세기가 커질수록 효과가 좋아지는 것을 확인하였다.(Fig.) 따라서 펄스자기장 자극이 LPS로 인하여 염증반응이 유도된 면역세포의 활성화에 기여하는 것으로 판단된다. 이러한 결과를 바탕으로 세포가 방출하는 사이토카인 농도와 펄스자기장의 효과 지속성을 관찰하여 펄스자기장의 항염증효과를 규명하고자 한다.

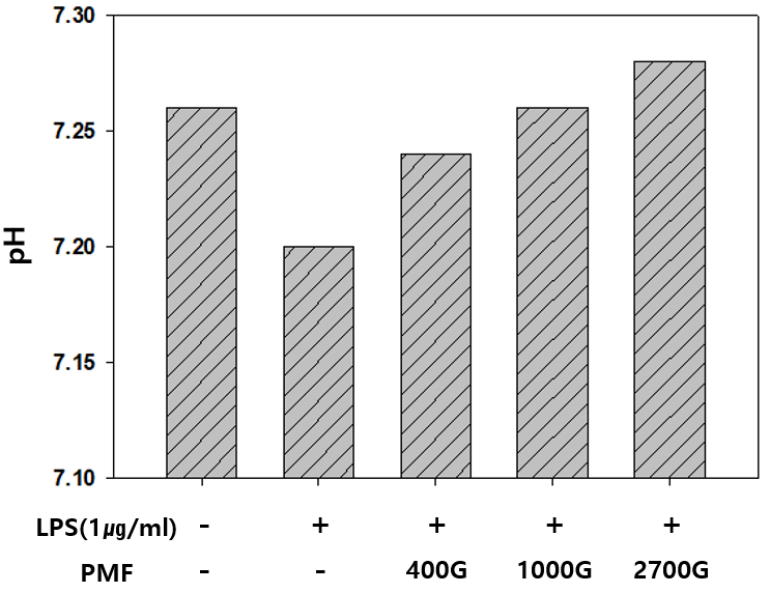

Fig. Effect of PMF stimulus after 18h on pH value.

References

[1] S. Sabatini, J Am Soc Nephrol 20, 4 (2009).

[2] S. H. Bang, AIP Advances 11, 015242 (2021).

Intravascular flow characteristics study for target induction of anti-CD3 monoclonal antibody conjugated to magnetic nanoparticles

Sang-Heon Choi[1*], Jong-Gu Choi[1], Ji-Won Ha[1], Yebin Bae[2], Hyunsook Lee[1], and Sang-Suk Lee[1†]
[1]Department of Digital Healthcare, Sangji University, Wonju 26339, Republic of Korea
[2]Department of Visual and Media Design, Sangji University, Wonju 26339, Republic of Korea

코로나-19 면역치료제로 사용되는 항-CD3 단클론항체(mAb)가 붙은 35 nm 크기의 자성나노입자(MNP)를 제조하였다. 인간화 마우스로부터 제조된 mAb를 동물 실험이 가능하도록 동일한 친화도를 유지한 토끼의 혈관에 투여하는 실험을 하였다. mAb-MNPs의 효과와 토끼의 혈관 내 직접 주입을 확인하기 위해 2021년 상지대학교 동물실험윤리위원회의 승인을 받아 비임상 동물실험을 적용하였다. 8주령의 1.8 kg 뉴질랜드산 토끼를 마취하여 안정된 자세로 눕힌 후에 동맥과 정맥 그리고 모세혈관이 모두 관찰되는 오른쪽 귀의 동맥 부근에 Fig. 1처럼 PBS×1에 담은 항체가 붙은 mAb-MNPs 접합 액상 75 μl를 우이동맥 아래 부분에 주입하였다. 액상 주입시 처음에는 Fig. 1(a)처럼 거부반응으로 인해 동맥 혈관이 끊어져 있으나 서서히 회복되어 10분 후에는 Fig. 1(b)처럼 정상적인 혈관을 나타내었다. 또한 검은색을 띤 자성나노입자가 혈관을 따라 흘러 들어가 정상적인 피의 색깔로 혈액이 순환되는 것을 확인하였다. 이로써 생체적합성 mAb-MNPs들은 혈관 순환시스템에서 잘 운동하는 특성을 보임으로써 이러한 나노 구조형 접합체는 생체에 접합한 액상구조로 이루어져 있음을 보였다.

PBS×1에 들어있는 순수한 MNPs 액상과 항체를 포함하는 mAb-MNPs 접합 액상을 각각 15 μL 만큼 Fig. 2과 같이 동맥, 정맥, 모세혈관이 모두 관찰되는 오른쪽 귀와 왼쪽의 동맥 근처에 주입하였다. Fig. 1(c)은 토끼 우이동맥의 한곳에 MNPs의 액상을 주사기하전 귀의 정상적으로 흐르는 혈관의 모습이다. Fig. 1(d)는 토끼의 우이동맥에 15 μL 만큼 MNPs의 액상을 주사하고 20분 이 지난 후의 혈관의 모습이다. 이 사진에서는 정상적인 혈관 내에 주입된 MNPs의 양이 흐르지 못하고 그대로 혈관에 남아 있음을 볼 수 있다. 한편 mAb-MNPs가 담긴 액상 주사 시 처음에는 거부반응으로 동맥혈관이 잘렸으나 약 5분 후에 서서히 회복되어 20분 후 모습을 보이는 Fig. 1(f)가 주입 전의 좌이동맥의 혈관을 보인 Fig. 1(e)와 같이 정상혈관으로 회복하였다. 또한, 흑색을 띤 mAb-MNP가 혈관을 따라 흐르고 혈액을 정상 혈액색깔을 보이며 혈액을 순환시키는 것으로 나타났다. 즉, mAb-MNPs는 생체에 적합한 구조로 혈관 순환계에서 좋은 움직임을 보였다.

인간화 항-CD3 단클론 항체인 포랄루맙(Foralumab)과 자성나노입자 접합체를 밀도 1 mg/cc로 PBS×1의 액상에 제조하여 생후 13주 무게 250 g인 쥐(rat, SD outbred model, 대한바이오링크 생산)에 투여하여 동물실험을 실시하였다. 1일에 1번 포랄루맙과 자성나노입자 접합 액상 1 cc의 양을 Fig. 2에 보인 사진에서 붉은색으로 나타낸 영상처럼 꼬리 정맥에 0.3 ml (Fig. 3(2)), 왼쪽 사타구니 근육에 0.3 ml (Fig. 2(b)), 그리고 오른쪽 복부 정맥에 0.3 ml (Fig. 2(c))로 총 0.9 ml를 2일간 2번 총 1.8 ml를 투여하였다.

포랄루맙 항체와 자성나노입자 접합체를 2일에 걸쳐서 총 1.8 ml를 투여한 후 혈액을 통해 이동하는 mAb-MNPs 접합체 액상을 Fig. 3(a)의 하얀색으로 표시한 것과 같이 쥐의 뒤쪽 목과 등 사이 중앙에 털을 깎고 본드를 이용하여 영구자석을 Fig. 3(b)처럼 붙였다. 사용한 네오듐 영구자석의 크기는 직경 10 mm, 두께 2 mm인 원통형 모양을 갖고 중앙에서 자기장의 세기는 1.5 kOe이고 가장자리 부근에서 1.0 kOe이었다. 부착한 영구자석은 2일 후 제거한 후 사진은 Fig. 3(c)이다.

혈관으로 흐르는 mAb-MNPs 접합체의 목표 부근에 부착한 영구자석으로 유도한 동물실험을 수행하였다.

Fig. 4(a)은 영구자석이 붙은 동일한 위치의 MNPs 주입없이 대조군의 쥐 등쪽 상처 사진으로 포랄루맙 항체와 접합한 MNPs를 주입 하기 전 표피층만 벗긴 후에 촬영되었다. Fig. 4(b)는 mAB-MNPs 접합체 액상을 쥐의 꼬리 중앙, 좌 사타구니, 우 복부에 총 1.8 ml 투여한 후, 등쪽 목 아래에 부착한 영구자석을 제거하고 난 후 영상이다. Fig. 4(b)는 영구자석을 붙인 부근의 피부의 표피층을 벗기고 난 후 바로 아래 진피층의 사진이다. Fig. 4(c)는 영구자석을 붙인 부근의 피부의 표피층 아래를 해부한 영상이다. 특히 Fig. 4(c)는 목과 등 쪽에 있는 혈관을 통하여 흐르는 혈관 내로 흐르는 혈액의 색깔이 진한 고동색으로 변화된 것을 알 수 있다. 이것은 mAb-MNPs 액상이 영구자석의 자기장 세기의 효과로 인하여 mAB-MNPs 접합체 액상이 타겟 부분에 도달하여 영구자석이 있는 중심부의 자기장이 센 곳에 머무른 것으로 볼 수 있다.

Acknowledgements : This research was supported by Basic Science Research Program through the National Research Foundation of Korea (NRF) funded by the Ministry of Education (2021R1I1A3054773).

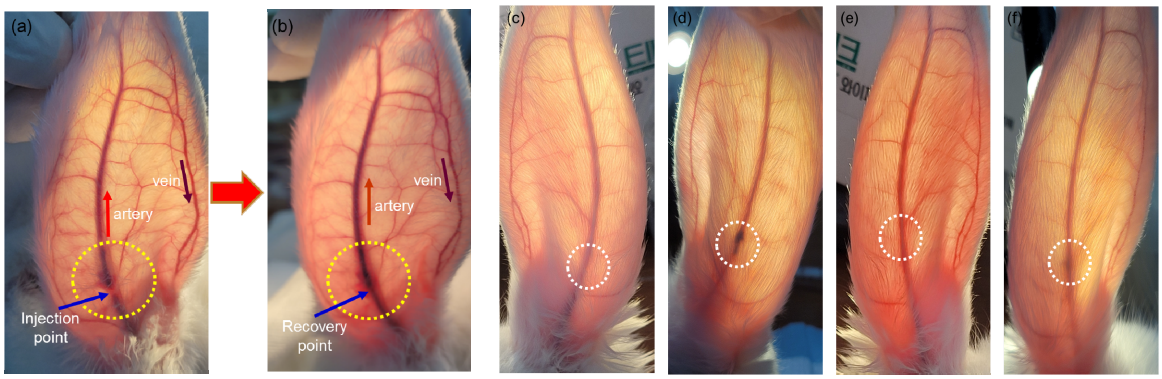

Fig. 1. Recovery flow property of mAb-MNPs in arterial blood vessels of rabbit's left ear (a) before and (b) after the injection of amount 75 µl. Non-recovery flow property from (c) before and (d) after 15 µL injection of pure MNPs in arterial blood vessels of a rabbit's right ear. Recovery flow property from (c) before and (d) after 15 µL injection of mAb-MNPs in arterial blood vessels of a rabbit's left ear. Here, the arrows in the dotted white circle indicate the injection site of MNPs and mAb-MNPs given in 1 mg/mL of PBS.

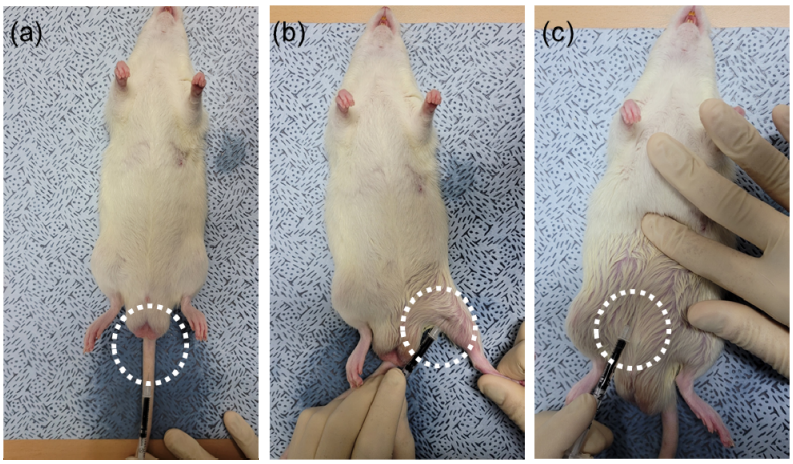

Fig. 2. (a) Intravenous injection, (b) intramuscular injection, and (c) intraperitoneal Injection of nanoparticles.

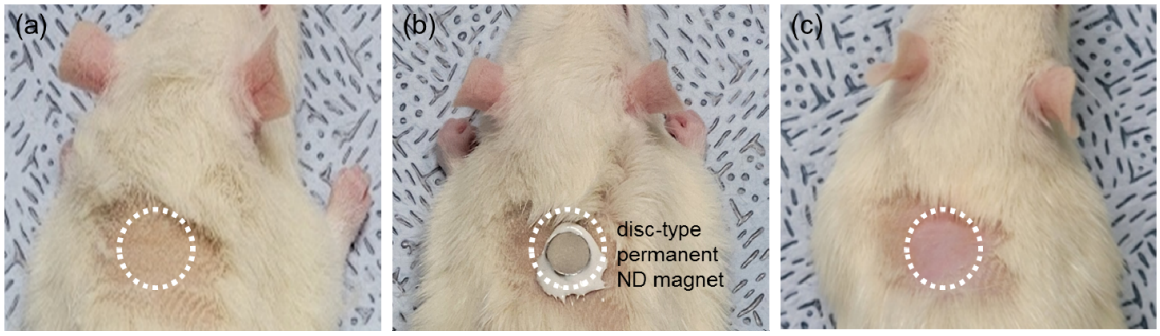

Fig. 3. Photos of the back of a rat. (a) Before and (b) after bonding one disc-type permanent magnet. (c) The permanent magnet is removed from the rat.

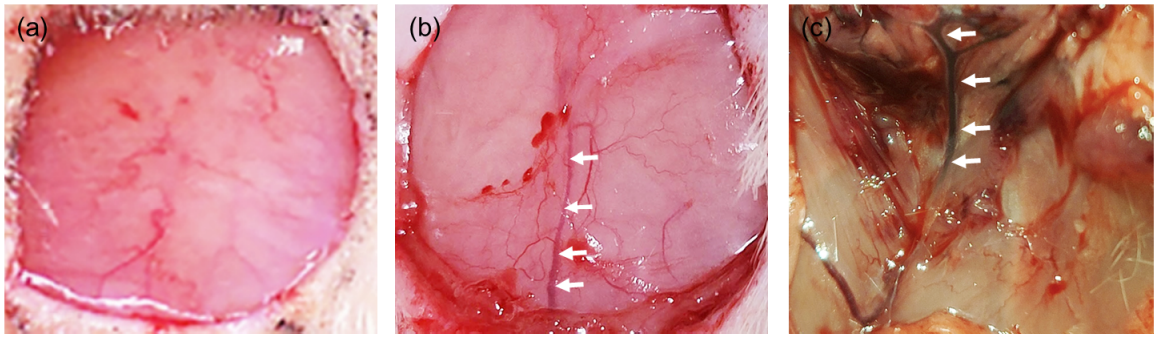

Fig. 4. The photos of the rat's dorsal wound were taken after applying MNPs conjugating Foralumab antibodies over both (a) before and (b) after 3 days. (c) The black-brown vessel marked white bold arrows at the top of the center is the induced state of mAb-MNPs by permanent magnet.

PM01

Na로 도핑한 La계 M형 페라이트 소결자석의 자기적 특성

손성우[1,2*], 김부안[1†], 권해웅[1], 최재영[3], 이정구[3†]
[1]부경대학교 재료공학과
[2](주) 태평양금속 연구팀
[3]한국재료연구원 분말재료연구본부 자성재료연구실

$AFe_{12}O_{19}$ (A = Ba, Sr, Pb)의 화학조성으로 알려져 있는 페라이트의 최대자기에너지적($(BH)_{max}$)은 대표적인 희토류(RE)-천이금속(TM)계 자석인 NdFeB계 자석의 1/10에 불과하지만 주원료가 산화철(헤마타이트)로서 가격대비 성능이 우수하고 화학적으로 매우 안정한 장점을 가지고 있다. 이러한 이유로 영구자석 중에서 가장 높은 생산량을 유지하고 있다. 각종 스피커나 모터 등 페라이트 소결자석이 사용되고 있는 다양한 용도 중에서 특히 페라이트 자석의 고특성화가 요구되고 있는 분야는 자동차용 모터나 가전용 모터이다. 최근 희토류 원료의 가격이 다시 상승하고 있고 조달 리스크 등으로 인하여 지금까지 NdFeB계 소결자석이 사용되고 있던 산업용 모터나 전기자동차용 구동모터 등에도 페라이트 소결자석의 적용이 검토되고 있다. 1990년대 이후 Sr계 및 Ca계 페라이트에서 Sr^{2+} 또는 Ca^{2+}의 일부를 La^{3+}로 치환하고 동시에 Fe^{2+}의 일부를 Co^{3+}로 치환하면 결정자기이방성과 저온에서의 보자력의 온도계수가 향상되는 것이 보고되고 있다. 그러나, 이러한 Sr-La-Co계 및 Ca-La-Co계 페라이트는 NdFeB계 소결자석을 대체하기에는 여전히 자기특성이 부족하여 페라이트 자석의 고특성화를 위한 연구가 계속되고 있으며 그 일환으로서 La계 M형 페라이트($LaFe_{12}O_{19}$)자석이 주목받고 있다. La계 M형 페라이트 자석은 0 K에서 기존 Sr계 및 Ba계 페라이트 자석대비 포화자화(M_s)는 유사하고 결정자기이방성이 대단히 큰 자석으로 알려져 있지만 M상 단상으로 합성하는 것은 어려운 것으로 보고되고 있다. 또한, Na로 도핑한 La계 M형 페라이트($La_{0.5}Na_{0.5}Fe_{12}O_{19}$)자석도 고상반응법으로 M상 단상으로 제조하는 것이 어렵고 주로 단결정으로 자기특성을 평가하는 수준에 머물러 있는 것으로 보고 되고 있다. $La_{0.5}Na_{0.5}Fe_{12}O_{19}$의 0 K에서의 포화자화는 일반적인 Sr계 및 Ba계 페라이트 자석에 비해서 약 10 % 이상 높은 것으로 보고 되고 있다. 만약 $La_{0.5}Na_{0.5}Fe_{12}O_{19}$의 M_s를 상온에서 더 높게 유지할 수 있다면 높은 잔류자속밀도를 구현할 수 있을 것으로 판단된다. 본 연구에서는 Na으로 도핑한 La계 M형 페라이트 소결자석의 Co치환량 변화에 따른 자기적 특성을 논의하고자 한다.

Keywords: 하드 페라이트, 페라이트 영구자석, La 계 M 형 페라이트 자석, Co 치환 M 형 페라이트 자석, Na 도핑

Hard Ferrites Composite Particles for Millimeter-wave Wideband Absorption

Gi-Ryeon Jo[1,2*], Da-young Jeong[1], Seung-hoon Song[1], Young-Guk Son[2], Youn-Kyoung Baek[1†]
[1]Powder Materials Division, Korea Institute of Materials Science (KIMS), Changwon, Republic of Korea
[2]School of Materials Science and Engineering, Pusan National University, Busan, Korea

High-performance electromagnetic wave absorbers are required for electromagnetic wave control particularly at a broad bandwidth in millimeter-wave spectrum, which will play a big role in future 5 G and 6G wireless networks. Traditional radar absorbing materials (RAMs) comprised of metals or soft ferrites and metamaterial absorbers (MA) have been developed for millimeter-wave absorption, but lack of widening the absorption bandwidth hinders their practical applications. In this study, we developed a facile and scalable method to synthesize the core-shell structured magnetic particles showing wideband absorption of millimeter-wave. The resulting ferrite composites show two different absorbance peaks around 54 and 84 GHz, measured by a vector network analyzer. It is note that broadband absorption from V (40~75 GHz) and W band (75~100 GHz) was shown in the magnetic loss particles.

This study was supported by the Fundamental Research Program of the Korea Institute of Material Science (PNK7630).

Keywords: Millimeter-wave, Magnetic loss material, 6G, Ferrite, Core-shell particle

Synthesis and characterization of FeCo-Mn_3O_4 hetero-nanostructures

Kavita Kumari[1*], Akshay Kumar[2], MinJi Shin[2], Seok Hwan Huh[3] and Bon Heun Koo[1,2†]

[1]Industrial Technology Research Institute, Changwon National University, Changwon, Gyeongnam, 51140, Republic of Korea

[2]Department of Materials Convergence and System Engineering, Changwon National University, Changwon, Gyeongnam, 51140, Republic of Korea

[3]Department of Mechatronics Conversion Engineering, Changwon National University, Changwon, Gyeongnam, 51140, Republic of Korea

[*]Corresponding Author - bhkoo@changwon.ac.kr

The magnetic hetero-nanostructures have gained immense attention of the scientific community due to their wide range of applications. The magnetic hetero-nanostructures have been exploited for the exchange bias effect which is highly desirable for the applications like magnetic sensors and non-volatile memory. Therefore, in the present work, the FeCo-Mn_3O_4 nanostructures have been prepared through chemical route method following two-pot synthesis. The heterostructure having the combination of ferromagnetic and antiferromagnetic materials can make an excellent system for the investigation of the exchange bias effect. The synthesized nanostructures were characterized with various characterization techniques such as x-ray diffraction (XRD), high resolution field emission scanning electron microscopy (HR-FESEM), electron dispersive x-ray spectroscopy (EDS) and dc-magnetization. The XRD spectra revealed the presence of cubic FeCo and tetragonal Mn_3O_4. The crystallite size has been calculated with in the nanometer range. The HR-FESEM micrographs demonstrated the formation of non-spherical particles. The histograms revealed a broad particles size distribution indicating that the average particle size remains with in the nanometer range. The EDS images displayed the presence of Fe, Co, Mn and O in the samples. The distribution of elements revealed that the manganese oxide surrounds the FeCo nanoparticles. The magnetic field dependent magnetization shows the ferromagnetic behaviour of the particles as shown by the M-H hysteresis curves. The field cooled and zero-field cooled M-H hysteresis curves evidenced the induced exchange bias effect.

Key words: Magnetic heterostructure, exchange bias, nano-composites

Phase transition and magnetic property of $La(Fe,Si)_{13}$ compound

Jae-Young Choi[1,2*], Jung-Min Lee[1], Youn-kyung Baek[1], Jung-Goo Lee[1], and Young-Kuk Kim[1†]
[1]Korea Institute of Materials Science, Changwon, Republic of Korea 51508
[2]Pusan National University, Pusan, Republic of Korea 46241

The magnetic property and phase fraction of the $La(Fe,Si)_{13}$ compound have been experimentally studied. In the near 200K, $La(Fe,Si)_{13}$ compound is phase transition occur. $La(Fe,Si)_{13}$ compound shows ferromagnetic or paramagnetic when the temperature is lower or higher than transition temperature, respectively. $La(Fe,Si)_{13}$ compound is paramagnetic in room temperature. To promote wider applications, it is highly desirable that the transition takes place near room temperature. Paramagnetic to ferromagnetic transition temperature enhances when light element is doped to $La(Fe,Si)_{13}$ compound. On the other hand, there is a problem that it takes a long time to form a single phase. To solve this problem, melt spinning was performed and annealed at high temperature to enhance the phase fraction of $La(Fe,Si)_{13}$ compound a short time. The amount of iron decreased during annealing in XRD data. The Fe and $La(Fe,Si)_{13}$ phases were identified by SEM images. VSM data showed a hysteresis loop close to a low paramagnetic material at room temperature, the remaining iron was existed in $La(Fe,Si)_{13}$ compound. PPMS analysis showed that the phase transition temperature is near to 200K and is consistent with $La(Fe,Si)_{13}$ reported. As a result of comparing magnetization at room temperature, 3% of Fe remains and a considerable portion of it was converted to paramagnetic materials.

PM05

Ca 환원을 통한 Nd-Fe-B 재생자석 제조 연구

노태성[1,2], 차희령[1], 김태훈[1], 이설미, 김태욱, 김양도[2*], 이정구[1*]
[1]한국재료연구원, 자성재료연구실
[2]부산대학교, 재료공학과

Nd-Fe-B계 자석은 우수한 자기특성으로 다양한 분야의 핵심소재로 이용되고 있다. 특히, 최근 친환경에너지 시장이 확대되면서 전기자동차 및 하이브리드 자동차의 수요가 크게 증가하였다. 이에 따라 구동모터의 핵심 소재인 Nd-Fe-B계 소결자석의 사용량이 급증하였다. 이로 인해, 가까운 미래에 관련 부품의 노후화로 인한 폐 Nd-Fe-B 자석이 대량 배출될 것으로 예상된다. 폐 Nd-Fe-B 자석의 경우 Nd-rich 상 및 $Nd_2Fe_{14}B$ 주상의 산화로 인해 자기적 특성이 매우 악화 되어 있는 상태이다. 따라서 폐자석의 산소농도를 저감하는 기술이 고특성의 재생자석 제조를 위한 핵심요소이다. 본 연구에서는 Ca을 이용하여 폐자석 내 Nd-rich 및 $Nd_2Fe_{14}B$ 산화물을 환원함으로써 고특성 재생자석을 제조하고자 하였다. 본 실험에서 사용된 폐자석의 조성은 $Dy_{1.98}Nd_{23.11}Pr_{5.72}Fe_{bar}B_{0.94}M(Co, Al, Cu, Ga, Zr)_{2.34}$ (wt.%)이다. 벌크 폐자석을 미세 분말화 하기 위해서 수소처리 및 jet-milling 공정을 수행하였고, 폐자석으로부터 제조된 폐분말은 Ca granule을 이용하여 환원하였다. Ca 사용량에 따른 폐분말의 환원거동을 살펴보기 위해서, Ca의 첨가량을 10 wt.%, 5 wt.%, 3 wt.% 로 달리하여 실험을 진행하였고, 환원공정은 850 ℃에서 진행하였다. 환원공정이 완료된 재생분말 내 잔존 Ca과 CaO를 제거하여 순수한 Nd-Fe-B 분말을 얻기 위해, 유/무기 solvent를 이용하여 다단의 세정 공정을 진행하였다. 제조된 분말은 자장 성형 및 소결 공정을 통해 이방성 재생소결자석을 제조하였다. 본 발표에서는 제조된 재생분말 및 재생자석의 산소농도, 미세구조, 그리고 자기적 특성 분석 결과를 토대로 고특성 재생자석 제조를 위한 폐자석 재생 연구의 가능성 및 방향을 제시해 보고자 한다.

Systematic process control for high performance MnBi

Su Yeon Ahn[1,2*], Yang Yang[1,3], Jung Tae Lim[1], Jihoon Park[1], Jong-Woo Kim[1], Soon Chul Hong[2], Chul-Jin Choi[1]

[1]Korea Institute of Materials Science (KIMS), Changwon

[2]Department of Physics, University of Ulsan

[3]School of Materials Science and Engineering, Pusan National University

In recent years, rare-earth-free permanent magnets have attracted considerable attention due to the concern over cost and supply crisis of rare-earth raw materials. Among the rare-earth-free permanent magnets, MnBi shows high magnetic crystalline anisotropy, high Curie temperature of 633 K and a noticeable positive temperature coefficient making it promising for possible industrial applications. For the future industrial applications, a detailed optimization process and mass synthetic process of qualified MnBi powder and bulk magnet should be established.

In this work, a systematic process control for *high performance* MnBi magnets has been investigated. A synthetic process of MnBi ingots via induction melting was tuned for high purity low-temperature phase (LTP) and mass production of MnBi powder. In addition, efficient particle size control and an inevitable post processes for homogeneity of LTP, microstructure, and finally, enhancement of magnetic property has been optimized. Meanwhile, the doping effect of the third element substitution on MnBi matrix has also been examined for enhancement of coercivity and higher energy products. A detailed optimization process and mass synthetic process of MnBi powder which has advantages for industrial applications will be presented in detail.

Magnetic properties and microstructure evaluation of $Sm(Fe_{0.8}Co_{0.2})_{11}Ti$ particles produced by reduction diffusion process

Hankuk Jeon[1,2*], Jung Tae Lim[1], Hui-Dong Qian[1], Jihoon Park[1*], Hyojun Ahn[2], and Chul-Jin Choi[1†]

[1]Korea Institute of Materials Science, Changwon, Gyeongsangnam-do 51508, Republic or Korea

[2]School of Materials Science and Engineering, Gyeongsang National University, Republic of Korea

Permanent magnets are increasingly used in transportation technology and sustainable energy production for EVs, hybrid vehicles and wind turbines. High performance permanent magnets, such as Nd-based magnets, have problems with stability at high temperature, supply and high price. Therefore, developing rare-earth free or rare-earth lean permanent magnets is becoming an important task to solve the abovementioned issues. Herein, iron-rich rare-earth alloys with tetragonal $ThMn_{12}$ structure, which can replace rare earth permanent magnets, is drawing attention due to its high saturation magnetization of 1.43 T, anisotropy field of 10.9 T, and Curie temperature of 800 K [1]. Although the magnetic properties of $SmFe_{12}$ with $ThMn_{12}$ structure have been already demonstrated, a number of studies to enhance coercivity are still underway. The coercivity increases as grain sizes approach to the single domain size. Therefore, in this work, we conducted experiments to obtain $SmFe_{12}$ particles with single domain sized grains to acquire high coercivity through the high energy ball milling and the reduction diffusion process.

In this experiment, Sm_2O_3(Samarium Oxide), Fe_2O_3(Iron Oxide), Co, TiO_2(Titanium Dioxide), Ca were used as starting materials. Sm_2O_3 and Ca, as a reducing agent, were excessively added in consideration of vaporization. The starting materials except Ca were crushed and homogeneously mixed for 4 hours using a high energy ball milling process. Then, the powders were processed by low energy ball milling with Ca powder for 2 hours. The resulting mixture was sealed in a graphite crucible and then heat treated in argon atmosphere. This heat treatment process including heat treatment temperature and time were optimized. Then, it was washed using a detergent that dissolves unreacted Ca and remaining CaO, followed by drying in vacuum. It was concluded that the purity of the samples varied with the initial contents of Sm and heat treatment time. The resultant particle size and magnetic properties of the products were also affected by the ball milling conditions. The detailed experimental procedures and physical and magnetic properties will be discussed.

Reference

[1] P. Tozman, H. Sepehri-Amin, Y. K. Takahashi, S. Hirosawa, K. Hono, Acta Materialia, 153, 354 (2018).

Magnetic properties and phase relations of $Sm(Fe_{0.8}Co_{0.2})_{10.8}Ti_{0.6}V_{0.6}$ + *x* wt.% Cu-Ga produced by melt-spinning method

Tianhong Zhou[1,2*], Hui-Dong Qian[1,2], Jung-Tae Lim[1], Jihoon Park[1], Yong-Rae Cho[2], Chul-Jin Choi[1†]

[1]Powder Materials Division, Korea Institute of Materials Science, Changwon, Gyeongsangnam-do 51508, Republic of Korea

[2]School of Materials Science and Engineering, Pusan National University, Busan 46241, Republic of Korea

In our previous work, we studied the influence of Ti and V content in the $Sm(Fe_{0.8}Co_{0.2})_{12-2x}Ti_xV_x$ (x = 0.5 - 1.0) alloys. The optimal x for high purity $ThMn_{12}$ phase was found to be 0.6, and the corresponding remanent magnetization, coercivity, and maximum energy product were 80.6 emu/g, 3379 Oe and 7.29 MGOe, respectively. However, an intergranular phase that could enhance the coercivity was not found in the $Sm(Fe_{0.8}Co_{0.2})_{10.8}Ti_{0.6}V_{0.6}$ sample, i.e., the grains of $ThMn_{12}$-phase were in direct contact. Therefore, in this work, we have introduced Cu-Ga as the intergranular phase to improve the coercivity.

First, $Sm(Fe_{0.8}Co_{0.2})_{10.8}Ti_{0.6}V_{0.6}$ and Cu-Ga alloys were separately fabricated. The produced alloys were then arc-melted together to produce $Sm(Fe_{0.8}Co_{0.2})_{10.8}Ti_{0.6}V_{0.6}$ + x wt.% Cu-Ga (x = 1, 2, 3) alloys. It is noted that an excess of Sm was added to crystallize Sm-Cu-Co-Ga in the alloys. The produced ingots include the $ThMn_{12}$ and α-Fe phases in the main grains and Sm-Cu-Co-Ga in the grain boundaries. The contents of the α-Fe and Sm-Cu-Co-Ga were dramatically reduced by melt-spinning at the wheel speed of 37 m/s due to the high cooling speed. It was found that the main phase of the melt-spun ribbons is $TbCu_7$ phase. The ribbons were manually ground and pressed under 12.5 GPa to produce high density green bodies. The green bodies were annealed at 800 °C for 15 minutes under vacuum conditions, which resulted in a nearly pure $ThMn_{12}$ phase in the main grains and Sm-Cu-Co-Ga in the grain boundaries. The resulted coercivities of the samples were 3399, 4054, and 4317 Oe for x = 1, 2, and 3, respectively, which are higher than the sample without Cu-Ga. However, compared to the small increase in the coercivity, the remanent magnetization declined to 64, 66 and 60 emu/g, respectively. This degradation resulted in a negative impact on the maximum energy product, which were 4.43, 6.44 and 4.75 MGOe, respectively.

Although the intergranular phase was successfully fabricated by introducing the Cu-Ga alloy in this work, it led to the deterioration of the remanent magnetizations and maximum energy products. Thus, it is necessary to further optimize the experimental procedures to improve the magnetic properties.

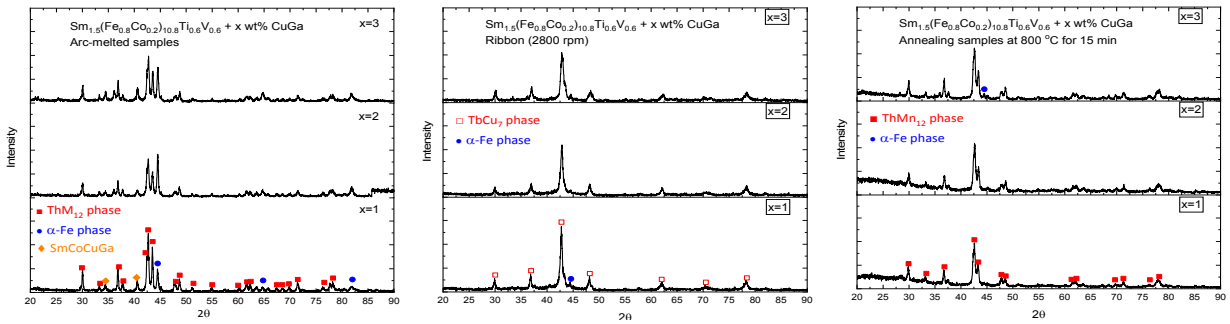

Fig 1. XRD patterns of the $Sm(Fe_{0.8}Co_{0.2})_{10.8}Ti_{0.6}V_{0.6}$+ x wt.% Cu-Ga (x = 1, 2, 3) (a) arc-melted ingots, (b) melt-spun ribbons, and (c) annealed bulks.

PM09

La-Co co-substituted M-type hexaferrites on magnetic properties prepared by solid-state reaction

Min-Kyung Seong[1*], Kang-Hyuk Lee[2], Sang-Im Yoo[2†], Hae-In Yim[1†]
[1]Department of Physics, Sookmyung Women's University, Seoul 04310, Korea
[2]Department of Material Science and Engineering, Seoul National University, Seoul 08826, Korea

M-type hexaferrites, which are widely used hard magnetic material, have high crystalline anisotropy (H_a), saturation magnetization (M_s), and coercivity (H_c). For enhancing magnetic properties, such as saturation magnetization, substitution is mainly used. La-Co substituted Strontium M-type hexaferrite has known superior magnetic properties among M-type hexaferrites. Previous research has focused on Co^{3+} substitution for the Fe^{3+} sites of Ca-La M-type hexaferrites. However, La-Co substituted La-Ca M-type hexaferrites remain unexplored. Therefore, in this work, we investigated the effect of La-Co co-substitution with the same ratio on the magnetic properties. $Ca_{1-x}La_xFe_{12-x}Co_xO_{19}$ ($0 \leq x \leq 1$) were synthesized by solid-state reaction. Calcination was performed at temperature 1200℃ for 2 hours in the air. The as-calcined samples were palletized and sintered at temperature 1250℃ for 2 hours in the air. The temperature was increased at a rate of 5℃ per minute. To define crystal structure, magnetic properties, and microstructure, the samples were characterized by X-ray diffraction (XRD), vibrating sample magnetometer (VSM), and the scanning electron microscope (SEM), respectively.

Effect of Heat Treatment Temperature on Rare-earth Elements Diffusion Process in Nd-Fe-B Sintered Magnets

Jaehyuk Kim[1,3*], Dong Hwan Kim[1], Sangchul Lee1, Donghwan Kim[2], Sang Hyub Lee[2], Dalhyun Do[3], Jeongmin Kim[1†]

[1]Division of Nanotechnology, DGIST, 333 Techno Jungang-daero, Hyeonpung-eup, Dalseong-gun, Daegu 42988, Republic of Korea

[2]R&D Center, Star Group, Daegu 42714, Republic of Korea

[3]Department of Advanced Materials Engineering, KEIMYUNG UNIVERSITY, 1095, Dalgubeol-daero, Dalseo-gu, Daegu, Republic of Korea

E-mail: jkim@dgist.ac.kr

Commercially used Nd-Fe-B sintered permanent magnets have been widely used in various applications such as hard disc drives, wind power generators, efficient air-conditioner compressors and motors for electric vehicles. Since these applications are often used in high-temprature environments, the required coercivity and remanence have been simultaneously obtained by using the heavy rare earth (HRE) grain boundary diffusion process (GBDP). In this study, we report the heat treatment temperature dependence of magnetic properties as a start to reduce the HRE content of GBDP-based high performance magnets. TbH coated commercial Nd-Fe-B sintered magnets were annealed under various temperatures and the coercivity and remanence were systematically measured. Further description of the microstructure will be discussed in detail.

Keywords: Grain boundary diffusion process / Nd-Fe-B / heavy rare earth / TbH / coercivity / remanence

Characterization and electromagnetic absorbing properties of sol-gel-processed $Sr_3Co_2Fe_{24}O_{41}$ hexaferrites-epoxy composites

Jae-Hee Heo*, Ji-Hye Lee, Young-Min Kang†
Department of Materials Science and Engineering, Korea National University of Transportation, Chungju, 27469, Republic of Korea
*Corresponding author email: ymkang@ut.ac.kr

$Sr_3Co_2Fe_{24}O_{41}$ hexaferrite powders were prepared through sol-gel synthesis and calcination at 1150–1260 °C. Almost single Z-type hexaferrite could be obtained at calcination temperature (T_{cal}) range in 1225–1245 °C. Below and above the temperature range, more than two types of hexaferrites phases were formed. Complex permittivities and permeabilities spectra (ε', ε", μ', and μ") of these calcined hexaferrite powders-epoxy (10wt%) composites were measured via network analyzer. Electromagnetic (EM) wave absorption properties were calculated based on the ε', ε", μ', and μ" spectra and analyzed by plotting reflection loss (RL) spectra and RL maps of the composite samples. Direct RL measurements confirmed that the calculations for RL spectra or RL maps derived based on transmission theory were very reliable. The Z-type hexaferrite-epoxy (10wt%) composites, where the powder calcined at 1230 °C, exhibited ferromagnetic resonance (FMR) at ~3.0 GHz and a strong EM wave absorbing performance with RL_{min} < -60 dB at around the FMR frequency. Z-type hexaferrite–epoxy composite is a highly promising material for EM absorption in the gigahertz band (2-10 GHz).

Acknowledgements: This work was supported by Korea National University of Transportation in 2021.

Tuning of electromagnetic wave absorption properties of Zn-Zr-substituted M-type hexaferrite-epoxy composites

Jae-Uk Kim*, Young-Min Kang†
Department of Materials Science and Engineering, Korea National University of Transportation, Chungju, 27469, Republic of Korea
*Corresponding author email: ymkang@ut.ac.kr

We report on synthesis, characterization, and electromagnetic (EM) wave absorption properties of Zn-Zr-substitued M-type Sr-hexaferrites (SrM). The hexaferrite powders with nominal chemical composition of $SrFe_{12-2x}Zn_xZr_xO_{19}$ (x = 0 – 2.0) were prepared by conventional solid-state reaction routes. The hexaferrite powder and epoxy binder were mixed at a 9:1 wt% ratio, and the mixtures were pressed into disk and toroidal shaped green compacts, respectively, and cured at 180 °C for 20 min air. M-H curves were measured using a B-H loop tracer on the disk samples. The real and imaginary parts of permittivities (ε', ε") and permeabilities (μ', μ") were measured on the toroidal samples using a vector network analyzer (E5063A, Keysight) with an airline kit in the frequency range from 0.1 to 18 GHz.

XRD analysis revealed that the solubility limit of Zn-Zr substitution into the M-type structure was about x = 1.0. The μ" spectra for the series of samples are presented in Fig. 1(a). Reflection losses (RLs) indicating the electromagnetic wave absorption performance were analyzed based on the ε', ε", μ', and μ" spectra. The EM absorption area could be figured out in the RL maps plotted as a function of the sample thickness (d) and frequency (f) for the composite samples. The RL spectra at the optimal thickness are plotted at Fig. 1(b). The coercivity, ferromagnetic resonance (FMR) frequency, and frequency range of the EM absorption decreased in large steps for an increasing substitution *x* of up to 0.9, and then decreased slightly with increasing *x* for 1.0 ≤ *x* ≤ *1.1. All these parameters are closely related to one another, and the changes are due to the magnetic crystalline anisotropy* change caused by the Zn-Zr substitution. The sample with x=0.9 exhibited a high absorption in the X-Band (8-12 GHz) with the lowest reflection loss of < 45 dB, and the sample with x = 0.8 exhibited EM absorption performance satisfying RL < 19 dB at 11 < f < 18 GHz. Tuning of EM absorption frequency could be achieved by Zn-Zr substitution, which gradually reduces the magnetic anisotropy, the FMR frequency, and the EM absorbing frequency area. It is believed that Zn-Zr substituted M-type Sr-hexaferrites are very promising candidates for X (8–12 GHz) and Ku band (12–18 GHz) EM absorbers.

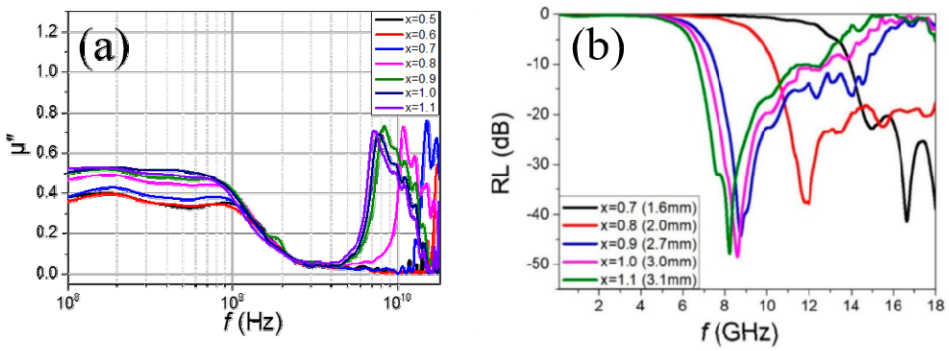

Fig. 1. (a) Imaginary part of permeability (μ") and (b) Reflection loss (RL) spectra of $SrFe_{12-2x}Zn_xZr_xO_{19}$ (x= 0.5, 0.6, 0.7, 0.8, 0.9, 1.0, 1.1)-epoxy composites

Comparison of magnetic properties of nickel powder according to magnetic field strength

Min Ji Shin[1*], Su Jeong Park[1], Akshay Kumar[1], Kavita Kumari[2],
Seok Hwan Huh[3*] and Bon Heun Koo[4†]

[1]Department of Materials Convergence and System Engineering, Changwon National University,
Changwon, Gyeongnam, 51140, Republic of Korea

[2]Industrial Technology Research Institute, Changwon National University,
Changwon, Gyeongnam, 51140, Republic of Korea

[3]Department of Mechatronics Conversion Engineering, Changwon National University,
Changwon, Gyeongnam, 51140, Republic of Korea

[4]School of Materials Science and Engineering, Changwon National University,
Changwon, Gyeongnam, 51140, Republic of Korea

[*]Corresponding Author - bhkoo@changwon.ac.kr

Nanomaterials are receiving a lot of attention these days. Transition metal elements such as iron (Fe), cobalt (Co) and nickel (Ni) have promising applications in the scientific community and for high utilization of optoelectronic materials in magnetic devices, magnetic memory bits, magnetic sensors and high-density data storage devices. showed In particular, among all magnetic elements, ferromagnetic Ni with low magnetic crystal anisotropy improves magnetic properties, which is useful for manufacturing various magnetic devices. Nickel, which has high saturation magnetization and low coercive force, has a high magnetic flux density and is easily reversible, was used in this study. Powders are prepared by solution synthesis, using $NiCl_2 \cdot 6H_2O$, NaOH, $N_2H_4 \cdot H_2O$, etc. at the right temperature, The strength of the magnetic field was changed as the reaction proceeded. After the specified time has elapsed, the generated powders are washed several times with deionized water and ethanol. Then dry using a vacuum oven. The collected samples are analyzed for composition and microstructure through XRD and high-resolution SEM, and the hysteresis curve is identified through the PPMS equipment. At this time, through the strength of the applied magnetic field, the evaluation of the magnetic properties of each sample can be compared.

Keywords: Magnetic Properties, Nickel, Powders, Magnetic, PPMS

The magnetic properties of Fe-Ni Nanoparticles according to the shape and strength of magnets

Su Jeong Park[1*], Min Ji Shin[1], Akshay Kumar[1], Kavita Kumari[2], Seok Hwan Huh[3*] and Bon Heun Koo[4†]

[1]Department of Materials Convergence and System Engineering, Changwon National University, Changwon, Gyeongnam, 51140, Republic of Korea

[2]Industrial Technology Research Institute, Changwon National University, Changwon, Gyeongnam, 51140, Republic of Korea

[3]Department of Mechatronics Conversion Engineering, Changwon National University, Changwon, Gyeongnam, 51140, Republic of Korea

[4]School of Materials Science and Engineering, Changwon National University, Changwon, Gyeongnam, 51140, Republic of Korea

[*]Corresponding Author - bhkoo@changwon.ac.kr

The properties of magnetic nanoparticles are affected by various factors such as particle size and shape, chemical composition, and crystal lattice. Among them, as the size of the magnetic nanoparticles decreases and the shape anisotropy increases, the magnetic recording density, material life, etc. are improved, so research on the magnetic nanoparticles is currently being conducted. Iron-nickel alloys, transition metal alloys selected in this experiment, are considered important in the field of wireless communication devices. Samples are prepared by solution synthesis using $FeCl_2 \cdot 4H_2O$, $NiCl_2 \cdot 6H_2O$, $N_2H_4 \cdot H_2O$, NaOH etc. Magnets of various shapes and strengths are used in the process of generating nanoparticles. After the appropriate time has elapsed, when the sample is formed, it is washed several times with deionized water and ethanol. Then dry using a vacuum oven. The collected samples are analyzed for composition and microstructure through X-ray Diffraction. Then, the surface and particle size of the samples are analyzed through high-resolution SEM, and the hysteresis curve, the saturation magnetization and the coercive force are identified through the Physical Property Measurement System equipment.

Keywords: magnetic properties, Fe-Ni alloy, Fe-Ni Nanoparticles, nanopowders

Ferromagnetic ReRAM in Sr(Fe,Co)O_x

Venkata Raveendra Nallagatla, Harisankar S, and Chang Uk Jung*
Department of Physics and Memory and Catalyst Research Center,
Hankuk University of Foreign Studies, Yong-in 17035, Korea

Redox based Resistive random-access memory (RRAM) devices is considered as one of the most promising candidates for the next generation nonvolatile memory due to its excellent storage capacity, high scalability, robust retention, good endurance, and stability [1,2]. Recent research shows that it has applicability in neuromorphic networks as an artificial synapsis is one of the major breakthroughs of the recent investigations [2]. Recently, we introduced brownmillerite $SrCoO_{2.5}$ and $SrFeO_{2.5}$ as a novel material platform to harness exceptional oxygen ion transport properties for resistive switching memory devices *for the first time* [3,4]. For $SrFeO_{2.5}$, we were able to demonstrate an excellent resistive switching performance with high endurance (> 10^6 cycles), fast switching speed (10 ns) and high uniformity in key switching parameters [4,5]. In this contest, compound with substitution of Co at the Fe lattice of $SrFeO_3$ is also found to be potential material for the resistive switching devices with excellent magneto-electrical coupling [6]. $SrFe_{1-x}Co_xO_3$ (SFCO) gained attention recently due to its redox-driven topotactic transformation with a brownmillerite nonmagnetic phase to perovskite ferromagnetic phase [7]. The solid-solution system SFCO exhibit antiferromagnetic-to-ferromagnetic transition as a function of Co concentration with a high Curie temperature of (T_C= 300K). $SrFe_{1-x}Co_xO_3$ shows multiple magnetic phases varying from helimagnetic to cluster glass for lower Co concentrations (0≥ x ≤0.07), whereas the system switches to ferromagnetic state for higher (x> 0.2) values [6,7]. In the present work we are interested to explore the electrical manipulation of magnetism and magnetic properties of PLD grown epitaxial SFCO thin films by varying the Co content as well as oxygen stoichiometry for the development of the high-quality magneto-electric switching devices.

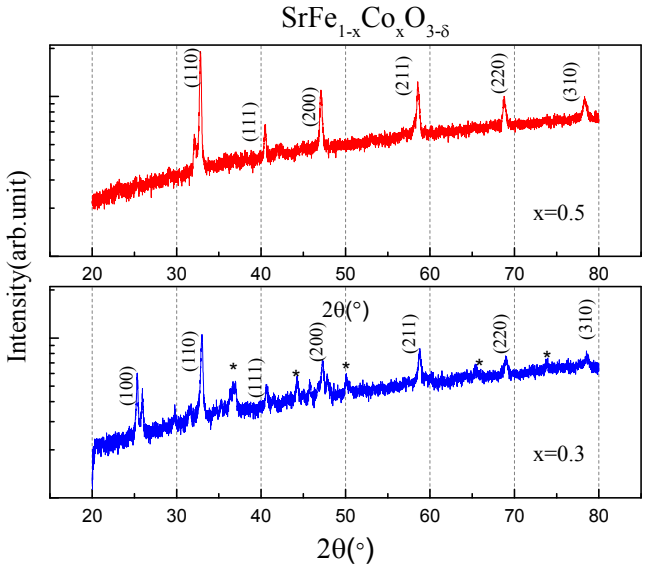

Figure 1. X-ray diffraction pattern of the $SrFe_{1-x}Co_xO_{3-\delta}$ bulk material with x=0.5 and x=0.3

References

[1] S. Pi, C. Li, H. Jiang, W. Xia, H. Xin, J. J. Yang, and Q. Xia, Nat. Nanotechnol. 14, 35 (2019)

[2] V. Raveendra Nallagatla, J. Kim, K. Lee, S. Chul Chae, C. Seong Hwang, C. Uk Jung, Cite This ACS Appl. Mater. Interfaces 12 (2020) 41740–41748.

[3] O.T. Tambunan, K.J. Parwanta, S.K. Acharya, B.W. Lee, C.U. Jung, Y.S. Kim, B.H. Park, H. Jeong, J.Y. Park, M.R. Cho, Y.D. Park, W.S. Choi, D.W. Kim, H. Jin, S. Lee, S.J. Song, S.J. Kang, M. Kim, C.S. Hwang, Appl. Phys. Lett. 105 (2014) 0–5.

[4] S.K. Acharya, R.V. Nallagatla, O. Togibasa, B.W. Lee, C. Liu, C.U. Jung, B.H. Park, J.Y. Park, Y. Cho, D.W. Kim, J. Jo, D.H. Kwon, M. Kim, C.S. Hwang, S.C. Chae, ACS Appl. Mater. Interfaces 8 (2016) 7902–7911.

[5] S. Kumar Acharya, J. Jo, N. Venkata Raveendra, U. Dash, M. Kim, H. Baik, S. Lee, B. Ho Park, J. Sung Lee, S. Chul Chae, C. Seong Hwang, C. Uk Jung, Nanoscale 9 (2017), 10502-10510 .

[6] Y. W. Long, Y. Kaneko, S. Ishiwata, Y. Tokunaga, T. Matsuda, H. Wadati, Y. Tanaka, S. Shin, Y. Tokura and Y. Taguchi, Phys. Rev. B 86 (2012), 064436-8.

[7] Shuai Ning, Qiqi Zhang, Connor Occhialini, Riccardo Comin, Xiaoyan Zhong, and Caroline A. Ross, ACS Nano 2020 14 (7), 8949-8957.

Microwave absorption properties of Co-substituted strontium W-type hexaferrites in Ka band (26.5-40 GHz)

Seung-Min Choi[1,2*], Jun-Sun Hwang[1], and Sang-In Yoo[1]

[1]Department of Materials Science and Engineering, Research Institute of Advanced Materials (RIAM), Seoul National University, Seoul 151-744, Korea

[2]Chang Sung Co Ltd, 1840-29, Seohae-ro, Cheongbuk-eup, Pyeongtaek-si, Gyeonggi-do, 17794, Korea

Currently, with the development of information-communication technology, telecommunication and microwave electronic systems operating in high frequency are being widely used. Simultaneously, electromagnetic interference (EMI) has been a challenging problem as it can cause a serious malfunction in electronic devices. To solve the EMI problem, much attention has been paid to microwave absorbers, because of a solution of electromagnetic noise and special usage in electronic devices. Among various hexaferrites, the W-type hexaferrites are well known for EMI suppression in the frequency region of gigahertz (GHz) because they have high saturation magnetization and magnetic anisotropy values. However, since strontium W-type hexaferrites (SrW) is stable at the high temperature region of 1350-1440℃ in air, it is hard to obtain a pure phase of SrW at room temperature. Thus, we fabricated Co-substituted SrW-type powders with the chemical formula of $SrFe_{(2-x)}Co_xFe_{16}O_{27}$ (x = 0.25, 0.5) in a reduced oxygen atmosphere. The complex permittivity ($\varepsilon_r = \varepsilon' - j\varepsilon''$) and permeability ($\mu_r = \mu' - j\mu''$) were measured in Ka band (26.5-40 GHz) by mixing SrW-type powders and epoxy resin. The microwave absorbing properties will be evaluated including reflection loss (RL) and presented for a discussion.

Effect of the Addition of Ni and Nb to the Fe-Co-V Alloy System on Magnetic Properties

Hyunsol Son*, Jihye Park, Hyunkyung Lee, Haein Choi-Yim†
Department of Physics, Sookmyung Women's University, Seoul 04310, Korea

Fe-Co-based alloy systems have outstanding soft magnetic properties, such as high saturation magnetization, suitable curie temperature, and low manufacturing cost. The last study added Vanadium to these FeCo alloys to make cold workable alloy without decreasing the soft magnetic properties. Further, in this study, the magnetic properties of the quaternary composition were tested by adding Ni and Nb to the three designs with the best magnetic properties among them to improve hysteresis loss, magnetic flux density, and mechanical properties. Therefore, we investigated the Fe-based alloys of Fe-Co-V-Ni and Fe-Co-V-Nb prepared by the arc-melting system with high purity metals under an Argon atmosphere. Then, we manufactured samples in bulk with a 5mm thickness, a width of 3mm, and a length of 50mm using injection casting equipment. After processing these samples, we analyzed the alloys' structural and magnetic properties using X-ray diffraction (XRD), vibrating sample magnetometer (VSM), and DC B-H loop tracer.

SM08

CoFe-MnIr 박막의 열처리 안정성 연구

김동영*, 윤석수
안동대학교 물리학과

교환 결합력을 갖는 CoFe-MnIr 박막의 열처리 온도에 따른 교환 바이어스 자기장 특성을 분석하였다. CoFe/MnIr 구조에서 열처리 온도에 따른 교환 바이어스 자기장은 300°C의 열처리 온도까지 급격하게 증가하다가 감소하는 특성을 보였다. 교환 바이어스 자기장의 급격한 증가는 박막의 증착 과정에서 무작위로 배열된 비상보성 스핀의 재정열로 설명하였으며, 열처리 온도가 300°C 이상에서 보인 교환 바이어스 자기장의 감소는 고온에서 활발하게 일어나는 Mn의 확산으로 설명하였다. MnIr/CoFe 구조에서는 교환 바이어스 자기장이 열처리 온도에 따라 일정하게 유지되었으며, 이는 박막의 증착 과정에서 한쪽으로 정렬된 비상보성 스핀의 영향으로 설명하였다. MnIr/CoFe 구조에서 측정한 교환 바이어스 자기장의 최댓값은 CoFe/MnIr 구조에서 측정한 값보다 약 반으로 감소하였으며, 이는 박막의 초기 증착 과정에서 발생한 계면 Mn의 성분비 감소로 설명하였다. 300°C에서 열처리한 박막은 MnIr/CoFe 구조와 CoFe/MnIr 구조 모두 열처리 온도까지 일정한 교환 바이어스 자기장 특성을 보였으며, 이들 결과로부터 CoFe-MnIr 박막은 열처리 온도까지 교환 결합력이 안정화 되고 있음을 확인하였다.

Thermal and Magnetic Properties of Fe-Co-B-P-Cu Amorphous Alloy System

Jihye Park*, Jiyoon Lim*, Hyunsol Son, Haein Choi-Yim†
Department of Applied Physics, Sookmyung Women's University, Seoul 04310, Korea

Over the past decades, Fe-based amorphous alloy systems have been spotlighted with remarkable soft magnetic properties such as high saturation magnetization (Ms), low coercivity (Hc), and good permeability. These advantageous properties provide a platform for essential components of commercial products.

In this study, we improved saturation magnetization and high-temperature magnetic properties by adding Cobalt at the expense of Fe. As a model system, Fe-Co-B-P-Cu amorphous ribbons fabricated by the melt-spinning method were employed. We measured the thermal properties of the alloy by using differential scanning calorimetry (DSC), including crystallization temperature. Structural characteristics of ribbons examined by X-ray diffraction (XRD) turned out to be a fully amorphous state. Magnetic properties such as Ms and Hc were inspected by vibrating sample magnetometer(VSM) and B-H loop tracer, respectively. The combination of excellent soft magnetic properties and thermal ability makes the FeCoBPCu alloys promising soft magnetic materials for industrial applications.

Effect of Composition on Magnetic Properties of CoNi Nanoparticles for Electromagnetic Waves Absorber in High-Frequencies

Drew Ahn*, Su-Jeong Suh*
Sungkyunkwan University, Department of Materials Science and Engineering, Suwon, Korea

Due to the development of the 4th industry, the problem of electromagnetic noise caused by electromagnetic waves continues to occur. Therefore, the need for electromagnetic wave absorbers in the high frequency band is becoming more important. The purpose of this study is to prepare CoNi nanoparticles for EMWs absorbers in the high frequency regions and evaluate magnetic properties according to the synthesis conditions. In order to synthesize CoNi, a polyol process that allows easy controls of composition, particle size, and shape and has small aggregation was used. In addition, to make the particle size smaller, AgNO3 was added to proceed to heterogeneous nucleation.

To investigate the characteristics, the morphology and composition of the materials are analyzed by SEM and EDS. XRD was performed to confirm the crystal structures of the prepared materials. TEM is used to determine the microstructures and sizes of the materials. Magnetic properties are confirmed using VSM. Electromagnetic properties (complex permeability, permittivity) are measured using VNA and reflection loss is calculated by transmission-line theory. CoNi nanoparticles with a different composition show feasibility for EMWs absorbers in high-frequency bands.

Keywords: polyol method, EMI absorber, CoNi nanoparticle

Improved magnetic properties of high saturation magnetization Fe-based amorphous flake-like powder core through temperature control

Hea-Ran Kim[1,2*], Min-Sun Jang[1], Yunseok Kim[2], Jae-Won Jeong[1]
[1]Powder/Ceramic Research Division, Korea Institute of Materials Science,
797 Changwondae-ro, Seongsan-gu, Changwon, 51508, Korea
[2]School of Advanced Materials Science and Engineering, Sungkyunkwan University, Suwon 440-746, Korea
[3]School of Materials Science and Engineering, Pusan National University, Busandaehak-ro 63beon-gil,
Geumjeong-gu, Busan, 46241, Korea

Fe-based amorphous soft magnetic powder is considered an ideal material for soft magnetic composite (SMC) due to its excellent magnetic properties such as a low coercivity, a high resistance, and good DC bias characteristics.[1] In general, the amorphous soft magnetic material is manufactured in the form of a ribbon or wire using a rapid solidification process. However, direct application in the form of ribbons or wires is very limited. Therefore, powder metallurgy has to be applied to manufacture soft magnetic parts with complex shapes.

Previously, the gas atomization process was attempted to make amorphous soft magnetic metal powder. However, it is difficult to maintain amorphous due to the low cooling rate, therefore a larger amount of glass-forming metals is added.[2] Accordingly, the iron content is limited and causes a low saturation magnetization. On the other hand, the melt spin process with a high cooling rate can manufacture a metal ribbon with high saturation magnetization.

However, manufacturing the powder core using the melt spin process requires a milling process. In particular, there is a problem in that the milling efficiency is low due to the low ductility of the amorphous. Most Fe-based amorphous metals become brittle after heat treatment at a temperature lower than the crystallization temperature.[3] Therefore, the temperature of pre-heat treatment is a factor that greatly affects the efficiency of the milling process, which is the next process.

In addition, the flake-like powder produced through the milling process causes a low filling rate. Therefore, high pressure is used in the pressing process, and stress is generated in the core. The core heat treatment process after pressing removes the stress generated during the pressing process, which is a factor that affects main soft magnetic properties such as magnetic permeability, core loss, and DC bias characteristics. Sufficient temperature is required to relieve the stress, but amorphous must be maintained.

Here, we demonstrated SMC using flake-like powder manufactured through the milling process and analyzed the effect of temperature during the manufacturing process. In this study, we demonstrate the milling effect according to the temperature of pre-heat treatment and analyze the soft magnetic properties according to the temperature of core annealing.

References

[1] Yoshida, S., Mizushima, T., Hatanai, T., Inoue, A. IEEE Trans. Magn. 36 (2000) 3424-3429
[2] Chen, H.S. Rep. Prog. Phys. 43 (1980) 353-432
[3] A.R. Yavari. Mater. Sci. Eng. 98 (1988) 491-493

Stable formation of high-Ms amorphous soft magnetic powder with $Fe_{82.5}B_xSi_2C_{0.5}Mo_x$ composition according to transition metal Mo and B content

Yeong Gyun Nam[1,2*], Hyun Ah Im[1,2], Su Bong An[1,2], Hearan Kim[1,3], Jung Woo Lee[2], Sangsun Yang[1], and Jae Won Jeong[1†]

[1]Metal Powder Research Division, Korea Institute of Materials Science, 797 Changwondae-ro, Seongsan-gu, Changwon, 51508, Korea

[2] Department of Materials Science and Engineering, Pusan National University, Pusan 46241, Republic of Korea

[3]Department of Materials Science and Engineering, Sungkyunkwan University (SKKU), 2066 Seobu-ro, Yulcheon-dong, Jangan-gu, Suwon, 16419, Korea

[*]Corresponding Author :jeongjw1204@kims.re.kr

As the operating frequency of the power conversion element increases for the purpose of miniaturization and weight reduction, the development of a soft magnetic material with high saturation magnetization is required to cope with the increase in current while exhibiting low iron loss even at high frequencies above 100. kHz. In the case of crystalline powder materials such as Fe-Ni, Fe-Si-Al, and Fe-Si, which were used in the past, the iron loss due to the eddy current increases rapidly as the frequency increases above 100 kHz. Current limiting use at high frequencies. Amorphous soft magnetic powder material is emerging as an alternative because it has no crystalline magnetic anisotropy and high specific resistance compared to conventional crystalline powder material and shows low iron loss even at high frequencies. A gas spraying method using an inert gas is used to prepare the amorphous powder, because the water spraying method has effects such as reducing saturation magnetization and increasing iron loss due to oxidation. In the gas injection method, it is important to achieve high GFA (glass forming ability) because the cooling rate is limited and it is difficult to make amorphous powder. In this study, a composition containing 80% or more of Fe was designed to obtain high saturation magnetization and high GFA. Based on the high-Ms Fe82.5B15Si2C0.5 quaternary composition, 1-2% of transition metal Mo and B were added in the direction of increasing GFA. The properties of the amorphous alloy were evaluated by fabricating a ribbon-shaped specimen through arc melting and melt spinning. The magnetic properties of the ribbon were measured using a vibrating sample magnetometer, a DC loop tracer and a BH analyzer. As a result, Fe82.5BXSi2C0.5Mox alloy containing Mo showed high saturation magnetization of 1.5T or more and high GFA for stable formation of high-Ms amorphous soft magnetic powder.

The Effect of Si/B Ratio on the Soft magnetic properties of $Fe_{80+x}(B_aSi_b)_{15-x}C_1Cu_1Nb_3$ Nanocrystalline Soft Magnetic Alloy

Su Bong An[1,2*], Hyun Ah Im[1,2], Yeong Gyun Nam[1,2], Sangsun Yang[1],
Jung Woo Lee[2] and Jae Won Jeong[1†]

[1]Metal Powder department, Korea Institute of Materials Sciene(KIMS),
797 Changwondae-ro Seongsan-gu, Changwon 51508, Korea
[2]Department of Materials Science and Engineering, Pusan National University, Pusan 46241, Republic of Korea
[*]E-mail of Corresponding Author: jeongjw1204@kims.re.kr

In this study, we attempted to optimize the composition of Fe-based nanocrystalline alloys with high saturation flux density, low coercivity and low core loss. To improve the saturation flux density, the alloy used in experiment is made up of over 80 at% of Iron. As the iron content of the alloy increases, the metalloid content of the alloy decreases, resulting in a decrease in glass forming ability(GFA). To improve the GFA and to obtain high Bs, we have researched to achieve optimal composition by adjusting the ratio of Boron and Silicon(a : b, a=1~5, b=1). Moreover, the metalloids elements, Carbon, and the transition element, Niobium, are added. The transition element, Nb, is known as an important element of nanocrystals by impeding a grain growth distinctly. The Cu can be a base of nanocrystalline alloy to form nucleation sites where nanocrystals occur. We fabricated a ribbon using Rapid Solid Process (RSP). To find optimal temperature for heat treatment analyzed using Differential Scanning Calorimetry, DSC. After that, we measured coercivity, permeability, core loss and saturation flux density using DC Loop Tracer, BH Analyzer and Vibrating-sample magnetometer(VSM). The results of that, we found optimized components of alloy, Si can improve GFA and the alloy of B : Si = 5 : 1 has remarkable magnetic properties. Based on these results, a way of adjusting ratio of components could deserve for designing alloys.

Keywords: Soft magnetic materials, Rapid solid process, Glass forming ability, Nanocrystals, Magnetic

Influence of C or Nb Addition on Magnetic Properties in NANOMET-based Alloy System

Jiyoon Lim*, Minkyung Seong*, Hyunsol Son, Halim Choi, Haein Choi-Yim†
Department of Applied Physics, Sookmyung Women's University, Seoul 04310, Korea

Until the present, Fe-based amorphous soft magnetic alloy systems have desirable properties such as low coercivity(H_C), high saturation magnetization(M_S), and good permeability. Because of these excellent properties can be applied to various components of inductors, magnetic cores, motors, and so forth. Especially Fe-Si-B-P-Cu alloys, as known as NANOMET, have attracted interest in variable soft magnetic properties such as high saturation magnetic flux density(B_S), and low manufacturing cost. However, NANOMET alloys have the limits of low glass-forming ability(GFA) and mechanical processing.

In this study, to improve the limits of soft magnetic properties and glass forming ability(GFA) on NANOMET alloys, we investigated the effect of C and Nb addition on the NANOMET-based alloy system. Using the induction-melting method with high purity metals, we prepared the alloys and produced ribbon samples by the melt-spinning process under the argon atmosphere. We analyzed the as-quenched ribbon's thermal and structural properties using differential scanning calorimetry(DSC) and X-ray diffraction(XRD). Measuring magnetic properties of the ribbons used vibrating sample magnetometer(VSM) and DC B-H loop tracer.

Electromagnetic Wave Absorption Film Incorporated with FeCo Nano-chained Particles

Mi Se Chang[1,2*], Min-Sun Jang[1], Sang-Sun Yang[1], Chong Rae Park[2], Byeongjin Park[3], Jae Won Jeong[1], and Young-Tae Kwon[1†]

[1]Metal Powder Department, Korea Institute of Material Science (KIMS), Changwon, Republic of Korea
[2]Department of Materials Science and Engineering, Seoul National University, Seoul, Republic of Korea
[3]Functional Composites Department, Korea Institute of Material Science (KIMS), Changwon, Republic of Korea
[*]E-mail: ykwon87@kims.re.kr

The wireless communication has revolutionized to meet the consumer demands in communication and mobility where the fifth generation (5G) telecommunications are rapidly developing for reliable data transmission and better connection in users. However, serious health hazards and malfunctioning in devices has become one of the issues when operating at high frequency bands around 26-30 GHz. Notable attempts have been made to solve these problems through recent breakthroughs in electromagnetic wave absorbing materials (EWAMs), composed of dielectric and magnetic materials for eliminating or attenuating electromagnetic waves. From this point of view, FeCo-based soft magnetic alloys is particularly attractive EWAMs due to their performances, including high saturation magnetization (M_s) of 2.45 T, small coercivity (H_c), and complex permeability. In addition, a structural modulation of the soft magnetic materials provides the magnetic anisotropy, resulting in enhancing the limit of ferromagnetic resonance (f_{mr}) to achieve high initial permeability.

Here, we prepare the FeCo nanochains using a highly-productive thermal plasma synthesis to be utilized as an electromagnetic absorber with exceptionally low reflection loss in the high frequency bands. The composition of FeCo nanochains ranging from 7:3 to 3:7 shows high saturation magnetization of 151 – 227 emu g^{-1}. Subsequently, the planetary ball milling is also implemented for a shape modulation in order to enhance the complex permeability and the reflection loss performance. The shape-modulated FeCo nanochains offer the enhancement in both the real and the imaginary part of the complex permeability. The shape modulation is one of the technological advancements in improving the complex permeability of FeCo alloys.

Keywords: Electromagnetic absorbing materials, FeCo nanochain, Thermal plasma synthesis, Shape modulation, and Permeability

Effect of Nb/Zr co-addition on the Microstructure and Magnetic Properties of $Fe_{77.5}Si_{11.5}B_{7.5}Nb_xZr_{3-x}Cu_1$ nanocrystalline soft magnetic Alloys

Hyun Ah Im[1,2*], Subong An[1,2], Yeong Gyun Nam[1,2], Sangsun Yang[1],
Jung Woo Lee[2] and Jae Won Jeong[1†]

[1]Metal Powder department, Korea Institute of Materials Sciene(KIMS),
797 Changwondae-ro Seongsan-gu, Changwon 51508, Korea
[2]Department of Materials Science and Engineering, Pusan National University, Pusan 46241, Republic of Korea
[*]E-mail of Corresponding Author: jeongjw1204@kims.re.kr

Soft magnetic materials require magnetic properties such as high permeability(μ), high saturation magnetic flux density(B_s), and low core loss. Silicon electronical is widely used due to high saturation flux density and low material cost, however it is difficult to satisfy low coercivity (H_c) and low core loss. Soft magnetic Fe-Si-B-Nb-Cu (Finemet) nanocrystalline alloys have been used as magnetic components in high frequency transformers, inductors due to their low coercivity, high permeability. Comparing to Silicon electronical Finemet has low saturation magnetic flux density(1.23T). Therefore, it is inevitable to develop Fe-based nanocrystalline soft magnetic materials with high saturation magnetic flux density and excellent soft magnetic properties. Nanocrystalline materials have the best soft magnetic properties when the crystal size is 10-15 nm. The purpose of this study is to minimize grain size and to enhance the soft magnetic properties. Zr distributed in amorphous residual matrix suppress grain growth, increasing the permeability and lowering the core loss and coercivity. Nb atoms also suppress grain growth and impending Fe_2B formations. However, Nb is problematic in terms of cost. To improve cost problem, we design our nanocrystlline alloys substitute Nb with Zr. Also according to previously studies **W. Lu et al**., it has been reported that simultaneous co-addition of transition elements resulted in a significant reduction in particle size to 10-20 nm. In this study, nanocrystalline ribbons with a composition of $Fe_{77.5}Si_{11.5}B_{7.5}Nb_xZr_{3-x}Cu_1$(x=0-3) have been fabricated by rapid-quenching melt spinning and thermal annealing. The ratio of (Zr/Nb) effects on microstructure and magnetic properties. Among the alloys investigated in this work, $Fe_{77.5}Si_{11.5}B_{7.5}Nb_1Zr_2Cu_1$ nanocrystalline ribbon annealed at 580 ^oC exhibits excellent soft-magnetic properties including low coercivity, low core loss, and high saturation magnetization. The uniform nanocrystallization in $Fe_{77.5}Si_{11.5}B_{7.5}Nb_1Zr_2Cu_1$ alloy has been also confirmed through high-resolution TEM analysis.

Keywords: soft magnetic materials. nanocrystalline, amorphous, magnetic properties, microstructures

Magnetic properties of Fe@SiO_x soft magnetic composites after high-temperature heat treatment

Jong-Min Park[1,2*], Min-Sun Jang[1], Bonuk Koo[1,2], Hea-Ran Kim[1,3], Young-Tae Kwon[1], Sangsun Yang[1], Jung Woo Lee[2], and Jae Won Jeong[1†]

[1]Metal Powder Department, Korea Institute of Materials Science (KIMS),
797 Changwondae-ro, Seongsan-gu, Changwon 51508, Korea
[2]School of Materials Science and Engineering, Pusan National University,
2, Busandaehak-ro 63beon-gil, Geumjeong-gu, Busan, 46241, Republic of Korea
[3]Department of Materials Science and Engineering, Sungkyunkwan University (SKKU),
2066, Seobu-ro, Jangan-gu, Suwon-si, Gyeonggi-do 16419, Korea

Soft magnetic composite (SMC) has the advantages of excellent magnetic properties and the three dimensions shape core manufacturing with insulation coated Fe powder [1]. In addition, SMC is attractive because it can overcome the output density limit of the currently produced electric motors made with two dimensions shape electrical steel plate. In the case of SMCs, comprising Fe@PO_4 powders, which is currently widely used, heat treatment above 650 °C damage of insulation properties. In order to solve this problem, this study focused on manufacturing SMC with low core loss characteristics, excellent magnetic properties, and maintaining insulation at heat treatment above 650 °C. Herein, SiO_2 coating was performed on the surface of Fe powder to reduce eddy current loss [2]. Fe powder was coated with tetraethyl orthosilicate by sol-gel method, and core was prepared by pressing and heat treatment for 1 hour at 600 °C, 700 °C, and 800 °C in the argon atmosphere. The phase identification was carried out by X-ray diffractometer (XRD) and the insulation coating layer was measured by scanning electron microscope and energy dispersive X-ray spectroscopy. Also, magnetic characteristics were figured out through vibrating sample magnetometer (VSM) as well as the core loss value were compared for each frequency band; 0.05 kHz, 0.4 kHz, and 1 kHz using AC BH analyzer (AC) and DC BH loop tracer (DC). XRD patterns were observed the α-Fe peak, VSM results suggested that the saturation magnetization value was reduced, which confirmed the existence of coating layers. The results of AC and DC measurements on the cores heat-treated at 600 °C, 700 °C, and 800 °C have presented that core loss increase rate is higher for the Fe@PO_4 than that for the Fe@SiO_2 because SiO_2 has superior ability to retain the coating layer at high temperature. Therefore, SiO_2 coated Fe powder has potential in high temperature atmosphere applications.

Keywords: soft magnetic composite, sol-gel, magnetic properties, heat treatment

References

[1] Liya Li et al., J. Alloys compd., **805**, 609-616 (2019).
[2] Sounghun Lee et al., IEEE Trans. Power Syst., **53**, 1-4 (2017).

Enhanced permeability of Fe-based amorphous powder core through the positioning of fine carbonyl iron powder at inter-particle voids

김혜란[1,2*], 장민선[1], 남영균[1,3], 김윤석[2], 양상선[1], 김용진[1], 정재원[1†]
[1]한국재료연구원 금속분말연구실
[2]성균관대학교 신소재공학과
[3]부산대학교 신소재공학과
[†]Corresponding author: Dr. Jea Won Jeong (E-mail: jeongjw1204@kims.re.kr)

In this presentation, we demonstrate hybrid mutimodal soft magnetic composite (SMC) comprising gas-atomized spherical amorphous powder (AP) and carbonyl-iron powder (CIP), and present enhanced electromagnetic properties of them. The CIPs are selectively incorporated in the voids between APs, and deforms during compression, effectively reducing the pores resulting in a high packing density of the core, where CIPs magnetically bridge APs each other and helping magnetic domain rotation much efficiently. Addition of 20 wt% CIP in the SMC showed constant effective permeability of 57 up to 1 MHz, a remarkable 63% increase compared with the AP core, while DC bias superimposing retention level of 61% was secured in the help of high magnetization of CIPs. In addition, effect of SiO_2 surface insulation, prepared by sol-gel process on the high-frequency magnetic properties of hybrid SMCs were also evaluated. Conclusionally, it has been revealed that high-frequency eddy current loss of the hybrid core is originated from intra-particle eddy currents, and inter-particle eddy currents are negligibly small. We believe that our approaches of AP/CIP multimodal hybrid SMCs are effective way of achieving high permeability as well as DC bias characteristics at high frequencies, and it will be highly beneficial for the miniaturization of power inductor.

Keywords: soft magnetic composite, amorphous powder, carbonyl iron powder, surface insulation, multimodal core

Strain dependent magentic properties of two dimensional 1T-VSe_2

Jicheol Son, Brahim Marfoua* and Jisang Hong†
Department of Physics, Pukyong National University, Busan 48513, Korea
E-mails: *hongj@pknu.ac.kr

We investigated the biaxial strain dependent magnetic properties of two dimensional (2D) VSe_2 single layer using the density functional theory. The ferromagnetic state of the pristine VSe_2 monolayer was preserved under the applied strain. Also, the pristine VSe_2 monolayer had an in-lane magnetic anisotropy of -0.47 meV/cell. The in-plane anisotropy was maintained in both tensile and compressive strain. However, the magnitude of magnetic anisotropy was dependent on the strain type. For instance, the in-plane magnetic anisotropy decreased under compressive strain whereas the opposite behavior appeared under tensile strain. We also explored the strain dependent Curie temperature. The pristine structure had a Curie temperature (T_C) of ~ 237K. By applying strains, the exchange energy was enhanced and subsequently, the T_C was increased as well. Particularly, we found that the T_C increased to 323 K under the tensile strain of 3%. Our finding illustrates the role of the strain in achieving tunable magnetic properties for potential spintronics and straintronics applications in the 2D 1T-VSe_2.

Acknowledgment: This research was supported by the Basic Science Research Program through the National Research Foundation of Korea (NRF) funded by the Ministry of Science, ICT and Future Planning (2019RA21B5B01069807).

Magneto-crystalline anisotropy of Co/Pt thin film: Ti insertion vs capping

Gyeong-Hye Kim*, Thi H. Ho, Soon Cheol Hong, and S. H. Rhim
Department of Physics and Energy Harvest-Storage Research Center, University of Ulsan, Republic of Korea

Magneto-crystalline anisotropy (MCA), originating from spin orbit coupling (SOC), is one of important properties for spintronics applications [1-3]. Here, MCA energy (EMCA) of Co/Pt thin film with Ti insertion or capping is studied using density functional theory. For both cases, two types of stacking sequence are considered, AB- and ABC-stacking (Fig. 1). EMCA of Ti capping is twice as large as that with Ti insertion. Moreover, both cases exhibit larger EMCA in AB-stacking than ABC-stacking. MCA is investigated in the flamework of the perturbation theory [4], where occupation change of bands is responsible. In particular, we analyze occupation change of low lying Ti d-states for all cases.

References

[1] S. Wolf et al., Science **294**, 1488 (2001).
[2] I. et al., Rev. Mod. Phys. **76**, 323 (2004).
[3] A. Brataas et al., Nat. Mater. **11**, 372 (2012).
[4] Ding-Sheng Wang et al., Phys. Rev. B **47**, 14932 (1993).

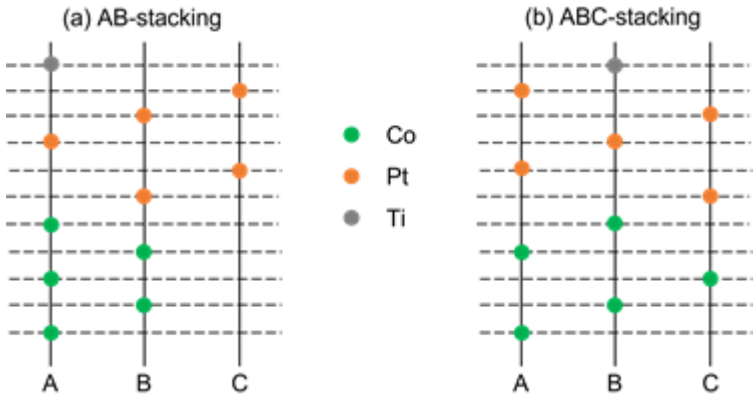

Fig. 1. Schematic diagram of stacking sequence of Co/Pt/Ti,
(a) AB- and (b) ABC-stacking. Each sphere denotes as green (Co),
orange (Pt) and Grey (Ti). Co/Pt/Ti consists of 5 layers of Co and Pt, and one layer of Ti.

First-principles study of shift current mechanism in various inversion-broken systems

Bumseop Kim[1*], Noejung Park[1*], Jeongwoo Kim[2†]
[1]Department of Physics, Ulsan National Institute of Science and Technology, Ulsan, 689-798 Korea
[2]Department of Physics, Incheon National University, Incheon, 406-772 Korea

Bulk photovoltaic effect characterized by the generation of a steady photocurrent without the aid of external *p-n* junction has attracted a lot of attention due to its novel physics and potential for high-performance solar cell device. We briefly introduce basic theory of bulk photovoltaic effect and show the electronic origin and photocurrent mechanism in organic molecular solids (TTF-CA), hybrid halide perovskite (MAPbI3 and FAPbI3), and transition metal dichalcogenides (TMDs). For TTF-CA, we show the electronic origin of the photovoltaic property of TTF-CA at low temperature (< 81 K). In the high-temperature phase, despite a net zero current, a non-vanishing shift current can be generated by the interchain effect. In addition, we find that the ferroelectric polarization of the hybrid halide perovskite is largely dominated by the ionic contribution of the molecular cation. In contrast, the photovoltaic nature is mostly determined by the intrinsic electronic band properties near the Fermi level, originating from iodine to lead atoms (inorganic backbone). At last, we investigate the underlying physics of the large bulk photovoltaic effect of the one-dimensional WS_2 nanotube and present the possibility of giant shift current over four times larger than the experimental value in the near-infrared region. Our results provide a fundamental understanding of intriguing bulk photovoltaic materials and pave a way for their practical applications.

Ultrafast Resonant Magnetic Responses of Non-magnetic 2D Semiconductors to Low-Frequency Optical Fields

Mahmut Sait Okyay*, Bumseop Kim, Noejung Park
UNIST, Dept. of Physics, 44919, Ulsan, South Korea

All-optical helicity-dependent switching of magnetism has attracted broad attention from the perspective of non-magnetic fast control of spins [1],[2]. We examine ultrafast spin dynamics of two-dimensional non-magnetic semiconductors, particularly focusing on alteration of material's time-reversal and valley symmetries driven by a circularly polarized light. Monolayer MoS_2 was selected as an exemplary system and the real-time time-dependent density functional theory (rt-TDDFT) calculations were carried out, together with a model Hamiltonian analysis. As a distinction from some of the previous reports, this study was circumscribed to the non-excitonic regime, i.e., an interval of frequency values below the band gap.

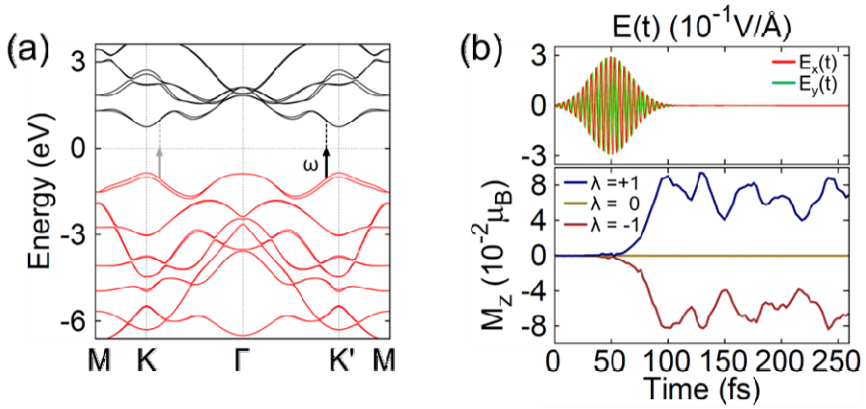

Fig. 1: (a) The band structure of MoS_2. (b) The real-time profile of the laser pulse (upper panel) and the induced magnetization as a response to left circular (λ=+1), right circular (λ=-1) and linear (λ=0) polarized laser field (lower panel). A finite magnetization remains after the pulse fades away at 100fs. The frequency of the applied field is selected as half of the band gap as depicted by an arrow in (a).

Our real-time *ab initio* calculations show that a circularly polarized light can induce a net magnetization in a non-magnetic two-dimensional material. We demonstrate that the magnetic responses are particularly amplified when the applied electric fields are in resonance with the spin-flipping band transition between valence and conduction bands through the second harmonic of the light. We forecast that a tunable spin dynamics can be achieved from these non-magnetic semiconductors when the light of the resonant frequency is combined with a proper setting of a few parameters such as field strength, pulse duration and the magnitude of spin-orbit coupling.

References

[1] A.R. Khorsand, M. Savoini, A. Kirilyuk, A.V. Kimel, A. Tsukamoto, A. Itoh, and T. Rasing, Physical Review Letters 108 (12), 1–5 (2012).

[2] A. Hassdenteufel, C. Schubert, B. Hebler, H. Schultheiss, J. Fassbender, M. Albrecht, and R. Bratschitsch, Opt. Express 22, 10017-10025 (2014).

Tunability of Structure and Magnetism in Heusler $Mn_{3-x}Co_xGa$ ($0 \leq x \leq 1$)

Quynh Anh Thi Nguyen*, Thi H. Ho, S. C. Hong, and S. H. Rhim
Department of Physics and Energy Harvest Storage Research Center,
University of Ulsan, Ulsan 44610, Republic of Korea.

Mn_3Ga has drawn interest in spintronics for potential applications due to large perpendicular magnetic anisotropy, high Curie temperature (~760 K), and low magnetization [1]. Motivated by previous studies on tunability of magnetism through transition metal substitutions in Mn_3Ga [2,3], we investigate magnetic and structural properties of Mn_3Ga upon Co substitution using first-principles calculations. In the absence of Co, Mn_3Ga is in tetragonal phase. With Co, both tetragonal and cubic phases occur. $x \leq 0.5$, tetragonal phase is preferred, while $x > 0.5$, cubic one is favored. Co magnetic moment in two phases exhibit different magnetic behaviors. In tetragonal phase, unlike other Co compounds, Co magnetic moment nearly vanishes. On the other hand, in cubic phase, it retains a usual moment at about 1 μ_B. Nearly vanishing Co magnetic moment in tetragonal structure is elucidated phenomenologically by the magnetic exchange coefficient [4], where coupling between Co and Mn is much smaller than cubic one. Furthermore, anomalous Hall conductivities (AHC) are investigated for x = 0, 0.5, and 1. The magnitude of AHC is about 100~500 S/cm, where the sign change occurs at $0.5 < x < 1$.

References

[1] B. Balke, G. H. Fecher, J. Winterlik, and C. Felser, Appl. Phys. Lett. **90**, 152504 (2007).
[2] V. Alijani, J. Winterlik, G. H. Fecher, and C. Felser, Adv. Mater. **99**, 222510 (2011).
[3] K. Lee, W. Yoo, Q. A. T. Nguyen, H.-W. Bang, H. Kim, M. Klui, S. H. Rhim, and M.-H. Jung, J. Alloys Compd. **858**, 158288 (2021).
[4] H. Yoon, T. J. Kim, J.-H. Sim, S. W. Jang, T. Ozaki, and M. J. Han, Phys. Rev. B **97**, 125132 (2018).

Mn_4C의 전이온도에 대한 제일원리 계산

이준규*, 이민영, 김상훈, 임성현, 홍순철†
울산대학교 물리학과, 울산시 남구 대학로 93, 44610

최근 새로운 자기 화합물 Mn_4C을 한국재료연구원에서 최초로 합성하는데 성공하였다[1]. 자기 구조는 준강자성으로 예측되었고, XRD 실험 결과에 의하면 Mn_4C은 격자 상수 a = 3.868 Å인 입방체 페로브스카이트로 보고되었다[1].

본 연구에서는 제일원리계산을 통해 자체일관계산을 수행하고 이를 통해 얻어진 고유함수에 Liechtenstein 공식[2]을 적용하여 교환 상호작용 상수를 계산하였다. 제일원리계산과 교환 상호작용 상수 계산은Open Source Package for Material Explorer(OpenMX)를 이용하였고, 전이온도에 대한 계산에는 VAMPIRE를 이용하였다. 전자들 간의 교환 상관 퍼텐셜은 Perdew-Burke-Ernzerhof에 의해 공식화한 일반물매근사(GGA-PBE)를 사용하였다. 자체일관계산에는 27 x 27 x 27 Monkhorst-Pack k-point 그물을 사용하였으며, 고유함수를 평면파로 전개하기 위한 차단에너지는 600 Ry를 주었다.

자체일관계산 결과, 입방체 Mn_4C의 격자 상수는 a=3.780 Å로 실험치 a=3.868 Å보다 0.088Å 만큼 작았고, 준강자성 상태가 가장 안정한 것으로 계산되어 실험결과와 일치하였다. 이 때 Mn_I과 Mn_{II}의 자기 모멘트는 서로 반평행이고 각각 3.878 μ_B, 1.470 μ_B로 계산되어 총 자기모멘트는 0.313 μ_B/unit-cell로 얻어졌다. 이 값은 실험치 0.258 μ_B/unit-cell[1] 보다 0.055 μ_B/unit-cell 만큼 컸다.

Mn_4C의 전이온도 계산에 앞서 대표적인 강자성체인 Fe, Co, Ni의 전이온도 계산을 수행하여 본 계산의 신뢰성을 확인하였다. 교환 상수 를 모두 더한 뒤 최인접 원자 z로 나눈 값을 평균 교환 상수 라 하면 $J=\frac{1}{z}\Sigma_{<ij>}J_{ij}$로 표현되며, 이 때 각 물질의 평균 교환 상수는 $J_{Fe}=6.7284\times10^{-21}J/pair$, $J_{Co}=5.4201\times10^{-21}J/pair$, $J_{Ni}=3.0540\times10^{-21}J/pair$이었다. 거리에 따른 교환 상수 계산 값을 그림 1에 나타내었다. 교환상수를 이용하여 Landau-Lifshitz-Gilbert(LLG) 방정식[3]과 평균장근사[2]로 계산된 전이온도를 표 1에 정리하였으며, Landau-Lifshitz-Gilbert(LLG) 방정식으로 계산된 값이 평균장근사로 계산된 값보다 실험값과 더 잘 일치함을 알 수 있었다.

표 1. 대표적인 자성원소 Fe, Co, Ni에 대해 계산된 전이온도(T_c) [K]

	MFA	LLG	Experimental
Fe (bcc)	1300	1036	1042
Co (hcp)	1570	1337	1388
Ni (fcc)	442	698	630

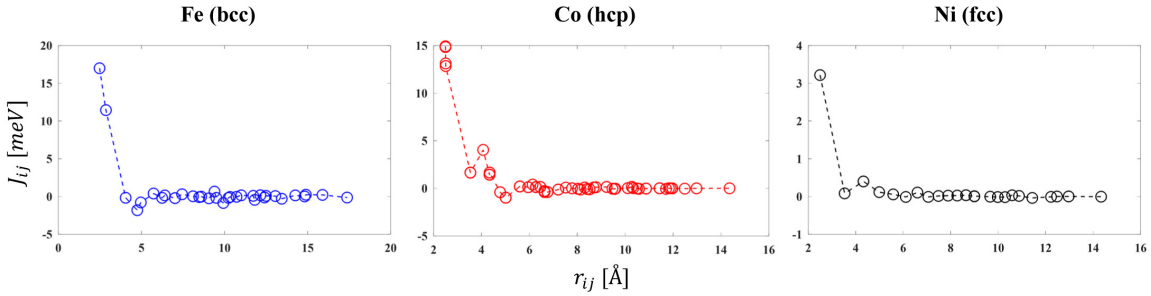

그림 1. Fe, Ni, Co 원자 간 거리에 따른 교환 상수.

Acknowledgment: 본 연구는 정부(과학기술정보통신부)의 재원으로 한국연구재단-미래소재디스커버리사업의 지원을 받아 수행된 연구임 (NRF-2016M3D1A1027831).

References

[1] Ping-Zhan Si, Hui-Dong Qian, Hong-Liang Ge, Jihoon Park, and Chul-jin Choi, *Appl. Phys. Lett*. 113, 049903 (2018).

[2] A. Terasawa, M. Matsumoto, T. Ozaki, and Y. Gohda, *J. Phys. Soc. Jpn*. 88, 114706 (2019).

[3] R F L Evans *et al* 2014 *J. Phys.: Condens. Matter* 26 103202 (2014)

Anomalous Hall and Nernst effect in Mn_3Al under volume change

Guihyun Han[1*], Minkyu Park[2], Soon Cheol Hong[1,3], and S. H. Rhim[1,3]
[1]Department of Physics, University of Ulsan, Republic of Korea
[2]Research Institute of Basic Science, University of Ulsan, Republic of Korea
[3]Energy Harvest-Storage Research Center, University of Ulsan, Republic of Korea

Anomalous Hall effect (AHE) is believed to be occur with non-zero magnetization. However, even with zero magnetization, anomalous Hall conductivity can exist [1-3]. In this context, AHC of compensated ferrimagnet Mn_3Al under hydrostatic pressure is investigated using *ab initio* calculations. Even with volume change, magnetization is still compensated. Volume change shifts bands thereby peak of density of states (DOS) moves under Fermi level. Anomalous Nernst conductivity (ANC) is also calculated. DOS, AHC, and ANC shows peaks in specific energy range where van Hove singularity (vHS) is found. To analyze interplay of ANC, AHC, and vHS, Fermi velocity and Berry curvature is investigated on Fermi surface.

References

[1] Hua Chen, Qian Niu and A. H. MacDonald, Phys. Rev. Lett. **112**, 017205 (2014).
[2] Yang Zhang, Yan Sun, Hao Yang, Jakub Zelezny´, Stuart S. P. Parkin, Claudia Felser, and Binghai Yan, Phys. Rev. B **95**, 075128 (2017).
[3] Libor Šmejkal, Rafael González-Hernández, T. Jungwirth, J. Sinova, Sci. Adv. **6** eaaz8809 (2020).

Oral Session 1

'Spintronics / Magnetization Dynamics'

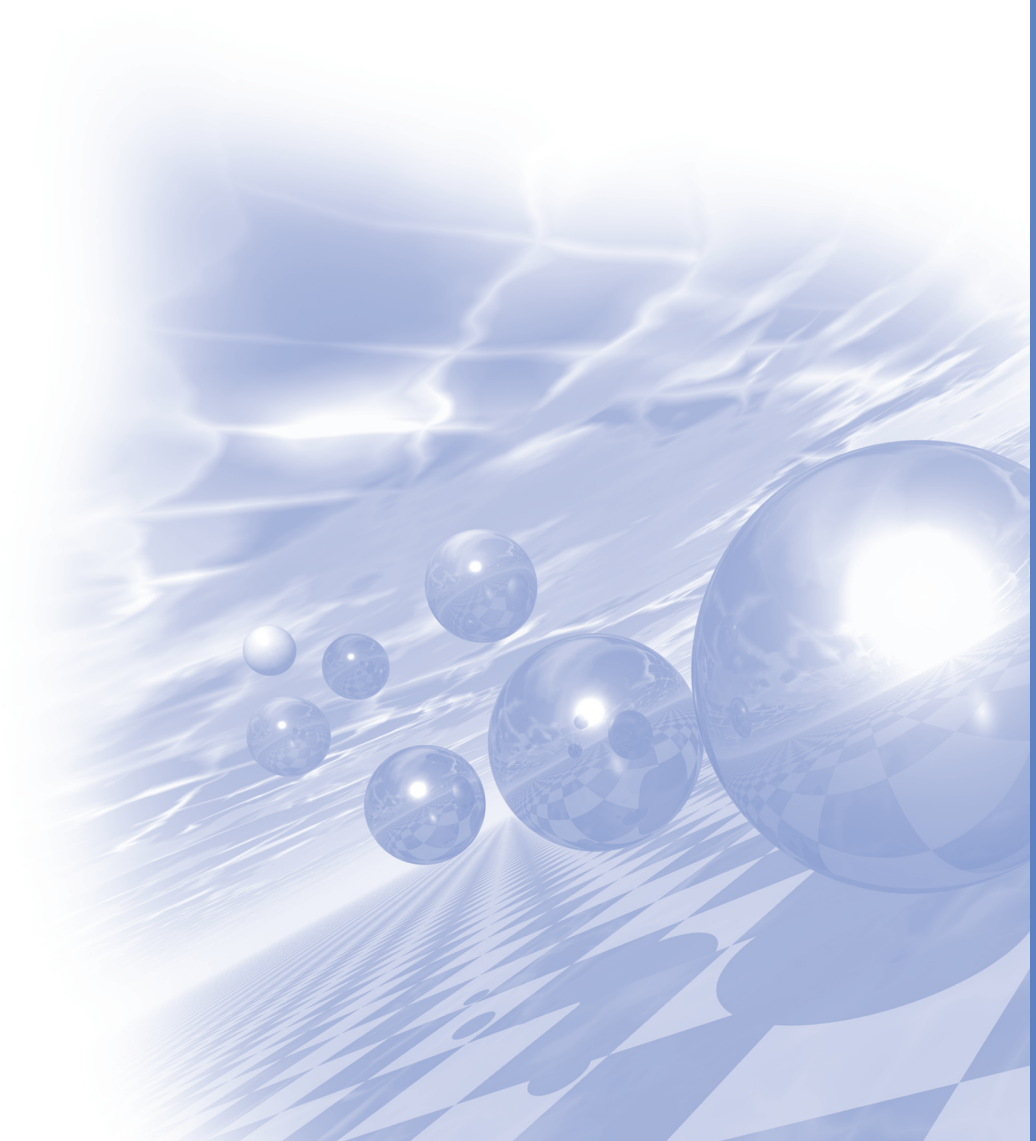

Stabilization and dynamical switching of skyrmions and skyrmioniums in magnetic hemispherical shells

Jaehak Yang[1*], Hyeon-Kyu Park[1], Gyuyoung Park[1], Claas Abert[2,3], Dieter Suess[2,3] and Sang-Koog Kim[1†]

[1]National Creative Research Initiative Center for Spin Dynamics and Spin-Wave Devices, Nanospinics Laboratory, Research Institute of Advanced Materials, Department of Materials Science and Engineering, Seoul National University, Seoul 151-744, South Korea

[2]Faculty of Physics, University of Vienna, Vienna, Austria

[3]University of Vienna Research Platform MMM Mathematics - Magnetism - Materials, University of Vienna, Vienna, Austria

[†]Correspondence and requests for materials should be addressed to S.-K. K. (sangkoog@snu.ac.kr)

We explored the topological magnetic textures of vortices, skyrmions, and skyrmioniums in magnetic hemispherical shells by varying surface-normal uniaxial magnetic anisotropy constant (Ku), Dzyaloshinskii-Moriya interaction (DMI) constant (D_{int}), and the shell diameter 2R. For given values of 2R, the combination of Ku and Dint plays a crucial role in the stabilization of those different spin textures [1]. With decreasing 2R, the geometrical confinement of hemispherical shells more significantly affects the stabilization of skyrmions owing to curvature-induced DM-like interaction. This effect is contrastingly dependent on the sign of Dint: skyrmion formation is more favorable for positive Dint values, whereas it is less favorable for negative ones. A quite promising feature is that skyrmions can be stabilized even in the absence of intrinsic DMI for 2R < 25 nm. We also explored characteristic dynamic properties of skyrmions excited by in-plane and out-of plane oscillating magnetic fields. Similar to the fundamental dynamic modes found in planar dots, in-plane gyration and azimuthal spin-wave modes as well as out-of-plane breathing modes were found, but additional higher-frequency hybrid modes also appeared due to coupling between radially quantized and azimuthal spin-wave modes. Finally, we found a switching behavior of skyrmion polarity through a transient skyrmionium state using very-low-strength AC magnetic fields [2]. This work provides further physical insight into the static and dynamic properties of skyrmions in curved-geometry nanodots and suggests potential applications to low-power consumption and ultra-high-density information-storage devices.

References

[1] J. Yang, C. Abert, D. Suess, and S.-K. Kim, *Sci. Rep.* **11**, 3886 (2021).

[2] J. Yang, H.-K. Park, G. Park, C. Abert, D. Suess, and S.-K. Kim, *Phys. Rev. B* (accepted).

Spin accumulation and spin-orbit torque driven by Rashba-Edelstein effect in an InAs quantum well layer

Won-Bin Lee[1*], Seong-Been Kim[2,3*], Kyoung-Whan Kim[3], Kyung-Jin Lee[1],
Hyun-Cheol Koo[2,3†], Gyung-Min Choi[4,5‡]

[1]Department of Physics, Korea Advanced Institute of Science and Technology, Daejeon 34141, South Korea
[2]KU-KIST Graduate School of Converging Science and Technology, Korea University, Seoul, 02841, South Korea
[3]Center for Spintronics, Korea Institute of Science and Technology, Seoul 02792, South Korea
[4]Department of Energy Science, Sungkyunkwan University, Suwon 16419, South Korea
[5]Center for Integrated Nanostructure Physics, Institute for Basic Science (IBS), Suwon 16419, South Korea
[*]These authors contributed equally to this work.

For semiconductor spintronics, efficient spin generation in semiconductor and spin transfer to ferromagnetic metal (FM) are essentially required. Two-dimensional electron gas (2DEG) of semiconductor quantum wells is a promising system for generating spin via Rashba–Edelstein effect (REE) because of its strong inversion symmetry breaking. In this study, we investigate spin accumulation through REE and spin Hall effect (SHE) in the 2DEG of an InAs quantum well. We use spatial- and vector-resolved measurements of spin, which reveals that REE dominates SHE in 2DEG. Furthermore, REE in 2DEG induces a spin-orbit torque on FM in a 2DEG/insulator/FM heterostructure. Using vector- and time-resolved measurements of FM magnetization, we determine a sizeable field-like torque, which is attributed to the phonon-mediated spin transport from 2DEG to FM.

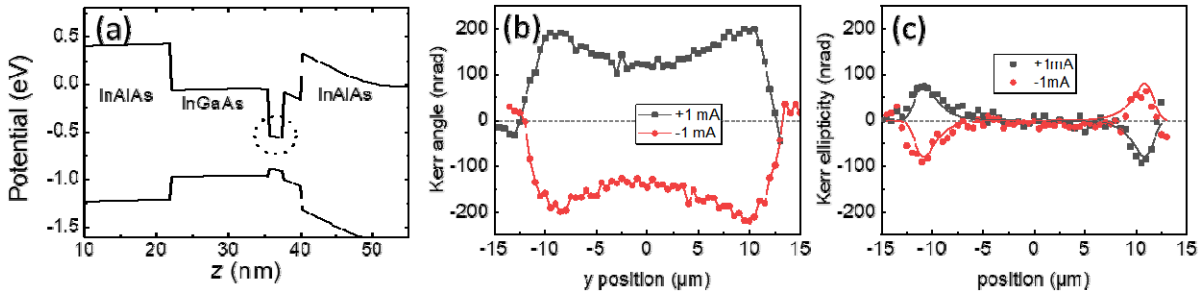

Fig. 1. Optical detection of spin accumulation in InAs quantum well.
(a) A quantum well of InAs 2 nm is formed between InGaAs and InAlAs layers. A 2DEG channel with the InAs quantum well is fabricated. (b) The REE-driven y-polarized spin along the channel position. (c) The SHE-driven z-polarized spin along the channel position. Black/red colors are with charge current of ±1 mA, corresponds to a 2D current density of 50 A m^{-1}.

Coupling of Distant Magnets via Standing Acoustic Waves

Kyongmo An[1*], Changsoo Kim[1], Chanyong Hwang[1], Olivier Klein[2]
[1]Quantum Spin Team, Korea Research Institute of Standards and Science, Daejeon, Republic of Korea
[2]Université Grenoble Alpes, CEA, CNRS, Grenoble INP, Spintec, 38054 Grenoble, France

We study the coupled dynamics of two magnets on both sides of a thick crystal spacer. The magnets communicate by acting as "speakers" as well as "microphones" for sound waves. The system can be tuned into tripartite hybridization by carefully tuning the two ferromagnetic resonance frequencies to a degenerate acoustic resonance of the crystal. Being in a regime where the interaction strength between the magnetic excitations is larger than their decay rate, the system is in the strong coupling regime in which the entire system of magnetization and lattice can only oscillate coherently. We show there that illumination of the bright and dark collective modes by a uniform microwave field depends on the parity of the phonon mode, which decides if the lattice displacement at the position of the two magnets is out-of-phase or in-phase. Depending on the parity of intermediate standing lattice waves, the interference is constructive or destructive, giving rise to the bright and dark collective modes.

Our solid state realization consists of a half-millimeter thick slab of nonmagnetic gallium gadolinium garnet coated epitaxially on both sides by the ferrimagnet yttrium iron garnet. The magnetoelastic coupling in itself is not so strong so it is the exceedingly high crystal quality and long lifetimes of magnons and phonons in garnets that are key to unveil strong coupling. The frequency can be tuned by applied magnetic field strength and directions, while we measure the magnetization dynamics electrically by induced voltages in Pt contacts and microwave absorption. Besides the electrical detection, we demonstrate the detection of magnon-phonon coupling using the inelastic light scattering technique. By virtue of the local detection, we obtain the line width close to the intrinsic value of magnetic damping. A clear signature of magnon-phonon coupling will be shown as a dip in the magnetic resonance spectrum.

Coexistence of coupling-induced transparency and absorption in photon-magnon coupling

Biswanath Bhoi*, Bosung Kim, Hae-Chan Jeon and Sang-Koog Kim†
National Creative Research Initiative Center for Spin Dynamics and Spin-Wave Devices, Nanospinics Laboratory,
Research Institute of Advanced Materials, Department of Materials Science and Engineering,
Seoul National University, Seoul 151-744, Republic of Korea

The prospect of a full control of electromagnetic waves has inspired intensive efforts on light-matter interactions in recent years. The two most interesting phenomena applicable to quantum information technology [1-3] are electromagnetically induced transparency (EIT) and absorption (EIA), arising from atomic coherences occurring in light–matter interaction. it is very difficult to construct a single system that exhibits both the phenomena simultaneously, due to the fact that conventional coupled systems often lack independent tenability and controllability of their eigenmodes. It is interesting to find a plausible method that would permit a single device where energy conversion or information transfer can be maximized through coupling induced transparency (CIT) or absorption (CIA).

In this regard, we fabricated a hybrid system composed of magnons (collective spin excitations) and microwave photons (electromagnetic excitations) in order to make them strongly couple with flexibly tailored dispersion and damping rate [4-5]. Here we report on an experimental demonstration of the simultaneous occurrence of CIT and CIA phenomena in photon-magnon coupling (PMC) in a planar hybrid system that consists of a yttrium iron garnet (YIG) film and a multi-concentric inverted-split-ring resonator (ISRR). The coexistence of both CIT and CIA behaviors is ascribed to magnon-mediated interactions between individual decoupled (or very weekly coupled) ISRRs. In order to capture the generic physics of the magnon-mediated photon-photon interactions, we made an analytical model based on competition between the coherent and dissipative photon-magnon interactions, which model precisely reproduces the experimental findings. The coupling parameters associated with the CIT/CIA behaviors are tunable by changing the direction of applied static magnetic fields and the position of YIG film on the microstripline. The demonstration of multifunctional characteristics of PMC in a single planar device provides a crucial stepping stone for the development of more complex, controllable, and sensitive photon-magnonics devices that are highly demanded in the development of quantum technologies.

References

[1] H. J. Kimble, Nature, 453, 1023 (2008).
[2] Z. Xiang, S. Ashhab, J. You, and F. Nori, Rev. Mod. Phys., 85, 623 (2013).
[3] Z. Xu, S. Liu, S. Li, and X. Yin, Phys. Rev. B 99, 041104(R) (2019)
[4] B. Bhoi, B. Kim, S-H. Jang, J. Kim, J. Yang, Y-J. Cho, and S-K. Kim, Phys. Rev. B 99, 134426 (2019)
[5] M. Harder, et al. Sci. China Phys. Mech. Astron., 59, 117511 (2016).

Highly efficient heat-dissipation power driven by ferromagnetic resonance in ferrite nanoparticles for hyperthermia application

Jae-Hyeok Lee*, Yongsub Kim, and Sang-Koog Kim†
National Creative Research Initiative Center for Spin Dynamics and Spin-Wave Devices, Nanospinics Laboratory, Research Institute of Advanced Materials, Department of Materials Science and Engineering, Seoul National University, Seoul 151-744, South Korea

The magneto-thermal effect, which represents the conversion of magnetostatic energy to heat from magnetic materials, has been spotlighted for potential therapeutic usage in hyperthermia treatments [1-3]. However, the realization of its potential has been challenged owing to limited heating powers from magnetic nanoparticles. Here, we explored a new paradigm of magneto-thermal modality using low-power driven spin excitations followed by consequent energy dissipation, which has yet to be realized for hyperthermia applications [4]. We experimentally demonstrated that distinctly efficient heat-dissipation power driven by ferromagnetic resonance (FMR) in ferrimagnetic MFe2O4 (M = Fe, Mn, Ni) nanoparticles gives rise to a targeted temperature increment. The power is two orders of magnitude higher than that of conventional Néel-Brownian mechanism. From micromagnetic simulation and analytical derivation, we found robust correlations between the temperature increment and intrinsic material parameters, the damping constant as well as the saturation magnetizations of nanoparticles' constituent materials. Furthermore, the temperature increments were reliably manipulated by extremely low strengths of applied AC magnetic fields under resonance field conditions. Our experimental results and theoretical formulations provide for a better understanding of the effect of FMR on the efficiency of heat generation as well as a straightforward guidance for the design of advanced materials for a control of highly localized incrementation of targeted temperatures using magnetic particles for magnetic hyperthermia bio-applications.

References

[1] X. Liu et al., Theranostics. 10(8): 3793-3815 (2020)
[2] M.-K. Kim et al., Phys. Rev. Applied 9, 054037 (2018)
[3] M.-K. Kim et al., J. Appl. Phys. 125, 063901 (2019)
[4] J.-H. Lee et al., Sci. Rep. 11, 4696 (2021)

Thickness-dependent spin-orbit torques in normal metal/Nb/ferromagnet tri-layers

Min Hyeok Lee[1*], Gyungchoon Go[2], Yong Jin Kim[1], In Ho Cha[1], Gyu Won Kim[1], Taehyun Kim[1], Kyung-Jin Lee[2], and Young Keun Kim[1†]

[1]Department of Materials Science and Engineering, Korea University, Seoul 02481, Republic of Korea
[2]Department of Physics, Korea Advanced Institute of Science and Technology, Daejeon 34141, Republic of Korea

When electrical current flows to normal metal (NM)/ferromagnet (FM) heterostructures, a transverse spin current that exerting torque to the magnetization is generated [1]. This torque, called spin-orbit torque (SOT), is drawing massive attention due to its applicability for the energy-efficient writing method of a next-generation memory device. For the application of SOT to memory or logic devices, it is crucial to quantify the mechanisms of this new physical phenomenon. Most SOT studies designed the simple NM/FM bilayer structures where NM (or NM/FM interface) serves as spin current source [2-4]. Recently, the experimental system has been improved to more complicate structures containing more than one source [5, 6]. This study discussed the thickness-dependent SOT efficiency in NM/Nb/FM tri-layer structures where either NM1/NM2 or NM/FM bilayer serves as an additional spin current source. We investigate two types of NM/Nb/CoFeB tri-layer in which the NM was either Ta or Pt. The SOT value increased and saturated with increasing the Nb thickness in both series. However, there is switching polarity reversal in Pt/Nb/FM structures due to the different spin-orbit coupling signs between Pt and Nb when t_{Nb} changed around critical thickness. In contrast, there would be no such reverse in the Ta/Nb/FM structure. We confirm this polarity reversal behavior by both second harmonics and current-induced SOT switching measurements, suggesting well-designed systematical observation of the thickness dependence of SOT. These results provide a systematic understanding of the thickness-dependent SOT properties.

References

[1] I. M. Miron *et al*., Perpendicular switching of a single ferromagnetic layer induced by in-plane current injection, *Nature* 476 (2011) 189–193.

[2] J. Kim *et al*., Layer thickness dependence of the current-induced effective field vector in Ta|CoFeB|MgO, *Nat. Mater*. 12, 240-245 (2013).

[3] I. M. Miron *et al*., Current-driven spin torque induced by the Rashba effect in a ferromagnetic metal layer, *Nat. Mater*. 9, 230 (2010).

[4] W. Zhang *et al*., Role of transparency of platinum–ferromagnet interfaces in determining the intrinsic magnitude of the spin Hall effect, *Nat. Phys.* 11, 496-503 (2015).

[5] Q. Ma *et al*., Switching a Perpendicular Ferromagnetic Layer by Competing Spin Currents, *Phys. Rev. Lett*. 120, 117703 (2018).

[6] S.-H. C. Baek *et al*., Spin currents and spin-orbit torques in ferromagnetic trilayers, *Nat. Mater*. 17, 509-513 (2018)

Prediction of large anomalous Hall conductivity in a compensated ferrimagnet quaternary Heusler compound TiZrMnAl

T. Thuy Hoang[1*], Minkyu Park[2], Do Duc Cuong[3], S. H. Rhim[1] and S. C. Hong[1]
[1]Department of Physics and Energy Harvest-Storage Research Center, University of Ulsan
[2]Research Institute of Basic Sciences, University of Ulsan
[3]Department of Physics and Computer Science, Vietnam National University, Ho Chi Minh City, Vietnam
(sonny@ulsan.ac.kr, schong@ulsan.ac.kr)

Recently, a combined experimental and theoretical study has shown that anomalous Hall conductivity (AHC) can be tailored via tuning Berry curvature regardless of magnetization[1], which may pave a new way to achieve large AHC without net magnetic moment. For instance, non-negligible AHC of 330(133) Ω^{-1}cm-1 and 300 Ω^{-1}cm^{-1} were predicted in non-collinear antiferromagnetic and compensated ferrimagnetic Heusler compounds Mn_3Ge (Sn)[2] and Ti_2MnAl[3]. In this work, using the PAW and FLAPW methods implemented in VASP and Fleur codes, AHC of a ferrimagnet quaternary Heusler compounds TiZrMnAl ($F\bar{4}3m$) is studied. Among three possible structural phases[4] (Fig. 1), α-phase is energetically most stable, by energy differences of 0.34 eV/fu and 0.03 eV/fu compared to β- and γ-phase. The local magnetic moment of Mn is antialigned with those of Ti and Zr. As a result, total magnetic moment is fully compensated ($m_t = 0.0\mu_B$) in α- and β-phase, and nearly compensated

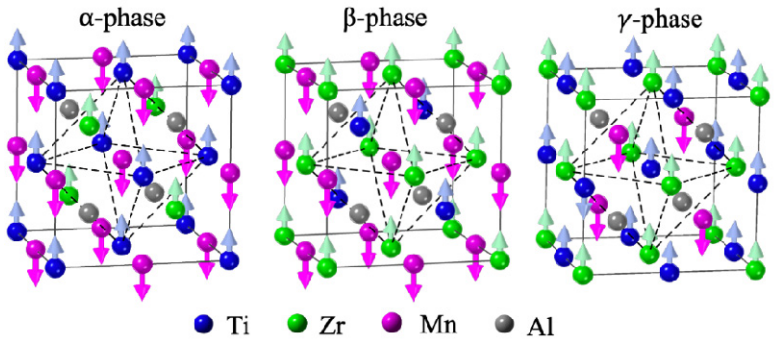

Fig. 1. Three possible structural phases of quaternary Heusler compound TiZrMnAl.

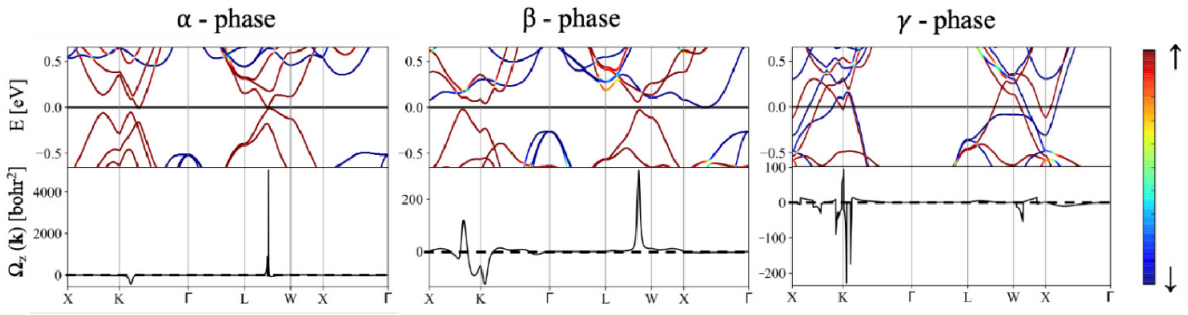

Fig. 2. Band structure and Berry curvature along the k-point symmetry lines.

(m_t = 0.1μ_B) in γ-phase. Interestingly, α-phase possesses a large AHC of 1470 $\Omega^{-1}cm^{-1}$, while β- and γ-phase show moderate AHC of 200 and 100 $\Omega^{-1}cm^{-1}$, consistently in both the PAW and FLAPW methods. The large AHC in α-phase stems from the direct gapless band along the symmetry line $\overline{LM}$, which shows a gigantic Berry curvature and nontrivial topology with non-zero Chern number x = ±1.

References

[1] K. Manna, L. Muechler, T. H. Kao, R. Stinshoff, Y. Zhang, J. Gooth, N. Kumar, G. Kreiner, K. Koepernik, R. Car, J. Kübler, G. H. Fecher, C. Shekhar, Ya. Sun, and C. Felser, Phys. Rev. X **8**, 041045 (2018).

[2] H. Yang, Y. Sun, Y. Zhang, W. Shi, S. Parkin, and B. Yan, New J. Phys. **19**, 015008 (2017).

[3] W. Shi, L. Muechler, K. Manna, Y. Zhang, K. Koepernik, R. Car, J. van den Brink, C. Felser, and Y. Sun, Phys. Rev. B **97**, 060406(R) (2018).

[4] Q. Gao, I. Opahle, and H. Zhang, Phys. Rev. Materials **3**, 024410 (2019).

자구벽 운동 임계전류의 보편성 이해

장준영[1,2*], 박민호[2], 유지성[2], 남윤석[2], 김대연[1], 민병철[1], 김세권[4], 김덕호[1*], 최석봉[2*]

[1]Center for Spintronics, Korea Institute of Science and Technology, Seoul, 02792, Republic of Korea
[2]Department of Physics and Institute of Applied Physics, Seoul National University, Seoul, 08826, Republic of Korea
[3]Department of Electrical and Computer Engineering, National University of Singapore, Singapore, 117576, Singapore
[4]Department of Physics, Korea Advanced Institute of Science and Technology, Daejeon, 34141, Republic of Korea

자구벽 메모리 소자에서 저전류 구동은 에너지 소비를 줄이고[1] 안정성을 향상[2]시키는 데 있어 중요하다. 소자는 임계 전류 이상에서 동작하는데, 임계 전류를 결정하는 요인으로 자성층의 두께[3,4], 자기 이방성 상수[4-6] 등이 있음이 알려져 있다. 기존 연구들의 경우 임계 전류와 개별 변수들의 관계를 설명하기 위한 모델에 시료의 피닝 에너지를 고려하지 않아[4,7], 소자 구동에 대한 물리적 이해가 부족하다. 본 연구는 피닝 에너지를 도입해 임계 전류의 이론 모델을 수립하고, 이를 바탕으로 얻은 중요 변수들과 임계 전류의 관계를 실험적으로 확인하고자 한다. 이를 위하여 DC 마그네트론 스퍼터 방식을 통해 Ta (5 nm) / Pt (3 nm) / Co (x) / TiOx (y) / Pt (2 nm) 의 구조에서 Co 층과 TiOx 층 두께를 바꿔가며 시료를 제작하였다. 광자기 커 효과 (MOKE) 현미경을 통해 전류 인가 자구벽 운동의 속도를 측정하여 임계 전류를 얻었다. 이론으로 수립한 관계식을 이용해, 자성층의 두께, 자기 이방성 에너지의 변화에 따른 임계 전류의 변화를 실험적으로 관찰하였고, 기존에 보고된 값들[3,8-10]과 비교하여 이 관계식에 보편성이 있음을 확인하였다. 따라서 본 연구를 통해 자구벽 구동 및 임계 전류에 대한 더 깊은 이해가 가능해, 자구벽 메모리 소자 개발에 큰 도움이 될 것으로 기대한다.

References

[1] Y. Xu et al., Handbook of Spintronics (Springer, 2016).
[2] A. Yamaguchi et al., Appl. Phys. Lett. 86, 012511 (2005).
[3] K. -S. Ryu et al., IEEE Trans. Mag. 52, 1400404 (2016).
[4] Y. Guan et al., Adv. Mater. 2007991 (2021).
[5] G. Tatara and H. Kohno, Phys. Rev. Lett. 92, 086601 (2004).
[6] Y. M. Hung et al., Appl. Phys. Express 14, 023001 (2021).
[7] S. Fukami et al., Appl. Phys. Lett. 95, 232504 (2009).
[8] Y. Guan et al., AIP Advances 7, 085123 (2017).
[9] K. -S. Ryu et al., Nat. Nanotech. 8, 527 (2013).
[10] I. M. Miron et al., Nat. Mater. 10, 419 (2011)

2021 KMS Winter Conference

Symposium 1

‘Permanent Magnetics’ & ‘Electro-Magnetic Energy Conversion’ 공동세션

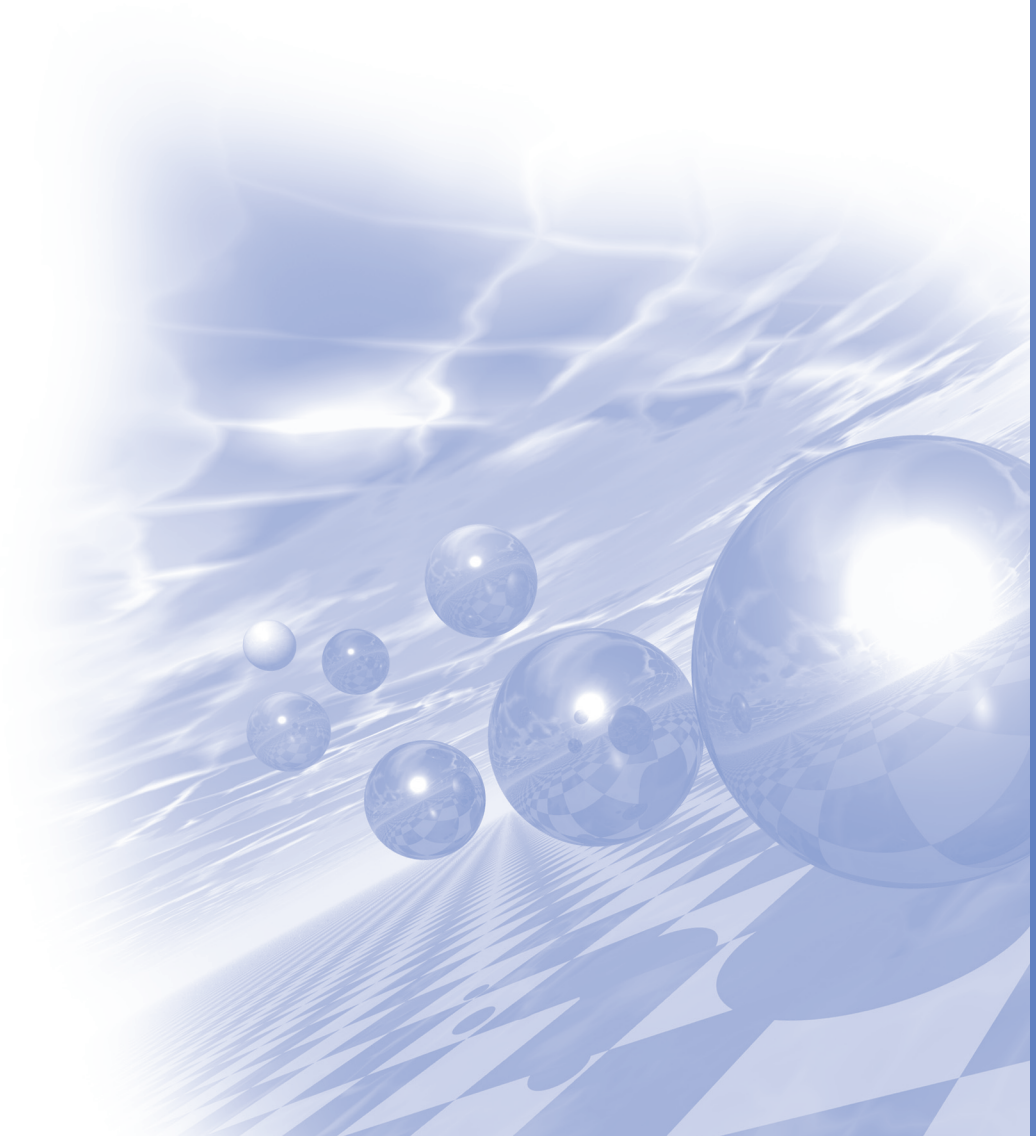

로봇용 서보모터 개발 및 고특성 분말 Soft Magnet Composite (SMC) 소재 개발에 관한 연구

양상선*, 김용진, 정재원, 권영태, 이정구
한국재료연구원, 분말재료연구본부

미래 모빌리티용 구동부품의 효율을 향상시키기 위한 다양한 연구가 시도되고 있다. 로봇용 서보모터의 경우 영구자석 회전자의 성능향상 및 연자성 고정자의 형상제어를 통한 효율을 향상시킬 수 있다. 현재 사용되는 모터의 고정자는 제한된 2차원 형상의 전기강판을 적층하여 제조되는 형태가 주를 이루고 있다. 따라서, 다양한 형상의 모터를 구현하기 위해서는 금속 분말의 표면에 절연층이 코팅된 분말 (soft magnetic composite: SMC)을 고압 성형하는 분말야급 공정 도입이 필요하다고 판단된다.

본 연구에서는 고포화자화를 갖는 수분사 순철 분말에 간단한 가수분해 방법을 통해 다층의 산화물 코팅을 진행한 SMC 를 제조하였다. 제조된 SMC 분말은 기존 Fe/PO_4 상용분말 대비 900 ^{o}C 이상의 열처리에서도 높은 자성 특성이 유지되는 것을 확인하였다. 또한, SMC 분말을 통해 제조된 코어는 낮은 투자율 특성을 갖는다는 고질적인 문제점을 해결하고자, Fe-Si-M (M = B, P, C, Mo 등)계 합금 설계를 진행하였다. 이러한 합금설계 결과를 통해 본 연구진은 Fe-Si-M 계 칩 (chip)을 제조, 순철 분말의 혼합비율에 따른 코어의 자기적 특성 연구를 수행하였다. 결과적으로 순철 분말로 제조된 코어의 투자율 ($\mu_{r,max}$ = 261) 대비 약 3배 높은 코어 ($\mu_{r,max}$ = 785)를 제작하였다.

본 발표에서는 로봇용 서보모터와 차량용 제너레이터 개발을 위한 소재 및 설계 기술 등을 전반적으로 소개하고, 형상자유도를 높은 고정자용 Fe-Si 계 기반의 분말 SMC 소재 개발 내용을 중점으로 발표하고자 한다.

Development of heat-resistant insulation coatings for pure iron SMCs (Soft Magnetic Composites)

Kwangdeok Choi[1,2], SoYeon Lee[1,3], Hyunyoung Kim[1], Jong-seung Hwang[4], Joo-youl Huh[3], Kyung-Woo Yi[2], Ji Young Byun[1*]

[1]Korea Institute of Science and Technology, Seoul, Korea

[2]Seoul National University, Seoul, Korea

[3]Korea University, Seoul, Korea

[4]Korea Polytechnic University, Gyeonggi-do, Korea

[*]jybyun@kist.re.kr

순철 SMCs (Soft Magnetic Composites)는 높은 자속 밀도, 우수한 성형성, 낮은 철손 및 높은 투자율을 나타낸다. 그러나 SMCs core를 만들기 위해 순철 분말을 가압 할 때 strain이 발생하고, 성형 공정 동안 생성된 residual strain 이 SMC core의 철손을 증가시킨다. strain을 제거하기 위해서는 고온 어닐링 공정이 필요하다. 그러나, 고온 어닐링 공정으로 SMCs 절연막의 열화로 인해 입자간 와전류 손실이 증가하여 열처리 온도에 한계가 있다. 일반적인 인산염 절연 코팅의 내열 온도는 400°C로 알려져 있어 residual strain을 제거하기에 충분하지 않다. 본 논문에서는 SMCs의 내열성을 향상시키기 위한 새로운 절연 코팅 방법을 제안하였다. 순철 분말 (Hoganas ABC100.30)의 표면을 고온 산화에 의해 산화물 물질로 코팅한다. 그리고 silicone resin을 코팅하면 내열 온도가 600°C까지 상승하는 것으로 관찰되었다. 어닐링 열처리 온도의 영향에 대한 절연층 분석 및 SMC 코어의 자기 특성의 자세한 논의는 발표를 통해 설명하고자 한다.

열간변형 공정을 이용한 고특성 희토자석 제조기술

차희령*, 김가영, 김태훈, 이정구
한국재료연구원, 분말재료연구본부

Nd계 희토자석은 자기특성이 우수하여 고출력/고효율/소형화가 요구되는 산업부품에 필수적으로 사용되고 있다. 그러나 고온 안정성 개선을 위해 첨가되는 중희토류 금속은 자원수급 및 가격 문제가 지속적으로 대두되고 있으며, 이러한 문제는 친환경 자동차, 산업용 로봇 시장의 성장과 함께 자석의 수요가 증가하면서 더 심화될 것으로 예상된다. 특히, 최근에는 중희토류 금속뿐만 아니라 향후 Nd 금속의 수급 역시 불안정해질 것으로 예상되며, 이에 사용되는 Nd의 일부를 Ce, La 등 생산량이 많고 산업에 활용도가 낮은 경희토 금속으로 대체한 Nd 저감형 자석을 개발하기 위한 연구가 주목받고 있다. 하지만, 자석에 사용되는 특정 희토류 금속을 저가의 다른 물질로 대체하게 되면 자석의 고유자기특성이 감소하여 자석의 특성이 크게 저하되는 문제가 있다. 자석의 특성을 개선하기 위해서는 결정립을 미세화하고 입계 조직을 정밀하게 제어하는 것이 중요하다. 열간변형 공정은 나노결정립을 가지는 등방성 분말을 소성변형을 통해 이방성벌크자석으로 제조하는 방법으로, 결정립 크기를 소결자석에 비해 1/10 수준으로 미세화가 가능하기 때문에 사용되는 중희토류 금속 또는 Nd를 저감하고도 자석의 보자력을 효과적으로 향상시킬 수 있는 방법이다. 본 연구에서는 고특성의 열간변형 희토자석을 제조하기 위한 미세구조 제어 기술 및 관련 연구동향을 소개하고 향후 연구 방향에 대해 논의하고자 한다.

영구자석 설계의 중요 파라미터, 인공지능에 물어보다

박현규[1*] 이재혁[1], 이제현[2], 김상국[1]
[1]서울대학교 재료공학부, 나노스피닉스 연구실
[2]한국에너지기술연구원, 플랫폼 연구실

20세기부터 지구 평균 온도가 점진적으로 증가하면서 환경 문제가 대두되고 있으며, 그 원인은 산업 발달에 따른 온실 가스 농도의 증가와 지구 온난화로 귀인되고 있다. 우리나라는 2015년 파리 협정에서 온실가스의 자발적인 감축 의무를 협약한 이래로 부분적인 수정과 목표 상향을 거치고 있으며, 이를 이행하기 위한 정책의 일환으로 전기차 보급을 전폭적으로 지원하고 있다. 그러나 전기차의 모터의 핵심 재료인 Nd 자석에 가격 및 공급이 불안정한 중희토류 원소가 전통적으로 쓰여오고 있기 때문에, 중희토류 없이도 미세구조와 같은 결정질 재료의 내재적 특성만을 이용해서 고성능의 Nd 자석을 설계하는 것이 시급하다. Nd 자석이 발명된 이래 수십 년간 실험과 시뮬레이션을 통해 미세구조와 내재적 특성 사이의 상관 관계를 물리적으로 설명하는 많은 기저 연구와 이를 실험으로 증명하는 연구들이 이루어져 왔다. 최근 컴퓨터의 발달로 미소자기전산모사를 이용하면 비교적 빠르게 대량의 데이터를 얻는 것이 가능하며, 이렇게 얻어진 데이터를 해석하는 방법론의 중요성이 대두되고 있다.

본 발표에서는 순수한 Nd 자석의 미세구조와 성능을 단기간 내에 연구할 수 있는 방안으로 미소자기전산모사 데이터에 기반을 둔 인공지능 분석 방법을 제안한다. 인공지능 분석에서는 기계학습 모델의 정확도와 품질이 중요하며, 정확도는 모델 하이퍼파라미터에 의해 결정된다. 본 연구에서는 하이퍼파라미터 최적화 과정에서 기존에 쓰이던 완전 탐색 (brute-force) 알고리즘을 담금질에 기반을 둔 휴리스틱 알고리즘으로 대체함으로써 효율성의 증대를 꾀하는 한편, 다양한 통계적 분석 방법들을 활용하여 모델의 품질을 검증했다. 이렇게 훈련된 인공지능 모델 내부를 들여다봄으로써 보자력에 영향을 미치는 파라미터의 우선 순위를 결정할 수 있었다. 더 나아가, 미소자기전산모사와 인공지능에 기반을 둔 분석은 다양한 자성 재료의 개발에 기여할 수 있을 것으로 기대된다.

References

[1] O. Gutfleisch *et al.*, *Adv. Mater.* **23**, 821 (2011).
[2] J. Jin *et al.*, *Sci. Rep.* **6**, 32200 (2016).
[3] Y. Zhang *et al.*, *Acta Mater*. **146**, 97 (2018).
[4] T. T. Sasaki *et al.*, *Acta Mater*. **84**, 506 (2015).
[5] T. T. Sasaki *et al.*, *Scr. Mater*. **113**, 218 (2016).
[6] S.-K. Kim *et al.*, *J. Magn. Magn. Mater.* **486**, 165257 (2019).
[7] H.-K. Park *et al.*, *Sci. Rep*. **11**, 3792 (2021).
[8] P. Linardatos *et al.*, *Entropy* **23**, 18 (2021).

신소재 적용 200W급 서보모터 및 1kW급 제너레이터 개발

전연도[1,3*], 이지영[1,3], 이지헌[1], 이대호[2]
[1]한국전기연구원, 전동력연구센터
[2]한국전기연구원, 절연재료연구센터
[3]과학기술연합대학원대학교, 한국전기연구원 캠퍼스

본 논문에서는 서보모터용 200W 급 전동기와 차량용 1kW 급 발전기를 대상으로 일반소재를 사용한 경우와 신소재를 사용한 경우에대해 부하 운전시 특성을 비교 분석하고자 한다. 본 논문에서 신소재라 함은 코어와 코일에 대한 두 가지를 다룬다. 코어의 경우, 규소강판을 적층하여 사용하는 것을 일반재료 코어라고 한다면 자성분말을 성형하여 만든 코어를 신소재 코어로 보았다. 코일의 경우에는 일반 에나멜 코팅 선재를 일반재료 선재라고 한다면, 특수 코팅을 통하여 내절연성을 높인 선재를 신소재 코일로 보았다. 전동기와 발전기 각각에 대해서 재료 조합에 따라 3가지 경우-(1)일반소재 코어와 코일을 사용한 경우, (2)신소재 코어와 일반 코일을 사용한 경우, (3)일반소재 코어와 신소재 코일을 사용한 경우-에 대해서 특성을 비교 분석한 내용을 본문에서 제시하도록 한다.

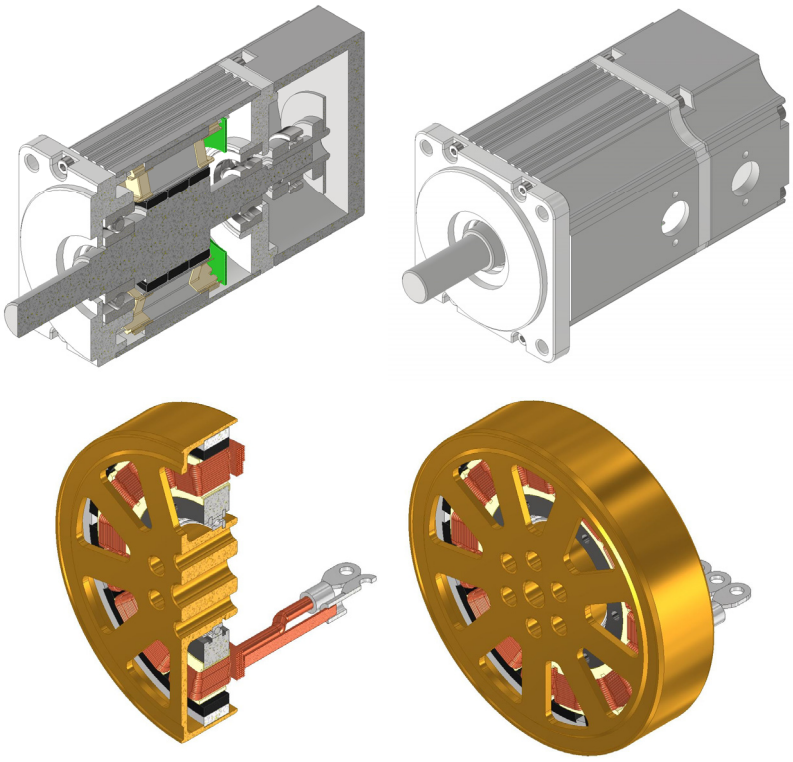

그림. 1. 개발된 200W급 전동기 (상)와 1kW급 발전기(하)

신소재 적용 200W급 서보모터 출력 특성 개선 설계

박예지[1*], 김정원[1], 이재준[2], 이주[1]
[1]전기공학과, 한양대학교, 대한민국
[2]전기공학과, 유한대학교, 대한민국

본 논문에서는 서보모터에 신소재를 적용하여 출력특성을 개선한 서보모터에 대한 연구를 진행하였다. 서보모터는 주로 제조용 로봇 및 각종 산업용 장비의 구동에 사용되며, 주어진 신호에 따라 위치, 속도 및 가속도 등을 신속하고 정확하게 제어하기 위해 사용되는 전동기이다. 과거에는 DC 서보모터가 산업분야 전반적으로 사용되었지만, 제어기술이 발달하고 유지보수 문제로 인해 현재 대부분의 서보모터는 AC 서보모터가 사용되고 있다. 공작 기계에 많이 사용되는 서보모터는 속응성, 정밀성이 가장 중요한 요소가 되며, 이를 고려한 설계가 필수적이다.

현재 상용되고 있는 타겟 서보모터 모델의 설계 제원 및 제약 사항 등의 분석을 통해 설계 인자를 선정하여 기본모델 설계를 진행하였다. 기본 모델을 바탕으로 신소재 적용을 하고 동등한 조건에서의 비교를 진행하기 위해 그림 1과 같이 개선 설계를 진행하고 시작품 제작을 통해 설계 결과의 신뢰성을 확보하였다.

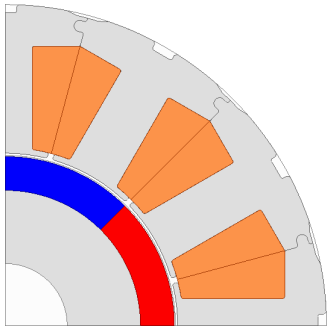

Fig. 1. 서보모터 개선 설계 모델

그림 1의 일반 재질의 설계 모델에 신소재 적용을 위해 동일 유효 부피의 Axial 타입 전동기 설계를 진행하였다. 실제 제작성을 고려하여 그림 2와 같이 Axial 개선 모델의 설계를 진행하였으며, 출력과 전류밀도를 설계 목적함수로 선정하였다. 고정자의 치 부분의 재질을 신 SMC 재질로 대체하고 유한요소 해석을 통해 특성을 비교하였다.

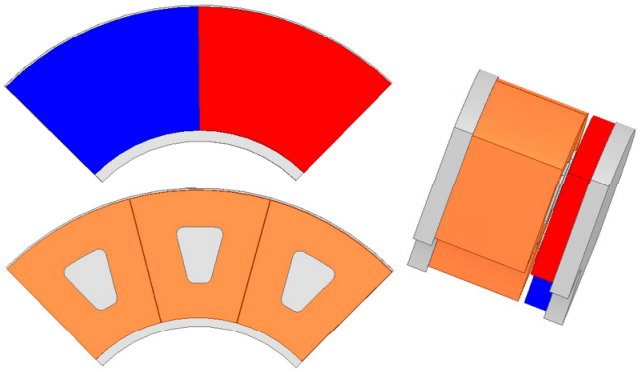

Fig. 2. 신소재 적용한 Axial 타입 서보모터 설계 모델

신소재 적용 1kW 급 제너레이터 출력 특성 개선 설계

김정원[1*], 박예지[1], 이재준[2], 이주[1]
[1]한양대학교, 대한민국
[2]유한대학교, 대한민국

Abstracts - 무인화 시대가 도래함에 따라 드론에 대한 관심이 지속적으로 커지고 있으며, 현재 드론의 운용 범위에 제약이 되는 짧은 체공시간을 늘리기 위해 배터리와 엔진을 조합한 하이브리드형 드론이 개발되는 추세이다. 이에 따라 에너지의 효율적 사용을 위해 보조 동력원으로 사용되는 배터리를 충전하기 위한 발전기의 성능 개선 연구의 필요성이 대두되고 있다. 본 연구에서는 신재료를 활용을 통한 1KW 급 드론용 AFG (Axial-flux Generator)의 출력 특성 개선 연구가 진행되었다. 각 비교 모델은 48V 배터리를 충전하기 위한 전압을 만족하도록 설계되었으며, 비교 및 분석을 위해 3D-FEA(Finite element Analysis) 시뮬레이션을 이용하여 해석을 진행하였다. 결과적으로 그림 1(b)와 같이 고정자 치 부분에 신 연자성 재료를 적용한 모델이 그림 1(a)의 일반재료 적용 모델에 비해 철손은 저감되며 출력은 증가하는 것을 확인하였다.

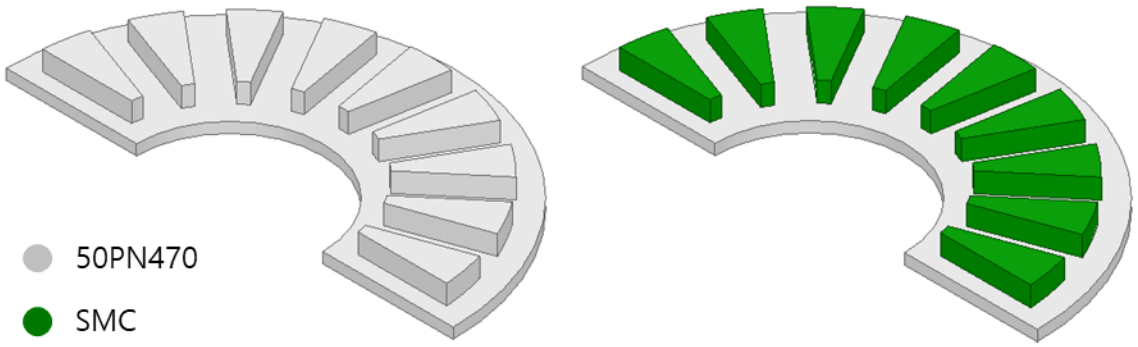

(a) (b)

그림 1. AFG의 신 재료 적용 부분 (a)일반 연자성재료 모델 (b)신 연자성재료 모델

회전 전기기계 기계적 성능 검증 프로세스 개발

Minjun Jang[1*], Hyunjun Jang[2], Junho Suh[3]
[1]Master Student, Graduate School, Dept. of Mechanical Systems Design, Pusan National University, Korea
[2]Ph. D. Candidate, Graduate School, Dept. of Mechanical Systems Design, Pusan National University, Korea
[3]Associate Professor, School of Mechanical Engineering, Pusan National University, Korea

최근 회전 전기기계의 초고속화, 경량화, 고출력화 됨에 따라 진동, 소음, 열에 대한 안정성 검증이 더욱 요구되고 있다. 따라서 본 연구를 통해 CAE 상용프로그램인 ANSYS를 기반으로 한 회전 전기기계에 대한 진동 해석 프로세스, 소음 해석 프로세스, 열 유동 해석 프로세스 개발을 하였다.

회전기계의 진동해석을 위해서 모달해석, 구조해석, 회전체 동역학 해석 순서대로 해석을 진행하며 이를 통해 위험속도 예측과 안정성 선도를 확인할 수 있다. 또한 불평형 회전체 제작시 제작오차와 재료의 불균일 등으로 인하여 회전체는 불평형 질량을 가지며, 이를 응답 해석을 통해 기계 진동을 예측할 수 있다.

소음 해석을 위해서 전자기해석, 모달해석, 조화응답해석, 방사소음 해석 순서대로 해석을 진행한다. 소음 해석 결과를 바탕으로 회전 전기기계에서 발생할 수 있는 가장 큰 소음원이 전자기력인지, 구조진동에 의한 소음인지를 예측할 수 있으며, 이 소음치가 기준 범위를 초과한다면 소음원의 설계 변경을 통해 소음을 감소할 수 있다.

열 유동 해석은 유동해석 모델링, Mesh 작업 및 민감도 테스트, 열 유동 해석 순서대로 진행한다. 열 유동해석을 통해 개발 예정 중인 회전 전기기계가 열이 잘 배출되는 구조인지를 확인할 수 있으며, 코일 발열로 인한 감자 여부 또한 예측 가능할 것으로 판단된다. 이를 통해 구조 변경을 통해 열 유동에 대한 안정성을 확보할 수 있게 된다.

후기 (Acknowledgments): 본 연구는 2021년도 정부(미래창조과학부)의 재원으로 한국연구재단의 지원을 받아 수행된 사업임. (No. 2020M3H4A3106186)

References

[1] K. N. Srinivas, R. Arumugam, IEEE, **4,** 40 (2004).
[2] D. K. Hong, B. C. Woo and D. H. Koo, IEEE, **6**, 45 (2009).
[3] D. K. Hong, B. C. Woo and D. H. Koo, IEEE (2012).
[4] D. K. Hong, B. C. Woo and B. H. Kim, Korean Society for Precision Engineering, **5** (2015).

Symposium 2

'Theory and Computational Magnetics'

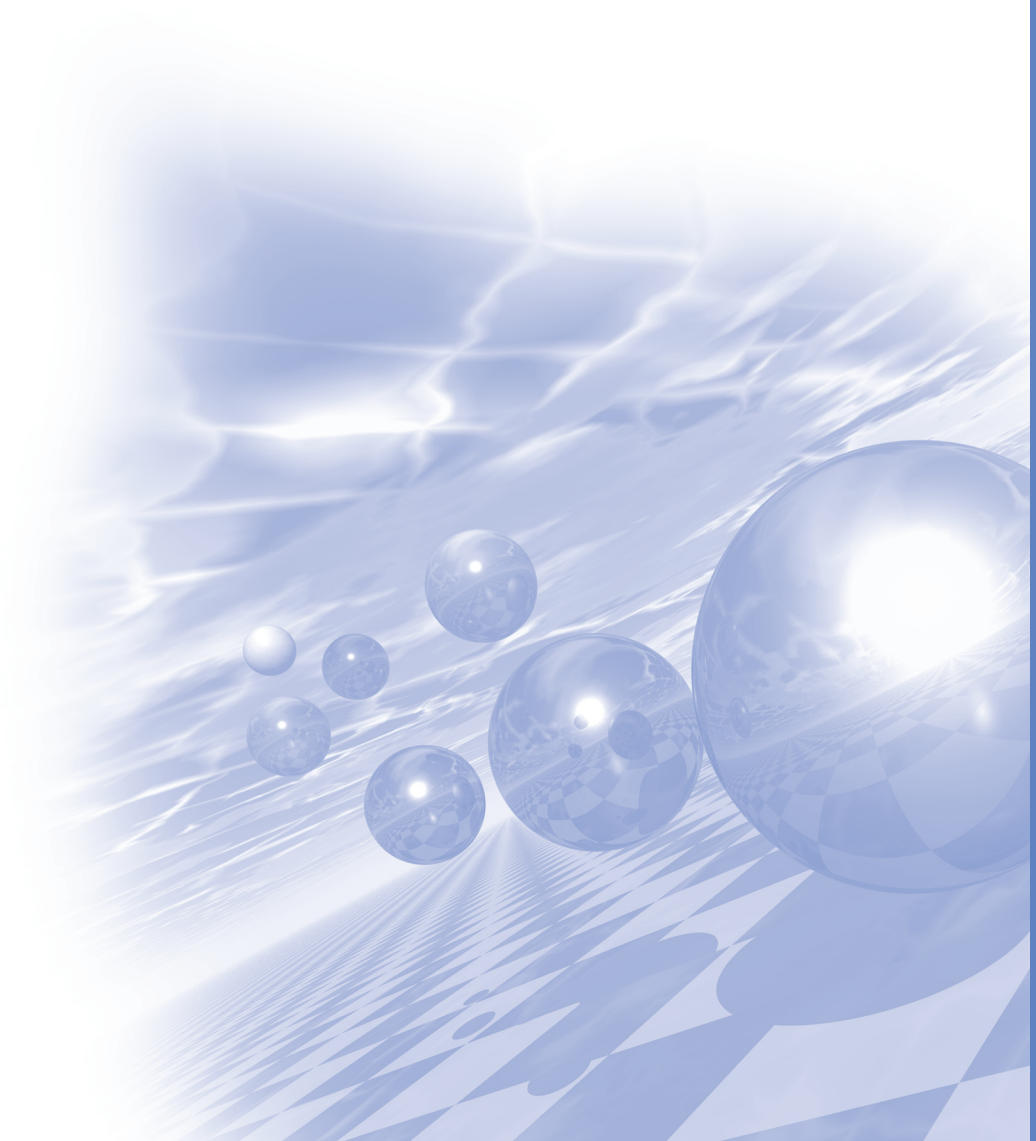

Field-induced Bose-Einstein condensation and supersolid in the two-dimensional Kondo necklace

Wei-Lin Tu[1], Eun-Gook Moon[2], Kwan-Woo Lee[1,3], Warren E. Pickett[4], and Hyun-Yong Lee[1,3,5*]

[1]Division of Display and Semiconductor Physics, Korea University, Sejong 30019, Korea

[2]Department of Physics, Korea Advanced Institute of Science and Technology (KAIST), Daejeon 34141, Korea

[3]Department of Applied Physics, Graduate School, Korea University, Sejong 30019, Korea

[4]Department of Physics, University of California, Davis, California 95616, USA

[5]Interdisciplinary Program in E·ICT-Culture-Sports Convergence, Korea University, Sejong 30019, Korea

We report our numerical calculation using two-dimensional tensor network ansatz, infinite projected entangled-pair state (iPEPS), on the 2D Kondo-necklace model where a local spin-singlet phase can be real- ized. By introducing an external magnetic field, the singlet-triplet gap reduces and eventually closes, leading to the well-known triplon condensation. Moreover, after introducing XXZ anisotropy, this model gives rise to a field-induced supersolid before entering a fully polarized phase. In 3D, the Kondo-sieve model is regarded as the spin Hamiltonian for Ba2NiO2(AgSe)2 (BNOAS), and thus we believe our numerical estimation can be realized and provide a new platform for such exotic field-induced condensation. Finally, we propose a t-J-K many-body Hamiltonian that is appropriate for exploring the expected superconductivity upon doping electrons into BNOAS.

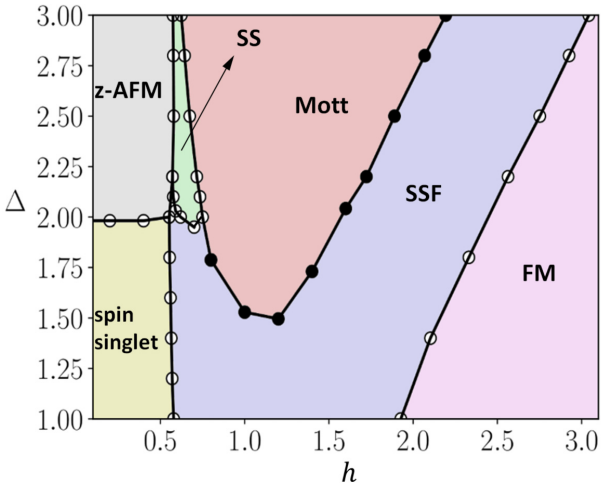

Figure 1. The anisotropy-field phase diagram for 2D XXZ Kondo necklace model

Design of $MgAl_2O_4$ Spinel-Oxide-Based Tunnel Barriers for Advanced Spintronics Devices

Kenji Nawa[1,2*], Keisuke Masuda[2], Shinto Ichikawa[3], Hiroaki Sukegawa[2], Tsuyoshi Suzuki[3], Katsuyuki Nakada[3], Seiji Mitani[2], Yoshio Miura[2,4]

[1]Graduate School of Engineering, Mie University, Japan

[2]Research Center for Magnetic and Spintronic Materials, National Institute for Materials Science (NIMS), Japan

[3]Advanced Products Development Center, Technology and Intellectual Property HQ, TDK Corporation, Japan

[4]Center for Spintronics Research Network (CSRN), Graduate School of Engineering Science, Osaka University, Japan

Tunnel magnetoresistance (TMR) in magnetic tunnel junctions (MTJs) is one of the central properties to develop high-performance spintronics devices. MgO(001) with bcc-Fe or CoFe electrodes has been mostly studied as a tunnel barrier of MTJs for the last decades because of its giant TMR ratio originating from the spin-filtering effect of Δ_1-symmetric evanescent states (s, p_z, $d_{3z^2-r^2}$ orbitals) [1], as predicted in 2001 [2,3]. However, the TMR ratio of MgO-MTJs reduces significantly by bias voltage applications, indicating a limitation of the output voltage of the MTJ. Recent experiments show that the use of a (001)-oriented spinel-type oxide, $MgAl_2O_4$, as a tunnel barrier improves the robustness of the TMR ratio under bias applications [4], but a theoretical TMR limit in Fe/$MgAl_2O_4$/Fe(001) MTJs is very small compared to the MgO-MTJs. This is because the in-plane lattice periodicity of Fe electrode is half of that of $MgAl_2O_4$ and a band-folding effect is induced in the two-dimensional Brillouin zone of the in-plane wave vector in the Fe electrode [5,6]. This effect provides additional conductive states at the Δ line in $MgAl_2O_4$-MTJ, contributing to the reduction of the TMR ratio. In this talk, we propose a combined trilayer tunnel barrier, MgO/$MgAl_2O_4$/MgO, to overcome the above issue of the small TMR limit of $MgAl_2O_4$-MTJs on the basis of the first-principles calculations.

We performed ballistic-conductance calculations in an Fe/MgO(n)/$MgAl_2O_4$/MgO(n)/Fe(001) MTJ using the non-equilibrium Green's functions method to clarify the TMR ratio under bias voltage application. Here, number of MgO layers (n-ML) is changed as n = 1, 2, 3. In the case of n = 1, a large TMR ratio of 1184% is obtained at a zero-bias voltage and this large value is almost maintained up to V = 1.2 V (see blue in Fig. 1), leading to a large voltage output. In contrast, a single barrier $MgAl_2O_4$ shows only a small TMR ratio (~125%), which is constant below V = 1.6 V (see orange in Fig. 1). These results indicate that both the models have a similar tendency in bias voltage dependence of TMR, except for the magnitude of a TMR ratio. Moreover, we clarified that the presence of an MgO interlayer between Fe and $MgAl_2O_4$ plays an important role in retaining (blocking) the Δ_1 evanescent state for majority (minority) spin. The former leads to the robustness of the TMR ratio against bias voltage as observed in single $MgAl_2O_4$ MTJs, while the latter does to the large TMR ratio as in single MgO MTJs [7].

This work is supported, in part, by TDK Corporation; Grants-in-Aid for Scientific Research (Grants No. JP16H06332, JP17H06152, JP20H02190, and JP20K14782) from the Japan Society for the Promotion of Science; the Tatematsu Foundation; and the Data-Science Research Center for Material, Quantum, and Measurement Technologies, Mie University. Computations are performed using the facilities of the Numerical Materials Simulator at NIMS.

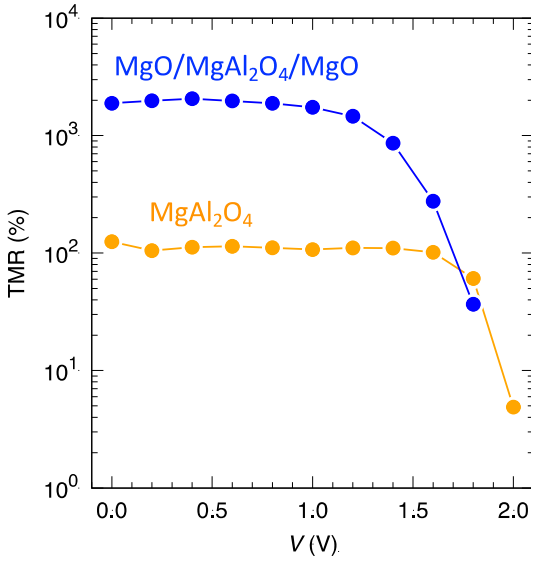

Fig. 1 Bias-voltage dependence of TMR ratio for $MgO/MgAl_2O_4/MgO$-MTJ and single MgAl2O4-MTJ.

References

[1] S. Yuasa *et al.*, Nat. Mater. **3**, 868 (2004).

[2] W. H. Butler *et al.*, Phys. Rev. B **63**, 054416 (2001).

[3] J. Mathon *et al.*, Phys. Rev. B **63**, 220403(R) (2001).

[4] H. Sukegawa *et al.*, Appl. Phys. Lett. **96**, 212505 (2010).

[5] Y. Miura *et al.*, Phys. Rev. B **86**, 024426 (2012).

[6] K. Nawa *et al.*, Phys. Rev. B **102**, 144423 (2020).

[7] K. Nawa *et al.*, Phys. Rev. Appl. **16**, 044037 (2021).

Magnetics in the two-dimensional layered materials

Wei Ren*
Physics Department, International Centre for Quantum and Molecular Structures,
Shanghai University, Shanghai 200444, China
*renwei@shu.edu.cn

Based on the first-principles prediction, we report the magnetoelectric coupling effect in two-dimensional multiferroic bilayer VS_2. The ground-state 3R-type stacking breaks space inversion symmetry, therefore introducing a spontaneous polarization perpendicular to the layer plane. We further reveal that the out-of-plane ferroelectric polarization of bilayer VS_2 can be reversed upon interlayer sliding of an in-plane translation. Each VS_2 layer has a ferromagnetic state with an opposite magnetic moment between two antiferromagnetically ordered layers. We found that ferroelectricity and antiferromagnetism can be coupled together by a ferrovalley in bilayer VS_2 to realize electronic control of magnetism. Remarkably, a net magnetic moment is generated by reducing the interlayer distance, and an electric field is able to achieve linear and second-order nonlinear magnetoelectric coupling in bilayer VS_2.

Reference

[1] Xingen Liu, Alexander P. Pyatakov, and Wei Ren, Phys. Rev. Lett. 125, 247601 (2020).

Manipulating emergent properties of Hund metal: $SrRuO_3$-$SrTiO_3$ heterostructure

Minjae Kim[1,2*], Chang-Jong Kang[3], Jaeho Han[4], and Bongjae Kim[5]

[1]Korea Institute for Advanced Study, Seoul 02455, South Korea
[2]Department of Chemistry, Pohang University of Science and Technology (POSTECH), Pohang 37673, South Korea
[3]Department of Physics, Chungnam National University, Daejeon 34134, South Korea
[4]Center of Theoretical Physics of Complex Systems, Institute for Basic Science (IBS) Daejeon 34126, South Korea
[5]Department of Physics, Kunsan National University, Gunsan 54150, South Korea

We investigate strain dependent emergent electronic properties of $SrRuO_3$-$SrTiO_3$ heterostructure in the theoretical framework of the combination of density functional theory and dynamical mean field theory (DFT+DMFT). The $SrRuO_3$-$SrTiO_3$ heterostructure in the presence of strain was recently proposed as a possible platform for studying unconventional superconductivity of Sr_2RuO_4, a paradigmatic Hund metal, in the DFT computation. [1] Here, from the DFT+DMFT method, we show that the $SrRuO_3$-$SrTiO_3$ heterostructure has a possibility of strain induced manipulation of low temperature emergent orders of Hund metal, covers ferromagnetic (FM) metal to Neel type antiferromagnetic (NAFM) insulator with orbital polarization. In between these emergent orders in the strain dependent phase diagram of the $SrRuO_3$-$SrTiO_3$ heterostructure, we confirmed that there is a regime in which a Fermi liquid quasiparticle experiences competing magnetic interactions of FM, NAFM, and spin density waves, indicating a clue for possible unconventional superconductivity.

Reference

[1] Bongjae Kim et al., Phys. Rev. B 101, 220502(R) (2020)

2-Dimensional van der Waals Antiferromagnets Studies with Optical Spectroscopy

Hyeonsik Cheong*
Department of Physics, Sogang University, Seoul 04107, Korea

Two-dimensional magnetic van der Waals materials are attracting much interest recently. Magnetism in low dimensional systems is an interesting topic for the fundamental physics, and atomically thin magnetic materials are promising candidates for novel spintronic devices. Antiferromagnetic 2-dimensional materials are particularly interesting both for fundamental physics and also for antiferromagnetism-based spintronic devices. However, traditional research tools to probe antiferromagnetic ordering such as neutron scattering cannot be employed for atomically thin materials due to the small sample volume. Although magneto-optical Kerr effect measurements can be used to monitor the magnetic ordering in ferromagnetic materials, the lack of net magnetization precludes the use of the Kerr effect in probing antiferromagnetic ordering. Optical techniques such as Raman spectroscopy or second-harmonic generation (SHG) are becoming increasingly important for the study of antiferromagnetic 2-dimensional materials. Raman spectroscopy, for example, can be an invaluable tool to probe the magnetic transition in antiferromagnetic van der Waals materials that show spectroscopic features that correlate with magnetic ordering. Furthermore, recent spectroscopic studies revealed a novel coherent state in some of these materials stabilized by the antiferromagnetic ordering. In this presentation, I will review recent achievements in the study of antiferromagnetism in 2 dimensions using optical spectroscopy.

Symposium 3

'Quantum Magnetism'

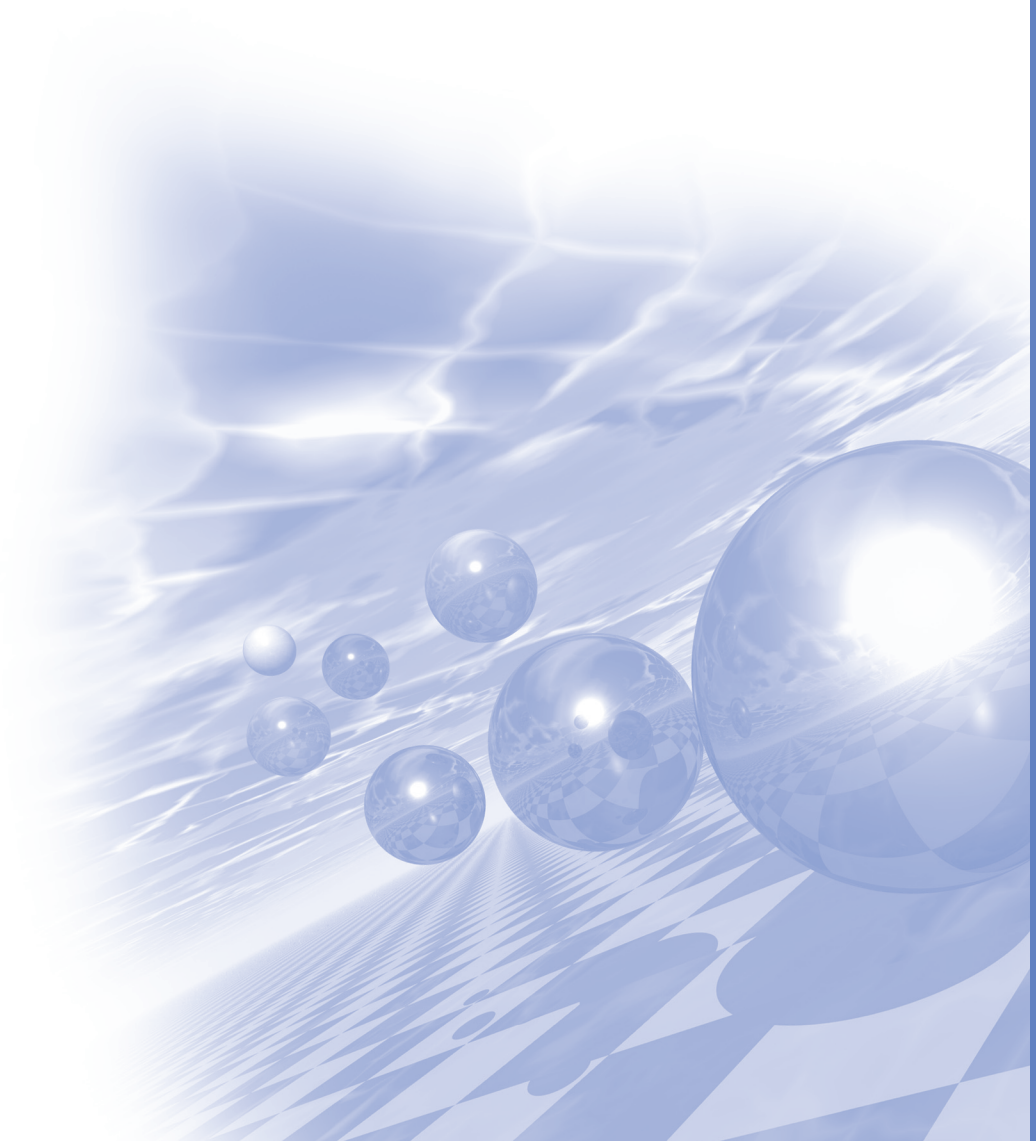

Machine Learning Quantum Data

Eunah Kim*
Department of Physics, Cornell University, USA

Impressive progress in classical and quantum simulations put us in the luxurious position of having rich quantum data at hand. However, it can be challenging to extract theoretical insight from quantum data for states that are intrinsically quantum mechanical and characterized by quantum fluctuations or topological properties. This talk will discuss recent successes using machine learning approaches to meet the quantum data challenge and discover new physics in unbiased and interpretable manners.

Artificial Neural Networks for Analyzing Quantum Many-Body Problems

Yusuke Nomura*
RIKEN Center for Emergent Matter Science, 2-1 Hirosawa, Wako, Saitama 351-0198, Japan

It is a great challenge to accurately represent quantum many-body states. In this talk, we will show that Boltzmann machines used in machine learning can be useful for analyzing quantum many-body systems.

First, we introduce a method for representing quantum states using Boltzmann machines proposed by Carleo and Troyer in 2017 [1]. Then, we discuss the progress of the neural-network wave function method for zero-temperature simulations [2-6]. Through various extensions, the neural-network wave functions are beginning to be applied to challenging problems (e.g., frustrated spin systems) in physics [5].

Next, we discuss two finite-temperature calculation methods using deep Boltzmann machines (DBMs) with two hidden layers [7]. Both methods use the idea of "purification," where a finite-temperature mixed state is represented by a pure state of an extended system. The former analytically constructs a pure state corresponding to thermal equilibrium, realizing quantum-to-classical mapping [3]. The latter method obtains the pure state by numerically optimizing the DBM parameters. This method can be applied to, e.g., frustrated systems for which the former method suffers from the negative sign problem. We will discuss the applications to the transverse-field Ising model and J_1-J_2 Heisenberg model.

These works were done in collaboration with Andrew S. Darmawan, Youhei Yamaji, Masatoshi Imada, Giuseppe Carleo, Nobuyuki Yoshioka, and Franco Nori.

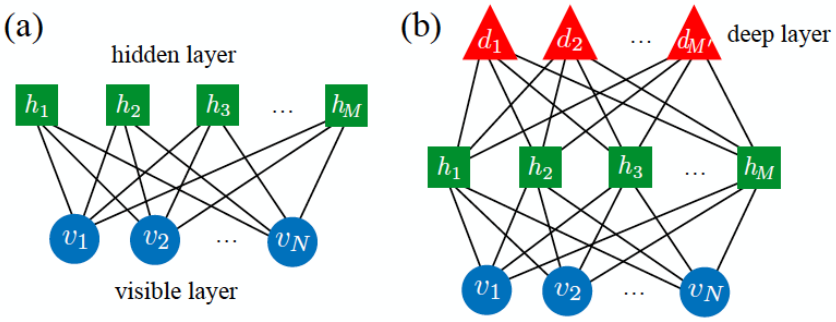

Fig. 1. Structures of (a) restricted Boltzmann machine (RBM) and (b) deep Boltzmann machine (DBM).

References

[1] G. Carleo and M. Troyer Science **355**, 602 (2017)
[2] Y. Nomura, A. S. Darmawan, Y. Yamaji, and M. Imada, Phys. Rev. B **96**, 205152 (2017)
[3] G. Carleo, Y. Nomura, and M. Imada, Nat. Commun. **9**, 5322 (2018)
[4] Y. Nomura, J. Phys. Soc. Jpn. **89**, 054706 (2020) [Editor's choice]
[5] Y. Nomura and M. Imada, Phys. Rev. X **11**, 031034 (2021)
[6] Y. Nomura, J. Phys.: Condens. Matter **33**, 174003 (2021) [special issue "Emergent Leaders 2020"]
[7] Y. Nomura, N. Yoshioka, and F. Nori, Phys. Rev. Lett. **127**, 060601 (2021)

Ground-state Properties via Machine Learning Quantum Constraints

Yi Zhang[1,2*]
[1]International Center for Quantum Materials, Peking University, Beijing, 100871, China
[2]School of Physics, Peking University, Beijing, 100871, China

Ground-state properties are central to our understanding of quantum many-body systems. At first glance, it seems natural and essential to obtain the ground state before analyzing its properties; however, its exponentially large Hilbert space has made such studies costly, if not prohibitive, on sufficiently large system sizes. Here, we propose an alternative strategy based upon the expectation values of an ensemble of selected operators and the elusive yet vital quantum constraints between them, where the search for ground-state properties simply equates to classical constrained minimization. These quantum constraints are generally obtainable via sampling then machine learning on a large number of systematically consistent quantum many-body states. We showcase our perspective on 1D fermion chains and spin chains for applicability, effectiveness, and several unique advantages, especially for strongly correlated systems, thermodynamic-limit systems, property designs, etc.

Thermal transport and thermodynamic properties of Kitaev quantum spin liquid candidate material α-$RuCl_3$

Yuji Matsuda*
Department of Physics, Kyoto University, Kyoto 606-8502, Japan

Half-integer thermal quantum Hall conductance recently reported in the two-dimensional honeycomb material α-RuCl3 indicates the presence of non-ablian anyons, which are relevant for fault-tolerant topological quantum computations, in a quantum magnet [1]. Here, based on recent studies of thermal transport and thermodynamic measurements in the magnetic field of α-RuCl3, we discuss the topological Chern number of Majorana band [2], Majorana gap [3], and field induced topological phase transition [4] of the Kitaev spin liquid.

References

[1] Y. Kasahara et al. Nature 559, 227 (2018).
[2] T. Yokoi *et al*. Science 373, 567 (2021).
[3] O. Tanaka *et al*. arXiv:2007.06757.
[4] S. Suetsugu *et al*. in preparation.

Terahertz spectroscopy of antiferromagnetic resonances in $YFe_{1-x}Mn_xO_3$ ($0 \leq x \leq 0.4$) across a spin reorientation transition

Howon Lee[1], Taek Sun Jung[1], Hyun Jun Shin[1], Sang Hyup Oh[1], Kyung Ik Sim[2], Taewoo Ha[2], Young Jai Choi[1] and Jae Hoon Kim[1*]

[1]Department of Physics, Yonsei University, 50 Yonsei-ro, Seoul 03722, Republic of Korea

[2]Center for Integrated Nanostructure Physics, Institute for Basic Science (IBS), Suwon 16419, Republic of Korea

We have conducted a terahertz spectroscopic study of the antiferromagnetic resonances in bulk orthoferrite $YFe_{1-x}Mn_xO_3$ ($0 \leq x \leq 0.4$). Both the quasi-ferromagnetic resonance mode and the quasi-antiferromagnetic resonance mode in the weak ferromagnetic Γ_4 phase disappear near the spin reorientation temperature, T_{SR}, for the onset of the collinear antiferromagnetic Γ_1 phase ($x \geq 0.1$). Below T_{SR}, an antiferromagnetic resonance mode emerges and exhibits a large blue-shift with decreasing temperature. However, below 50 K, this mode softens considerably, and this tendency becomes stronger with Mn doping. We provide a deeper understanding of such behavior of the antiferromagnetic resonance modes in terms of the influence of the Mn^{3+} ions on the magnetocrystalline anisotropy. Our results show that terahertz time-domain spectroscopy is a useful, complementary tool in tracking magnetic transitions and probing interaction between disparate magnetic subsystems in antiferromagnetic materials with multiple ionic species.

Oxide Heterostructures for Quantum Magnetism

Changhee Sohn*
Department of Physics, Ulsan National Institute of Science and Technology (UNIST), Korea

Magnetism with strong quantum fluctuation and entanglement has received rising attention due to its exotic excitations and potential application to spintronics and quantum computations. However, realizing genuine quantum magnetic ground state in real matter remains extremely challenging up to now. In almost every candidate for Kitaev quantum spin liquid, for example, the presence of additional spin exchange interaction results in classical long-range antiferromagnetic ground states. In this regard, heterostructure approach on quantum magnet might provide a unique route to realize quantum magnetism owing to its wide tunability of spin Hamiltonian. Here, we will introduce our recent attempt to realize quantum magnetic ground states in strongly correlated oxide heterostructures. We will present successful growth of quantum spin liquid candidates in thin film geometry and its basic characterization including structure, stoichiometry, electronic and magnetic ground states. The similarity and difference between bulk and thin film will be discussed.

Finite-Temperature Spin Dynamics and Transport Phenomena in Kitaev Quantum Spin Liquids

Joji Nasu*
Department of Physics, Tohoku University, Sendai 980-8578, Japan

Quantum spin liquids (QSLs) have been the subject of great interest since Anderson's suggestion. Recently, Kitaev proposed a canonical model of QSLs termed the Kitaev model on a honeycomb lattice (Fig. 1), which provides exact realizations of QSLs with topological order and fractional excitations. Moreover, exchange interactions in transition metal compounds with the strong spin-orbit coupling, such as iridium and ruthenium compounds, are suggested to be dominated by the Kitaev-type interaction.

To discuss experimental results in the viewpoint of the Kitaev physics, we investigate the thermodynamic properties and spin dynamics of the Kitaev model [1]. We calculate the specific heat using the quantum Monte Carlo simulations and find a double-peak structure, where half of the entropy is released at each peak. The result suggests that a quantum spin is fractionalized into two types of elementary excitations, itinerant Majorana fermions and localized Z_2 fluxes, due to quantum many-body effects. We also find fingerprints of fractionalization in the spin dynamics. The fermionic temperature dependence in the Raman scattering and incoherent broad structure in the dynamical spin structure factor are the manifestations of the itinerant Majorana fermions [2,3]. We also examine the thermal transport governed by the itinerant emergent Majorana fermions in the presence of the magnetic field [4]. The thermal Hall conductivity shows nonmonotonic temperature dependence due to the Majorana chiral edge mode and the thermally fluctuating Z_2 gauge field emergent from the fractionalization of quantum spins.

Finally, we discuss disorder effects on the Kitaev QSL, which inevitably exist in real materials. We investigate the impact of two types of disorder, bond randomness and site dilution, on the spin dynamics and transport in the Kitaev model [5,6]. We compare the calculation results with experimental ones. The relevance to real materials will be discussed in the presentation.

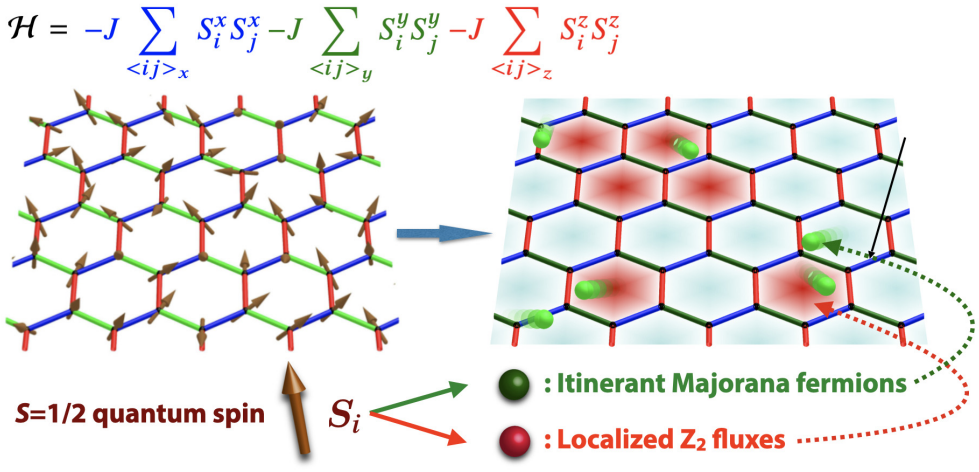

Fig. 1. Schematic picture of Kitaev model and spin fractionalization.

References

[1] J. Nasu, M. Udagawa, and Y. Motome, Phys. Rev. Lett. **113**, 197205 (2014), Phys. Rev. B **92**, 115122 (2015).

[2] J. Nasu, J. Knolle, D. L. Kovrizhin, Y. Motome, R. Moessner, Nat. Phys., **12**, 912 (2016).

[3] J. Yoshitake, J. Nasu, and Y. Motome, Phys. Rev. Lett. **117**, 157203 (2016).

[4] J. Nasu, J. Yoshitake, and Y. Motome, Phys. Rev. Lett. **119**, 127204 (2017).

[5] J. Nasu and Y. Motome, Phys. Rev. B **102**, 054437 (2020).

[6] J. Nasu, Y. Motome, Phys. Rev. B **104**, 035116 (2021).

Assessments of Kitaev physics in 3d transition metal magnets via first-principles calculations

Heung-Sik Kim*
Kangwon National University, Korea, heungsikim@kangwon.ac.kr

Since the first suggested realization of Kitaev's exchange Hamiltonian in layered 5d-transition metal oxide systems by G. Jackeli and G. Khaliullin, 4d- and 5d-transition metal elements have been considered "a must" ingredient to conjure Kitaev physics in solid state systems. In search of other candidate systems, recently there have been several studies on reducing the need of the spin-orbit-entangled j_{eff}=1/2 orbitals as the basic building block. There have been generally two different approaches in that direction; i) employing S=1 or S=3/2 higher-spin elements or ii) many-body J=1/2 states. Both approaches involve in the presence of 3d transition metal elements despite their apparently weak spin-orbit coupling. In this talk I'd like to review both approaches, make assessments on candidate systems for each cases via first-principles electronic structure calculations, and try to suggest a couple of ways to enhance Kitaev physics in the relevant systems.

2021 KMS Winter Conference

Symposium 4

미래소재디스커버리 사업

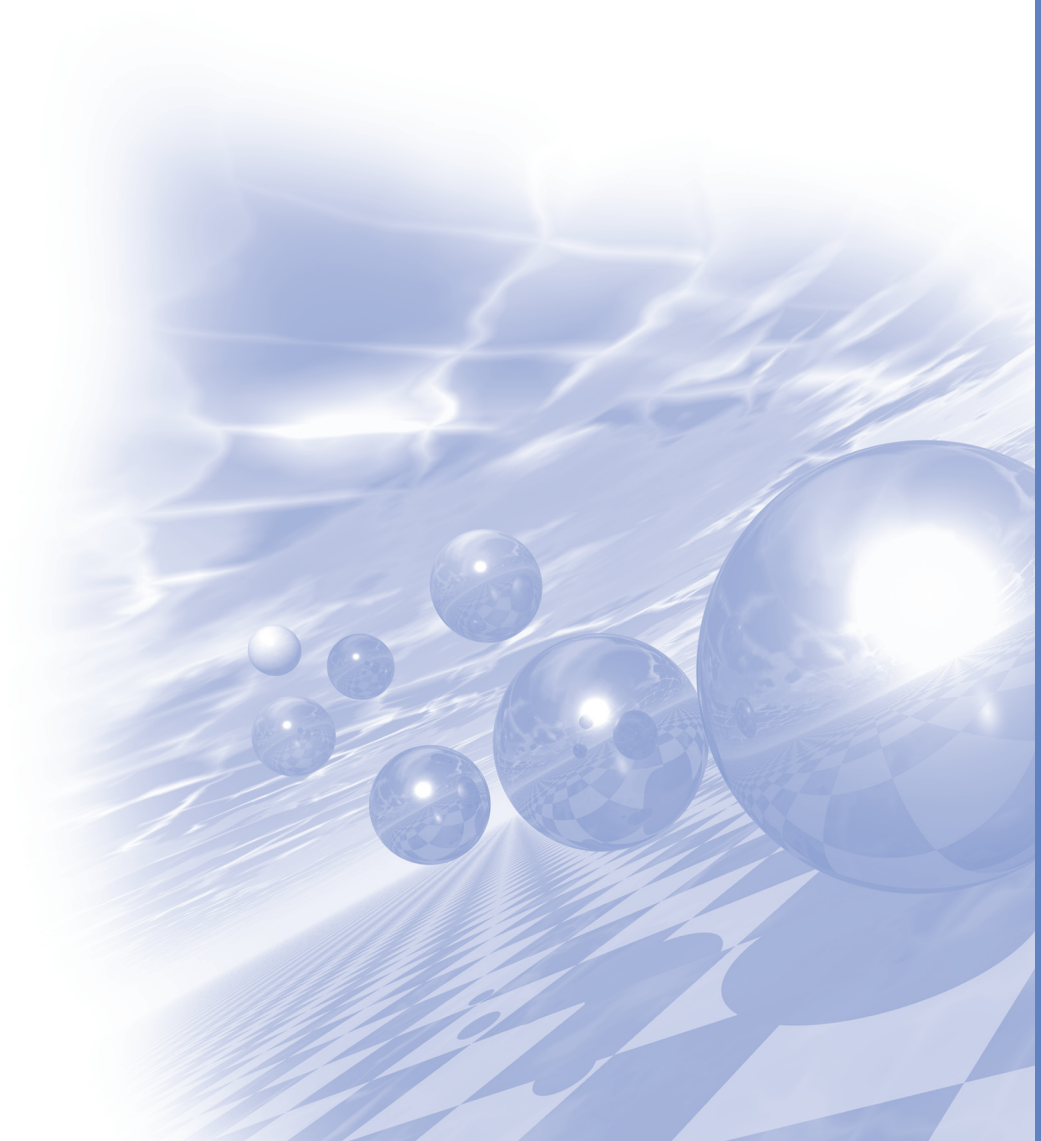

스핀궤도소재연구단의 연구 현황과 성과

Young Keun Kim*
Department of Materials Science and Engineering, Korea University, Seoul, Korea

본 연구단은 2015년 과학기술정보통신부 미래소재디스커버리사업의 일환으로 출범되어 지난 6년간 '저전력, 초고속, 비휘발성 logic-in-memory 구현이 가능한 스핀궤도소재 원천기술 개발'을 목표로 연구를 수행하고 있다. 비자성층과 강자성층으로 구성된 소재 접합구조에서 발생하는 스핀궤도토크(spin-orbit torque, SOT)로 낮은 에너지로 자화의 방향을 스위칭시켜 향후 MRAM의 기록성능을 월등히 높일 가능성이 있는 새로운 소재와 구조를 발굴하고 있다. 수직자화를 갖는 여러 접합에서 소재 계면과 미세구조 제어로 SOT 효율을 높이는 기술, 외부자기장 없이 스위칭이 가능한 기술들을 개발한 바 있다. SOT 효율이 높으며, 수직자기이방성 에너지가 7 Merg/cm^3 이상인 소재들을 확보하였다. 본 연구실에서는 β-상을 갖는 W 박막에 이종 원소 합금화를 시도하여 SOT 효율이 0.5 이상을 갖는 W-N, W-V 같은 비자성 스핀생성층 소재들을 개발하였다. 또한 DMI 에너지가 MgO 박막의 두께에 따라 RKKY 거동을 보이는 소재구조를 확인한 바 있다. 개발된 소재 물성치를 기반으로 회로를 설계하였을 때, 7 nm 기술 노드에서 SRAM (100%) 대비 에너지 및 면적이 20~30% 수준으로 감소할 수 있음을 확인하였다. 또한, 미래기술로 비대칭교환결합력인 DMI 에너지 1 erg/cm^3 이상이며 자구벽 이동속도 50 m/s의 소재와 스커미온 소재 기술을 개발하였다. 연구단에서는 SOT 소재의 이론 설계, 소재 공정, 측정 평가와 관련하여 192 편의 SCI 등재 학술논문 게재와 44건의 국내외 등록 특허를 확보하였다.

New spin hall system for high spin efficiency materials

Young Chan Won[1*], Young Rae Kim[2], Jae Ho Jung[2] and Sang Ho Lim[1,2]
[1]Department of Nano Semiconductor Engineering, Korea University, Seoul 02841, Korea
[2]Department of Materials Science and Engineering, Korea University, Seoul 02841, Korea

In this study, various experiments have been performed to develop a new system for the spin-orbit torque (SOT) device. In Pd/Co/Pt/MgO structure, 0.2 nm thick Ti layer is inserted in the Pt layer to control SOT efficiency. The SOT efficiency is changed by a thickness of Pt layer and position of Ti layer. The perpendicular magnetic anisotropy (PMA) and crystalline structure of Pt/Co/AlN structures are also investigated. Before the annealing, the stack shows no magnetic moment with a 0.5 nm thick Co layer. However, dramatic increase in magnetic moment value is observed after annealing at 300°C. Simultaneously, strong PMA is obtained. The magnetic dead layer and interfacial PMA energy density are investigated to determine a relative interfacial effect. The microstructural experiments are also performed by XRD and TEM experiments. The AlN layer is inserted in Pt/Co/MgO structure which is known for a strong PMA. The variation of PMA and SOT is studied by changing a position of AlN layer.

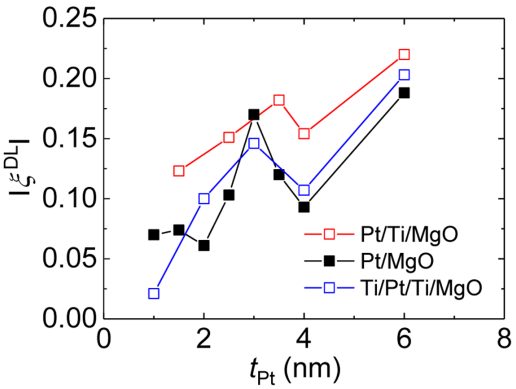

Fig. 1. Damping like efficiency with depends on Pt thickness layer

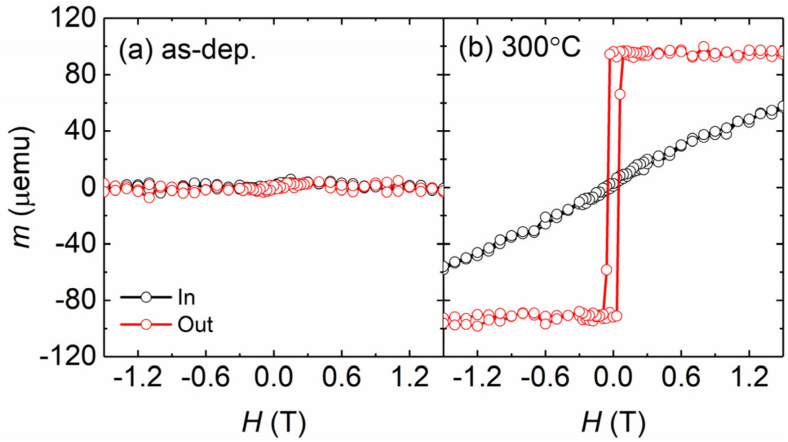

Fig. 2. *m-H* loops for [Pt/Co/AlN] structures: (a) as-deposited sample and annealed sample at (b) 300°C

Pd/Co/Pd 구조에서 강자성층 두께에 따른 전자기적 특성 변화

이상호, 강범승, 홍종일*
연세대학교 신소재공학과

자기저항메모리(magnetoresistive random-access memory, MRAM)는 쓰기 속도가 빠르고, 전력 소모는 적은 특징이 있어 차세대 메모리로써 많은 주목을 받고 있다. 한편, 지속되는 스케일에 부합하기 위하여 MRAM 셀의 집적도는 더욱 증가해야만 한다. 셀의 집적도가 증가할수록 강자성체의 열적 안정성이 감소하고, 이에 따라 소자가 오작동할 확률이 높아진다. 따라서, MRAM 셀의 열 안정성 확보를 위하여 자기이방성에너지를 증가시키는 구조 또는 물질에 대한 연구가 주목받고 있다. Pd/Co/Pd 박막은 계면에서 병진 대칭성(translational symmetry)이 깨져있고 d-밴드와 p-밴드의 혼성화로 상당히 큰 수직자기이방성에너지를 가지고 있어[1]많은 연구가 이루어지고 있다.

본 연구에서는 Pd/Co/Pd 박막에서 Co 강자성층을 쐐기(wedge) 모양으로 증착하여 강자성층의 두께에 따른 전기적 특성 및 자기적 특성을 홀(Hall) 소자와 진동시료형자력계(vibrating sample magnetometer, VSM)를 사용하여 분석하였다. 자성층의 두께가 증가할수록 자기모멘트는 증가하는데 이에 반하여 비정상 홀 효과의 크기는 감소하는 경향을 보였다. 강자성층의 두께를 감소시키면 음극성(negative polarity)의 비정상 홀 효과에 기여하는 표면 산란(surface scattering)이 상대적으로 벌크 산란(bulk scattering)에 비해 큰 영향을 미치기 때문으로 생각한다.[1,2,3] 이로 인해 Pd/Co/Pd 구조에서 강자성층의 두께가 0.35nm 이하에서는 음극성을 나타내고, 0.35 nm 이상에서 극성이 반전되어 양극성(positive polarity)를 나타나게 된다. 비정상 홀 효과는 페르미 준위 근처의 전자들이 주로 수송에 기여하는 반면, 자기모멘트는 페르미 준위 아래 d-밴드와 p-밴드 혼성화 밴드의 전자들이 기여하여 나타난다. 본 발표에서는 Co 강자성층 두께에 따른 비정상 홀 효과의 변화에 관하여 논의한다.

References

[1] Z. B. Guo et al., Phys. Rev. B 86, 104433 (2012)
[2] G. Winer et al., J. Appl. Phys. 118, 173901 (2015)
[3] T. H. Dang et al., Phys. Rev. B 102, 144405 (2020)

Field-free spin-orbit torque switching of perpendicular magnetization

Soogil Lee and Byong-Guk Park*
Department of Materials Science and Engineering, KAIST, Korea

Spin-orbit torque (SOT) arising from spin-orbit coupling has gained much attention because it promises efficient magnetization switching in spintronic devices [1]. It is important for device applications that the SOT switches perpendicular magnetizations without an external magnetic field. In this talk, I will present two approaches to field-free SOT switching of perpendicular magnetization. First, we investigate SOT in antiferromagnet IrMn/CoFeB/MgO structures, where an in-plane effective field and a sizable SOT generated from IrMn can switch the magnetization perpendicular CoFeB without an external magnetic field [2]. Second, we demonstrate that out-of-plane SOT created at a ferromagnet/non-magnetic interface deterministically switches magnetization in a magnetic trilayer [3].

References

[1] J. Ryu, S. Lee, K.-J. Lee, and B.-G. Park, Adv. Mater. 32, 1907148 (2020)
[2] Y.-W. Oh, et al., Nat. Nanotech. 11, 878 (2016)
[3] S.-h.C. Baek, et al., Nat. Mater. 17, 509 (2018)

Various approaches for the more effective spin-orbit torque switching

Suhyeok An, Eunchong Baek, Yeh-Ri Kim, Dongryul Kim, Jin-A Kim,
Hyeongjoo Seo, and Chun-Yeol You*
Department of Emerging Materials Science, DGIST, Daegu 42988, Korea

Spin orbit torque (SOT) induced magnetization switching is promising technique for the logic-in-memory applications [1]. SOT switching has many advantages compare to the spin transfer torque switching: separated read/write current paths, faster switching speed, independent switching behavior on the free layer damping constant, and less energy consumption. Despite many advantages, there are still unresolved issues in SOT switching. We studied various technique to improve the efficiency of SOT switching. First, we will discuss about the effect of the He+ ion irradiation on the SOT switching, He+ ion irradiation leads not only the magnetic anisotropy, but also the spin Hall angle variations. We will also introduce several approaches in order to achieve field-free SOT switching by introducing lateral in-plane symmetry breaking.

Reference

[1] I. Y. Vedmedenko, *et al.* J. Phys. D. Appl. Phys. **53**, 45 (2020).

Interfacial Dzyaloshinskii-Moriya Interaction in Ferromagnetic Thin Films

Sug-Bong Choe*
Department of Physics and Institute of Applied Physics, Seoul National University, Seoul, 08826, Korea

Interfacial phenomena play decisive roles in modern science and technology as the scale shrinks down to a few atomic layers. Such minute nanostructures require more comprehensive understanding beyond the conventional concepts of interfaces and interfacial phenomena generated at interfaces. The Dzyaloshinskii–Moriya interaction (DMI) generates intriguing chiral magnetic objects such as magnetic skyrmions and chiral domain walls that can be used as building blocks in emerging magnetic nanodevices. Precise control of the DMI strength is one of the key issues to achieve better stability and functionality of these chiral objects. Here we present two major experimental results on the interfacial DMI and spin-orbit torque (SOT) in ferromagnetic films. First, we report an experimental observation that in magnetic trilayer films, the DMI strength exhibits a noticeable correlation with the work functions of the nonmagnetic layers interfaced to the magnetic layer [1]. Such correlation with the intrinsic material parameters provides a guideline for material selection to engineer the DMI strength. Second, from series of a-few-atomic-layer-thick magnetic films, here we demonstrate experimentally that, contrary to the common notion, interfacial phenomena require finite thickness for their full emergence [2]. The layer thickness dependences revealed that the interfacial DMI begins to appear with thickness and emerges completely in the thickness of 2 to 3 atomic layers, at which the magnitude is maximized. This implies that the DMI is suppressed, when the “bulk” layer adjacent to interfaces is thinner than the threshold thickness. The existence of the threshold thickness indicates the need to refine conventional perspectives on interfacial phenomena and imposes the lowest structural bound and optimum thickness to maximize interfacial effects for technological applications.

References

[1] Y.-K. Park, D.-Y. Kim, J.-S. Kim, Y.-S. Nam, M.-H. Park, H.-C. Choi, B.-C. Min, S.-B. Choe, “Experimental observation of the correlation between the interfacial Dzyaloshinskii–Moriya interaction and work function in metallic magnetic trilayers.” NPG Asia Materials 10, 995-1001 (2018).

[2] Y.-K. Park, J.-S. Kim, Y.-S. Nam, S. Jeon, J.-H. Park, K.-W. Kim, H.-W. Lee, B.-C. Min, S.-B. Choe, “Interfacial atomic layers for full emergence of interfacial Dzyaloshinskii–Moriya interaction”, NPG Asia Materials 12, 38 (2020).

SRAM 기반 cache memory 대체를 위한 SOT-MRAM의 설계 사양 검증

박종선*
고려대학교 전기전자공학과

스핀 궤도 토크 자기메모리 (SOT-MRAM)는 다른 자기 메모리 보다 더 적은 쓰기 에너지로 인하여 최근 가장 많은 주목을 받고 있으며 이에 따라서 대용량 메모리, 뉴로모픽 하드웨어, 사물인터넷기기 (IoT device) 등 다양한 분야에서 응용될 것으로 기대되고 있다. 특히, SRAM 기반 L3 cache는 공정 감소로 인한 누설 전력으로 인하여 어려움을 겪고 있는데 SOT-MRAM으로 대체할 경우 낮은 누설 전력으로 기존의 문제를 해결할 수 있다. 본 연구에서는 그림 1에 나와 있는 SOT 소자 파라미터를 기반으로 SOT-MRAM회로 및 시스템 시뮬레이션을 통해 SOT-MRAM 기반 cache 에너지를 SRAM 기반 cache와 비교하였다. 소자-회로 통합 시뮬레이션을 위해 SPICE language 기반 모델링을 구축하였으며, SOT-MRAM macro 설계를 통해 SOT-MRAM의 쓰기/읽기/누설 에너지를 측정하였다. 또한, Gem5 시뮬레이션을 통해 cache의 access pattern을 산출하여 SRAM 및 SOT-MRAM 기반 cache의 에너지를 측정하였다. 그림 2는 본 논문에서 사용한 Gem5 시뮬레이터의 시스템 구성도이다. 그림 3은 SRAM 및 SOT-MRAM 기반 cache의 에너지 측정 결과를 보여준다. 측정 결과 10nm 공정에서 무자기장 SOT-MRAM의 경우 SRAM 대비 19%의 에너지 소모를 보였으며 유자기장 SOT-MRAM의 경우 SRAM 대비 18%의 에너지 소모를 보였다. 7nm 공정에서 무자기장 SOT-MRAM의 경우 SRAM 대비 24%의 에너지 소모를 보였으며 유자기장 SOT-MRAM의 경우 SRAM 대비 22%의 에너지 소모를 보였다. 그림 4는 2T SOT-MRAM cell의 레이아웃을 보여준다. 7nm 공정에서 무자기장 SOT-MRAM의 경우 SRAM 대비 27%, 유자기장 SOT-MRAM의 경우 SRAM 대비 32%의 면적을 확인하였다. 다음과 같은 결과들을 통하여 SRAM 기반 L2 cache를 SOT-MRAM으로 대체하였을 경우 충분한 에너지 감소 및 면적 감소를 확인하였으며 대체 가능성을 확인하였다.

Parameter	Value	
	유자기장	무자기장
Switching current duration	0.8nsec	
MTJ free layer dimension	13.5 x 35 x 1 (nm)	
Heavy metal dimension	13.5 x 90 x 2 (nm)	
Spin hall angle	0.984	0.69
Apllied external field	200 Oe	50 Oe
TMR	200%	
Saturation Magnetization	800 emu/cc	972 emu/cc
Perpendicular anisotropy energy density	8.02 x 10^6 erg/cm^3	8.85 x 10^6 erg/cm^3
Effective Perpendicular anisotropy energy density	4.5 x 10^6 erg/cm^3	3.65 x 10^6 erg/cm^3

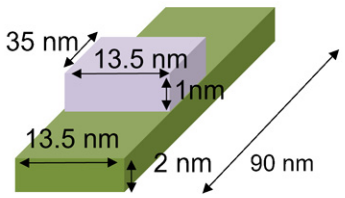

	유자기장	유자기장
Thermal stability	51.2	41.5
Switching current	40uA	50uA

그림 1. SOT 소자 파라미터

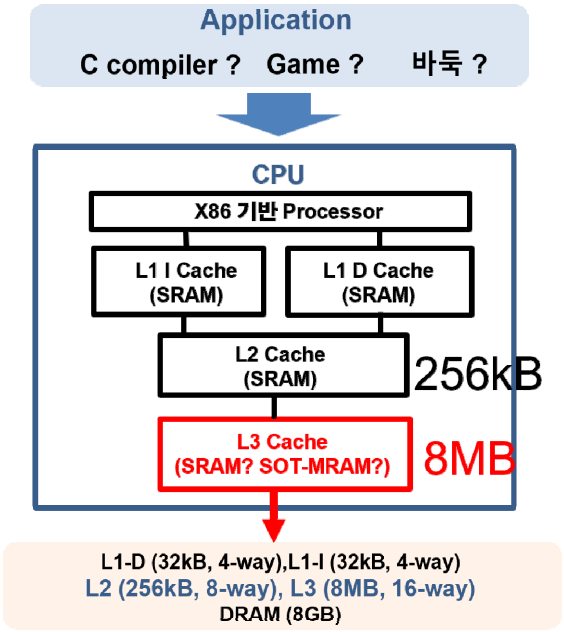

그림 2. Gem5 시뮬레이터의 시스템 구성도

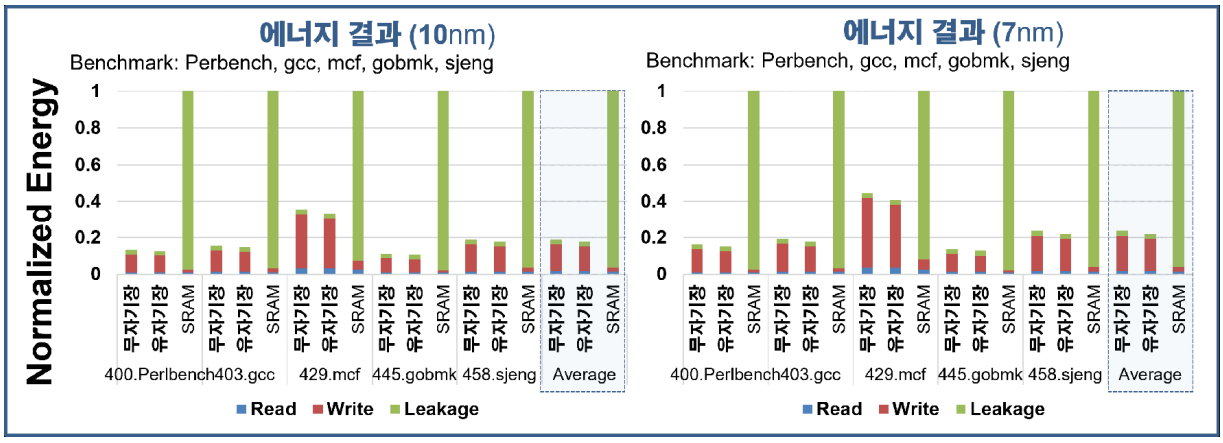

그림 3. SPEC 2006 benchmark 별 cache의 에너지 측정

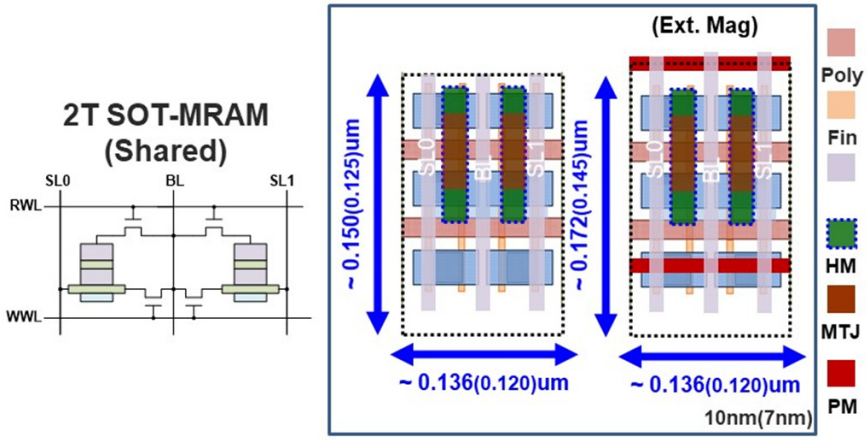

그림 4. SOT-MRAM cell 레이아웃

Spin Hall conductivity of Tungsten alloys

Sonny H. Rhim[1*], Quynh Anh T. Nguyen[1], Do Duc Cuong[1], and Soon Cheol Hong[1]
[1]Department of Physics, University of Ulsan, Korea
[2]Department of Physics and Computer Science, Faculty of Physics and Engineering Physics, University of Science, Vietnam National University, Ho Chi Minh City, Vietnam

In this talk, spin Hall conductivities of three Tungsten alloys, W-V alloy, W-Nitrides, and W-Silicide, are presented with comparison of their values and underlying Berry curvatures. First-principles calculations are performed using VASP package along with Wannierization, where Kubo formula is used to evaluate Berry curvature and spin Hall conductivities. In all cases, anti-crossing regions guaranteed by symmetry, crossing due to symmorphic and nonsymmorphic little group, are responsible for large Berry curvature: each stemming from bcc structure and rock-salt structure. Regarding W-Si, we show preliminary result of 6.25 % Si concentration comparing other higher concentrations with less stability. Further, unexplored task in spin Hall conductivity using DFT calculations is revealed.

Ferromagnet-induced spin-orbit torques

Kyung-Jin Lee*
Department of Physics, KAIST, Korea

Spin-orbit torque (SOT), which is considered as a write scheme for next-generation MRAMs, arises from the charge-to-spin conversion via spin-orbit coupling (SOC). For commercialization of SOT-MRAMs, it is of critical importance to enhance the charge-to-spin conversion efficiency, which requires a detailed understanding of various SOC effects. In addition to the widely studied spin Hall effect of non-magnet (NM), recent studies found that SOC of ferromagnet (FM) also contributes to the SOT [1], including (i) interface torque [2-4], (ii) anomalous torque [5-7], and (iii) orbital torque [8-10]. In this talk, we will discuss about FM-induced SOTs, which provide additional knobs to enhance the net SOT efficiency.

References

[1] D. Go et al. Theory of current-induced angular momentum transfer dynamics in spin-orbit coupled systems, **Phys. Rev. Research 2**, 033401 (2020).

[2] S.-h. C. Baek et al., Spin currents and spin-orbit torques in ferromagnetic trilayers, **Nat. Mater. 17**, 509 (2018).

[3] V. P. Amin, J. Zemen, and M. D. Stiles, Interface-generated spin currents. **Phys. Rev. Lett. 121**, 136805 (2018).

[4] D.-K. Lee and K.-J. Lee, Spin-orbit torque switching of perpendicular magnetization in ferromagnetic trilayers, **Sci. Rep. 10**, 1772 (2020).

[5] W. Wang et al., Anomalous spin–orbit torques in magnetic single-layer films, **Nat. Nanotechnol. 14**, 819 (2019).

[6] V. P. Amin, Junwen Li, M. D. Stiles, and P. M. Haney, Intrinsic spin currents in ferromagnets, **Phys. Rev. B 99**, 220405(R) (2019).

[7] K.-W. Kim and K.-J. Lee, Generalized spin drift-diffusion formalism in the presence of spin-orbit interaction of ferromagnets, **Phys. Rev. Lett. 125**, 207205 (2020).

[8] H. Kontani et al., Giant orbital Hall effect in transition metals: Origin of large spin and anomalous Hall effects, **Phys. Rev. Lett. 102**, 016601 (2009).

[9] D. Go and H.-W. Lee, Orbital torque: Torque generation by orbital current injection, **Phys. Rev. Research 2**, 013177 (2020).

[10] D. Lee et al., Orbital Hall effect in magnetic bilayers, submitted.

[11] H.-J. Park Lee et al., Spin swapping effect of band-structure origin in centrosymmetric ferromagnets, submitted.

Oral Session 2

'Permanent Magnetics' & 'Electro-Magnetic Energy Conversion' 구두발표

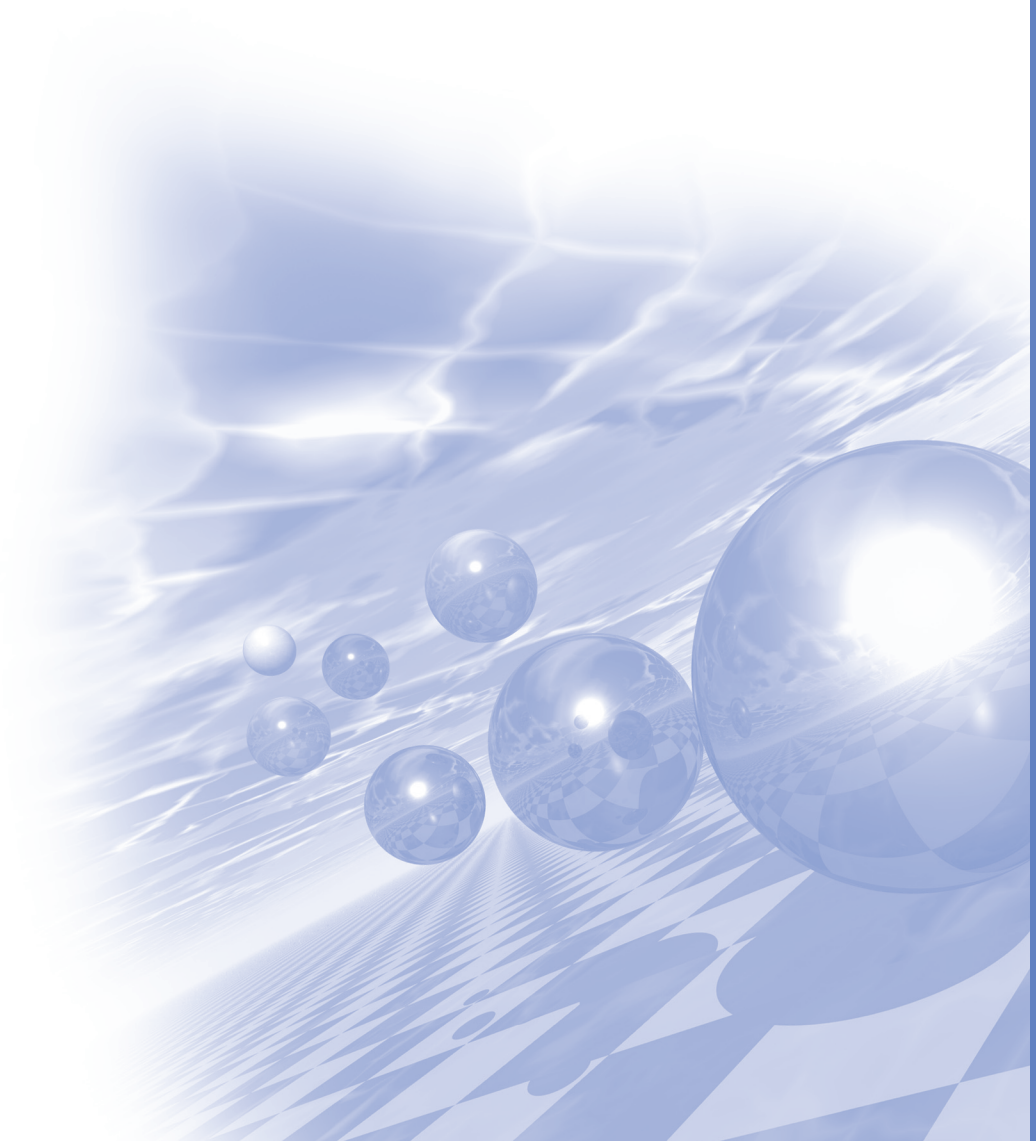

High-performance Ce-substituted Nd-Fe-B hot-deformed magnets produced by dual alloy method

Ga-Yeong Kim[1,2*], Tae-Hoon Kim[1], Hee-Ryoung Cha[1], Yang-Do Kim[2*] and Jung-Goo Lee[1†]
[1]Department of Magnetic Materials, Korea Institute of Materials Science, Changwon, Korea
[2]Department of Materials Science and Engineering, Pusan National University, Busan, Korea

Nd-Fe-B magnets have been used for the traction motor of hybrid or electric vehicles due to its excellent magnetic properties. With increasing demand on Nd-Fe-B magnets, the shortage of Nd resource is becoming more serious. Ce and La is the most abundant rare earth elements and constitute more than 70% of the total rare earth element, and the price of Ce is about 10 times lower than Nd. Hence, from both industrial and academic viewpoints, it is a technologically important to develop high-performance Ce or La substituted Nd-Fe-B magnets. However, the magnetic properties of Nd-Fe-B magnets could be drastically deteriorated after replacing Nd with Ce and La due to inferior intrinsic magnetic properties of $Ce_2Fe_{14}B$ ($4\pi M_s$ = 11.7 kG, H_a = 26 kOe) and $La_2Fe_{14}B$ ($4\pi M_s$ = 13.8 kG, H_a = 20 kOe) compared to $Nd_2Fe_{14}B$ ($4\pi M_s$ = 16 kG, H_a = 73 kOe). Despite of the inferior intrinsic magnetic properties of $Ce_2Fe_{14}B$ and $La_2Fe_{14}B$ to $Nd_2Fe_{14}B$, it is reported that deterioration of magnetic properties due to Ce and La substitution could be largely suppressed by constructing a multi-main-phase (MMP) structure in Nd-Fe-B sintered magnets. RE elements are inhomogeneously distributed within a 2:14:1 grains when sintering a mixture of Ce, La-free and Ce, La-containing $RE_2Fe_{14}B$ powders. Compared to single-main-phase (SMP) magnets, where Ce and La is homogeneously substituted Nd in the 2:14:1 phase, MMP magnets show much better magnetic performance. In this study, effect of dual-phase of Nd-Ce-Fe-B hot-deformed magnets using melt-spun powder was investigated. Initial ribbons with the nominal compositions of $Nd_{13.6}Fe_{bal}B_{5.6}Ga_{0.6}Co_{6.6}$ and $(Nd_{0.6}Ce_{0.4})_{13.6}Fe_{bal}B_{5.6}Ga_{0.6}Co_{6.6}$ were prepared by a single-roller melt-spinning technique and then pulverized into powders. By tuning the mass ratios of the Ce-free and Ce-containing powder, Ce-containing magnets with 0-30 wt.% (named as ND, CE0.2 and CE0.3, respectively) Ce content were prepared by dual alloy method. The melt-spun powders were then hot-pressed and subsequently die-upsetted. In our previous study, the remanence and coercivity gradually decreased with increasing Ce content. This dependence of magnetic properties on Ce content could be ascribed to the magnetic dilution effect that Ce substitution for Nd in the 2:14:1 phase decreased the intrinsic magnetic properties. However, dual-phase hot-deformed magnets shows higher magnetic properties than single-phase hot-deformed magnets at the same composition. From SEM observation, it was confirmed that the Ce-free and Ce-containing area is quite different, the crystallographic alignment of Ce-containing area is inferior to that of Ce-free area. After annealing at 973 K, the composition of the flake interface changes due to interdiffusion during the annealing process. In sintered magnet, it has been reported that the peculiar chemical heterogeneity of dual-phase magnet is that the short-range exchange coupling and long-range magnetostatic interaction can induce higher remanence and coercivity simultaneously than those of single-phase magnets with the same composition. In this study as well, it is thought that the coercivity and remanence were improved due to the interdiffusion of elements between the flake interface by annealing. Compared to the Nd-Fe-B magnet ($4\pi M_r$ = 13.1 kG, H_c = 17.3 kOe), with CE0.3, H_c decreases drastically to 15.6 kOe, accompanied with significant falls in $4\pi M_r$ to 11.5 kG. In contrast, for the dual-phase magnet with CE0.3, H_c reaches 16.74 kOe and $4\pi M_r$ is 12.1 kG, which are 7.3% and 9.2% higher than those of single-phase magnet, respectively. Based upon these results, effect of interdiffusion conditions of magnetic properties of Nd-Ce-Fe-B hot-deformed magnets will be discussed.

Synthesis and Characterization of $SmFe_{12}$-based compounds prepared by reaction-diffusion reaction

Kang-Hyuk Lee[1*], Jun-sun Hwang[1], Min Kyung Seng[2], and Sang-Im Yoo[1†]
[1]Department of Material Science and Engineering, Research Institute of Advanced Materials (RIAM), Seoul National University, Seoul, Korea
[2]Department of Physics, Sookmyung Women's University, Seoul 04310, Republic of Korea

The $ThMn_{12}$-type structure has attracted attention as permanent magnetic material due to the high anisotropy field, saturation magnetization (M_s), and Curie temperature (T_C). The $Sm(Fe_{0.8}Co_{0.2})_{11}Ti$ (SFCT) materials have been intensively studied to synthesize high permanent magnets by controlling the doping element. In this study, we tried to investigate SFCT materials prepared by reaction-diffusion reaction. we prepared the $Sm_x(Fe_{0.8}Co_{0.2})_{11}Ti$ (x= 1~4) precursor was prepared by a common co-precipitation method. The samarium nitrate hexahydrate, cobalt nitrate hexahydrate, titanium tetrachloride, and iron nitrate hexahydrate were dissolved in deionized water at 70 C to form a homogeneous solution. The 3M KOH solution was slowly dropwise in the solution. Then the pH of the solution was adjusted slowly to pH 12 by adding dropwise ammonium hydroxide solution. The precipitates were collected by filtration. The precursors were heat-treated at 600℃ for 4h in H_2 gas. The hydrogen-reduced powders were mixed with calcium granules and pelletized. The pelletized samples were heated at 950 - 1050 ℃ for 1 h in Ar gas. Samples were characterized by using an x-ray diffractometer (XRD) with Cu-Kα radiation source, a vibrating sample magnetometer (VSM), and scanning electron microscopy (SEM). The samples were obtained $ThMn_{12}$-type phase at 1050 ℃ for 1 h in Ar gas. The M_s and H_c values of $Sm(Fe_{0.8}Co_{0.2})_{11}Ti$ samples were 95 emu/g and 1935 Oe. Detailed microstructures and magnetic properties will be presented for discussion.

SmFe12-based compounds, ThMn12-type, hard magnetic material

Acknowledgments: This research was supported by Future Materials Discovery Program through the National Research Foundation of Korea(NRF) funded by the Ministry of Science and ICT (2016M3D1A1027835).

Magnetic performance of hybrid Nd-Fe-B/Ce-Fe-B hot-deformed magnets

Ye Ryeong Jang[1*], Wonjin Kim[1], Seung Yong Lee[2], Hyun-Sook Lee[1], and Wooyoung Lee[1†]
[1]Department of Materials Science and Engineering, Yonsei University, Seoul 03722, Republic of Korea
[2]KIURI Institute, Yonsei University, Seoul 03722, Republic of Korea

With a rapid increase in demand for Nd–Fe–B magnets, Ce-based magnets have received a lot of attention in recent years for their potential use of permanent magnets. This is because Ce has much more natural reserves and a relatively lower selling price compared to Nd and Pr. However, Ce substitution for Nd in the 2:14:1 phase weaken the magnetic properties due to the low intrinsic magnetic properties of $Ce_2Fe_{14}B$ (saturation magnetization 11.7 kG, magnetocrystalline anisotropy field 30 kOe). Therefore, the fabrication of high performance Nd-Fe-B magnet, in which Nd is partially or completely replaced by Ce, is still challenging issues. In this study, we investigated the magnetic performance of hybrid Nd-Fe-B/Ce-Fe-B hot deformed magnet. We designed a dual main phase (DMP) hot deformed magnets by mixing Ce-free and Ce-containing Nd-Fe-B powders. The melt-spun ribbons of Ce-Fe-B and Nd-Fe-B were mixed in various ratios and prepared into powders. The magnetic performance of the magnets was investigated by changing the contents of Ce-Fe-B and Nd-Fe-B in the range of 50–100 wt% and 50–0 wt%, respectively. For best magnetic performance, the hot deform temperature was adjusted in the range of 700–850 ℃. We analyzed the microstructure of the DMP magnets compared to SMP (single main phase) magnets. Finally, we evaluated the possibility of the hybrid Nd-Fe-B/Ce-Fe-B hot deformed magnet as a potential candidate for low-cost medium performance ($(BH)_{max}$ = 20 MGOe) permanent magnet.

Fabrication and magnetic properties of Iron-rich intermetallic compounds with $ThMn_{12}$ structure

Hui-Dong Qian[1,2*], Jung Tae Lim[1], Yang Yang[1,2], Jong-Woo Kim[1], Tian Hong Zhou[1], Su Yeon Ahn[1], Hankuk-Jeon[1], Kyung Mox Cho[2], Jihoon Park[1*], Chul-Jin Choi[1†]

[1]Powder Materials Division, Korea Institute of Materials Science, Changwon, Gyeongsangnam-do 51508, Republic of Korea

[2]School of Materials Science and Engineering, Pusan National University, Busan 46241, Republic of Korea

Rare-earth intermetallic compounds of $R(Fe,M)_{12}$ (R = rare earth elements, M = transition metals) with $ThMn_{12}$ structure have been known to be promising permanent magnetic materials since the 1980s [1]. Recently, increasing rare earth price has pushed the industry to seek ways to reduce the R-content in the hard magnetic materials. In case, strong magnets with the $ThMn_{12}$ type of structure received much attention [2]. However, during the several tens of years, the research about $ThMn_{12}$ magnetic materials was not made a breakthrough. As a turning point of the $ThMn_{12}$-type Fe-rich compounds research, $ThMn_{12}$-type $Sm(Fe_{1-x}Co_x)_{12}$ compound films with a saturation magnetization of 1.78 T, an anisotropy field of 12 T, and a Curie temperature of 586 °C, all of which are superior to those for $Nd_2Fe_{14}B$ [3], were successfully produced. However, it still has difficulty in stabilizing the unstable $ThMn_{12}$ phase in magnetic powders and bulks. In previous research, the $ThMn_{12}$ structure is also unstable and partial Fe atoms must be substituted with phase stabilizing element(s), such as Ti, V, Cr, Mn, Mo, W, Al, and Si, which results in magnetization reduction. So, decreasing magnetization or coercivity with the non-magnetic elements substitution is a new challenge for the $ThMn_{12}$-type $Sm(Fe_{1-x}Co_x)_{12}$ compound research. Therefore, we have developed a new fabrication method to produce a high-density $Sm(Fe_{0.8}Co_{0.2})_{11}Ti$ bulk with high purity and magnetic properties and investigated Si substitution or doping effects on this work's magnetic and physical properties.

The purity of the hard magnetic $ThMn_{12}$ phase in the bulk magnet reached higher than 97 *wt*.%. The remanent magnetization and maximum energy product of the prepared $Sm(Fe_{0.8}Co_{0.2})_{11}Ti$ bulk reached high values of 96.0 emu/g and 12.22 MGOe, respectively. The phase transformation behavior from amorphous to $ThMn_{12}$ phase during

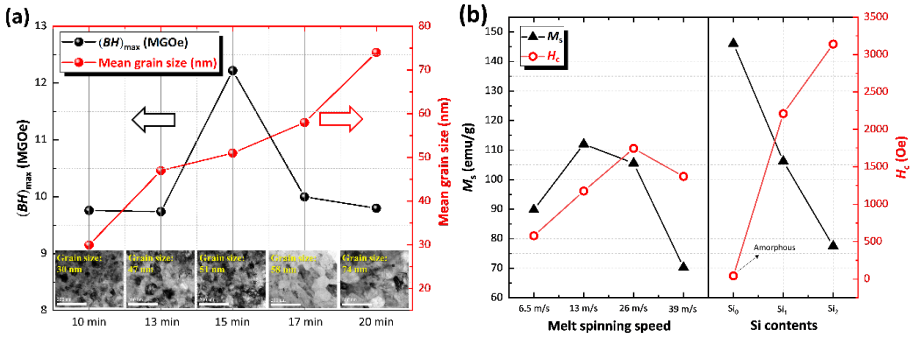

Fig. 1 (a) Magnetic properties and grain sizes of $Sm(Fe_{0.8}Co_{0.2})_{11}Ti$ bulk magnets with different annealing times and (b) magnetic properties of $Sm(Fe_{0.8}Co_{0.2})_{10}Si_2$ with different wheel speeds and $Sm(Fe_{0.8}Co_{0.2})_{11}Ti+Si_x$ (x = 0, 0.5, and 1) ribbons with wheel speed of 39 m/s.

heat treatment was systematically investigated by transmission electron microscopy. The magnetic properties and grain sizes of $Sm(Fe_{0.8}Co_{0.2})_{11}Ti$ bulk magnets with different annealing times were shown in Fig. 1 (a). To investigate the effect of substituted elements in the $ThMn_{12}$-type Fe-rich compounds and compare with the Ti substitution, Si was selected to dop into the $ThMn_{12}$-type Fe-rich compounds. $Sm(Fe_{0.8}Co_{0.2})_{10}Si_2$ and $Sm(Fe_{0.8}Co_{0.2})_{11}Ti+Si_x$ (x = 0, 0.5, and 1) ribbons were produced using a melt spinning method. The magnetic properties of the $Sm(Fe_{0.8}Co_{0.2})_{10}Si_2$ ribbons with different melt spinning speeds and the $Sm(Fe_{0.8}Co_{0.2})_{11}Ti+Si_x$ ribbons with melt spinning speed of 39 m/s are shown in Fig. 1 (b). The maximum coercivity of the $Sm(Fe_{0.8}Co_{0.2})_{10}Si_2$ and $Sm(Fe_{0.8}Co_{0.2})_{11}Ti+Si_x$ ribbons reached 1745 and 3140 Oe, respectively. The details of the fabrication procedure, microstructure, and magnetic properties of as mentioned compounds will be discussed.

References

[1] G.C. Hadjipanayis, A.M. Gabay, A.M. Schönhöbel, A. Martín-Cid, J.M. Barandiaran, D. Niarchos, *Engineering* **6** (2020) 141-147.

[2] I. S. Tereshina, N. V. Kostyuchenko, E. A. Tereshina-Chitrova, Y. Skourski, M. Doerr, I. A. Pelevin, A. K. Zvezdin, M. Paukov, L. Havela, and H. Drulis, *Scientific Reports* **8** (2018) 3595.

[3] Y. Hirayama, Y.K. Takahashi, and S. Hirosawa, and K. Hono, *Scripta Mater.* **138** (2017) 62-65.

Microstructure and Magnetic Properties of Sn added MnBi Bulk Magnets

Yang Yang[1,2*], Jung Tae Lim[1], Jihoon Park[1], Hui-Dong Qian[1,2], Oi Lun Li[2], Jong-Woo Kim[1†], Chul-Jin Choi[1†]

[1]Korea Institute of Materials Science, Changwon 51508, Republic of Korea

[2]School of Materials Science and Engineering, Pusan National University, Busan 46241, Republic of Korea

Rare-earth free permanent magnets are current emerging issues of industry for the growing market demands. Among the rare-earth free permanent magnets, MnBi has attracted attention for large magnetocrystalline anisotropy constant ($K_1 \approx 1.6$ MJ/m^3, at 300 K) [1] and unique positive temperature coefficient of coercivity (H_c) [2]. The low-temperature phase (LTP) of MnBi exhibits a saturation magnetization (M_s) of 80 emu/g, and the theoretical maximum energy product $(BH)_{max}$ 17.7 MGOe at room temperature [3]. However, it is a challenge to fabricate MnBi bulk magnets while maintaining the superior magnetic properties of the powder, especially to prevent the reduction of H_c from powder to bulk. The effects of Sn adding on the microstructure and magnetic properties of MnBi bulk magnets have been systematically investigated. As kwon, the pure MnBi bulk magnets are challenging to reach high H_c in previous studies, and a few reference works have been reported about research on fabrication of high H_c MnBi bulks by adding the third element. It was found that the Sn-added MnBi bulk magnets show the increased H_c and the improved squareness, apparently related to restructuring the intergranular phase due to Sn element addition. The H_c of MnBi bulk magnet with 3 *wt.*% Sn reaches 11.6 kOe, which is 35 % higher than that of the pure MnBi magnet. In the sample of 1 *wt.*% Sn added MnBi bulk magnet, the H_c was elevated to 10.0 kOe, and the maximum energy product $(BH)_{max}$ was recorded of 7.84 MGOe at room temperature. This makes Sn added MnBi bulk magnet a promising candidate for next-generation rare-earth-free bulk magnets.

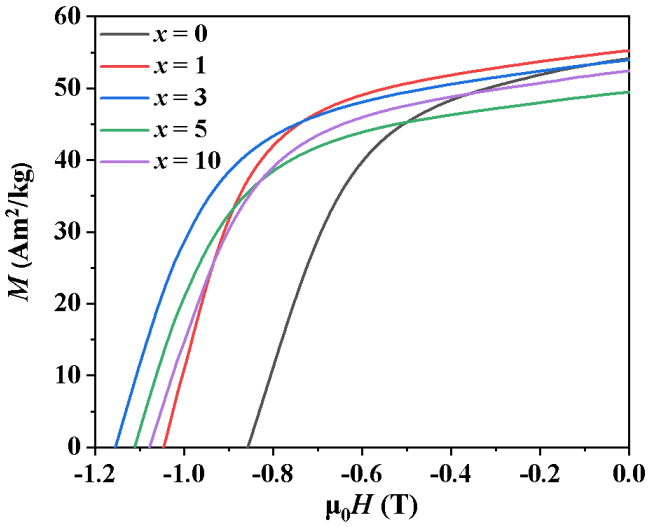

Fig. 1. Room temperature demagnetization curves of the MnBi bulk magnets added with Sn contents of (0, 1, 3, and 5 *wt.*%).

References

[1] B.W. Roberts, Neutron diffraction study of the Structures and magnetic properties of Manganese Bismuthide, Phys. Rev. 104 (1956) 607-616.

[2] J.B. Yang, K. Kamaraju, W.B. Yelon, W.J. James, Q. Cai, A. Bollero, Magnetic properties of the MnBi intermetallic compound, Appl. Phys. Lett. 79 (2001) 1846.

[3] J. Park, Y.-K. Hong, J. Lee, W. Lee, S.-G. Kim, C.-J. Choi, Electronic structure and maximum energy product of MnBi. Metals 4 (2014) 455-464.

O-2-6

Giant Magnetic Anisotropy in Metastable FePt Alloy

T. Ochirkhuyag[1*], S. C. Hong[2], D. Tuvshin, E. Uranbaigal, and D. Odkhuu[1†]
[1]Department of Physics, Incheon National University, Incheon 22012, South Korea
[2]Department of Physics, University of Ulsan, Ulsan, South Korea

As information storage and high-speed permanent magnet motor technologies have evolved, high-performance permanent magnetic materials with large saturation magnetization and magnetic anisotropy (MA) become indispensable. In this presentation, we report results of first-principles calculations on structural and intrinsic magnetic properties of L10-ordered FePt alloy along the so-called Bain path. Our total energy calculations reveal that the body centered tetragonal (bct) structure of FePt with c/a=0.85 is identified as a metastable phase, which can be epitaxially grown on an appropriate substrate. More remarkably, both saturation magnetization and uniaxial MA of this bct metastable phase are significantly larger compared with those of the ground state L10-FePt and other known magnetic materials. Single-particle energy spectrum analyses indicate that while the Pt 5d orbital states determine the MA-driven permanent magnetic properties in L10-FePt alloy, the large enhancement of MA in the metastable structure mainly originates from the Fe 3d orbital states. We will also discuss our more recent findings on possibilities of further improving the performance of the metastable permanent magnet FePt with a series of 3d and 4d transition metal dopant elements.

Effect of Cu addition on the magnetic and microstructural properties of multi-main phase Nd-Ce-Fe-B sintered magnet

Kyoung-Hoon Bae[1*], Jung-Goo Lee[1], Sang-Hyup Lee[2], Dong-Hwan Kim[2]
[1]Powder Materials Division, Korea Institute of Materials Science, Changwon, Korea
[2]R&D center, Star Group, Daegu, Korea

As the demand for Nd-Fe-B magnets increases, replacing Nd in the magnets with abundant and inexpensive Ce has become an important technology to develop cost-effective Nd-Fe-B magnets [1]. Developing a multi-main phase (MMP) microstructure by the mixture of Ce-free and Ce-containing powders is an efficient way to improve the coercivity (H_c) and to minimize the remanence reduction of Nd-Ce-Fe-B sintered magnets [1]. Nevertheless, the insufficient H_c of the MMP Nd-Ce-Fe-B sintered magnet, owing to the low intrinsic magnetic properties of the $Ce_2Fe_{14}B$ phase, is still a major obstacle to be overcome. The practical H_c of Nd-Ce-Fe-B sintered magnet can be improved when the 2:14:1 grains are magnetically isolated by continuous and uniform non-magnetic grain boundary phase (GBP) [2]. A small amount of Cu addition promotes the effects of post-sintering annealing (PSA) on microstructural improvements in the magnetic properties of Nd-Fe-B sintered magnet because of the reduced melting point of the Nd-rich GBP [3]. However, in the case of MMP Nd-Ce-Fe-B sintered magnet, the role of Cu in the rare-earth (RE)-rich triple-junction phase (TJP) and GBP has not yet been clearly clarified. In addition, since the melting temperature of the RE-rich phase is sensitive to the Cu content, the effect of the Cu content on the optimal PSA conditions should be considered. Therefore, we investigated the effects of various amounts of Cu addition on the microstructural and magnetic property changes of MMP Nd-Ce-Fe-B sintered magnet and clarified the optimum PSA temperature for the Cu-doped MMP sintered magnet. Ce-free and Ce-containing magnetic powders with nominal compositions of $(Pr,Nd)_{31.0}Fe_{bal.}M_{1.90}B_{1.0}$ and $[(Pr,Nd)_{19}Ce_{12}]_{31.0}Fe_{bal.}M_{1.90}B_{1.0}$ M(wt.%, M=Al, Ga, Nb, Cu, and Co) were prepared using the powder metallurgical method. Ce-free and Ce-containing powders, with a mean particle size of less than 3.0 ㎛, were mixed (ratio of 20:80) and these powders were mixed with Cu powder (0.05 and 0.15 wt.%). The Cu contents of the magnets were 0.15, 0.2, 0.3 wt.%. The green compacts were sintered at 1060°C for 2h. The 1st PSA temperatures were varied from 850 to 600°C to optimize the PSA temperature, then annealed again at 480°C for 2h (2nd PSA). The microstructure, phase identify and magnetic properties of samples were investigated by using EPMA, HRTEM, DSC, and BH-tracer. In this presentation, the role of Cu in MMP Nd-Ce-Fe-B sintered magnets and the change in the triple junction and grain boundary structures and phases will be discussed, and the optimum PSA temperature according to the change in Cu content will be proposed.

References

[1] T. Ma, M. Yan, K. Wu, B. Wu, X. Liu, X. Wang, Z. Qian, C. Wu, W. Xia, Acta Maters. 142 (2018) 18-28.
[2] K.H.Bae, S.R. Lee, K.H. Bae, H.J. Kim, M.W. Lee, T.S. Jang, Intermetallics 92 (2018) 93-100.
[3] T.H. Kim, S.R. Lee, M.W. Lee, T.S. Jang, J.W. Kim, Y.D. Kim. H.J. Kim, Acta. Maters.

Fabrication of fine-grained Nd-Fe-B hot-pressed magnet using anisotropic HDDR powders aligned by a pulsed magnetic field

Jae-Gyeong Yoo[1,2*], Tae-Hoon Kim[1], Hee-Ryoung Cha[1], Yang-Do Kim[2†], Jung-Goo Lee[1†]
[1]Department of Magnetic Materials, Korea Institute of Materials Science, Changwon, Korea
[2]Department of Materials Science and Engineering, Pusan National University, Busan, Korea

The hot-deformation process is the most promising industrial process to fabricate fine-grained anisotropic Nd-Fe-B bulk magnets using melt-spun or HDDR powders. However, the problem of the hot-deformed magnets produced from the isotropic melt-spun powders is that an abnormal grain growth occurs during the hot-deformation process or the grain boundary diffusion process due to the fine nature of grains in the initial melt-spun powders. To use the isotropic HDDR powders with a relatively larger grain size as an initial powder is an effective way to fabricate the anisotropic hot-deformed magnets while suppressing the abnormal grain growth. However, the hot-deformed magnet produced from isotropic HDDR powders is difficult to obtain high remanence, B_r. Because the [001] texture is not well developed during the hot-deformation due to the higher deformation resistance of the HDDR powders.

Therefore, magnetically aligning the anisotropic HDDR powders before the densification can be a great solution for achieving higher Br in the magnets. In addition, if the HDDR powders can be magnetically well aligned before the densification, the fine-grained anisotropic bulk magnet could be obtained by the hot-press alone without undergoing subsequent die-upsetting process. Thus, in this study, we fabricated the anisotropic Nd-Fe-B hot-pressed using the anisotropic HDDR powders aligned by a pulsed magnetic field, and observed the influences of the magnetic and microstructural properties of initial HDDR powders on the magnetic alignment and hot-press behaviours.

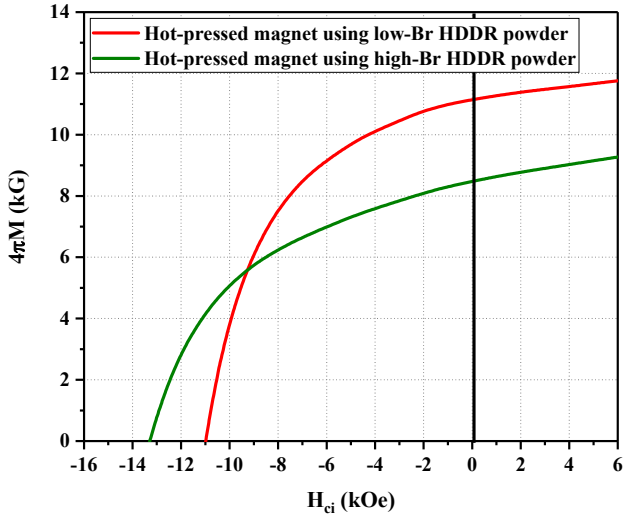

Figure 1. Demagnetization curves of hot-deformed magnets using low-and high-Br HDDR powders.

Especially, higher Br is obtained after the hot-press of the anisotropic HDDR powders when the remanence of the HDDR powders are controlled to be lower. This implies that higher-remanence HDDR powders generate stronger local magnetic field during the magnetic alignment, thereby disrupt the alignment of adjacent particles as observed by R. Soda et al [1]. A detailed influences of the magnetic and microstructural properties of initial HDDR powders on the magnetic alignment and hot-press behaviours will be discussed, and a method to further increase the remanence of the hot-pressed magnets when align the anisotropic HDDR powder by pulsed magnetic field will be proposed based on the results.

Reference

[1] R. Soda et al, Scr. Mater., 41-44, 120 (2016).

화학공정용 마그네틱 드라이브 펌프에 적용되는 영구자석에 대한 연구

윤명환*, 신용우, 이기덕, 유세현, 이정종
한국전자기술연구원 지능메카트로닉스 연구센터

화학공정용 원심펌프는 중화학 관련 여러 산업의 핵심 모듈이며 에너지 소비가 높은 기기이다. 원심펌프는 메카니컬 씰을 사용하는 펌프와 마그네틱 드라이브 펌프로 크게 나뉜다. 기존에 많이 적용된 메커니컬 씰 펌프는 축과 하우징 사이를 밀봉하는 구조를 갖는다. 이 구조는 제작이 쉽고 가격이 저렴하지만 씰에 문제가 생기는 경우 유해한 화학약품이 펌프 운전 중에 유출되는 사고가 발생할 가능성이 크다. 하지만 마그네틱 드라이브 펌프의 경우 임펠러를 포함, 화학약품이 흐르는 주변을 모두 밀봉하는 구조로 축과 마그네틱 드라이브는 분리되어 있어 매우 안전하다. 마그네틱 드라이브는 동력을 전달해주는 장치로 Inner Part와 Outer Part로 구성되어 있고 안쪽과 바깥쪽은 운전 환경이 다르다. 안쪽의 경우 액체의 최대 온도가 150도까지 올라가기 때문에 그 온도에서의 성능 및 자석의 불가역감자가 일어나지 않아야 한다. 목표 출력 및 토크를 만족하기 위해서는 영구자석의 온도에 따른 특성을 분석을 해야한다. 이 논문에서는 운전 온도에 따른 자석 성능 및 불가역 감자 등 자석 특성에 대한 검토를 진행하였다.

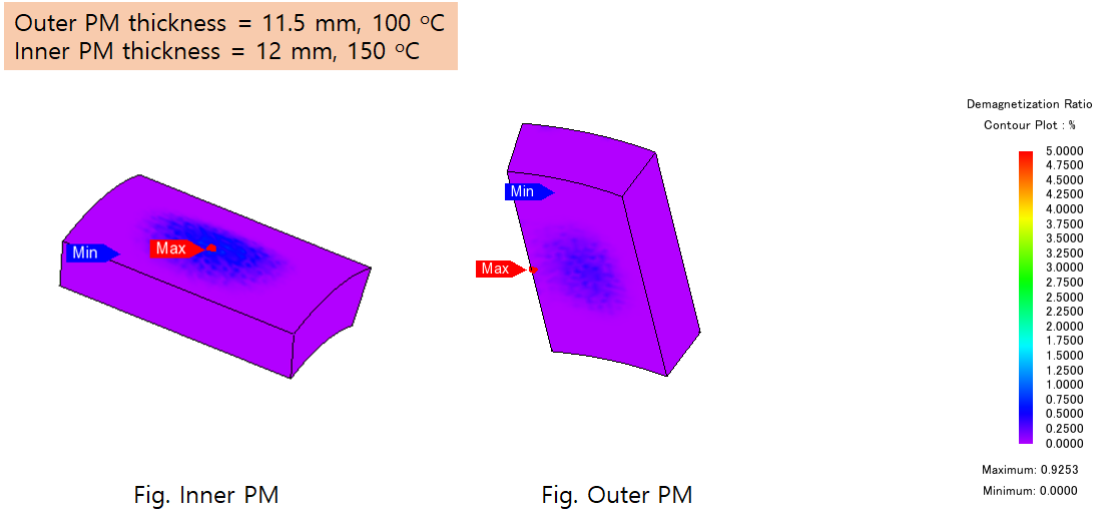

Fig. Inner PM　　Fig. Outer PM

그림 1. 영구자석 감자특성

사사: 본 연구는 2021년도 중소벤처기업부의 기술개발사업 지원에 의한 연구임. (S3153495)

할박 배열 영구자석을 갖는 비 접촉 동력 장치의 구조에 따른 특성 해석 및 검증

우종현[1*], 박하나[2], 이정훈[2], 최장영[1†]
[1]Department of Electrical Engineering, Chungnam National University,
99 Daehak-ro, Yuseong-gu, Daejeon 34134, Korea
[2]Human Cooperate Company, Korea

산업이 발달함에 따라 여러 분야에서 1차측 에너지를 2차측으로 전달하는 동력 전달 장치에 대한 수요가 많아지고 있으며, 그 중 하나인 직접 구동 기기는 벨트, 볼스크류 등의 기구 장치를 거치지 않고 구동 축과 부하 축을 직접 구동하는 시스템을 의미한다. 직접 구동 기기는 상대적으로 간단한 구조, 제어, 용이한 제작성 및 높은 효율의 장점을 가지며 산업용 로봇, 세탁기, 자동차 등에 사용된다. 그러나 이런 직접 구동 기기는 구동 축과 부하 축의 결합으로 인해 기기의 접촉부에 발생하는 기계적 손실이 불가피한 요소로 작용한다. 따라서 반도체 제조 장비 등, 응용 처에 따라 기계적 손실에 따른 분진 및 진동에 민감한 분야에서는 적용되기 어렵다. 그에 대한 대안으로 영구자석을 사용한 비 접촉 식 동력 전달 장치가 떠오르고 있으며, 많은 연구가 수행되고 있다. 이러한 자기 장치는 기계적 장치에 비해 유지보수, 효율, 토크 전달 메커니즘 측면에서 장점을 보유하고 있기 때문에, 큰 동력을 전달할 때 탁월한 효과를 얻을 수 있고, 다양한 문헌들을 통해 마그네틱 기어의 장점을 확인 할 수 있다.

비 접촉식 동력 전달 장치의 경우, 기어와 벨트와 같은 접촉식과 달리 1차측과 2차측의 간극과 자석의 극수 및 배열에 따라 많은 전달 토크의 차이를 가진다. 따라서 마그네틱 기어의 구조에 따른 영향에 대한 분석이 매우 중요하다. 본 연구의 경우 회전 운동을 선형 운동으로 변환하는 것을 목적으로 랙-피니언 구조를 선정하였다. 랙-피니언 기어는 선형 기어와 회전형 기어의 결합된 기어로써, 회전력인 토크를 선형 추력으로 변환해 주는 역할을 한다. 고정된 축을 피니언이 회전하면 랙은 선형 운동을 하게 되고 이러한 움직임을 이용하여 랙-피니언 기어는 조향장치, 반송장치, 공작기계 등에 널리 이용된다. 따라서 본 논문에서는 랙-피니언 마그네틱 기어의 구조를 선정하여 할박 배열을 갖는 피니언을 적용 및 구조에 따른 추력 특성 및 진동 특성을 비교 분석하여 최적의 모델을 제안한다.

본 연구에 적용된 할박 배열은 수직 방향으로 자화된 자석배열 보다 공극에서 자속밀도가 약 1.4배 크게 얻을 수 있고 그 파형 또한 정현적이기 때문에 기기의 출력 밀도를 높이는 장점이 있다. 따라서 할박 배열 영구자석을 갖는 피니언을 적용하였을 경우, 공극 자속 및 추력에 미치는 영향을 분석 하였다. 먼저, 1차측을 회전 운동, 2차측을 선형 운동으로 적용하여 영구자석의 극수에 따른 동작 분석을 통해 초기 모델을 선정하였다. 이 후 1차측과 2차측의 구조에 따른 추력 분석을 수행하였고, 1차측의 움직임을 통한 최대 정지력을 얻었다. 이때 한 주기의 1차측 Pull Out 토크를 THD(Total Harmonic Distortion) 분석하였고, 다음으로 과도 해석을 통하여 1차측이 구동 할 때 발생하는 동력이 2차측 기어에 선형 운동으로 전달되는 해석 결과를 분석하였다. 분석 결과를 바탕으로 최적 모델을 선정하였으며, 이후 제작 모델을 통한 실험을 통해 검증을 수행하였다. 본 논문의 모든 해석 과정은 3차원 유한요소 해석법을 이용하였고, 각 구조에 따른 비교를 통해 본 논문에서 제시하는 랙-피니언 비 접촉 동력 전달 장치의 가능성 및 신뢰성을 제안하고자 한다. 이는 다양한 종류의 자기장치들을 설계 시 참고 할 수 있을 것으로 사료된다.

방향성 전기 강판을 적용한 고고도 장기체공 무인항공기용 외전형 방식 표면 부착형 영구자석 동기전동기의 성능 분석

안종민*, 임동국†
Department of Electrical, Electronic and Computer Engineering, University of Ulsan

본 논문에서는 방향성 전기 강판을 적용한 HALE(High Altitude Long Distance, 고고도 장기체공) UAV (Unmanned Aerial Vehicle, 무인항공기)용 외전형 SPMSM(Surface-mounted Permanent Magnet Synchronous Motor, 표면 부착형 영구자석 동기전동기)의 성능 분석을 다루고 있다. 무인항공기는 현재 농업, 교통, 물류 항공 촬영 등 다양한 분야에서 사용되고 있고 활용도가 커질 것으로 기대되어 앞으로 무인항공기는 항공시장의 성장을 주도할 것으로 예상됩니다. 고고도 장기체공 무인항공기의 경우 고고도인 성층권에서 비행하므로 고도의 환경에서도 안정적인 성능 발휘를 위한 전동기가 필요합니다. 영구자석 동기 전동기의 경우 높은 효율성, 출력밀도, 좋은 응답특성 등으로 인해 자동차, 가전제품, 항공 분야 같은 고성능 어플리케이션에 넓게 사용됩니다. 그 중 표면 부착형 영구자석은 상대적으로 제어가 간단하고 공극자속밀도를 사인파로 설계하여 코깅 토크와 토크 리플을 줄일 수 있고 정속 운전에 유리하므로 급격한 가감속 운행보단 지속적인 운행을 필요로 하는 고고도 장기체공 무인항공기에 적합합니다. 전기 강판은 자화가 일어나기 쉽도록 결정배열을 조정하고 규소를 첨가하여 다른 철강재료에 비해 전자기적 특성이 우수합니다. 그 중에서 방향성 전기강판은 강판의 압연방향으로 자화가 용이하도록 제작된 강판으로 Fig. 1에 보이듯이 압연 방향으로 자기적 특성을 대폭 향상시킵니다. 반면에 압연 수직 방향으로는 오히려 낮은 자기적 특성을 보입니다. 따라서, 전동기의 경우 고정자에 흐르는 자속의 방향이 바뀌기 때문에 큰 효과를 보기 힘들 것입니다. 그러나, 본 논문에서는 상대적으로 자속 방향이 일정한 고정자 치 부분에 방향성 강판을 적용하여 SPMSM 모델을 설계하였고 유한요소해석을 통해 부하, 무부하 해석을 진행하였습니다. 토크 리플과 코깅 토크, 역기전력 전 고조파 왜곡은 진동을 발생시키므로 전동기 설계에 있어서 이들을 저감하는 것은 매우 중요합니다. 따라서, 부하 해석을 통해 정격 토크를 만족하는 방향성 강판 적용 SPMSM과 무방향성 강판 SPMSM의 토크 리플을 비교하고 무부하 해석을 통해 코깅 토크, 역기전력 전 고조파 왜곡을 비교하였습니다. Fig. 2는 제안된 SPMSM 모델로서 48극 36슬롯 구조이고 고정자 치에 방향성 강판이 적용되어 있습니다. 해석 결과 무방향성 강판과 비교하여 부하 해석에서 토크는 약 12.33% 증가하였고 토크 리플은 약 73.81% 감소하였으며 철손의 경우 약 93.42% 감소하였습니다. 토크의 증가와 철손의 감소로 인해 효율이 1.34% 증가하였습니다. 또한, 무부하 해석에서는 THD와 코깅토크가 각각 67.42%, 86.35% 감소하였습니다. 따라서, 전동기 설계에서 방향성 강판의 자속이 압연방향으로 흐를 수 있도록 고려하여 적절한 위치에 방향성 강판을 사용한다면 다양한 어플리케이션에 적용하여 좋은 성능을 나타낼 것으로 기대됩니다.

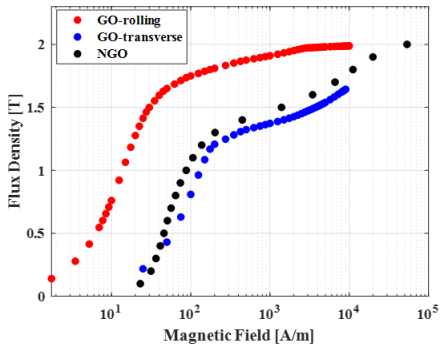

Fig. 1. B-H curve of GO and NGO Steel

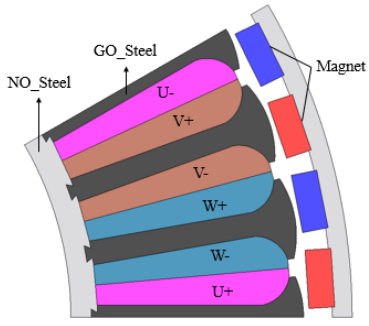

Fig. 2. Proposed SPMSM model for HALE UAV

고정투자율법을 이용한 고조파 전류 입력 철손 해석 방법

유준열*, 진준우, 임명섭
한양대학교 미래자동차공학과, 한국

최근 산업에서 많이 사용되는 전기 모터의 운전 영역이 넓어짐에 따라 철손 예측에 대한 관심이 늘어나고 있다. 하지만, 고속 영역에서 정확한 모터 성능을 예측하기 위해 고조파 전류를 고려한 철손이 요구된다. 이를 위해 본 논문에서는 고정투자율법을 이용한 고조파 전류 입력 철손 해석 방법을 제안한다. 모터-인버터 coupling 모델을 통해 모터에 입력되는 고조파 전류를 예측하고, 해석 시에 반영하기 위한 고조파 차수 및 주파수를 결정한다. Steinmetz 식을 통해 결정된 주파수까지 철손 데이터를 fitting하여 해석에 반영하고, 고조파 차수를 고려하여 수식적인 방법을 통해 공극 mesh 개수 및 해석 step을 결정한다. 2D 유한요소해석을 통해 고조파 성분을 반영하기 위해서는 많은 수의 해석 step이 요구되지만, 이는 해석 시간이 고조파 차수에 비례하여 증가한다는 단점이 있다. 이를 해결하기 위해 기본파 전류에 대해 비선형 해석을 진행하여 투자율을 저장하고, step별 투자율 보간 방법을 적용하여 선형 해석을 통해 고조파 전류 반영 철손을 계산한다. 제안한 방법을 통해 계산한 철손은 정현파 전류 인가하여 계산한 철손 및 동일 전류 파형을 인가하여 3D 유한요소해석을 통해 계산한 철손과의 비교를 통한 검증을 진행하였다. 따라서, 제안한 방법을 통해 예측한 고조파 전류를 통해 해석 모델링 및 해석 조건을 결정한다. 추가적으로, 2D 유한요소해석 시에 투자율 보간 방법을 통해 높은 신뢰성을 갖는 철손을 빠르게 계산하여 정확한 전기 모터 성능 예측에 반영할 수 있다.

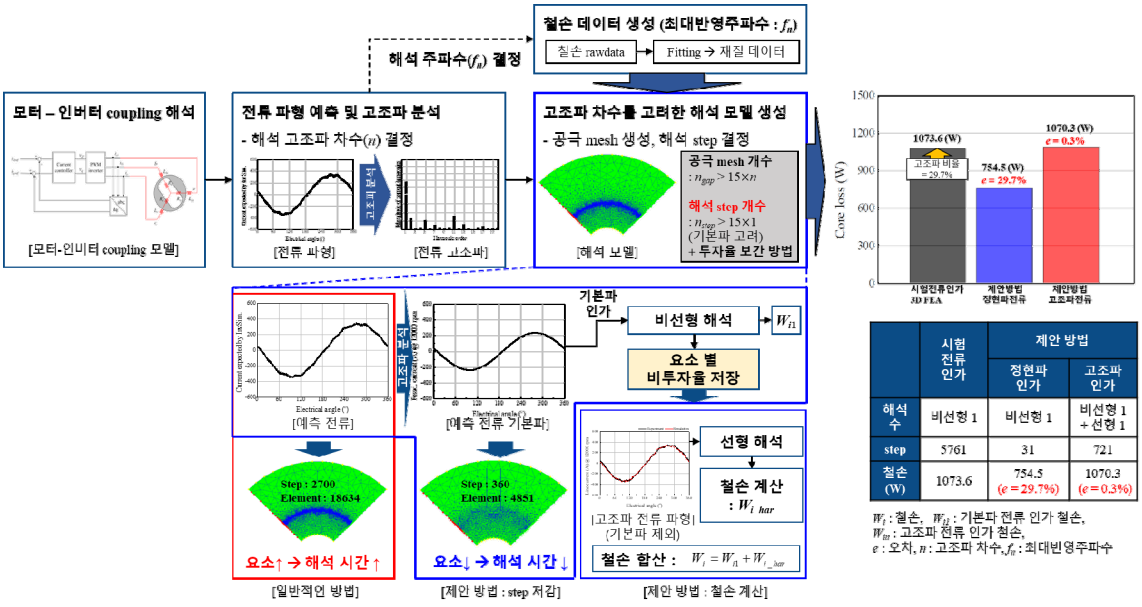

	시험 전류 인가	제안 방법	
		정현파 인가	고조파 인가
해석 수	비선형 1	비선형 1	비선형 1 + 선형 1
step	5761	31	721
철손 (W)	1073.6	754.5 (e = 29.7%)	1070.3 (e = 0.3%)

W_i : 철손, W_{i1} : 기본파 전류 인가 철손,
W_{ih} : 고조파 전류 인가 철손,
e : 오차, n : 고조파 차수, f_n : 최대반영주파수

2021 KMS Winter Conference

Symposium 5

‘Soft Magnetics’

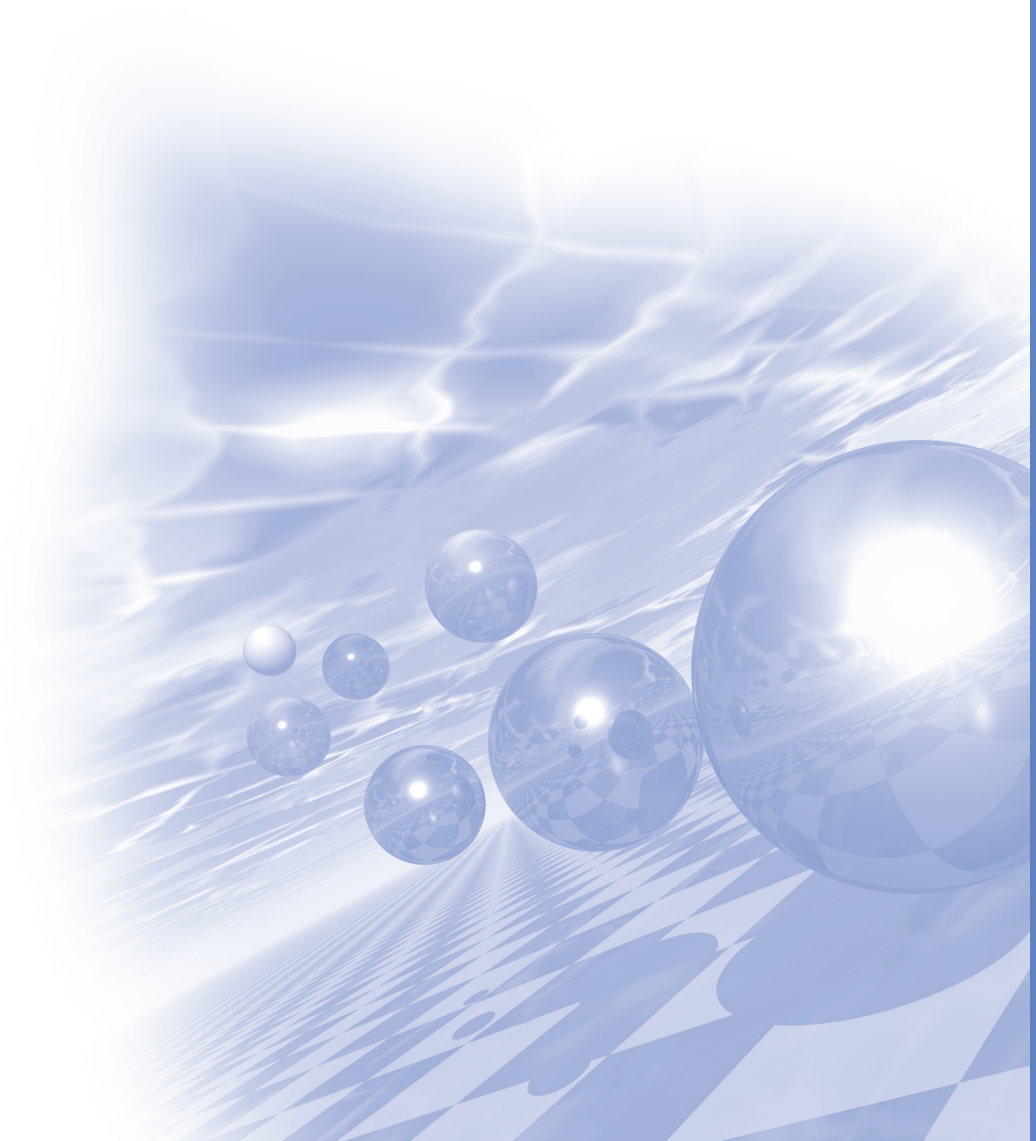

Fabrication of high-M_s amorphous/nanocrystalline soft magnetic materials for high-frequency and high-efficiency electromagnetic applications

Jae Won Jeong[1*], Yeong Gyun Nam[1,2], Hyun Aha Im[1,2], Su-Bong An[1,2], Hea-Ran Kim[1,3], Min-Sun Jang[1], and Sangsun Yang[1]

[1]Metal Powder Department, Korea Institute of Materials Science (KIMS), 797 Changwondae-ro, Seongsan-gu, Changwon 51508, Korea

[2]School of Materials Science and Engineering, Pusan National University, Busandaehak-ro 63beon-gil, Geumjeong-gu, Busan 46241, Korea

[3]Department of Materials Science and Engineering, Sungkyunkwan University (SKKU), Suwon 16419, Korea

Soft magnetic materials are widely used in diverse fields of applications including electronics, motor/ generators, electromagnetic wave shielding/absorbing. As the working frequency of electronic devices is continuously increasing and high-efficiency operation is required, the development of reliable and low-loss soft magnetic materials has become an import work.

Fe-based soft magnetic amorphous/nanocrystalline materials are considered ideal materials for magnetic powder cores due to their excellent magnetic properties such as low coercivity, high resistance, and good DC bias characteristics. Due to the disordered configuration of atoms in amorphous alloys, these materials have zero magnetocrystalline anisotropy, which ensures high permeability and low coercivity. In addition, due to their high resistivity, Fe-based amorphous alloys exhibit extremely-low eddy current loss at high frequencies, making them suitable as high frequency soft magnetic composite (SMC) materials.

The most significant limitation of SMCs comprising low-M_s amorphous/nanocrystalline materials is poor DC bias. Enhancing the M_s of amorphous/nanocrystalline materials by carefully managing alloy composition is the best way to enhance permeability retention even with high bias field; however, increasing Fe content in the alloy significantly deteriorates the glass-forming ability of the alloy, and processing through gas or water atomization becomes extremely difficult due to the limited cooling rate (10^2~10^6 K/s) of the process

In this presentation, the fabrication and processing of novel amorphous/nanocrystalline soft magnetic materials for high-frequency and high-efficiency electromagnetic applications will be discussed. Ultra-fine soft magnetic micro powders having amorphous phase were prepared by high-pressure gas/liquid co-injection atomization and their soft magnetic properties were examined. High-M_s nanocrystalline soft magnetic ribbons were also fabricated through the rapid-cooling planar flow casting process. The examination of their soft magnetic properties and demonstrations of commercial applications will also be presented.

초S-5-2

Changes in magnetic properties and microstructure according to composition and annealing conditions of Fe-based nanocrystalline alloys

Kwiyoung Lee* and Jongryoul Kim
Department of Materials and Chemical Engineering, Hanyang University, Ansan 15588, South Korea

급속응고법(Rapid solidification process, RSP)은 Fe 기반 나노결정합금을 제조하는데 널리 사용된다. 급속응고법으로 비정질 구조의 합금을 얻기 위해 합금 내 Fe 함량은 비정질 형성 원소의 첨가량에 의해 제한된다. 최근 전자 장치의 에너지 효율성에 대한 이슈로 Fe 계 나노결정 합금은 높은 자속 밀도를 갖도록 요구된다. 그러나, 높은 자속 밀도를 위한 Fe 의 과첨가는 소재의 비정질 형성을 방해할 뿐만 아니라 열 안정성을 저하시킨다. 열적 불안정성은 어닐링 공정에 의한 나노결정합금의 보자력을 급격히 증가시키며 최종 어플리케이션 사용 환경의 제약을 가져온다. 이러한 이유들로 나노결정합금의 우수한 자기적 특성을 얻기 위해 급속응고법 이후 후속 어닐링 공정의 중요성이 강조된다. 이 연구에서 우리는 Fe-B-Cu-C 합금 비정질 리본을 제조하였고, 1.8T 이상의 고포화자속밀도와 저손실을 갖는 최적 어닐링 조건을 탐색하였다. 어닐링 조건은 시차열분석(Differential thermal analysis : DTA)으로 측정된 제1결정화 온도(First crystallization temperature, T_{x1})를 기준으로 수행하였으며, 온도, 유지시간 등의 조건들을 고려하였다. 빠른 결정 핵 생성을 도모하고 결정 성장 억제를 위해 구간별로 온도를 다르게 설계한 2단계 어닐링도 수행 되었다. 그림 1은 다양한 어닐링 조건에서 제조된 나노결정합금의 미세구조를 보여준다. T_{x1}+30℃에서 어닐링 된 그림 1의 (a)에서 각진 육면체 형상의 나노결정립이 관찰되었다. 형성된 결정립은 어닐링 유지시간이 증가함에 따라 면방향으로 성장하여 매우 불규칙한 입자로 성장한 반면, 2단계의 어닐링을 수행한 그림 1의 (c)는 균일한 핵 생성으로부터 결정의 성장이 억제되어 미세한 나노결정이 균일하게 형성 되었음을 알 수 있다.

Fe계 나노결정합금의 연자성 특성은 어닐링 과정에서 형성되는 나노 결정의 크기, 형상, 분포 및 분율에 의해 결정된다. 앞서 제조된 Fe-B-Cu-C 나노결정합금은 우수한 자기적 특성에도 불구하고 84 at% 이상의 Fe 함량에 의해 매우 민감한 어닐링 조건이 요구된다. 따라서, 앞선 4원계 나노결정합금의 열 안정성을 향상시키고, 균일한 나노 결정립 형성을 위해 Fe 기반 합금 내 Nb와 Cu의 함량을 변화하여 5원계 합금 리본들을 제조하였다. 제조된 합금 리본은 비정질 형성능, 합금 조성에 따른 결정화 온도 변화, 어닐링 조건에 따른 자기적 특성 및 미세구조가 분석되었다. 이러한 원소의 첨가는 재료의 열 안정성을 높여 균일한 핵 생성을 도모하고 급격한 결정의 성장을 억제하게 된다. 결과적으로, Nb의 첨가는 합금의 T_{x1}을 증가시킴으로써 열 안정성을 향상시켰으며, 결정 성장 억제의 효과로 그림 2의 (a)-2와 같이 10nm 이하의 미세한 *a*-Fe 나노결정립을 형성하였다. 그림 2의 (c)는 Cu-free 합금 리본의 어닐링 된 미세구조를 보여준다. 그림 2의 (a), (b)와는 대조적으로 *a*-Fe 나노결정립은 비정질 매트릭스 내에 고르게 분포하지않고 응집된 클러스터의 형상으로 관찰되었다. 일반적으로 과냉각 된 이원 합금의 국부적인 조성 변동으로 인해 그 구조가 응집된 것으로 보여진다. 이것은 Cu 원자가 Fe 기반 비정질 합금에서 핵 생성 사이트로 작용한다는 것을 명확하게 확인시켜준다.

결과적으로, Cu의 첨가는 균일한 핵 생성을 유도하고 *a*-Fe 나노 입자의 응집을 억제하였다. 또한, Nb의 첨가는 편석에 의해 *a*-Fe나노 입자의 성장속도를 조절하였다. 이러한 효과는 Fe 기반 합금 리본의 열 안정성을 증가시키고 결정의 급속한 성장을 억제하여 구형 결정의 생산을 유도한다. 따라서, Fe계 나노 결정 합금의 연자성 특성은 어닐링 온도의 변화로써 핵 생성 및 결정 성장속도를 제어 할 수 있을 뿐만 아니라, Nb와 Cu의 첨가량을 조절함으로써 두 가지 효과의 상충으로 제어 할 수 있다

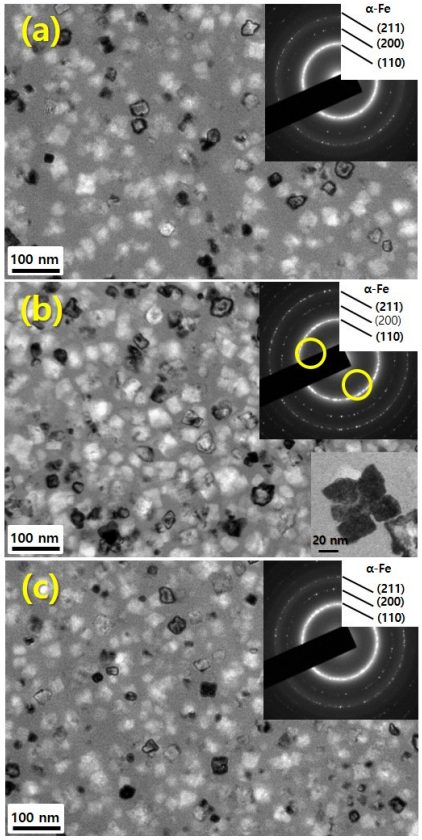

Fig. 1. TEM images and SAED patterns of one-step and two-step annealed $Fe_{84.3}B_{13.7}Cu_1C_1$ ribbons. (a) T_{x1}+30 °C for 1 s. (b) T_{x1}+30 °C for 300s. (c) T_{x1} for 150s after T_{x1}+30 °C for 1s.

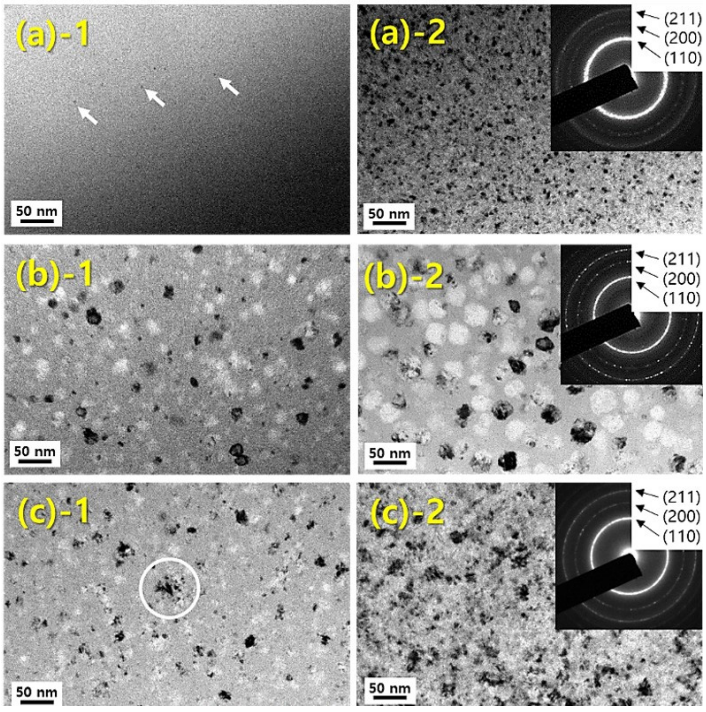

Fig. 2. TEM image and SAED pattern of the annealed Fe-B-C-Cu-Nb alloy ribbons at T_{x1}+10℃(left side) and T_{x1}+40℃ (right side). (a) : $Fe_{80}B_{12.5}C_1Cu_1Nb_{5.5}$, (b) : $Fe_{80}B_{12.5}C_4Cu_1Nb_{2.5}$, (c) : $Fe_{81}B_{12.5}C_1Nb_{5.5}$

Soft magnetic properties and nanocrystallization behavior of cast-iron based bulk amorphous alloy

Ji Yong Hwang and Hyo Yun Jung*
Korea Institute of Industrial Technology

With great potential for extensive industrial application, iron-based bulk amorphous alloy developed with industrial raw materials have attracted increasing attention. Among them, multi-component cast-iron (CI) based bulk amorphous alloy have emerged as one of the promising amorphous materials characterized by their low cost, good mechanical strength and excellent magnetic softness. In addition, it has been revealed that nanocrystalline phases precipitated in amorphous matrix can enhance tensile strength as well as soft magnetic properties of CI-based bulk amorphous alloy. Thus, more recently, the development of nanocrystallized CI-based bulk amorphous alloy has also drawn significant attention. In the present study, we aimed to investigate the effect of minor elements addition on soft magnetic properties and nanocrystallization behavior of cast-iron based bulk amorphous alloy. The alloy with basic compositions of Fe76.5C6.0Si3.3B5.5P8.7 was synthesized by melt spinning and Cu mold casting. As indicated by increased critical diameters (dmax) for the amorphization, the minor alloying of Cu and Al enhanced the glass-forming ability of the alloy. However, it was revealed that the decreased thermal stability of the amorphous phase is strongly related to the enhanced crystallization tendency to form primary a-Fe phase. Upon the nanocrystallization of primary a-Fe phase the alloy shows enlarged Ms of 176 emu/g, still keeping a reasonable small Hc value of 0.086 Oe. However, due to the increased tendency to form secondary Fe3C and Fe2P phase, the bulk metallic glass with combined Cu and Nb addition had a reduced processing window for nanocrystallization. It was revealed that the classical nanocrystallization strategy introducing combined Cu and Nb addition is not a suitable alternative to facilitate nanocrystallization of the cast-iron based bulk metallic glasses.

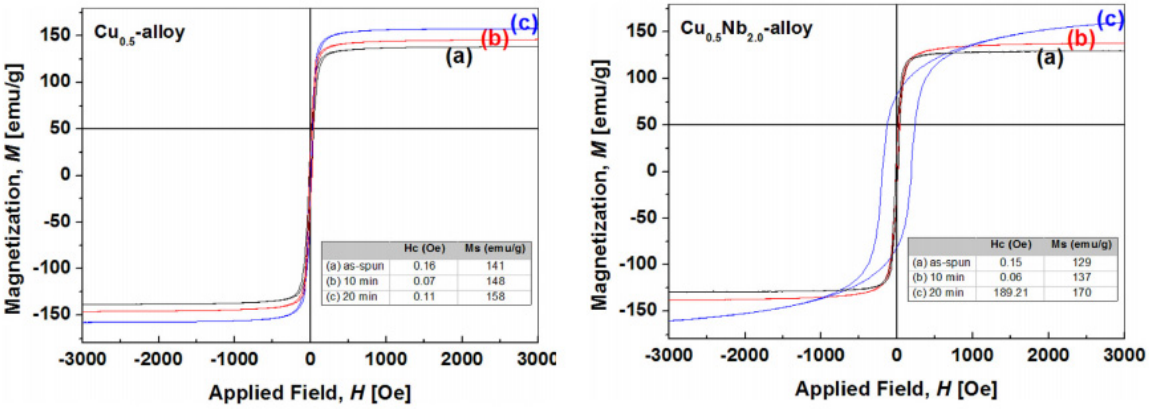

Fig. 1. M-H hysteresis loops of Fe76.0-xC6.0Si3.3B5.5P8.7Cu0.5Nbx (x=0, 2.0) ribbon upon different annealing time.

Development of hexaferrite-based electromagnetic wave absorbers

Young-Min Kang*, Jin-Young You, Su-Mi Lee, Jun-Pyo Lim, Min-Gu Kang
Department of Materials Science and Engineering, Korea National University of Transportation, Chungju, 27469, Republic of Korea
*Corresponding author email: ymkang@ut.ac.kr

Recently, needs of electromagnetic interference (EMI) suppression by the EM wave shielding or absorbing are increasing because a large increase in electronic devices that are working in an environment of electromagnetic (EM) radiation raises the EMI issues among the electric devices and circuits. One of the promising candidates for EM wave absorbers working at several tens gigahertz (GHz) range is the hexaferrite materials. The hexaferrites are magneto-dielectric materials and have high ferromagnetic resonance (FMR) frequencies in the range of a few to several tens gigahertz owing to their high magnetocrystalline anisotropies. EM wave absorption of insulating hexaferrites is mostly dependent on the magnetic loss mechanism, which is closely related to the imaginary part of the permeability (μ"). The μ" of hexaferrites increases at the FMR frequency, which is proportional to magnitude of magnetic anisotropy field (H_{ani}). Herein, we report the EM wave absorption characteristics of various types of hexaferrite-based composites. The methods of tuning and broadening of EM absorption frequency range by compositional and structural controls, the correlation between the substitutional composition, structure, magnetic properties, and EM absorption properties will be presented and discussed.

Machine Learning Directed Prediction of Saturation Magnetization

Chunghee Nam*
Department of Electrical and Electronic Engineering, Hannam University, Daejeon 34430, Korea

Research to predict the various physical properties of inorganic materials using material data has been actively conducted in recent years. Among them, magnetic properties are important features for functional material applications and have been predicted, such as the Curie temperature, coercivity and magnetocaloric properties. In this study, saturation magnetization value was predicted using the DFT quantum calculation-based material data (open source) via machine learning. Ensemble algorithms have been used to compare the performance of models with two metrics of R^2 (coefficient of determination) and RMSE (root-mean-squared error), as shown in Fig. 1. Detailed results will be presented.

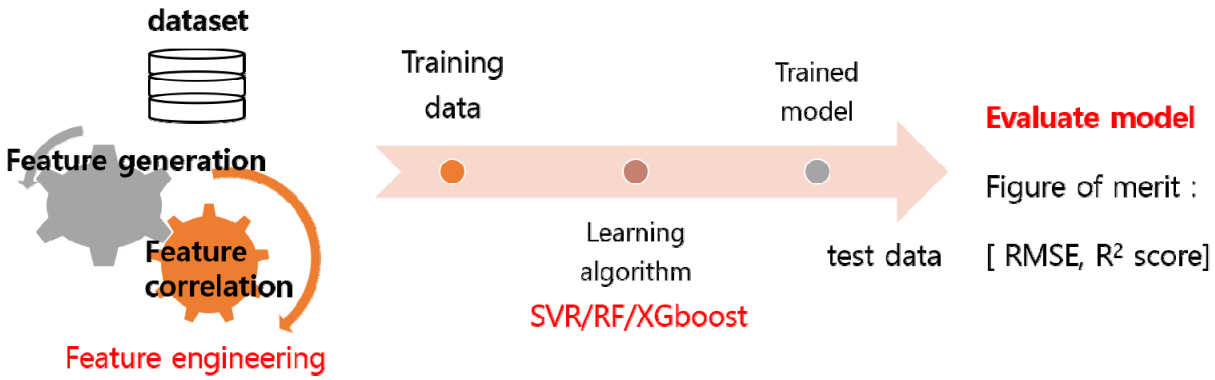

Fig. 1. Machine learning Architecture

Current Status and Research Trend of Soft Magnetic Core

JinBae Kim*
H&A Research Center, LG Electronics, Seoul, Korea

High performance non-oriented electrical steels have become the subject of considerable attention because of the potential applications in electrical appliances and devices, such as transformers and motor cores, because of its excellent soft magnetic properties and low cost. Significant reductions of the magnetic core losses in electrical steel have been sought in order to improve efficiency in electrical appliances. It is well known that the magnetic properties of electrical steel are strongly dependent on the strip thickness, silicon concentration, grain size, and crystallographic texture. Among these factors, the increase in crystalline alignment is one of the most effective ways to reduce magnetic core loss. This article describes the research trend in high performance non-oriented electrical steels.

Manufacturing strategy for a powder-based Fe-6.5%Si steel with high density

Ki Hyuk Kwon[1*], Do Hee Kim[1], Eon Sik Lee[2], Tae-Wook Na[3], Yong Seok Choi[4]
[1]Materials Research Division, RIST, Pohang, Korea
[2]Department of Material Science and Engineering, POSTECH, Pohang, Korea
[3]Functional Materials and Components R&D Group, KITECH, Gangneung, Korea
[4]Material Division R&D part, ZENIX Co., Ltd., Gumi, Korea

In order to manufacture the high performance of high speed and high horsepower electric vehicles, it is essential to use the traction motors that operate efficiently in higher frequency. However, since the core loss of soft magnetic materials increase in the high frequency band, it is required to develop the soft magnetic material capable of exhibiting low core loss with high magnetic flux density even in high frequency. Among the several soft magnetic materials, Fe-6.5%Si steel is a promising candidate because it can simultaneously show high magnetic flux density, low core loss and low magnetostriction in high frequency compared to the existing Fe-3.5%Si steel and amorphous materials. However, in order to realize the mass production of this material, it is needed to develop the new manufacturing process with lower cost compared to the commercial CVD process even using $SiCl_4$ toxic gas.

Among the various candidate of manufacturing processes, the powder rolling process is promising with the advantage of low cost and being able to manufacture alloys containing high Si and Al, which are traditionally difficult to cast. In order to commercialize this process, manufacturing the steel sheets with high density and design of manufacturing process are important. In this study, the technical ideas for the densification of steel sheet were verified such as a modification of powder size distribution and addition of metal powders with low melting point resulting in a liquid phase sintering. For improving a cold rolling properties, the degree of silicon diffusion was optimized to avoid a brittle phase of $B2/DO_3$.

Soft Magnetic Composites: Basics and Methods to Minimize Core Loss

Min-Sun Jang[1*], Bonuk Koo[1,2], Jong-Min Park[1,2], Hea-Ran Kim[1,3], Young-Tae Kwon[1], Sangsun Yang[1] and Jae Won Jeong[1]

[1]Metal Powder Department, Korea Institute of Materials Science (KIMS), 797 Changwondae-ro, Seongsan-gu, Changwon 51508, Korea

[2]School of Materials Science and Engineering, Pusan National University, Busandaehak-ro 63beon-gil, Geumjeong-gu, Busan 46241, Korea

[3]Department of Materials Science and Engineering, Sungkyunkwan University (SKKU), Suwon 16419, Korea

Soft magnetic composite (SMC) which can produce an innovative 3-dimensional core has been much attraction as the potential in various electrical machinery fields because of their superior soft magnetic properties such as a high magnetic permeability and a low core loss at a high frequency range [1]. In general, SMC is composed of Fe-based ferromagnetic particles, and the surface of the iron particles is covered with an inorganic or organic insulation layer. It is possible to improve the surface resistance and thus form an insulated space between them, which can remarkably reduce the eddy-current losses [2]. SMC is generally used as a part of a machine, but in the case of some electric machines, the need for developing high-strength SMC parts is being raised against the material is damaged by fatigue due to exposure to continuous vibration or external shock. There is a method to develop high-strength SMC by the densification of the surface insulating materials through annealing at high temperature (600 °C~1000 °C). However, in general, there is a disadvantage in that insulation is weakened after annealed at high temperature, so an evaluation is necessary to secure both strength characteristics and insulation coating layer retention. Herein, SMC with different inorganic coating materials which is well-known to withstand at high temperature; SiO_2, MgO, and PO_4 and stacking layer; mono or double parameters have been considered for magnetic characterization. All of the coated iron particles were prepared by a chemical sol-gel method, and the thickness of the formed coating layer was confirmed to be 500-600 nm on average through a scanning electron microscope and an energy dispersive X-ray spectrometer. Based on the excellent insulating layer condition (i.e. mono-layers and double-layers, @SiO_2@MgO and @MgO@SiO_2), the core loss evaluation were conducted at high temperature (> 600 °C). Toroidal cores with an outer/inner diameter of 25/15 mm and a thickness of 3 mm were manufactured by cold pressing under a pressure of 500 MPa and then annealed for 1 h at 600 °C, 700 °C, 800 °C, and 900 °C, respectively, in Ar atmosphere to figure out the retention of insulation layer. As a result, as the annealing temperature increased, the core loss with phosphating layer rapidly increased at 1 kHz and 1T because it was carbonized and lost above 650 °C. As compared to the phosphating layer, on the other hand, the SMCs coated with SiO_2 or MgO or double layers annealed at 800 °C exhibited higher retained flux density as well as a significantly low increasing rate of core loss as the frequency and external magnetic field strength increased (at 0.05~1 kHz and 0.3~1 T). This work might be offered a noticeable ideal to design inorganic insulation layer for SMC applications under the high temperature atmospheres.

References

[1] L.Y. Li, et al., J. Alloys Compd. 805, 609-616 (2019).

[2] S.H. Lee, et al., IEEE Trans. Power Syst. 53, 1-4 (2017).

A Study on the Magnetic Properties of Soft Magnetic Powder using Water Atomized Iron Powder for Eco-Friendly Automotive Application

Joonchul Yun[1*], Hyungon Lyu[1], Jinwoo Kim[1], Wonseog Koo[1] and Shingyu Kim[2]
[1]Powder Development & Quality Management Team, Hyundai Steel, Korea
[2]Powder Materials Development Team, Hyundai Motors, Korea

This study has developed technology for manufacturing process of soft magnetic iron powder for eco-friendly automotive part application. Especially, this study investigated the effect of particle size distribution and impurity contents on the magnetic properties of iron powder. The iron based soft magnetic powder was prepared by fluidized bed process using water atomized iron powder, phosphoric acid solution and additional insulation materials. The measurement of magnetic property revealed that the iron based soft magnetic powder had a magnetic flux density of 1.5~1.6T and core loss of 140~200W/kg at frequency of 1kHz. It is expected that the magnetic properties of soft magnetic iron powders can be improved by follow research which is controlling the insulation coating process based on this study.

Additive manufacturing of soft magnetic Fe-Si alloys: a new strategy for 3D components of novel high-performance motors

Bonuk Koo[1,2*], Yeong Gyun Nam[1,2], Min Sun Jang[1], Sangsun Yang[1], Jihun Yu[1], Hak-sung Lee[1], Won-Ho Kim[3], and Jae Won Jeong[1]

[1]Powder/Ceramic Research Division, Korea Institute of Materials Science(KIMS), 797 Changwondae-ro, Seongsan-gu, Changwon, 51508, Korea

[2]School of Materials Science and Engineering, Pusan National University, Busandaehak-ro 63beon-gil, Geumjeong-gu, Busan, 46241, Korea

[3]Department of Electrical Engineering, Gachon University, 1342 Seongnamdaero, Sujeonggu, Seongnam, 13120, Korea

Fe-6.5 wt% Si alloys have been reported excellent magnetic properties such as high permeability over than 20000, low core loss, and zero magnetostriction. In particular, Fe-6.5wt%Si alloys are expected to be suitable for electric motor applications, because they can significantly increase power density and efficiency of the motors by virtue of their high permeability and low core loss. However, Fe-6.5wt%Si alloys have high brittleness and poor formability so that they are difficult to manufacture electrical sheets by cold rolled process which is traditional manufacturing process.

In order to apply the electrical sheets as the motor components, it goes through the process of casting or powder compaction and cutting and lamination. However, they do not have design freeform of 3-dimensional structures, it is difficult to fabricate a next-generation electric motor component with a complex and complicated shape which have optimized magnetic path and considerably increased power density.

Additive manufacturing (AM) have been considered to be suitable for solving the 3D design freeform. Accordingly, many researchers have reported successful fabrication of Fe-6.5wt%Si alloys through various AM processes including selective laser melting, direct energy deposition, and binder jetting but the problems of the insertion of the insulating layer inside the alloy has not been solved.

In this work, we demonstrate additive manufacturing designs for two difference types of soft magnetic stator cores that one is single-rotor-type and the other is dual-rotor-type based on selective laser melting. First design is novel shell-shaping of single-rotor-type stator core, it has inner insulation layers based on selective laser melting. Secondly, design of dual-rotor-type stator core, we devised an inter-racking structure which consists of some separate parts with coated surface insulation layer.

In particular, we analyzed soft magnetic properties of each shells (or sheets) heat-treated at temperatures of 1000-1200 ^{o}C and surface-insulated with silica. Finally, we demonstrated single-rotor-type stator cores for electric motors which are hard to be realized with conventional electrical steel sheets.

2021 KMS Winter Conference

총회초청강연

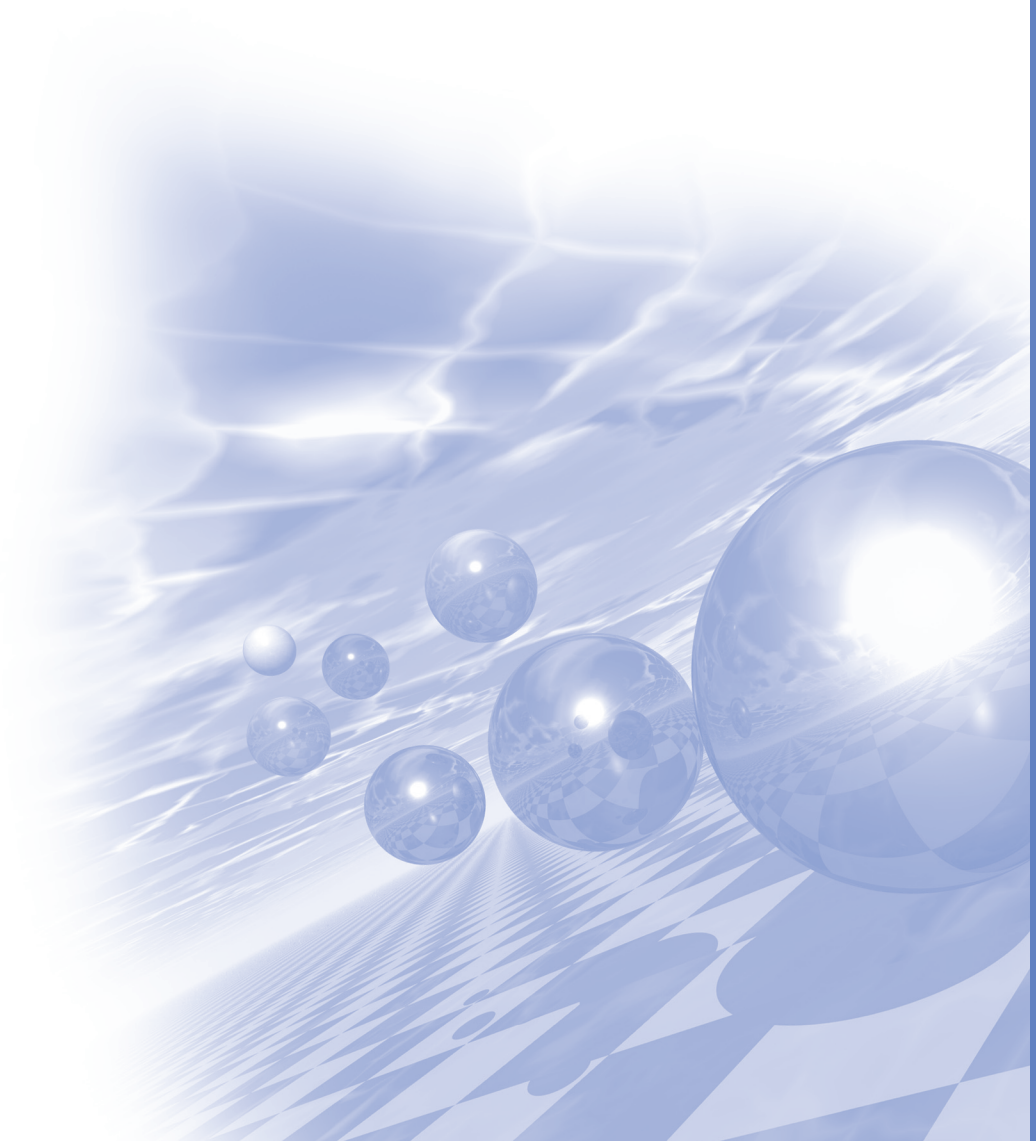

총회초청강연

오환원*
㈜우원테크놀로지 대표이사

약력

1987년 2월 광운대학교 전자재료공학 학사
1990년 9월 ~ 1995년 10월 우원교역 대표이사
1992년 8월 광운대학교 전자재료공학 석사
1995년 10월 ~ 현재 ㈜우원테크놀러지 대표이사
2011년 8월 국민대학교 물리학 박사
2015년 9월 ~ 2016년 2월 서울대학교 공과대학 나노융합IP최고전략과정 이수

2021 KMS Winter Conference

Symposium 6

'Magnetics in Medical Science'

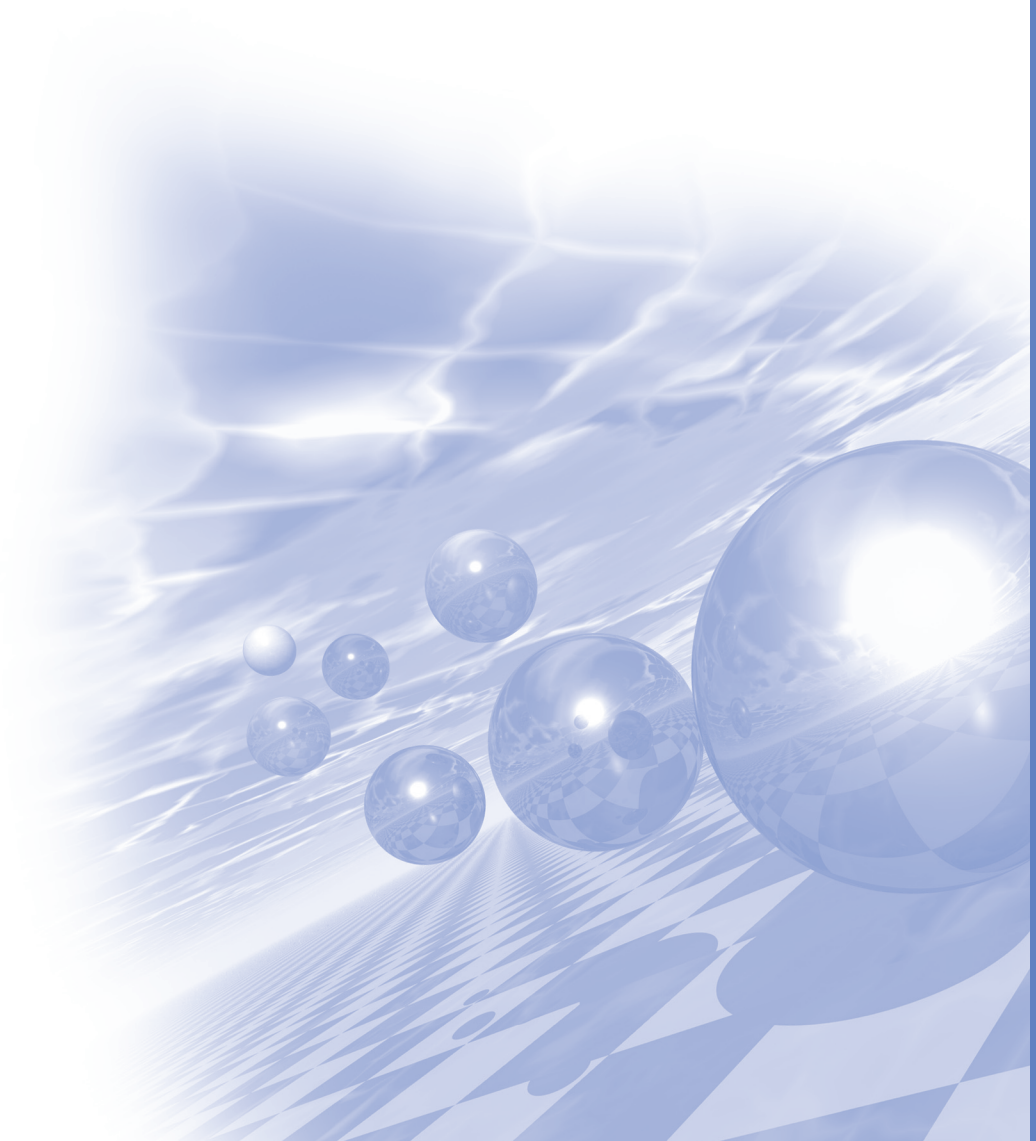

Effects of Neuromuscular Electrical Stimulation Applied After 1 Hz Low Frequency Repetitive Transcranial Magnetic Stimulation on Upper Limb Motor Function and Electroencephalography in Chronic Stroke Patients

Jung-Woo Jeong*
Department of Occupational Therapy, Bobath Memorial Hospital, Seongnam 13552, Republic of Korea

The purpose of this study was to investigate the effect of neuromuscular electrical stimulation applied after 1 Hz low-frequency repetitive transcranial magnetic stimulation on upper extremity motor function and EEG in chronic stroke patients. For 16 chronic stroke patients who satisfied the selection criteria, 8 patients in the neuromuscular electrical stimulation group applied after 1 Hz low-frequency repetitive transcranial magnetic stimulation and 8 patients in the neuromuscular electrical stimulation group combined with intrinsic muscle treatment of the hand were classified into 4 weeks. times, the study was conducted for 3 weeks. In the experimental group, the intervention was performed for a total of 40 minutes, including 15 minutes of 1 Hz repeated transcranial magnetic stimulation and 25 minutes of neuromuscular electrical stimulation. In the control group, 15 minutes of intrinsic hand muscle treatment and 25 minutes of neuromuscular electrical stimulation treatment were performed for a total of 40 minutes. For the evaluation used in this study, electroencephalography, electromyography, and fugl-meyer assessment were performed, and all groups were evaluated before, after, and 2 weeks after the intervention. As a result, the experimental group showed a significant improvement in sensorimotor rhythm wave during the electroencephalography, and there was no significant difference in the control group. In the electromyography among upper extremity motor functions, there was a significant improvement in the experimental group and no significant difference in the control group. In the fugl-meyer assessment, there was a significant difference in both the experimental group and the control group. Through the results of these studies, it was possible to confirm the positive effect of neuromuscular electrical stimulation applied after 1 Hz low-frequency repetitive transcranial magnetic stimulation on upper extremity motor function and electroencephalography in chronic stroke patients.

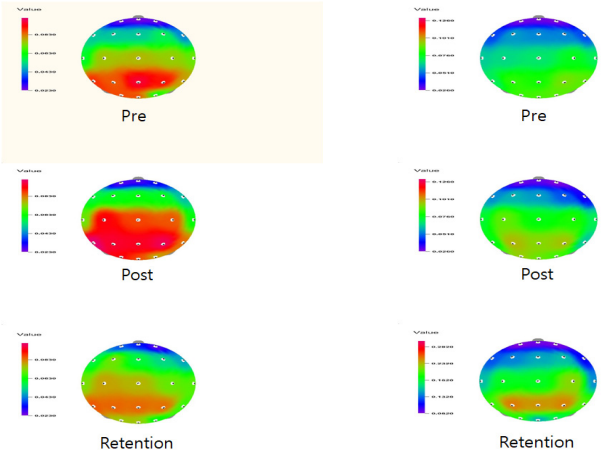

Fig. 1. Comparison of changes in electroencephalography between the two groups.

A Computational Algorithm to Classify Active and Resting Motion during Finger Tapping Task for evaluation of Rehabilitation Therapy

Na-Yeon Seo[1*], Seung-Min Hwang[2], Young-Jin Jung[1,2†]
[1]School of Healthcare and Biomedical Engineering, Chonnam National University, Korea
[2]Interdisciplinary Program of Biomedical Engineering, Chonnam National University, Yeosu-si, Republic of Korea

With the aging of the population approaching, digital health care technology for the elderly has become important. The most elderly people who have a stroke or a brain dysfunction will take a brain therapy including Transcranial magnetic stimulation (TMS) and transcranial direct current stimulation (tDCS) to enhance their brain function. Especially, the preventive rehabilitation therapy for brain function will be requested using digital health care technology. In order to provide the preventive rehabilitation therapy, quantitative and object tool to estimate brain function is essential. In this study, the AI based digital health care technique that can easily classify the human motion was proposed to evaluate a brain function indirectly. To demonstrate, the finger tapping task was employed. Although the finger tapping test is made by subjective judgment based on human eyes currently, the proposed technology will be a first step (preprocessing) for objective judgment index using motion information (range of motion, velocity etc.). To estimate the velocity and angle, a computation algorithm was developed to classify the Active and Resting period to identify the starting point of the motion during the finger tapping task. Then, motion feature can be calculated from video data with AI-based motion estimation algorithm. The results showed that the proposed computational algorithm provide significantly result to how people evaluate. We believe that the algorithm will be a useful tool in medical field.

Effect of Gradient physical linearity and Static Magnetic Field homogeneity on diffusion weighted image : A phantom study

Ho-Beom Lee[1*], Yong-Soo Han[2]
[1]Korea2Asan medical center, 88, Olympic-ro, Songpa-gu, Seoul 05505, Korea
[2]Department of Radiological Science, Hanlym Polytechnic University, Chuncheon 24210, Korea

Gradient strength affects spatial resolution and imaging scan time, as well as the gradient switching rates (dB/dt) for simultaneously switching the encoding gradients in all three axes, and these parameters are critical for MRI. The linearity of the gradient coil describes the deviation from an ideal linear 'steepness' of the magnetic field. A low physical linearity of the gradient coil will result in image distortions and in a smaller maximum field of view (FOV). In this study, we assessed image quality and geometric accuracy as a function of the gradient physical linearity used for diffusion-weighted imaging (DWI) on both conventional-bore and wide-bore scanners. The signal to noise ratio (SNR) was calculated using b = 1000 DWI images for all acquisitions. To evaluate geometric accuracy, the diameter of a phantom on an image slice was measured in four directions. In comparison with the enhanced gradient mode, the default and maximum gradient modes showed higher SNRs with both bore sizes. There were significant differences in SNR among the various gradient modes of the two bore sizes ($p < 0.05$, ANOVA). The geometric accuracy evaluations showed no statistically significant differences in the measured lengths among the various gradient modes and both bore sizes ($p > 0.05$). The wide bore using default and maximum gradient mode showed higher SNR than the conventional bore, and comparable geometric accuracy.

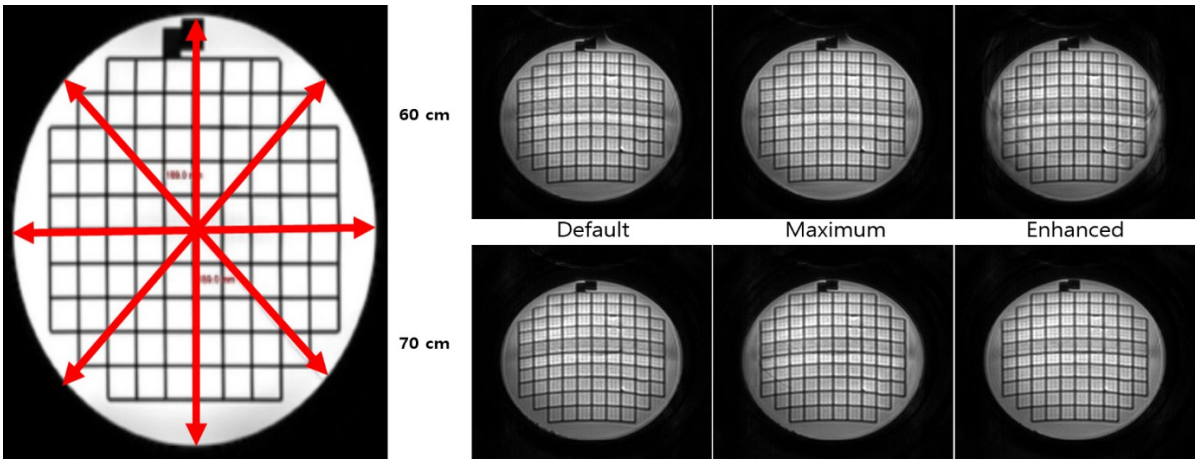

Fig. 1. Images used to assess geometric accuracy. The diameter of the phantom image on slice 5 was measured in four directions on images acquired for each of the gradient modes and both scanner bore sizes.

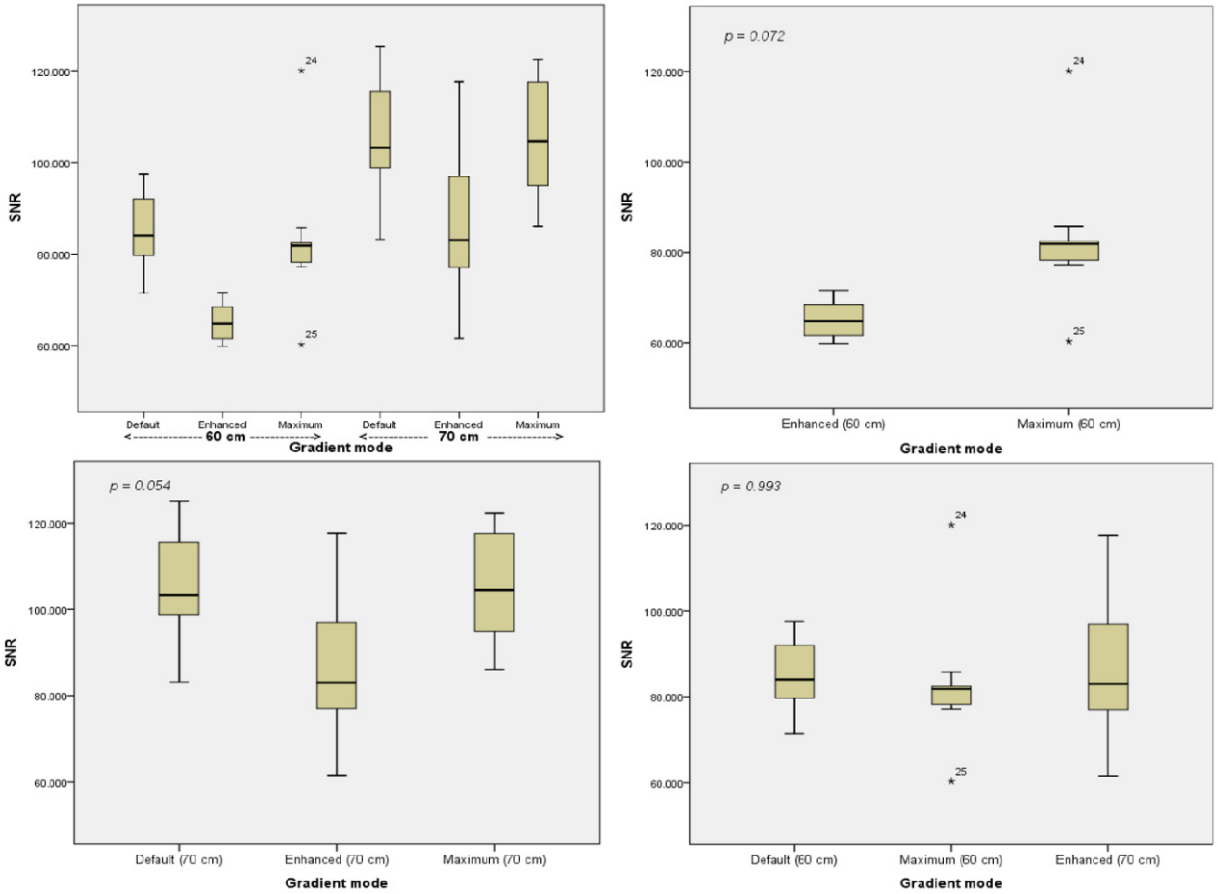

Fig. 2. Box-plot graph showing the distribution of the signal to noise ratio (SNR) as a function of the gradient mode for both bore sizes. *Outliers indicate values more than 1.5 times the upper quartile.

Conjugation element analysis and Brownian motion observation of magnetic nanoparticle structure conjugated with Corona-19 immune antibody

Jong-Gu Choi[1], Sang-Heon Choi[1], Ji-Won Ha[1], Yebin Bae[2], Hyunsook Lee[1], and Sang-Suk Lee[1*]

[1]Department of Digital Healthcare, Sangji University, Wonju 26339, Republic of Korea

[2]Department of Visual and Media Design, Sangji University, Wonju 26339, Republic of Korea

Magnetic nanoparticles (MNPs, Fe_3O_4) are getting a lot of attention as substances widely applied in medical/science fields such as separation of cells, genetic cloning, biosensor, magnetic resonance imaging (MRI), etc for use biomolecular diagnosis and biological application. In a very serious pandemic situation around the world, even after vaccination, coronavirus disease 2019 (COVID-19) treatments for cytokine inhibition has cytokine receptor inhibition and specific immune cell depletion other than steroid hormone. Among them there is a monoclonal antibody (mAb) treatment among the methods of depletion of specific immune cells. Monoclonal antibody treatment is a way that inhibits cytokine secretion by inhibiting cluster of differentiation 3 (CD3) that is one of the important signaling molecules for activation of T cell receptors. An optimal Fc-directed conjugate of humanized anti-CD3 monoclonal antibody (Foralumab) and amine group-MNPs was prepared by the SiteClick antibody labeling kit. The SiteClick antibody labeling kit, which includes antibody control, buffer exchange, antibody carbohydrate domain modification, azide attachment, and azide-modified antibody purification and concentration procedures, was used. The mAb-MNP conjugate was confirmed by observing transmission electron microscopy (TEM) and energy dispersive spectrum (EDS) mapping images included of S elemental spectra and images. The average values of drift movement speed due to Brownian motion of MNPs and mAb-MNPs in phosphate-buffered saline (PBS) were measured as +3.16 pix/frame, 0.76 pix/frame, and +6.70 pix/frame and +1.98 pix/frame on the x-axis and y-axis, respectively. In the case of MNPs and mAb-MNPs having an actual size of 35 nm, from the graphs of the particle size, concentration distribution, and intensity distribution analyzed by nanoparticle tracking analyzer (NAT). For mAb-MNPs, the size of the hydrodynamic diameter was found to be 180.0 nm and 218.8 nm on average, respectively. For mAb-MNPs, the reason why the drift velocity was in-creased by 2 times due to Brownian motion was proved to be increased by 2 times in proportion to the square of the radius of the particle according to Stokes' law. This means that the anti-CD3 antibody (Foralumab) having a biocompatible ligand functional group conjugated to the surface of the MNP has better fluidity in PBS.

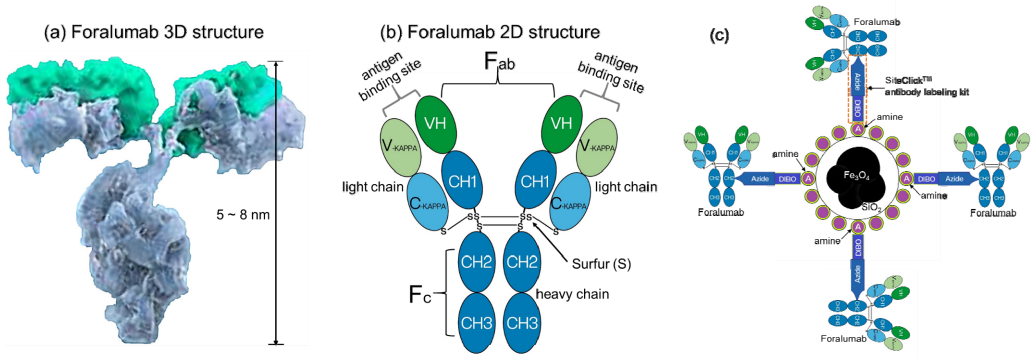

Fig. 1. (a) Hypothetical 3D structure and (b) schematic diagram of 2D structure of Fc-directed Foralumab as anti-human CD3 epsilon therapeutic antibody with a magnitude of a few nm. (c) The schematic diagram of conjugation between monoclonal antibody-azide-DIBO and amine-magnetic nanoparticles.

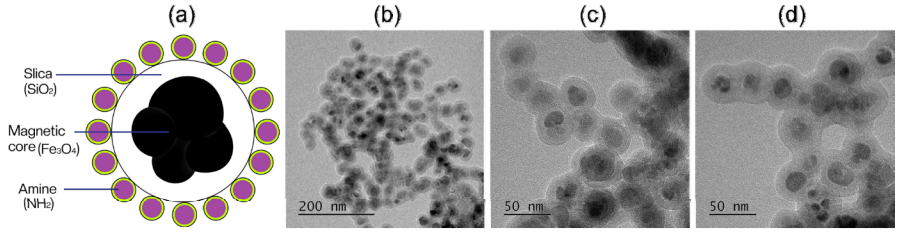

Fig. 2. (a) Structure of one aminated silica shelled magnetite (F_3O_4), (b), (c), and (d) TEM photos of amine-SiO_2-Fe_3O_4 of nanocomposix Cat. No. SCM0067 with surface area of Dia.: ~ 33 ± 5 nm and particle surface: aminated.

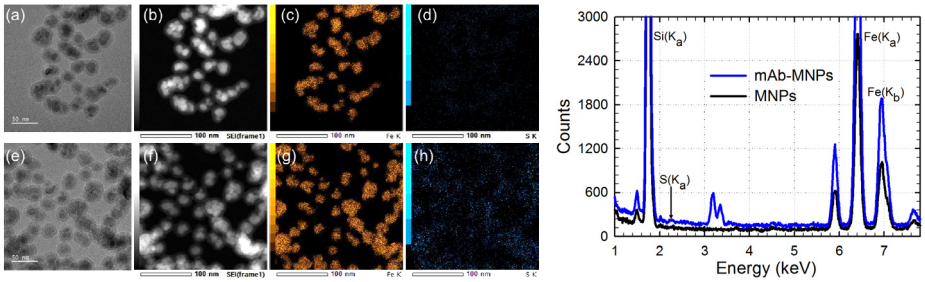

Fig. 3. TEM images and atomic intensities of elements and EDS spectrum of mAb-MNPs (anti-CD3 Foralumab mAb-azide-DIBO-MNPs of aminated silica shelled magnetite).

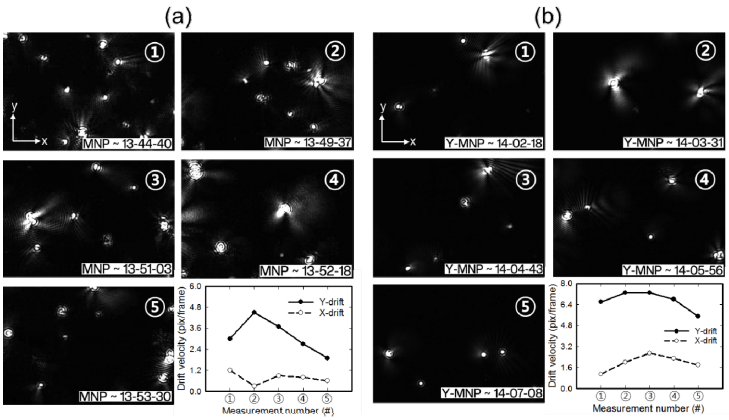

Fig. 4. Single shots of flow images and analysis results of Brownian motion obtained by NTA device in 5 different groups of MNPs and mAb-MNPs samples immersed in a liquid with PBS×1 magnetic particles of 1 μg/mL.

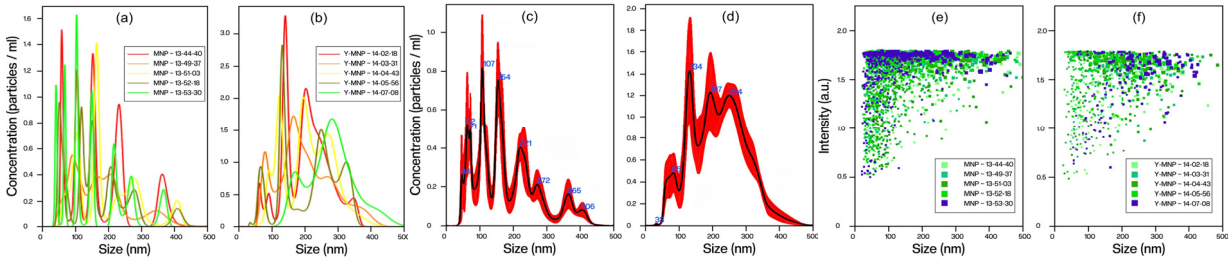

Fig. 5. Finite track length adjustment (FTLA) Concentration versus Size graphs for NTA analysis of particles in (a) MNPs and (b) mAb-MNPs. Averaged FTLA Concentration in (c) MNPs and (d) mAb-MNPs. Intensity versus Size graphs in (e) MNPs and (f) mAb-MNPs. Hydrodynamic mean sizes: MNPs = 180.0 nm and mAb-MNPs = 218.8 nm.

Keywords : Foralumab, Magnetite, Mapping image, Brownian motion, Drift velocity, Stokes' law

Acknowledgements : This research was supported by Basic Science Research Program through the National Research Foundation of Korea (NRF) funded by the Ministry of Education (2021R1I1A3054773).

New CT Scanner with Photon-Counting Detector

Chang-Lae Lee*
PCD R&D Group, Health and Medical Equipment Business Unit,
Samsung Electronics, Suwon-si, Gyeonggido, Korea

Dual-energy computed tomography (DECT) has provided new opportunities for X-ray CT. The major advantage of DECT is that it shows different attenuations of two materials using two different energy spectra, thereby allowing the separation of two materials that can hardly be distinguished by single energy CT. DECT reduces the use of contrast media as it improves the contrast among different tissues. Several applications of DECT have been reported since its introduction. For example, virtual monochromatic images (VMIs), synthesized from DECT data, are utilized to locate abdominal tumors (such as liver and kidney tumors), intracerebral hemorrhage, pulmonary embolism, and vascular calcification. Moreover, VMI enables the detection and characterization of chemical compositions of materials that help in assessing specific disease processes. However, the DECT approach suffers from certain limitations related to its mechanism of image acquisition. For instance, difference in the acquisition time of high- and low-energy datasets and acquiring images with substantial spectral overlap are major challenges. Recently, photon-counting detector (PCD) CT scanners, which use an X-ray detector with improved energy-resolving power, have emerged as a diagnostic technique. Energy-integrating-detectors (EID) integrates all photon energies while PCD can discriminate by counting the number of photons according to the energy of a defined threshold (Figure 1). PCD CT provides significant benefits such as reduced electronic noise, increased contrast-to-noise ratio, decreased metal artifacts, and improved spatial resolution, material decomposition, and dose efficiency compared to conventional EID CT.

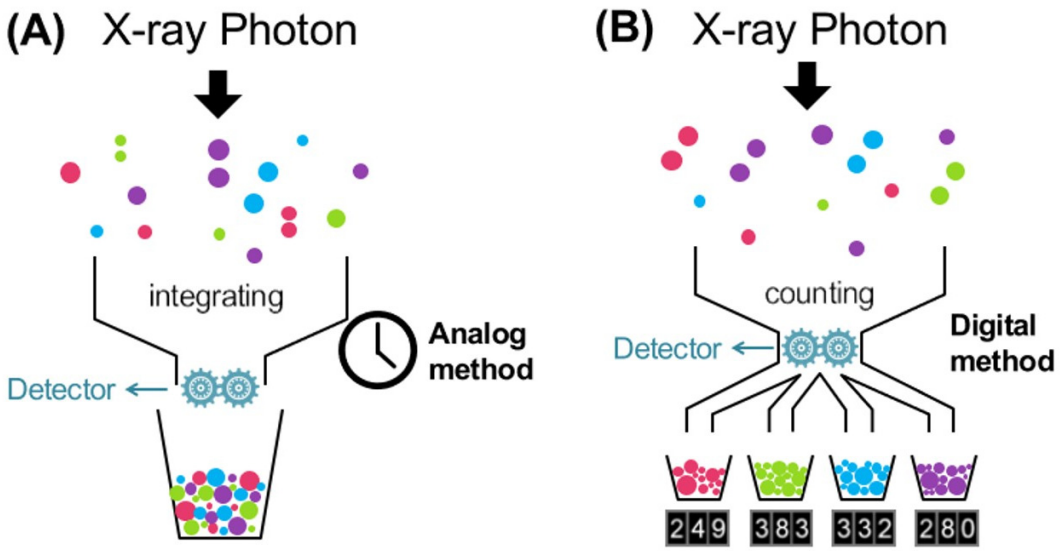

Fig. 1. Schematic particle detection schemes of x-rays (a) Conventional EID and (b) PCD. Different color indicates energy of photons. Conventional EID integrates all photon energy, while PCD counts the number of photons corresponding energy level.

몬테카를로 시뮬레이션을 이용한 친환경 의료용 차폐 시트개발

권다은[1*], 한동희[1], 정경환[1], 김장오[3], 이승재[4], 백철하[2†]
[1]강원대학교, 보건의료과학과
[2]강원대학교, 방사선학과
[3]강원대학교, 보건의료융합연구소
[4]동서대학교, 방사선학과

의료방사선은 세계적 고령화와 질병의 증가에 따라 이용되는 필수적인 전자기파 방사선인 동시에 인공방사선의 약 80%를 차지하고 있다. 방사선이 인체에 미치는 영향에는 결정적 영향과 확률적 영향이 있으며, 특히 확률적 영향은 문턱선량이 없어 적은 선량에서도 암 발생 확률이 증가되기 때문에 전자기파의 물리적 성질을 가진 엑스선차폐를 위해 의료방사선 검진 시 방사선방호용기구의 착용이 권고되고 있다. 현재까지 높은 원자번호와 밀도의 납 소재를 활용한 방사선방호용기구가 사용되고 있지만, 방사선방호용기구의 노후 시 납자체 독성으로 인체와 환경에 유해하다는 단점이 제시되었다.[1] 이후 납을 사용하지 않은 친환경 물질 기반의 차폐복이 개발되었으나 대부분이 교반 방식에 편중되어 있으며, 선행연구에 따르면 교반 방식은 나노 입자의 불균등한 분포와 그에 따른 공극으로 인해 방사선 차폐성능이 불균등하다는 문제점이 보고되었다.[2] 이에 본 연구는 몬테카를로 시뮬레이션 GATE 를 이용하여 성인의 진단 엑스선 에너지 범위 중 고 영역인 120, 150 kVp 에서 단일 원소 물질을 적층으로 쌓아 각 층별 물질과 두께를 최적화하였으며, 그 결과를 바탕으로 또 다른 시뮬레이션 도구인 MCNP 에서 최적화된 차폐 시트결과를 표준 한국인 체형 기반인 HDRK(High-Definition Reference Korean-Man)팬텀에 적용하여 각 장기별 선량을 도출하였다. 차폐물질은 주석(Tin), 텔루륨(Tellurium), 텅스텐(Tungsten), 비스무트(Bismuth)을 이용하였으며 원자번호, 밀도, k-edge 등의 특성을 고려하여 적층구조로 구현하였다. 본 연구 결과는 엑스선이 활용되는 의료분야뿐 아니라 지질탐사, 보안시스템등 다양한 분야에서 피폭저감화에 기여할 수 있을 것으로 기대된다.

중심단어: 몬테카를로 시뮬레이션, HDRK 팬텀, 적층구조, 단일 원소 물질

Acknowledgement: This research was supported by the National Foundation of Korea (NRF) funded by the Ministry of Education, Science and Technology(2020R1C1C1004584)

References

[1] Z Li, W Zhou, X Zhang, Y Gao, S Guo. “High-efficiency, flexibility and lead-free X-ray shielding multilayered polymer composites: layered structure design and shielding mechanism,” Scientific Reports, Vol. 1, No. 11, pp. 1-13, 2021.

[2] Sazali, M. A., Rashid, N.K.A. M.,&Hamzah, K. “A preliminary study to metaheuristic approach in multilayer radiation shielding optimization,” IOP Conference Series: Materials Science and Engineering, Vol. 298, No. 1, p. 012042, 2018.

A review of AAPM Task Group 241: A medical physicist's guide to MRI-guided focused ultrasound body systems

So Hyun Park*
Department of Radiation Oncology, Jeju National University Hospital, Jeju University College of Medicine, Korea

As treatment techniques such as intensity-modulated radiation therapy (IMRT) and volumetric arc therapy (VMAT) are actively applied in radiation therapy, accurate and localized radiation delivery is becoming more important. Accordingly, image-guided therapy plays a very important role in accurate radiation delivery. Currently, the most active work for image-guided is cone beam computed tomography (CBCT) coupled to a linear accelerator. In the case of CBCT, not only radiation is used, but additional doses are delivered to the patient depending on the number of uses, not for the purpose of treatment. Recently, the magnetic resonance linear accelerator (MR-linac) equipment, which combines the magnetic resonance imaging (MRI) and linear accelerator, has started to be used. Instead of images acquired with the radiation before treatment, images are acquired using MR without radiation, and the setup is being done in consideration of the patient's position and anatomical structure. And Hyperthermia was also used because it can help cancer treatment without radiation. A number of techniques have been developed and applied for cancer treatment that allow the body to be minimally or not exposed to radiation while focusing only on the treatment area. As the latest trend in non-ionizing image guided and treatment, AAPM 241 reported the Magnetic resonance image-guided focused ultrasound (MRgFUS) in 2021. The MRgFUS uses ultrasound instead of radiation during treatment, and apply MRI as image-guided. It is completely non-invasive, potentially resulting in shorter recovery times and reduced infection risks. In this report, integrated procedures such as patient preparation, positioning, treatment planning, assessment, and safety are covered in detail. The process recommendations are also dealt with. It emphasized that key points and best practice recommendations will allow the identification and management of the uncertainties that can potentially arise during MRgFUS body treatments, ultimately affecting the treatment outcome. The review for the AAPM 241 will help to understand and effectively deal with novel MRgFUS.

Implementation and Clinical Considerations of Elekta MR-linac

Kwang Hyeon Choo*
Elekta Ltd Korea, Republic of Korea

Major advantages of online magnetic resonance-guided radiotherapy are the superior soft-tissue contrast and the acquisition of continuous imaging without additional exposure over X-ray based imaging. In this presentation, a MR-Linac (magnetic resonance linear accelerator) system Unity (Elekta AB, Stockholm, Sweden) consisting of a 1.5T MRI (magnetic resonance imaging) and a 7 MV photon beam will be introduced including implementation and clinical considerations.

Experience with 1.5T MR-Linac system: a medical physicist's point of view

Ho Lee*, Jiwon Sung, Yeonho Choi
Department.of.Radiation Oncology, Gangnam Severance Hospital, Yonsei University College of Medicine, Korea

This talk will discuss the 1.5T MR Linac Unity equipment installed at Gangnam Severance Hospital for the first time in Korea. First, the physical characteristics are briefly described compared to conventional linear accelerators. Second, we describe the implementation of MR-based workflows for adaptive radiation therapy. Third, we introduce the experience of commissioning, including beam data acquisition/validation and patient-specific quality assurance, as well as device acceptance test after Unity installation. Finally, we provide information on clinical applications that have been treated with Unity.

Oral Session 3

'Theory and Computational Magnetics' / 'Others'

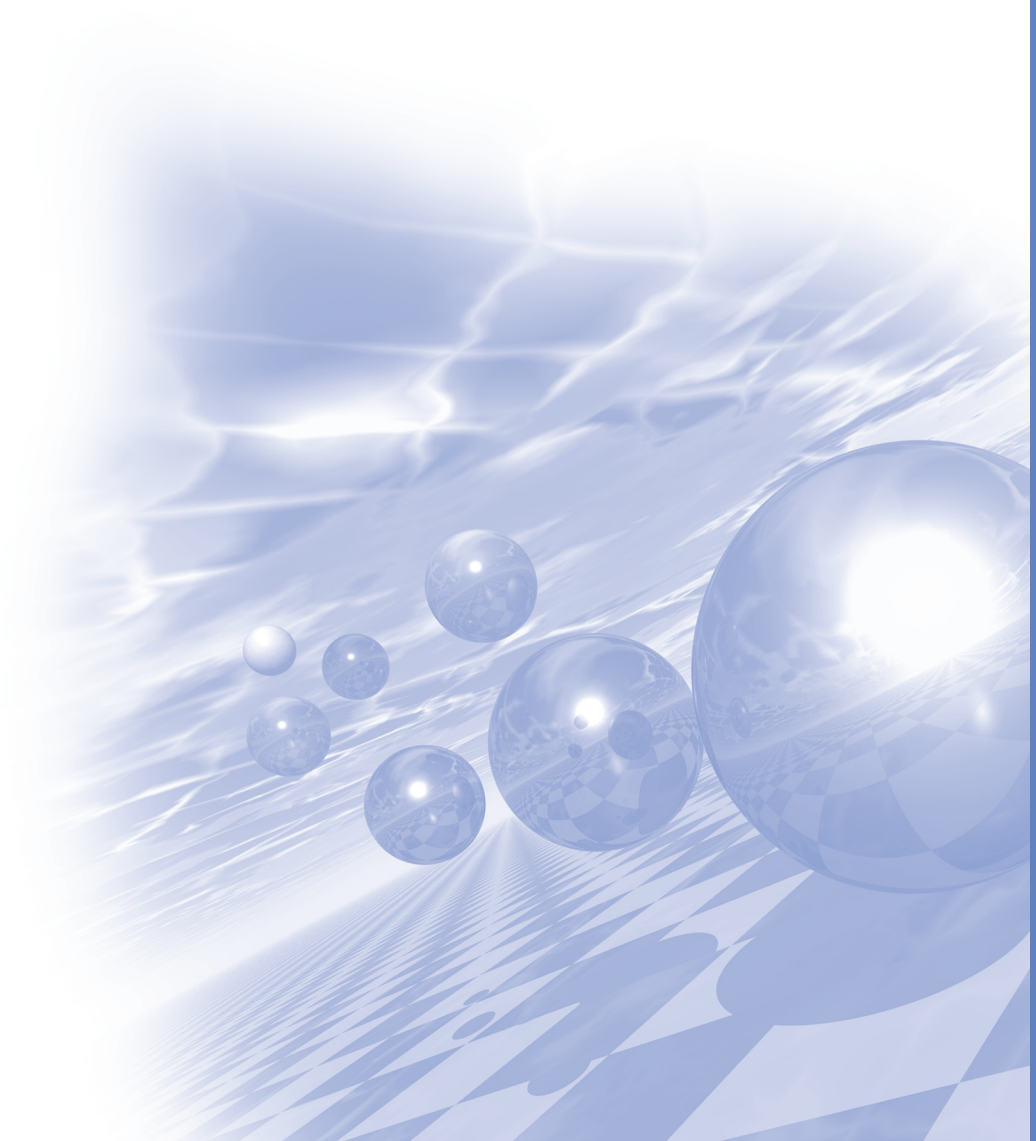

Semimetallic Nature of and Magnetic Polarons in EuB_6 Studied by using Angle-Resolved Photoemission Spectroscopy

Hyeong-Do Kim[1*], Chul-Hee Min[2], Boyoun Kang[3], Beong Ki Cho[3], En-Jin Cho[4], Byeong-Gyu Park[1]

[1]Pohang Accelerator Laboratory, Pohang 37673, Korea
[2]Institut für Experimentelle und Angewandte Physik, Christian-Albrechts-Universität zu Kiel, D-24098 Kiel, Germany
[3]School of Material Science and Engineering, Gwangju Institute of Science and Technology, Gwangju 500-712, Korea
[4]Department of Physics, Chonnam National University, Kwangju 500-757, Korea

Temperature-dependent angle-resolved photoemission spectroscopy (ARPES) was carried out on single-crystalline EuB_6 samples. By measuring ARPES spectra in an extended Brillouin zone, we clearly observed a B 2p hole pocket centered at the X point as shown in Fig. 1, thus proving the semimetallic nature of EuB_6. Below the Curie temperature T_C, ARPES spectra show two B 2p bands of which separation is due to an exchange interaction between local Eu 4f and itinerant B 2p electrons. The exchange splitting becomes smaller as the temperature increases and disappears well above T_C. Additionally, a diffuse structure near the Fermi level survives at temperatures just above T_C. Such behavior is well described by using Monte Carlo simulations of a Kondo lattice model, thus supporting the formation of magnetic polarons in EuB_6, which accounts for the resistivity upturn slightly above T_C as the temperature is lowered.

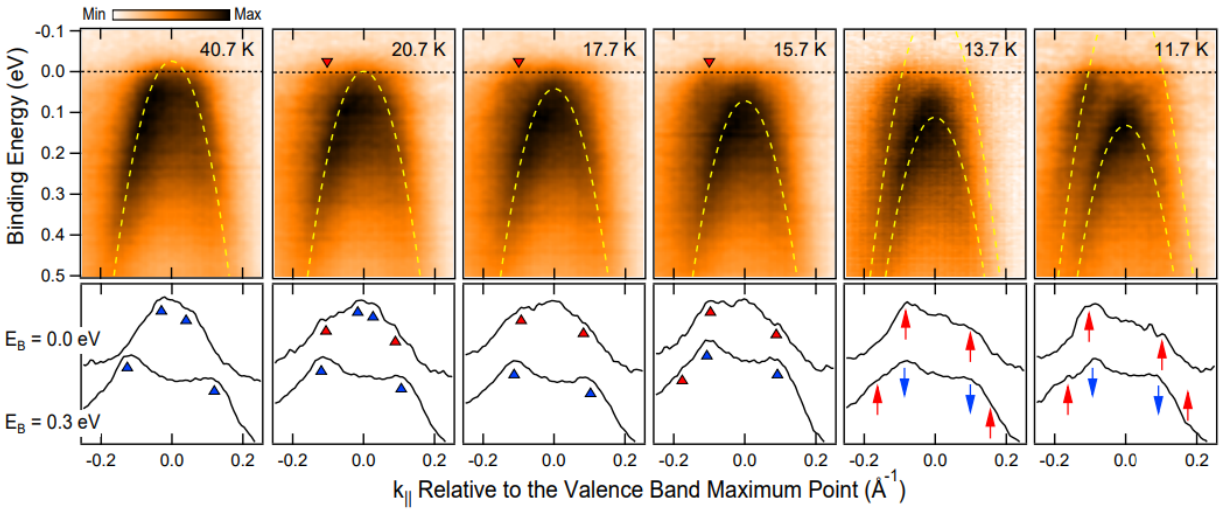

Fig. 1. Upper panels: ARPES spectra of EuB6 at various temperatures above and below Tc. Lower panels: MDCs at the binding energies of 0 and 0.3 eV.

O-3-2

자동차 럼버서포트용 모터의 토크향상을 위한 전자기해석

Mangi Lee[1*], Sejung Kim[1], Yong Chol[1], Young Jin Hong[1], Sujung Lee[2]
[1]Korea Institute of Robotics & Technology Convergence, [2]Gyeongbuk Technopark

Abstracts 자동차 부품의 개발 방향은 경량화에 맞춰 연구개발이 진행되고 있음. 이에 발맞춰 럼버서포트에 사용되는 모터를 전자기해석을 통해 토크를 향상시키는 방법을 연구하여 같은 토크에 무게가 가벼운 모터를 설계하고자 함. 여기서 설계 변수는 자석의 배열/크기/패턴, 요크의 형상/개수, 전선의 두께/턴 수로 총7개의 변수를 조정하여 설계를 수행함.

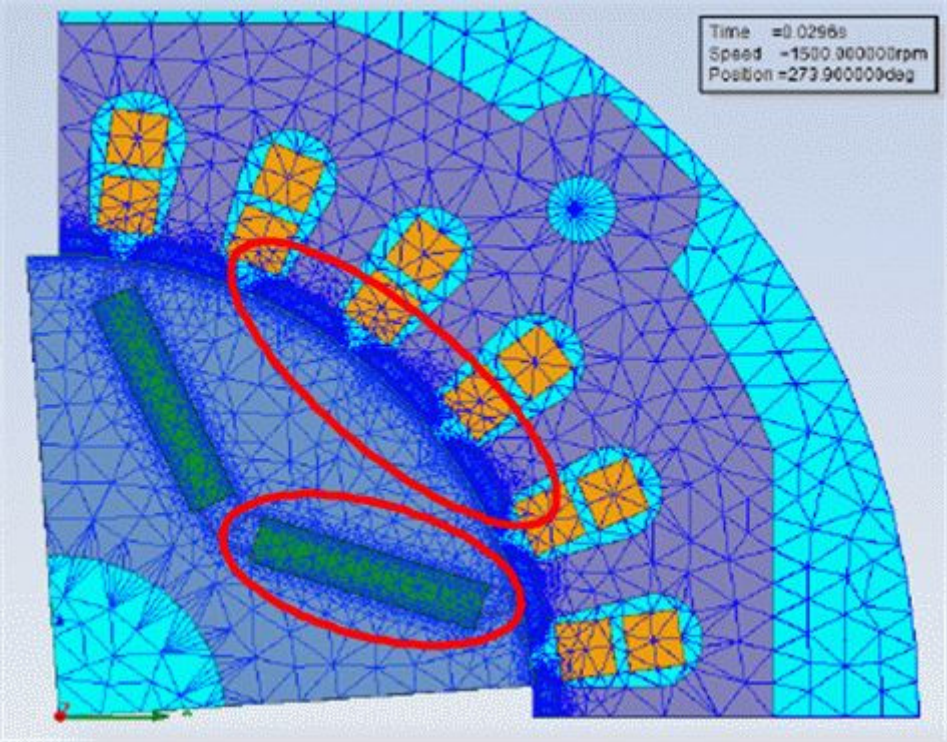

Fig. 1. Mesh 구성

위 fig1과 같이 Mesh를 구성하였고, Mesh의 Segment Setting을 컴팩트하게 설계하면 해석 시간이 크게 단축됨. 회전자, 고정자 사이에 Airgap에 대한 Mesh 설정이 아주 중요함. 회전이 되면서 Segment간 연결이 원활하게 되어야 자속의 흐름이 모터 토크에 큰 영향을 주기 때문임.

또 Mesh 설계를 Log Scale로 설정하면 한 개체의 Segment의 수만큼 일정하거나 비슷한 크기의 Mesh가 설계되는 것이 아니라 Log Scale로 설계 시, 한 개체와 다른 개체 사이에 접촉되어 있는 부분은 Mesh 크기가 작고 Segment가 많도록 구성을 하게됨.

전기 코일, 영구자석, 자성체, Band에 특히 Mesh 설정에 따라 손실 계산에 영향이 큼. 위와 같은 설정으로 전자기해석을 수행하면 아래 fig2와 같은 자기장 분포와 밀도를 확인할 수 있음.

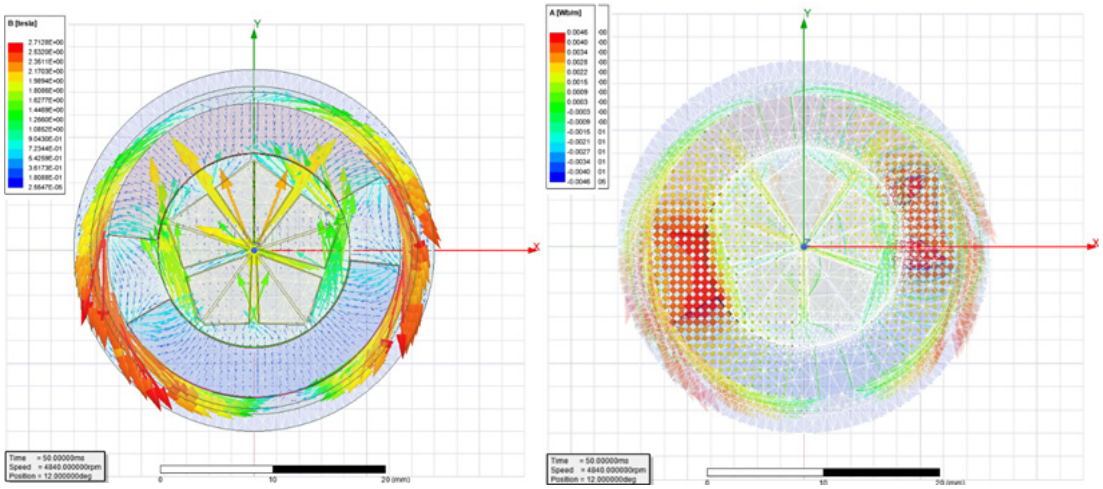

Fig. 2. 자기장 분포 및 밀도

위 fig2는 (왼)자기장 분포, (오른)자기장 밀도의 해석 결과를 확인하였음. 자기장 분포 및 방향 결과에서 화살의 방향은 자기장의 방향, 화살의 크기는 자기장의 세기를 의미함.

자기장 밀도 결과에서 양측의 붉은 색을 띄는 부분이 자기장의 밀도가 높은 부분이며, 토크 발생 부 임을 알 수 있음.

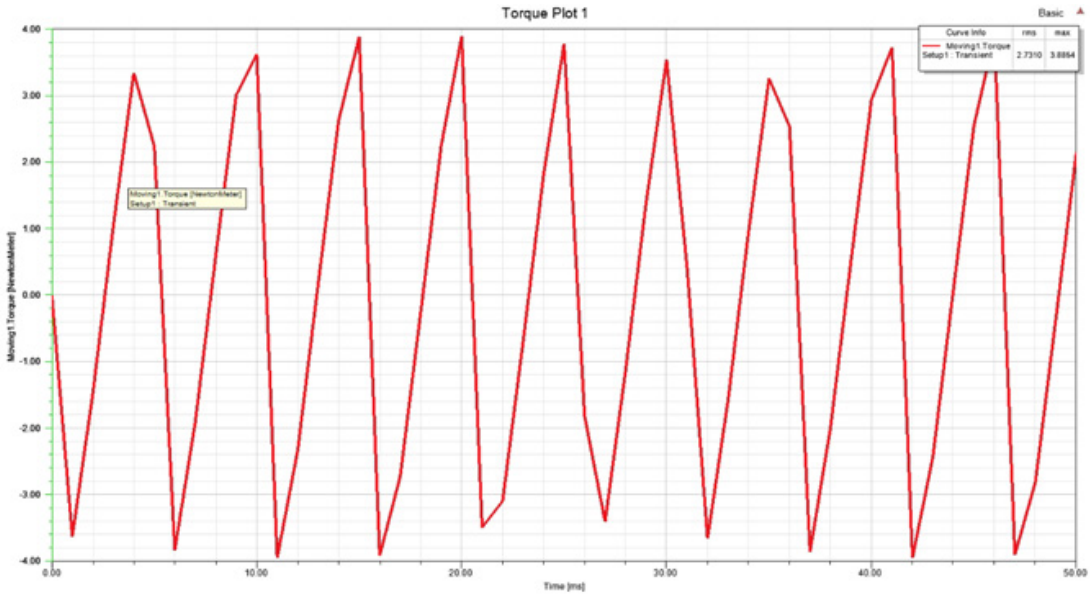

Fig. 3. 토크 그래프 및 RMS 값

Transient 해석에서 기존 모터 모델에서의 토크를 출력한 결과 RMS 값은 2.73N/m 임을 알 수 있음.

O-3-3

Weyl points in magnetic metals

Minkyu Park[1*] and S. H. Rhim[2]
[1]Research Institute of Basic Sciences, University of Ulsan, Ulsan, 44610, Republic of Korea
[2]Department of Physics, University of Ulsan, Ulsan 44610, Republic of Korea

In three-dimensional crystals, Weyl points are ubiquitous as long as *PT* (spacetime reversal) symmetry is broken. If Weyl points are close to the Fermi energy as in Weyl (semi)metals, small and topologically nontrivial Fermi surface leads to many fascinating physics such as chiral magnetic effect. In ordinary metals, on the other hand, the Fermi surface is not small and does not necessarily possess nontrivial Chern number. In this work, we study Weyl points in magnetic metals in the context of anomalous Hall effect. We show avoided crossings are equally crucial as Weyl points in general. We also discuss some mplications of the Nielsen-Ninomiya theorem on magnetic metals.

Author Index

Digests of the KMS 2021 Winter Conference

The Korean Magnetics Society

사단법인 한국자기학회

2021년 동계학술대회 논문개요집 제 31권 2호

(06130) 서울특별시 강남구 테헤란로 7길 22(역삼동635-4) 한국과학기술회관 신관 905호

TEL. (02)3452-7363, **FAX.** (02)3452-7364

E-mail. office@magnetics.or.kr, **Home-page.** www.magnetics.or.kr

연세대학교 '초임계 소재 산업기술거점센터'

연세대학교 '초임계 소재 산업기술거점센터(센터장 이우영 교수)'는 산업통상자원부에서 주관하는 사업으로 대학 연구소를 통한 미래 산업의 원천핵심기술 개발, 축적 및 산업계 기술 공급 체계를 마련하는 사업이다. 총 2단계의 사업 중 1단계는 53억, 2단계는 200억 규모로 지원하며 산업 혁신을 위한 원천핵심기술 개발하고 지식재산권을 확보하는 사업이다.
초임계 소재 산업기술거점센터는 30여개의 기업체가 협력하여 소재합성과 공정개발, 소재설계, 부품화를 통한 응용 물성까지 확보하는 완성형 연구를 추진하고 있다. '산업기술거점센터'는 글로벌 소재-부품 First Mover 도약을 비전으로 설정하였으며, 대학 연계 소재-부품 R&D전략 다변화, 성과 창출을 위한 R&D기반 강화, 협력-축적-공유 기반 R&D생태계 구축의 3대 추진전략을 수립하였다. 이를 바탕으로 연구개발 수행 인프라와 협의체 운영 및 지원 시스템을 구축할 계획이다.

1. 금속, 세라믹, 고분자 소재와 관련 부품화 기술을 포괄하는 산업기업지원센터
2. 기업 수요 파악, 개발 목표 설정, 전략 수립 컨설팅 및 기술 개발 전주기 페이스 메이커 역할 수행
3. 기업별 맞춤형 산학 연구 수행, 원천기술 확보 및 상용화 지원
4. 참여 기업간 물적 인적 교류 중계
5. 소재부품 전문 인력 양성 및 산업계 공급 기능 수행

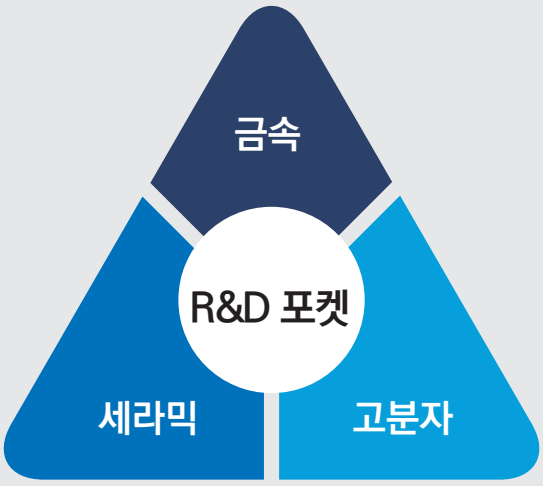

난제 해결형 Task Force

연구개발 기술공유
해결 및 협력연구 추진

기업별 타켓형 산학연구 지원

기획 · 운영 전주기적 점검
지속적인 수요변화 대응
AI 기반 맞춤형 솔루션 제공

기술이전

참여기업 우대

- 참여기업 우수기술 확보 권리 부여
- 공동위착과제 산업체 선용 실시권 제공
- 양산을 위한 공정설비 공동개발

기술이전 안심 보장제도

- 기업의 기술도입비용 부담 최소화
- 상용화 시 기술료로 보상체제 전환
- 지속적인 기술보완 A/S 제공
- 추가 위탁과제 수행 통한 공동 개발

민간 R&D 수탁

상용화 기획

- 수요기업 섭외
- 운영 및 개발 경비 확보
- 중소 · 벤처기업 대상 지원 사업 추진
- 벤처캐피털 통한 외부 투자 유치

브릿지기술 개발

- 기술 보완 단기 연구 활성화
- 임무 완수형 연구과제 개발
- 선연구 후지급 연구위탁 시스템 구축